The Role of Transglutaminases in the Development of Abdominal Aortic Aneurysms

Kathryn Jane Griffin

Submitted in accordance with the requirements for the degree of

Doctor of Philosophy

Thrombosis and Tissue Repair Group,

Department of Cardiovascular and Diabetes Research (DCDR),

Leeds Institute of Cardiovascular and Metabolic Medicine (LICAMM),

School of Medicine,

The University of Leeds

July 2016

Intellectual Property and Publication Statement

The candidate confirms that the work submitted is her own and that appropriate credit has been given where reference has been made to the work of others.

Acknowledgements

Undertaking a PhD thesis is not to be underestimated; in terms of workload, stress and personal effort, but also in terms of the number of people who will come in to your life and help you along the way…and in my case, there have been many!

Although the work presented in this thesis is predominantly my own, it would not have been possible without the combined effort of a team of people and I would like to take this opportunity to thank them all here. Thanks, firstly to my supervisors – Dr. Richard Pease and Prof. Julian Scott – who have provided countless hours of support, guidance and intellectual challenge, and also to mentors in the form of Dr. Chris Jackson in Bristol and Dr. Ric Cubbon here in Leeds. Thanks also, to my external collaborators; Prof. Bob Graham who kindly provided the TG2-deficient mice used in this project and Prof. Timothy Baxter and Dr. Wanfen Xiong who welcomed me so warmly to a freezing Nebraska back in January 2013 and provided advice relating to the calcium chloride aneurysm model throughout this project.

I would like to mention each member of the Thrombosis theme for treating me as part of their team, but specific thanks must go to the Grant lab group, within which I have found a home over the last 4-years. Thank you, to Mrs. Jane Brown for your help with the FXIII-A assay and in providing technical support for the histological staining work included in this thesis, to Dr. Cora Beckers for your expert management of our mouse colonies whilst I was away and to Dr. Lih Cheah for your help with the wire myography setup and histological analysis. Thanks also to the students (Eleanor Cawthorne, Tejal Parekh and Callum Taylor) who have joined (and left) our group and have asked me probing questions about methodology and results, forcing me to analyse my own work continually. The largest debt though, is owed to Mr. Kingsley Simpson who has taught me (pretty much) everything I now know about working in a lab and who stopped me from making countless “medic mistakes”. Your help and support has been invaluable (particularly with regards the real-time PCR data) and I wish you every luck in finishing your own PhD and continuing what I know will be a hugely successful academic career.

Outside of my own lab group, I have received histological support from Mr. Mike Shires, animal husbandry support from the staff of CBS (but especially Mr. Andy Horner) and personal support from Drs Kerrie Smith and Karen Porter. Dr. Nadira Yuldasheva has been my patient teacher of animal surgery (as well as husbandry, histology and general lab practice) for a number of years and I am eternally grateful to her for sharing her expert skills and knowledge with me – thank you.

This brings me to a group of people without whom I would not be submitting this thesis; Katy Paradine, Marc Bailey, Anshu Sengupta, Andy Walker, Noman Ali, Peysh Patel and Nadeem Mughal – you have not provided technical support, and may even have hindered my progress at times with your “witty” banter and in-jokes but I could not have done this without you and the lunches and coffee breaks we have shared. I know I have made some life-long friends through this process and I look forward to watching your careers progress and flourish in the future. This group should also include Mrs Anne Johnson – my “work Mum” – hopefully I have told you how much I value your support, but if not, I do, and thank you.

I would also like to extend my sincerest thanks to the British Heart Foundation for funding this work through my Clinical Research Training Fellowship. Your supporters and fundraisers work tirelessly to improve the lives of patients with cardiovascular disease and I am immensely grateful for all the opportunities that this fellowship has provided.

And finally, my boys; my long-suffering husband Nick and my gorgeous sons Thomas and Edward who both arrived during this PhD and turned my world upside down. Thank you for filling my life with fun and silliness and for being my reason for wanting to work hard and succeed. None of you have a clue about this project (!) but you still support me every single day and I love you all so much.

Abstract

Abdominal aortic aneurysms (AAA) are dilatations of the abdominal aorta that are prone to rupture with fatal consequences. AAAs (diameter >3cm) are present in ~4% of men aged >65years.

AAA formation is initiated with the loss of medial elastin. Responses to this include synthesis of tropoelastin and deposition of collagen. Dilatation occurs following degradation of this collagen, secondary to release and activation of matrix metalloproteinases (MMPs) by invading macrophages. Elastin is strengthened and protected from proteolysis by cross-linking.

Transglutaminases (TGs) introduce cross-links between protein chains and have been implicated in arterial repair; TG2 has been shown to be induced early in experimental aneurysm development. The literature suggests that TG2 and the homologous enzyme FXIII-A may act cooperatively or may compensate for each other in the face of deficiency.

We have bred $TG2^{-/-}$, $FXIII\text{-}A^{-/-}$ and $TG2^{-/-}.FXIII\text{-}A^{-/-}$ double knockout (DKO) mice to characterise their basal vessel structure and function and investigate their susceptibility to aneurysm formation.

This work has shown that both FXIII-A and TG2 are involved in the maintenance of basal vessel integrity and that aortic permeability is increased in mice lacking FXIII-A. In the absence of the repair function of TG2, the DKO mice develop extensive cardiovascular fibrosis and exhibit decreased vessel tension.

We have not seen evidence of a clear protective effect of TG2, however our DKO animals showed an (unexpected) decreased propensity to aneurysm formation. In an extended model there is evidence that aneurysm initiation and progression occur by different mechanisms and that TG2 plays a role in prevention of the latter. This thesis has also shown that TG2 and/or FXIII-A are not essential for vascular calcification.

The results presented here help to define the common and distinct functions of FXIII-A and TG2 in arterial structure and function, and provide evidence in their evaluation as potential therapeutic targets.

Table of Contents

List of Tables

List of Figures

Chapter 1: General Introduction

Chapter 1: General Introduction

This chapter discusses normal aortic physiology and elastogenesis and the pathology of aneurysmal disease. The various animal models of aneurysms are introduced and compared and an introduction is given to the key enzyme families related to this thesis; the transglutaminases (TGs) and the matrix metalloproteinases (MMPs).

The primary focus of this work pertains to the vascular biology and development of abdominal aortic aneurysms (AAA), which are discussed in detail in section 1.3. However, in summary, a AAA is a focal dilatation of the abdominal aorta to 1.5 times the normal diameter, or approximately 3.0 cm. The UK prevalence of AAA is ~4% in men and ~1% in women over the age of 65 (England, 2013) and the natural history of AAAs is to expand and eventually rupture. AAA rupture accounts for ~6000 deaths per year (Earnshaw et al., 2004) in the UK and mortality rates approach 90% if rupture occurs out of hospital and remain high (~41%) (Bown et al., 2002) even if the patient is transferred into a tertiary Vascular Surgery centre and intervention is undertaken.

Current guidelines recommend aneurysm screening, and all men in the UK are invited for a “one-off” abdominal ultrasound scan when they reach 65 years of age. Detection of aortic dilatation (diameter >3.0cm) by ultrasound (or by imaging for another reason) prompts regular surveillance and/or review by a Vascular Surgeon with the ultimate aim of repair at a threshold diameter of 5.5cm,(Moll et al., 2011) or when risk of intervention is balanced by risk of rupture. Repair is either by surgical replacement of the aneurysmal segment of vessel (using a prosthetic graft) or by endovascular insertion of a stent-graft, usually via a femoral approach. Both of these options have considerable potential complications and side effects, and patients with AAA have increased cardiovascular risk when compared with the normal population. It is obvious therefore, that medical treatments to prevent AAA development and/or slow progression would be of great therapeutic benefit to this high-risk patient population and are, at present, woefully lacking. This thesis will investigate the role of two transglutaminases (transglutaminase 2 (TG2) and (F)actor XIII-A) in the development of AAA and will discuss novel insights into AAA pathophysiology as well as directions for future research.

1.1 Aorta structure and function

1.1.1 Layers of the aortic wall

The human aorta is an elastic artery, with a large lumen relative to wall thickness, which acts as a conduit of blood from the heart to the muscular arteries. Its structure consists of three distinct layers (tunica adventitia, media and intima) with two elastic lamina (internal (IEL) and external (EEL)) which are differentially present and delineate the media from the intima and adventitia respectively (see Figure 1).

The tunica adventitia, or outermost layer, is composed of loose, irregularly organised connective tissue (collagen and elastin) with scattered fibroblasts and smooth muscle cells (SMCs). The adventitia is the location of the vasa vasorum; the network of small blood vessels that supply the aorta itself. This network is notably absent in the abdominal portion of the aorta which is comparatively thinner than the thoracic component and is reliant on the diffusion of nutrients for its metabolic needs.

In contrast to the irregularly organised adventitia, the aortic tunica media (0.5-2mm thick) contains abundant elastic fibres arranged into distinct fenestrated concentric lamellae interspersed with contractile SMCs; the so-called “lamellar unit”. In new born humans the aorta contains approximately 25 lamellar units, with this number rapidly increasing to 50-75 units as elastin is synthesised in response to changes in haemodynamic stress. This elastin structure, which comprises up to 50% of the dry weight of the aorta,(Rosenbloom et al., 1993) is complemented by an extracellular matrix (ECM) containing large amounts of collagen I and II as well as proteoglycans which impart strength and stiffness to the vessel. Indeed, these collagen fibres have been shown to be the main ECM component imparting tensile strength to the aortic wall.(Wagenseil and Mecham, 2009)

The tunica intima is separated from the media by the IEL and comprises an endothelial-cell lined luminal surface supported by a deeper connective tissue layer. The integrity of the luminal endothelial layer is particularly important to prevent the initiation of thrombus formation and atherosclerosis development but endothelial cells are also capable of synthesising elastin to contribute to the formation of the IEL. The sub-endothelial layer upon which the endothelium is situated is a supportive medium made up of collagen, elastin and an amorphous gelatinous structure known as “ground substance” which retains water and within which occasional fibroblasts and SMCs can be found.

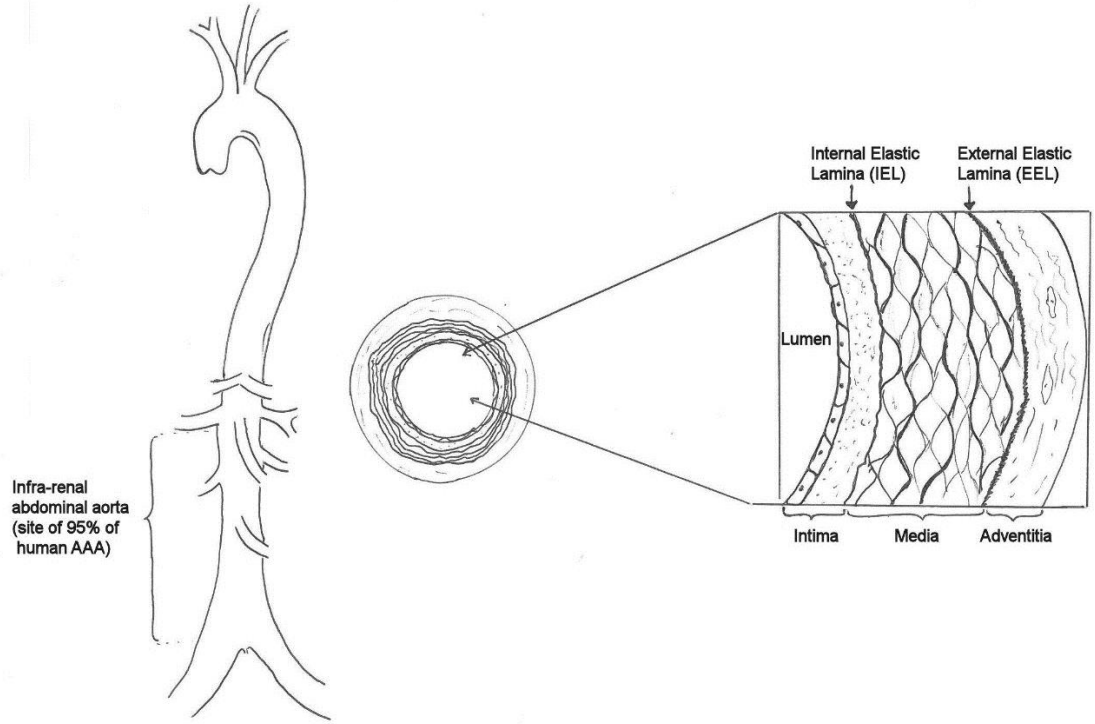

Figure 1. Structure of the aorta

Figure depicting the anatomy and structure of the aorta, highlighting the three distinct layers of the vessel wall; intima, media and adventitia. See text for further detail.

1.1.2 Elastin and the elastic fibre

Elastin is the ECM protein responsible for the elasticity of connective tissues including blood vessels, skin, lung and ligaments. In arteries, elastin allows vessels to stretch and absorb the force generated by ventricular contraction in systole. This stored haemodynamic energy is released during diastole such that a relatively high diastolic blood pressure is maintained and end-organ blood flow is more constant and less pulsatile in nature.

The elastin (*ELN*) gene is a single copy gene of 36 exons localised to chromosome 7 in humans (chromosome 5 in mice), the product of which is the 70kDa soluble protein tropoelastin which has a highly conserved structure of hydrophobic domains alternating with lysine cross-linking motifs.(Wagenseil and Mecham, 2009) Various isoforms of tropoelastin are generated as a result of alternative splicing of the primary transcript and gene expression is controlled by factors including insulin-like growth factor-1 (IGF-1) and transforming growth factor-β (TGF-β).

Occurring in the last third of foetal gestation in fibroblasts and SMCs, the process of elastin fibre formation, or elastogenesis (see Figure 2), is complex and begins with the binding of tropoelastin to a galactolectin chaperone protein called elastin binding protein (EBP) which prevents intracellular aggregation. Tropoelastin is then localised to the cell surface and is cross-linked following deamination and oxidation of its lysyl residues to allysine by lysyl-oxidase (Lox). This process is copper-dependent and mice with abnormal copper metabolism (Brophy et al., 1988) (the so called “blotchy” mouse) or Lox-deficiency (Maki et al., 2002) are unable to cross-link elastin and collagen and demonstrate a propensity to AAA development and tortuous aortas with thickened vessel walls. Histologically the aortas of these mice show fragmentation of the elastin fibres as expected, however they are limited in their usefulness because of systemic pathologies (including emphysema) and vessel rupture which occurs before, or soon after, birth.

The next stage of elastic fibre development requires the orientated immobilisation of tropoelastin onto a microfibril structure to facilitate the covalent cross-linking of tropoelastin to form the functional insoluble polymer. The highly cross-linked structure of elastin (15-20 cross-links per “unit”) results in its unique elastic recoil function and relative stability over the adult life span.(Wagenseil and Mecham, 2009) A number of proteins have been identified as components of this stabilising scaffold in arterial walls, including fibrillin-1 and microfibril-associated glycoprotein-1 (MAGP-1), both of which are substrates for TG2. TG2 also cross links tropoelastin to protease-inhibitors such as elafin (an elastase specific inhibitor, absent in mice), thus helping to protect the ECM from degradation.

Human AAA tissue has been shown to contain greater amounts of tropoelastin than normal arteries, (Minion et al., 1994) however these novel elastin fibres are disorganised with frequent discontinuities and reduced cross-linking.This so called “maturation arrest” of elastin may therefore be a key trigger in aneurysm formation. It is reasonable to suppose that TG2 may be up-regulated in an attempt to restore normal elastin structure and Munezane *et al* (Munezane et al., 2010) have shown increased mRNA expression of TG2 in experimental aneurysm formation in rats, possibly in response to increased tumour necrosis factor-α (TNF-α) activity. Our previous work has shown that TG2 is present in striated deposits in human aneurysmal tissue, interspersed between cellular tissue (Figure 3), and this project aims to help delineate the role of TG2 in 1) normal aortic elastin formation and 2) the structural and functional response to aneurysm induction.

Within the arterial wall, each layer of insoluble elastin is non-covalently associated with orientated collagen fibres and circumferentially arranged SMCs which together make up the lamellar unit. The importance of the lamellar unit structure was first recognised in 1967 (Wolinsky and Glagov, 1967) and the number of units found at a given anatomical site is directly proportional to the wall tension experienced at that site.(Clark and Glagov, 1985) Of note, there is a lower density of lamellar units found in the infra-renal segment (~25 units) of the human abdominal aorta when compared with the thoracic (55-60 units) and supra-renal regions,(Halloran et al., 1995) perhaps contributing to the significant predisposition of this site to aneurysmal dilatation.

Remodelling and fragmentation of elastin fibres occurs with increasing age,(Tsamis et al., 2013) and in certain disease states, and eventually leads to arterial stiffening because of a compensatory increase in collagen production. Elastin fibre assembly is essentially “turned off” in adult animals and hence collagen (which is >100 times stiffer than elastin) is produced instead to reinforce the arterial wall, which ultimately results in vessel stiffening.(Wagenseil and Mecham, 2012) This can be measured *in vivo* as an increase in pulse wave velocity (PWV) and is an independent predictor of cardiovascular risk and mortality.(Blacher et al., 1999) Calcification of elastin fibres (which occurs with increasing age and in atherosclerosis) and elastin cross-linking by advanced glycation end products (AGEs) (found with increasing age and in excess in Diabetes Mellitus) can also lead to arterial stiffening.(Aronson, 2003)

Elastin-derived peptides (EDPs) (including those released within human aneurysmal tissue) have important chemotactic roles and have been shown to be involved in the recruitment of endothelial and smooth muscle cells and inflammatory monocyte/macrophages.(Hance et al., 2002) These degradation products promote

proliferation of arterial SMCs via a complex tyrosine kinase-cytokine signalling cascade triggered by binding to the cell-surface elastin receptor,(Mochizuki et al., 2002) whilst in isolated SMC preparations proliferation is inhibited by the presence of soluble tropoelastin.(Karnik et al., 2003) Elastin is also required to maintain SMC quiescence and orientation (Li et al., 1998a) and *eln*-null mice die in utero or shortly after birth due to aortic obstruction secondary to excess SMC proliferation. These cells exhibit an abnormal longitudinal, rather than circumferential orientation, yet the mice show no evidence of endothelial damage, inflammation, ECM disruption, or haemodynamic stress, suggesting that it is the absence of elastin itself that results in this fatal phenotype.

The importance of elastin is further emphasised by study of the heterozygous $eln^{+/-}$ mice (Li et al., 1998b) which are viable with normal life expectancy, but have altered vessel morphology. These mice have approximately half the normal amount of elastin and as such their vessels show reduced compliance (i.e. are “stiffer”) with thinner elastic lamellae and a greater number of individual lamellar units. In order to maintain cardiac output in the face of increased vascular resistance these mice are hypertensive (Faury et al., 2003) and show varying degrees of cardiac hypertrophy and/or fatigue. The autosomal dominant condition Supravalvular Aortic Stenosis (SAS) is due to loss-of-function mutations in the elastin gene, elastin haploinsufficiency and decreased total elastin levels. Like the $eln^{+/-}$ mice, these patients are hypertensive with decreased aortic compliance and mortality from cardiac failure and, as in the mouse models, they reinforce the direct relationship between elastin quantity and phenotype severity.(Wagenseil and Mecham, 2012)

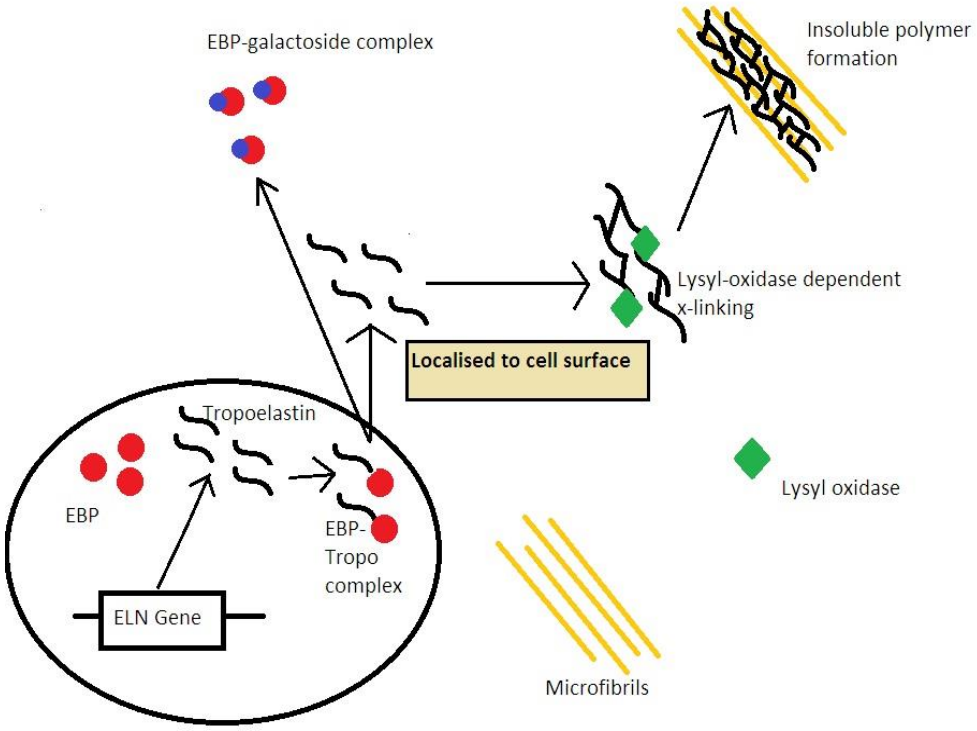

Figure 2. Elastogenesis

Schematic diagram outlining the main steps in the process of elastogenesis as described in detail in section 1.1.2 (adapted from Mithieux et al.)(Mithieux and Weiss, 2005). EBP = Elastin binding protein

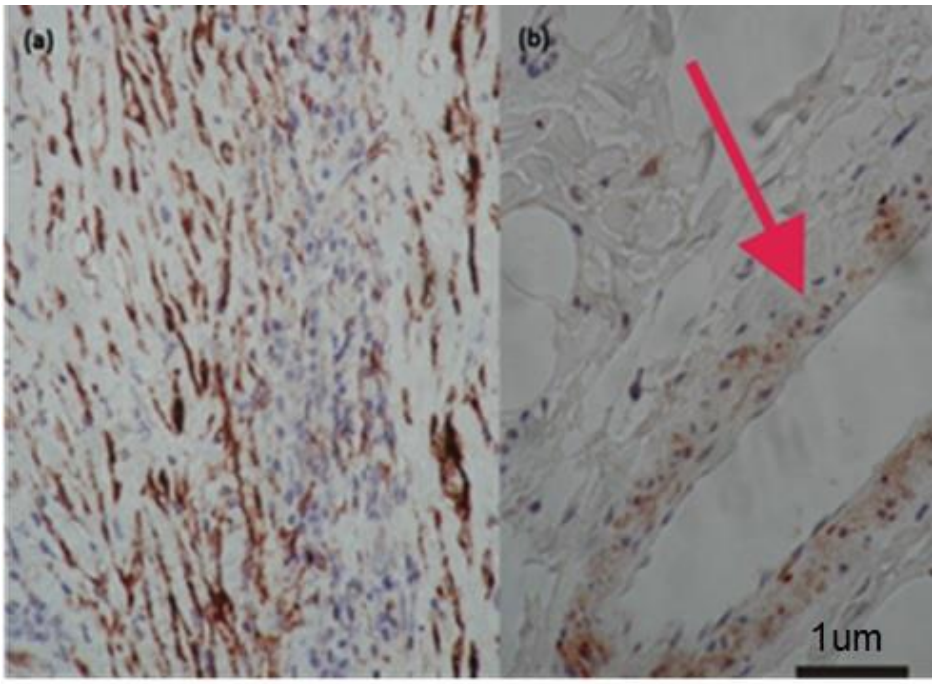

Figure 3. TG2 localisation in AAA tissue

Histological sections from human aneurysmal tissue. The DAB reaction product (brown) shows localisation of TG2 in striations **(a)** and capillaries **(b)** within the sample.

1.1.3 The microfibril

Microfibrils are small (10-15nm) fibrillin-rich filaments which appear in developing embryonic tissues prior to tropoelastin and form a stabilising scaffold onto which tropoelastin is localised to enable polymerisation and elastic fibre formation. Long thought to be structural molecules only, microfibrils are now recognised as having a number of diverse facilitative roles in growth factor signalling and cell-matrix interactions (particularly through their interaction with members of the TGF-β family) and Mecham *et al* have recently proposed the idea of the "microfibrillar niche" within which cellular phenotype and behaviour can be altered.(Mecham and Gibson, 2015)

Fibrillins are the primary component of microfibrils and consist of three (two in the mouse) ancient homologous glycoproteins with epidermal growth factor (EGF)-like domains interspersed with 8-cysteine domains. Aside from their role in elastin fibre assembly, fibrillins regulate the availability and activation of latent TGF-β (Kaartinen and Warburton, 2003) and other growth factors which (via Smad signalling) are involved in a host of cellular and developmental processes.(Ramirez et al., 2007) The signalling pathways of TGF-β are summarised in Figure 4 but essentially TGF-β is held in a latent form through binding to a latency associated peptide (LAP). Upon release, active TGF-β is able to bind its receptor, leading to receptor heterodimer formation, phosphorylation and downstream signalling through numerous "cross-talking" pathways. TGF-β availability is tightly regulated by components of the ECM and TGF-β signalling has been shown to inhibit the development of AAA and has been proposed as a potential therapeutic target (see (Wang et al., 2013b) for a review).

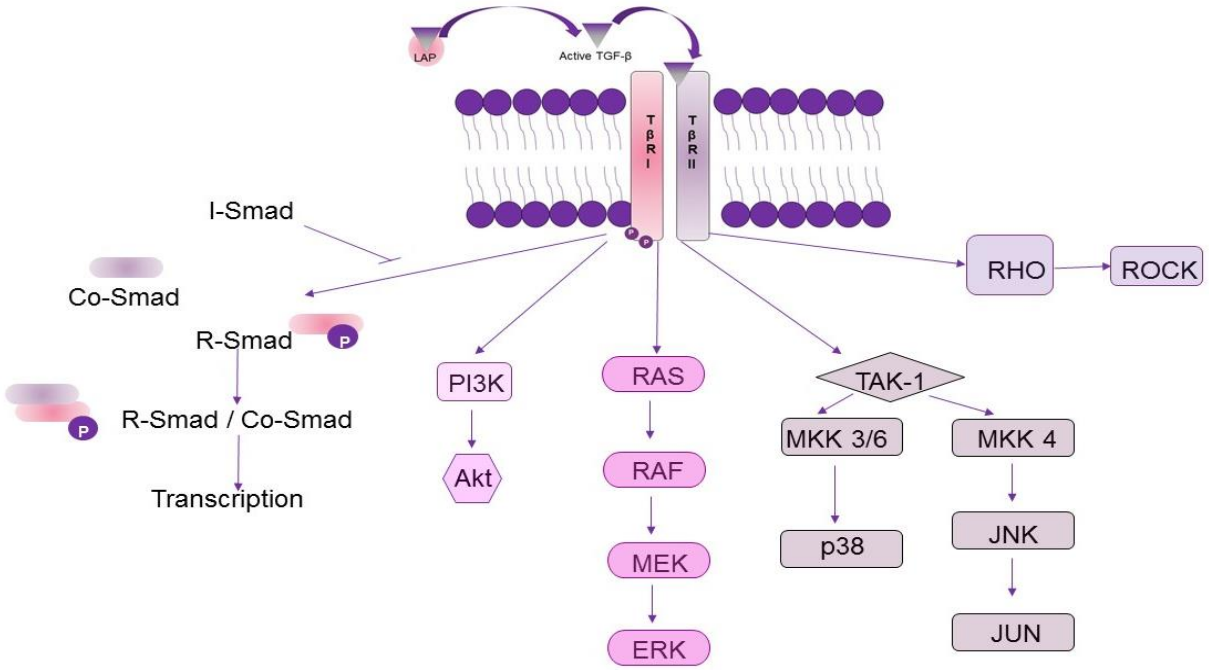

Figure 4. TGF-β Signalling

The TGF-β family of growth factors consist of three TGF-β isoforms, at least 4 TGF-β activins, at least 10 bone-morphogenic proteins (BMPs) and several growth factors. The TGF-β isoforms are held in an inactive state by a “latency associated peptide” (LAP) and, when released, bind to the TGF-β-receptor II (TβRII) and cause heterodimerisation with TβRI and phosphorylation. Downstream signalling is effected via a number of pathways including Smad signalling (with receptor-specific Smad (R-Smad) recruiting a common-mediator Smad (Co-Smad) before translocation of these complex to the nucleus where it mediates gene transcription), the PI3/Akt pathway, the RAS/Erk pathway, the Rho pathway and via TGF-β activated kinase-1 (TAK-1) signalling through mitogen activated kinases (MAPK). Through these various pathways (and their extensive crosstalk), TGF-β is able to influence cell survival, growth, migration and proliferation as well as multiple other cellular processes. TGF-β signalling has been shown to be downregulated in human AAA samples and TGF-β can inhibit AAA development and/or progression in various mouse models. See section 1.3.3 and Wang *et al* (Wang et al., 2013b) for further detail.

Due to its early and predominant expression in the developing mouse aorta it would seem that fibrillin-1 is the major player in elastic artery development and certainly *Fbn1*$^{-/-}$ mice die within a fortnight of birth from aortic aneurysms and complete diaphragmatic failure leading to impaired ventilation. In fibrillin-2 deficiency there is an absence of arterial pathology however Fbn1$^{+/-}$.Fbn2 $^{-/-}$ results in a more severe phenotype than Fbn1 KO alone and dual deficiency results in death in utero with little or no evidence of elastic fibre production in the aorta, suggesting an overlapping, compensatory, role for these two proteins.(Wagenseil and Mecham, 2009) In humans, missense mutations in the *Fbn1* gene give rise to an excess of TGF-β and the spectrum of cardiovascular, musculoskeletal and ophthalmic defects of Marfan syndrome; which include aortic root dilatation and its associated aortic valve regurgitation, aneurysm formation and dissection.

MAGP-1 is a small (20-30kDa) protein which is a component of almost all microfibrils, and is expressed in the aortic media at the surface of the elastic lamellae where it is able to facilitate cell-matrix interactions by binding various ECM molecules (including tropoelastin and collagen VI) as well as numerous growth factors. The MAGP-1 deficient mouse (Weinbaum et al., 2008) has revealed numerous potential functions of MAGP-1 including wound healing, haematopoiesis and fatty acid metabolism, although a number of reported phenotypes appear to be dependent on mouse genetic background and thus may not be truly reflective of the role of MAGP-1 in wild-type (WT) animals

Despite the constitutive presence of MAGP-1 in elastic vessels, the KO mouse shows no cardiovascular defect and MAGP-1 appears not to be required for elastin fibre assembly in mice. Of interest though is the increased thrombotic occlusion time (following laser injury of the carotid artery) and increased venous bleeding time seen in the MAGP-1$^{-/-}$ line.(Werneck et al., 2008) This persistent phenotype was independent of platelet or coagulation function and the mice showed no defect in vascular structure or evidence of hypertension. Given that MAGP-1 is a substrate for transglutaminase reactions (via its conserved “amine acceptor” glutamine at position 20) Mecham *et al* (Mecham and Gibson, 2015) hypothesise that these findings may be evidence of impaired interaction between the developing fibrin thrombus and constituents of the vessel wall, analogous to the stabilisation of fibrin by transglutaminase FXIII-A.

MAGP-2 is a 25kDa protein which is found exclusively in microfibrils and which shows similar matrix-binding properties to MAGP-1, although numerous studies have shown it to be a functionally distinct entity with important roles in angiogenesis,(Albig et al., 2008) tumour invasion and inflammation. Transgenic

mouse studies of MAGP-2 deficiency have not shown an essential role for this protein in elastic artery development despite recent genetic studies highlighting a loss-of-function mutation in the *Mfap-5* gene (encoding MAGP-2) as a cause of hereditary thoracic aortic aneurysm and dissection (TAAD) in humans.(Barbier et al., 2014) MAGP-2 KO mice are phenotypically relatively normal, without the multiple abnormalities shown by MAGP-$1^{-/-}$ mice, although both lines do show haematopoietic disturbances.(Combs et al., 2013) Of particular interest for this work is the observation that in double knockout of both MAGP-1 and MAGP-2, mice display spontaneous aortic dilatation (site not reported) at 6 months of age. This dilatation is not due to hypertension and is not associated with aortic dissection however it is age-dependent and suggests that MAGP-1 and -2 have overlapping roles in the establishment of vascular integrity and/or vascular remodelling, which require further study.

The fibulins are a group of 7 ECM proteins of which fibulins-1,2,4 and 5 are found in association with the (tropo)elastin core and/or the surrounding microfibril scaffold. Although their importance and function(s) are yet to be fully elucidated, mutations of the *Fbln1* gene cause loss of fibulin-1 (normally located within the elastic core of the developing fibre), defects in the integrity of small blood vessel endothelium and bleeding which ultimately leads to death soon after birth.(Kostka et al., 2001) Loss of fibulin-4 or -5, (McLaughlin et al., 2006, Nakamura et al., 2002) in contrast, gives rise to tortuous large blood vessels with interrupted elastin fibres and visible aggregates of elastin within the media.

EMILIN-1 or elastin microfibril interface located protein is a cysteine rich glycoprotein located at the interface between the supporting microfibril and the amorphous elastin core.(Wagenseil and Mecham, 2007) EMILIN-1 is expressed early in the development of the embryonic aorta and, in cell culture, antibodies to EMILIN-1 lead to the production of elastin aggregates rather than organised fibre formation.(Bressan et al., 1993) Insights from mouse models have revealed that EMILIN-1 is not essential for elastin fibre development, however KO mice display significant arterial hypertension when compared to WT littermates which is due to a generalised increased peripheral vascular resistance caused by arteries which are smaller in luminal diameter with thinner tunica media and irregular lamellae.

Some authors have suggested that as EMILIN-1 can bind both tropoelastin and fibulin-5 it likely acts as a bridging molecule during elastin fibre formation. Whilst this may be true, work by Zacchigna *et al* (Zacchigna et al., 2006) has shown that EMILIN-1 may regulate the availability of TGF-β by inhibiting the conversion of pro-TGF-β to the latent TGF-β complex; hence in the KO model excess TGF-β

signalling could lead to reduced cell proliferation and the impaired vessel growth exhibited by these animals. Further work is needed, but this example and others discussed above serve as a reminder that the ECM is not just a passive structural background but instead regulates growth factor availability and activation in ways that are only now being understood. As many of these ECM components are substrates for transglutaminase cross-linking, elucidating the role that TG2 (and other TGs) has in these various cellular processes will become increasingly important as new functions for the ECM are discovered.

1.1.4 Vascular collagens

Collagens are a group of 19 distinct proteins, 13 of which have been found within the vessel wall, that make up ~20% of the dry weight of the aorta and which are critical for vessel wall strength and integrity. Produced by vascular SMCs (VSMCs), as well as endothelial cells, macrophages and fibroblasts, collagens have a characteristic triple helical structure composed of 3 intertwined pro-collagen α-chains and are broadly classified as 1) fibrillar collagens, 2) non-fibrillar collagens and 3) network forming collagens.

Although a detailed discussion of collagen synthesis is beyond the scope of this work (see Prockop *et al*,(Prockop et al., 1979a, Prockop et al., 1979b) for an overview) there are many similarities with elastogenesis with a proline- and glycine-rich “pro-collagen” structure formed initially, prior to hydroxylation of proline and lysine residues and extracellularisation as tropocollagen. Tropocollagen is then crosslinked in a lysyl-oxidase dependent manner to form collagen fibrils which are bound together (with various glycoproteins and proteoglycans) to produce collagen fibres.

Within the aortic wall, type I collagen predominates and makes up 75% of the collagen content, with types III and IV (basement membrane collagen) also found in relative abundance.(Thompson et al., 2002) Collagen I and III form discrete bundles of fibrils 10-200nm in size which are found between the elastic lamellae and SMCs of the aortic media and as a loose mesh in the aortic adventitia. Biomechanical studies have shown that fewer than 10% of collagen fibres are circumferentially orientated at physiological pressures,(Wagenseil and Mecham, 2009) with this proportion rapidly increasing as pressures rise, more fibres are recruited, and the aorta becomes less distensible. This has particular relevance in AAA where the distended vessel is at the limit of mechanical strain that can be offset by elastin, and tensile strength is instead determined by the collagen contained within the vessel wall.(Thompson et al., 2002) The aged aorta contains a greater collagen concentration than that seen in developing or young vessels (~30% vs 20%) with

an increase in production occurring from middle age (Tsamis et al., 2013) and aneurysmal tissue contains greater amounts of collagen again (both in total and relative to diminished elastin) with increased turnover and synthesis.

Transgenic mouse studies and various genetic human disease states illustrate the importance of the collagen structure for the vasculature, as well as in skin, bone and other organ systems.(Wagenseil and Mecham, 2009) Mice with *Col1α1* mutations, for example, die in utero from vessel rupture whilst mutations in human *Col3α1* give rise to the autosomal dominant (type IV or vascular-type) Ehlers-Danlos Syndrome (EDS) with patients showing joint laxity, propensity to bruising without trauma (ecchymosis) and abnormal scarring. Sadly, however, this complex condition is often only diagnosed at presentation with life-threatening arterial rupture in early adulthood.

Collagen I is a potential substrate for TG2 and transglutaminase cross-linked collagen shows resistance to proteolysis and degradation *in vitro*.(Wang and Griffin, 2012) Various applications for TG2-collagen matrices have been proposed in bioengineering as cells seeded on these scaffolds show increased adhesion and proliferation when compared to seeding in non-cross linked collagen templates.(Chau et al., 2005) Conversely, excess TG2-mediated collagen crosslinking has been implicated in fibrosis (Johnson et al., 2003b) and the pathogenesis of abnormal wound scarring,(Verderio et al., 2004) diabetic nephropathy (Zsoldos et al., 2006) and atherosclerosis (Van Herck et al., 2010) where a loss of regulation by NO has been proposed as the mechanistic basis of TG2 over activity.(Telci et al., 2009) Clearly the potential links between aneurysm formation (with initial collagen synthesis and eventual insufficiency), collagen cross-linking (which increases resistance to breakdown) and TG2 warrant further investigation, as does the role of TG2 in the maintenance of normal arterial structure and function.

1.1.5 Smooth muscle cells

Vascular smooth muscle cells have been identified as a “key player” in aneurysm formation and VSMC apoptosis is a histological feature of human aneurysmal tissue, hence they will be discussed in brief below.

Originating from a number of embryonic sources (including the cranial neural crest and mesoderm in the case of the aorta)(Wagenseil and Mecham, 2009) arterial SMCs are the predominant stromal cells of the vascular wall and are found within the tunica media. Arranged in helical layers between elastic fibres, these cells are the source of ECM constituents during vascular development and following vessel injury when repair/regeneration is required. The primary function of VSMCs is

contraction, to enable regulation of blood vessel tone and thus systemic blood pressure and the adult (differentiated) phenotype of these cells have decreased proliferation rates and relatively little synthetic ability (Owens et al., 2004) but show high sensitivity to mechanical stress.

In contrast to most differentiated cells however, VSMCs retain phenotypic plasticity and are able to switch to a predominantly synthetic phenotype with high proliferative capacity. It is likely that these two “extreme” phenotypes actually represent opposing ends of a continuum of phenotypic profiles which can be assumed depending on local stimuli which may be acute (triggering ligand-receptor interactions) or more chronic (leading to epigenetic modifications).(Lacolley et al., 2012)

VSMCs are critical for the response to changes in pressure or strain experienced at the vessel wall. With raised blood pressure, for example, VSMCs sense “stretch” which triggers an increase in contractility (and tone) initially and then the coordinated process of hypertrophic inward remodelling to ultimately increase media:lumen ratio and restore normal stress levels.

Age-related changes in VSMC phenotype and function have been linked to arterial stiffness with VSMC hypertrophy and increased collagen production evident in the aortic wall. Important changes are also seen in VSMCs in aneurysmal tissue as VSMC density is reduced in the media of tissue samples from human aneurysms (Lopez-Candales et al., 1997) with evidence of p53 production and cell apoptosis.

Aside from their matrix producing capabilities, VSMCs can also recruit inflammatory cells via cytokine and chemokine release, synthesise proteases and are the primary source of inhibitors of tissue proteases (including the TIMP (tissue inhibitor of metalloproteinases) family and plasminogen-activator inhibitor-1 (PAI-1) amongst others). Numerous studies have shown that VSMCs constitutively express MMP-2 and can be induced to express MMPs 3, 7, 9 and 12 under conditions of stress (e.g. inflammation and vascular injury).(Curci, 2009) VSMCs could, therefore, potentially contribute to aneurysm pathogenesis by increased matrix degradation or by decreased inhibition of this proteolysis and/or reduced ECM synthesis.

Although the evidence in this area is conflicting, some authors hypothesise that aneurysmal VSMCs represent a unique sub-population of cells with a distinctive gene expression profile and enhanced elastolytic activity.(Airhart et al., 2014) It would be attractive to assume that such cells are different due to their mesodermal embryonic origin, and hence the infra-renal aorta shows a “regional predominance of cells with a differentiation bias towards matrix degradation”.(Curci, 2009) VSMCs certainly represent an important area for future study; key to this will be a clearer

understanding of the factors that influence and control VSCM phenotype “switching” or dedifferentiation. A number of signalling pathways have been implicated in dedifferentiation, including the PDGF/Akt1 and the β-catenin pathways, both have which have been linked to neointimal formation and re-stenosis following injury. A recent study by Nurminskaya *et al* in Baltimore (Nurminskaya et al., 2014) suggests that these pathways may be dependent on extracellular TG2, acting as a receptor agonist and/or a bridging molecule between signalling receptors, however further work is required to validate this proposed mechanism.

1.2 Matrix metalloproteinases

1.2.1 MMPs in general

The matrix metalloproteinases or MMPs are a family of structurally related endopeptidases which (among other functions) are able to catalyse the proteolytic breakdown of the extracellular matrix. Twenty-three distinct enzymes are recognised in humans,(Page-McCaw et al., 2007) which, although structurally and evolutionarily related, show diverse substrate specificity, enzymatic efficiency and tissue location. The structure of MMPs in general will be discussed briefly and then the key MMPs implicated in aneurysm pathogenesis will be introduced and their roles in cardiovascular disease outlined. An overview of the role of MMPs in AAA formation and development is given in section 1.3.4

The first member of the MMP family (MMP-1 or interstitial collagenase) was described in 1962 by Gross *et al* (Gross and Lapiere, 1962) in relation to the loss of the tadpole tail during normal metamorphosis. Subsequently, further enzymes were discovered which showed a similar three-domain structure with a conserved methionine residue and histidine bound zinc ion at the enzyme active site. These “metzincin” proteases have a characteristic structure which comprise a pro-peptide domain, a catalytic domain and a hemopexin-like C-terminal domain (Nagase et al., 2006) (Figure 5) and are synthesised (+/- secreted) in an inactive or pro-MMP form. The pro-peptide contains a conserved cysteine residue which interacts with the active site zinc ion, thus preventing the binding of an essential water molecule and inhibiting catalysis;(Nagase et al., 2006) MMP activation requires removal of this pro-peptide, usually as the first stage of a multi-step activation process (see (Visse and Nagase, 2003) for more detail). MMPs can also be activated without pro-domain cleavage by disruption of the zinc-cysteine bond, for example by reactive oxygen species (ROS) binding.(Van Wart and Birkedal-Hansen, 1990) The third, hemopexin-like, domain is joined to the catalytic domain by a flexible “hinge” region and has a “four-bladed-β-propeller” structure which determines substrate specificity

and is the site of binding of the endogenous inhibitors of MMPs, the TIMPs.(Page-McCaw et al., 2007)

The MMPs were initially named based on their observed function, location and substrate specificity however recently discovered MMPs do not fit neatly into this classification system and there is increasing evidence that some MMPs may straddle more than one group. These groups are summarised in Table 1 and are the collagenases, the gelatinases, the stromelysins, the matrilysins, the membrane-type MMPs (which are transmembrane or membrane-anchored proteins) and then those that fall outside these groups which include MMP-12 or macrophage metalloelastase.(Visse and Nagase, 2003) MMP activity is tightly regulated by an endogenous group of four inhibitors (TIMPs 1-4) which are wedge shaped molecules (Visse and Nagase, 2003) that form tight 1:1 complexes with the catalytic domain of the active enzyme. The TIMPs are able to inhibit the MMP family with varying efficiency depending on which enzyme-inhibitor relationship is studied and they are also able to interact with other proteases (including the ADAM and ADAMTS proteases) as well as components of cell signalling pathways (such as growth factor receptors and integrins).(Newby, 2012) As well as TIMP inhibition, MMPs are subject to regulation at a transcriptional level via cytokine signalling, by post-translational modification and by the action of other MMPs and serine proteases (such as thrombin and plasmin).(Yabluchanskiy et al., 2013) Hence, in health, MMP activity is tightly controlled and held in balance with its natural inhibitors. Upset of this balance, by whatever means, is implicated in numerous disease processes including cancer, arthritis, atherosclerosis, fibrosis and, of course, aneurysm formation.(Visse and Nagase, 2003)

MMPs do not *just* promote ECM breakdown and instead participate in a plethora of cellular processes. Some of these functions occur as a direct result of MMP action on ECM components which may, for example, produce biologically active cleavage fragments or release sequestered stores of growth factors, whereas other functions result from MMP interaction with non-ECM substrates which include cytokines, tyrosine kinase receptors, growth factors and other MMPs.(Page-McCaw et al., 2007) Given the vital processes in which MMPs participate it seems likely that knockout of these genes in transgenic mouse models would have devastating consequences. However, no reported MMP gene knock out has been shown to be embryonically lethal and most show remarkably mild phenotypes. This suggests that MMPs are either not required during embryonic development (which seems unlikely) or instead that there is a high degree of “enzymatic redundancy [and] compensation”(Page-McCaw et al., 2007) during development that allows for loss

of one member of the enzyme family without complete loss of function. This redundancy, along with the complex networks of interactions within which MMPs and TIMPs act, contribute to the difficulties in developing therapeutic modulators of MMP activity. These potential therapies are discussed by Newby in reference to the treatment of atherosclerosis and MI and would need to “target a specific adverse effect of MMPs whilst leaving intact essential physiological functions”.(Newby, 2015)

Subgroup	MMP	Name	ECM Substrate(s) (if known)
Collagenases	MMP-1	Collagenase-1	Col I, Col II, Col III, Col VII, Col VIII, Col X, Gelatin
	MMP-8	Collagenase-2 / Neutrophil Collagenase	Col II, Col III, Col VII, Col VIII, Col X, Aggrecan, Gelatin
	MMP-13	Collagenase-3	Col I, Col II, Col III, Col IV, Col IX, Col X, Col XIV, Gelatin
Gelatinases	MMP-2	Gelatinase A	Gelatin, Col II, Col III, Col IV, Col VII, Col X
	MMP-9	Gelatinase B	Gelatin, Col IV, Col V
Stromelysins	MMP-3	Stromelysin-1	Col II, Col IV, Col IX, Col X, Col XI, Gelatin
	MMP-10	Stromelysin-2	Col IV, Laminin, Fibronectin, Elastin
	MMP-11	Stromelysin-3	Col IV, Fibronectin, Laminin, Aggrecan
Matrilysins	MMP-7	Matrilysin-1	Fibronectin, Laminin, Col IV, Gelatin
	MMP-26	Matrilysin-2	Fibrinogen, Fibronectin, Gelatin
Membrane Type MMPs	MMP-14	MT1-MMP	Gelatin, Fibronectin, Laminin
	MMP-15	MT2-MMP	Gelatin, Fibronectin, Laminin
	MMP-16	MT3-MMP	Gelatin, Fibronectin, Laminin
	MMP-17	MT4-MMP	Fibrinogen, Fibrin
	MMP-24	MT5-MMP	Gelatin, Fibronectin, Laminin
	MMP-25	MT6-MMP	Gelatin
Others	MMP-12	Macrophage Metalloelastase	Elastin, Fibronectin, Col IV
	MMP-19	-	Aggrecan, Elastin, Fibrillin. Col IV, Gelatin
	MMP-20	Enamelysin	Aggrecan
	MMP-21	XMMP	Aggrecan
	MMP-23	CA-MMP	Gelatin, Casein, Fibronectin
	MMP-27	CMMP	-
	MMP-28	Epilysin	-

Table 1. Members of the matrix metalloproteinase family

Table showing a summary of the current knowledge about human matrix metalloproteinases, including the traditional classification system, MMP number, alternative names (if any) and information about known ECM substrates.
Col = collagen

1.2.2 Matrix metalloproteinase 2 (MMP-2)

Matrix metalloproteinase 2 is a 72kDa protein, also known as type IV collagenase or gelatinase A (reflecting its membership of the gelatinase sub-group of MMPs (see Table 1)), that is encoded by the *MMP2* gene at human chromosome locus 16q12.2. MMP-2 is able to degrade denatured collagen (gelatin) through binding at its fibronectin-repeat region which lies adjacent to the catalytic domain (see Figure 5) as well as degrading collagens IV, V and IX and laminin and, with less efficiency, collagens I and II.

MMP-2 is secreted constitutively from VSMCs and endothelial cells,(Galis and Khatri, 2002) however is inactive in non-diseased vessels, becoming upregulated and activated under conditions of stress, after injury, or with changes in stretch and haemodynamic flow.(Galis and Khatri, 2002, Newby, 2006) Although the mechanisms by which upregulation occurs are yet to be fully elucidated they are likely to be multifactorial and effected through various cell types and signalling pathways. For example; ROS produced by foam cells within atherosclerotic lesions can upregulate *MMP2* gene expression as well as activate latent pro-MMP2 complexed within the vessel wall,(Rajagopalan et al., 1996) an effect mitigated by overexpression of endothelial nitric oxide synthase (eNOS) to reduce ROS.(Gurjar et al., 1999) ROS also promote VSMC migration and proliferation (Papaharalambus and Griendling, 2007) (which is facilitated by MMP-mediated ECM breakdown), thus increasing the numbers of a cell type which produces MMP-2. This is just one example of the typical amplificatory cascades seen in MMP regulation and emphasises how important the fine balance between proteolysis and inhibition is in preventing pathology.

Although predominantly extracellular, there is increasing evidence that MMP-2 has important intracellular roles which are mediated through non-matrix substrates. In the cardiovascular system such substrates include α-actin, myosin light chain and troponin I found within myocytes (DeCoux et al., 2014) and the intracellular action of MMP-2 mediates the reperfusion syndrome seen after myocardial ischaemia.(Wang et al., 2002) Although the means by which MMP-2 is targeted to the cytosol are not yet fully understood, there are splice variants of *MMP2* which, when translated, would lack the ER signal sequence seen in the conventional form of the gene,(Ali et al., 2012) thus representing a presumed mechanism for specific targeting of the intracellular protease.

MMP-2 is activated by a unique mechanism whereby the latent form (pro-MMP-2) is secreted extracellularly and is recruited to the cell surface by a complex of membrane-type MMP-1 (MT1-MMP) and TIMP-2. An additional MT1-MMP

molecule (in close proximity within the cell membrane) is then required to cleave the pro-peptide of pro-MMP2 to generate the active form.(Lafleur et al., 2003) This process requires sufficient TIMP-2 (to generate the initial MT1-MMP.TIMP-2 complex) but an excess of TIMP-2 will bind and inhibit all available MT1-MMP and prevent pro-MMP2 activation, thus highlighting, again, the importance of balance between these proteases and their inhibitors. Crucially the activation complex described here is different from that formed during inhibition of active MMP-2 by TIMP-2 (Morgunova et al., 2002) hence the potential for specific modulation of MMP-2 activity.

Despite its multiple extra- and intra-cellular substrates, MMP-2 does not appear to be essential for any key developmental processes and MMP-$2^{-/-}$ mice are fertile and phenotypically normal although show smaller birth weights and slower growth rates when compared to WT mice.(Itoh et al., 1997) Mutations in human MMP-2 lead to a rare autosomal recessive form of multicentric osteolysis (Martignetti et al., 2001) characterised by bone resorption particularly in the hands and feet, suggesting that MMP-2 has a key role in bone formation and/or turnover.

Aside from its evidenced roles in AAA pathogenesis (see section 1.3.4) and ischaemia/reperfusion syndrome, MMP-2 has been implicated in other cardiovascular diseases such as atherosclerosis (MMP-$2^{-/-}$ mice show reduced atherosclerotic plaque formation in an apolipoproteinE (ApoE) deficiency model)(Kuzuya et al., 2006) and hypertension.(Azevedo et al., 2014) It also has a key role in angiogenesis or neovascularisation (van Hinsbergh and Koolwijk, 2008) both in normal development, and under pathological conditions of injury and tumorigenesis and MMP-2 is thought to be required for the “angiogenic switch” seen in many tumour types (see Bergers et al (Bergers and Benjamin, 2003) for a review). Interestingly TG2 has been shown to be a potential target of MMP-2 (and MT1-MMP)(Belkin et al., 2004) and there is a single report of TG2 regulating MMP-2 transcription (via CREB phosphorylation) in ovarian cancer cell lines,(Satpathy et al., 2009) perhaps suggesting a reciprocal relationship between the transglutaminases and the metalloproteinases which warrants further investigation.

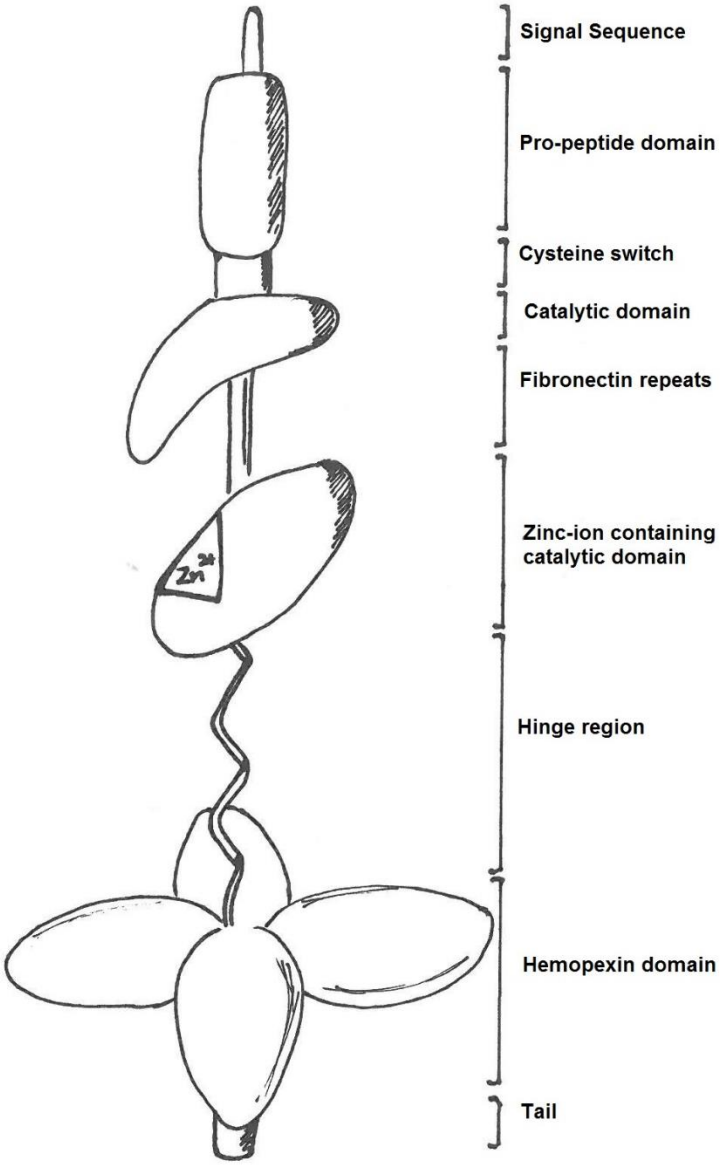

Figure 5. Structure of matrix metalloproteinase-2

Schematic showing three-dimensional structure of MMP-2 illustrating three key domains (pro-peptide, catalytic and hemopexin domains) common to all metalloproteinases as well as the fibronectin-repeat region which confers the ability of MMP-2 to bind gelatin. Image based on modification of (Sigma-Aldrich, 2016).

1.2.3 Matrix metalloproteinase 9 (MMP-9)

MMP-9 is a gelatinase of molecular weight 92kDa in the zymogenic form and 88kDa in the active form in humans. Also known as type IV collagenase, MMP-9 has a triple repeat fibronectin-like domain which, as in MMP-2, gives rise to its ability to bind gelatin for proteolysis. MMP-9 is secreted by a number of cell types including neutrophils, macrophages (particularly foam cells) and fibroblasts and is inhibited and bound to TIMPs -1 and -3 via its hemopexin domain prior to secretion.(Yabluchanskiy et al., 2013, Siwik et al., 2001) As previously discussed, there is increasing evidence that matrix metalloproteinases may be activated and function intracellularly although the evidence for this is limited with regards MMP-9.(Pereira et al., 2005)

Transgenic MMP-$9^{-/-}$ mice have been generated by Vu *et al* (Vu et al., 1998) by replacement of part of exon 2 and all of intron 2 of *MMP9* with a neomycin resistance cassette. These mice are fertile although pups show defects in bone development and impairment of vascularisation and ossification of cartilage, corresponding to the rare human condition of Metaphyseal Anadysplasia Type 2 (MANDP2) seen with homozygous loss-of-function mutation of *MMP9.*

A number of insights have been gained through the study of the MMP-9 KO mouse, particularly with regards the role of MMP-9 in cardiovascular pathology; MMP-9 is required for SMC migration and neointimal formation (Johnson and Galis, 2004) and contributes to the angiogenesis seen after femoral artery ligation in a murine critical limb ischaemia model.(Johnson et al., 2004) Mice deficient in MMP-9 show decreased atherosclerosis (Luttun et al., 2004) and MMP-$9^{-/-}$ animals show decreased rates of left ventricular rupture and ventricular dilatation following experimentally induced myocardial infarction (MI).(Ducharme et al., 2000) This change in cardiac re-modelling is thought to be due to decreased macrophage recruitment however increases in MMP-9 activity are also seen in cardiac fibroblasts subjected to oxidative stress (Siwik et al., 2001) and have been implicated in cardiac fibroblast migration and differentiation to a myofibroblast phenotype. Roles in embryo implantation, embryogenesis, immune cell functioning and nerve myelination amongst others have also been ascribed to MMP-9.(Yabluchanskiy et al., 2013)

As with all the MMPs, regulation of MMP-9 is complex and multifaceted, and includes transcriptional regulation, activation by other MMPs and by other proteases, regulation via cytokine (e.g. TNF-α and IL1β) stimulated signalling pathways and post-transcriptional modifications to confer mRNA stability.(Yan and Boyd, 2007) Many of the stimulators of MMP transcription signal via nuclear factor

kappa B (NFκB) and binding sites for this factor are seen in *MMP1*, *3*, *9*, *14* and *19* (Fanjul-Fernandez et al., 2010) although not yet reported within the *MMP2* gene. This differential expression of transcription-binding domains in functionally related proteases is discussed in (Yan and Boyd, 2007) and a detailed description of the genetic regulation of MMPs is given by Clark *et al*.(Clark et al., 2008) Given the complex nature of MMP-9 regulation and the fact that TG2 has been implicated in the induction of NFκB,(Lee et al., 2004) it is perhaps not surprising that there are reports of TG2 activity influencing MMP-9 expression via this (Lin et al., 2011) and other intermediates (Ahn et al., 2008) in cancer cell lines; whether this relationship is borne out *in vivo* remains to be seen.

1.2.4 Matrix metalloproteinase 12 (MMP-12)

MMP-12, also known as macrophage metalloelastase, is a 54kDa protein encoded on chromosome 11 in humans. MMP-12 is induced in response to injurious stimuli (such as cigarette smoke) and is found only at low levels in health, being primarily expressed by inflammatory macrophages (although also osteoclasts and chondrocytes). Despite its pseudonym, MMP-12 has multiple ECM substrates in addition to elastin, including fibronectin, collagen IV and laminin, and its protease activity is crucially important for normal macrophage migration and emigration through the basement membrane.(Shipley et al., 1996)

The catalytic form of MMP-12 is produced by cleavage of the pro-domain and a mature (22kDa) form is also seen following subsequent cleavage of the hemopexin domain.(Nar et al., 2001) Like the other MMPs, MMP-12 expression and activation is tightly regulated and can be initiated by numerous pathways including the plasmin/thrombin-PAR-1 (protein activated receptor 1) cascade, TNF-α signalling and via interferon-γ (IFN-γ) released from circulating lymphocytes.(Houghton, 2015) Complete deficiency of MMP-12 (Shipley et al., 1996) results in offspring that are phenotypically normal and show conventional development, however, litter sizes in this line are reduced by as much as 60%. In human pregnancy, placental macrophages express MMP-12 during the first trimester (Harris et al., 2010) when it is thought to have a role in vascular remodelling and maintenance of blood flow to the developing foetus; MMP-12 deficiency presumably therefore results in placental abnormalities which are unable to sustain normal litter sizes.

Much of the evidence about MMP-12 function and regulation has been generated from the study of cigarette-smoke-induced lung injury in murine models of emphysema since; 1) inherited deficiencies of alpha-1-antitrypsin (an inhibitor of *neutrophil* elastase) lead to early-onset emphysema, and 2) MMP-$12^{-/-}$ mice fail to develop lung destruction in this model.(Hautamaki et al., 1997) Emphysema is one

of the disease entities seen under the umbrella of chronic obstructive pulmonary disease (COPD) which results in over 25,000 deaths each year in Great Britain (Executive, 2015) and (in emphysema) results in enlarged bronchiolar and alveolar air spaces due to destruction of the elastin walls of these structures, ultimately causing impaired ventilation and oxygenation. The role of MMP-12 in emphysema is complex but involves direct elastolysis of pulmonary constituents, production of a chemotactic gradient (MMP-12 recruits inflammatory macrophages and neutrophils to sites of injury), and production of EDPs which are themselves chemotactic to macrophages.(Houghton, 2015) MMP-12 can also degrade alpha-1-antitrypsin (α1AT) (Nar et al., 2001) - removing its potent inhibition of neutrophil elastase - and facilitate TNF-α release, thus potentiating an inflammatory cascade which ultimately results in disease.

Aside from its role in emphysema, MMP-12 also has a physiological function in host defence both through a direct bactericidal action of the C-terminal domain on bacterial cell walls (Houghton et al., 2009) and via its regulation of IFN-γ in response to viral infection.(Dandachi and Shapiro, 2014) In the cardiovascular system, MMP-12 is involved in the control of angiogenesis by generating angiostatin (from plasminogen) (Dong et al., 1997) which is a specific and highly effective inhibitor of angiogenesis (and hence tumour growth and metastasis) *in vivo* (Sang, 1998) and MMP-12 has also been implicated in the VSMC mediated arterial stiffening seen with age or vascular injury,(Liu et al., 2015) and atherosclerosis.(Liang et al., 2006) Its role in aneurysm formation is discussed in section 1.3.4. Clearly MMP-12 represents a potential therapeutic target for the treatment of chronic lung diseases but its multiple actions in this, and other, organ systems will need to be better understood before its potential can be realised.

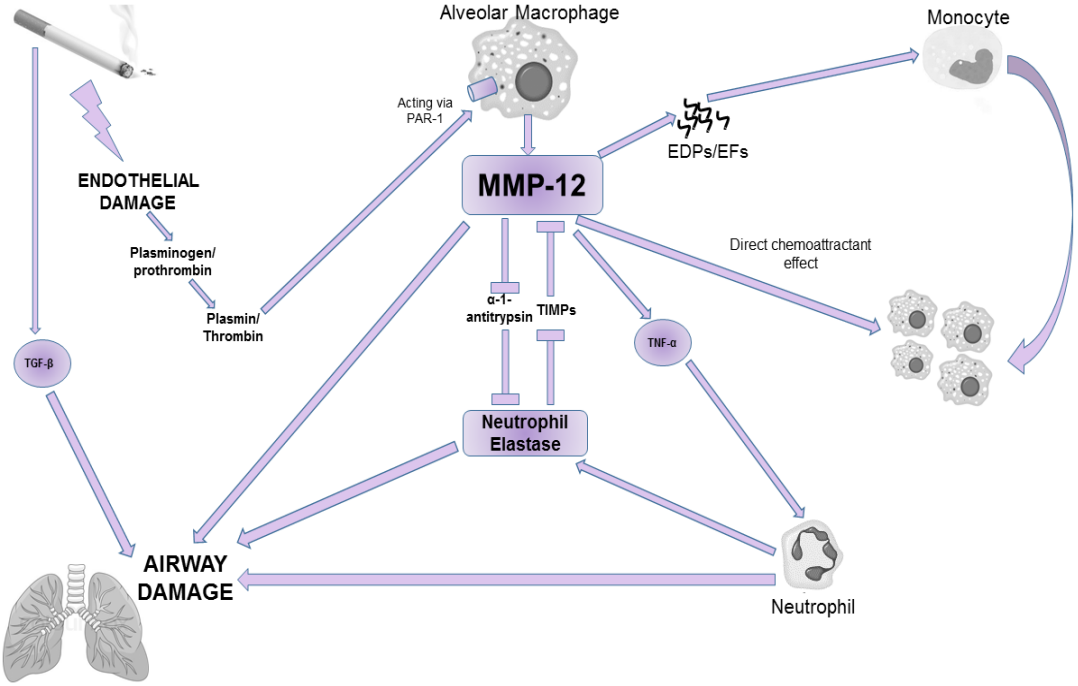

Figure 6. Role of MMP-12 in emphysema

Schematic showing some of the multiple mechanisms by which MMP-12 (predominantly released from inflammatory macrophages) facilitates the bronchiolar and alveolar elastin wall damage seen in emphysema. MMP-12 is both directly chemoattractive to inflammatory cells and also generates elastin degradation products (EDPs) or elastin fragments (EFs) which recruit monocytes and macrophages to the site of injury. MMP-12 can also cleave α-1-antitrypsin, thus removing the inhibition of neutrophil elastase which can cause damage directly or via inhibition of TIMPs. Endothelial damage promotes MMP-2 production via the action of plasmin/thrombin acting via protein activated receptor-1 (PAR-1).

1.2.5 Tissue inhibitors of metalloproteinases (TIMPs)

MMP activity is regulated (amongst other mechanisms) by TIMPs 1-4. These proteins are highly evolutionarily conserved and inhibit MMP catalytic activity by chelation of the active site zinc molecule via a conserved cysteine residue in the N-terminal domain of the TIMP.(Visse and Nagase, 2003) The TIMPs, which are 21-29kDa in size, show different affinities for the various MMPs, with TIMP-3 – a membrane bound TIMP – having the broadest action and TIMP-1 the most restrictive.(Brew and Nagase, 2010) As well as MMP-inhibition, the TIMPs (and particularly TIMP-3) are also capable of inhibiting the activity of the ADAM and ADAMTS proteases,(Newby, 2012) can affect pro-MMP activation, and they have a number of identified MMP-independent functions. These include promotion of cell growth, suppression of cell growth and anti-angiogenesis and anti-apoptotic activity.(Brew and Nagase, 2010)

As shown by the complex nature of MMP activity, it is unlikely that TIMPs act in a uniquely MMP-dependent *or* MMP-independent fashion, instead displaying multiple actions simultaneously. For example; in angiogenesis, by inhibiting MMP-mediated breakdown of the ECM, TIMPs can influence the migration of endothelial cells and subsequent sprouting and tube formation preceding new vessel development.(van Hinsbergh and Koolwijk, 2008) Concurrently, TIMP-2 acting via the MAPK signalling pathway (Feldman et al., 2004) can inhibit endothelial cell proliferation and migration whilst direct binding of TIMP-3 to vascular endothelial growth factor (VEGF) can prevent the interaction of this growth factor with endothelial cells,(Qi et al., 2003) thus limiting its angiogenesis promoting effects. Similar coordinated networks of action can be seen in the nervous system (Jourquin et al., 2005) which requires neuronal turnover and differentiation to facilitate learning and memory, and in the inflammatory system.

Mouse models of TIMP deficiency have contributed to evidence of the above, as well as additional important roles of TIMPs in development. However, single-TIMP deficient mice are viable and fertile (Page-McCaw et al., 2007) and show no obvious compensatory upregulation of other TIMPs. TIMP-$3^{-/-}$ mice primarily show features of “unbalanced matrix degradation”(Brew and Nagase, 2010) with development of spontaneous emphysematous change in the lungs, dilated cardiomyopathy and age-related arthritis, thus confirming its broad inhibition of ECM proteolysis. Specific roles within the cardiovascular system have been identified for TIMP-1 in relation to cardiac remodelling and atherosclerosis (TIMP-$1^{-/-}$ mice show reduced atherosclerosis (Silence et al., 2002) with more stable, more

calcified plaques (Orbe et al., 2003)) and several studies have investigated the role of TIMPs in abdominal aortic aneurysm formation and progression.

The relationship between MMPs (and other proteases) and TIMPs (and other protease inhibitors) is finely balanced and targeted modulation of this balance may allow the development of novel therapies for a number of pathological conditions (see (Newby, 2012) for a review in vascular diseases); it is important, however, that the effects of these proteins outwith their traditional ECM roles are fully elucidated and understood in order that the potential side effects of such therapies are mitigated without causing harm.

1.3 Abdominal aortic aneurysms

1.3.1 General pathology, epidemiology and clinical course

An abdominal aortic aneurysm or AAA is the term given to a localised increase in diameter of the abdominal aorta; the blood vessel supplying the abdominal viscera which commences at the level of the diaphragm and terminates at its bifurcation into the iliac vessels at the L4 vertebral level.(Feller and Woodburne, 1961) The normal aorta measures approximately 2.0cm in diameter and aneurysmal dilatation is classified as an increase in size by 50% of normal. Such dilatation is often diagnosed incidentally on imaging or examination for another presenting complaint and is increasingly discovered in England through the NHS AAA Screening Programme (NAAASP) which was established nationally in 2014 and offers “one-off” ultrasound imaging of the abdomen to all men over the age of 65.

AAA Diameter (mm)	12-month Rupture Risk (%)
30 – 39	0
40 – 49	1
50 – 59	1 – 11
60 – 69	10 – 22
>70	30 – 33

Table 2. Annual rupture risk by AAA diameter

From the European Society for Vascular Surgery (ESVS) AAA Guidelines 2011 (Moll et al., 2011)

The prevalence of detected AAA in the screening programme has been much lower than predicted (just 1.4%)(NAAASP, 2014) – due predominantly to a reduction in the “lifestyle” related risk-factors of AAA such as smoking and an increased population use of cardiovascular (CV) preventative medications such as anti-hypertensives and statins. Despite this, the NAAASP is cost effective (Glover et al., 2014) because of the potential fatal consequences of AAA which, if left unchecked,

will continue to increase in size and eventually rupture. As discussed earlier, mortality rates from aneurysm rupture are high whether rupture occurs with (41%)(Bown et al., 2002) or without (90% out-of-hospital mortality)(Earnshaw et al., 2004) intervention and hence patients with AAA are closely monitored with serial imaging and offered repair when the risk of intervention is balanced by the risk of rupture (Table 2).

AAA disease is estimated to cost in excess of $3 billion per year in the United States,(Go et al., 2013) and much of this cost is associated with either aneurysm repair itself (either surgical graft repair or endovascular with stent-device insertion) or with the complications of intervention. Complications from open surgical repair can be considerable and range from minor wound problems through to bowel ischaemia, organ failure and death (mortality rate 3-10% depending on population) whilst endovascular repair has a not insignificant risk of kidney injury, graft failure and need for re-intervention. Given that the risk factors for AAA are also those that increase risk of all cardiovascular disease it is easy to see why this population represents a co-morbid group which is at high risk of complications, and specifically post-intervention cardiovascular events such as stroke and MI. Clearly, therapeutics that could either stop aneurysm development or, more likely, slow progression after early detection, would be incredibly valuable and would have huge potential benefit in reducing morbidity and mortality in this population.

Although aneurysms do form at other sites in the vascular tree, the abdominal aorta is unique in terms of the frequency of aneurysm development and the fact that 90% of aortic aneurysms are located infra-renally (i.e. below the origin of the renal arteries). The aorta is a non-uniform structure with distinct regions (Tsamis et al., 2013) which have differing embryological origins and which are subject to vastly different haemodynamic forces. The abdominal aorta, for example, has a mesodermal origin (with the ascending aorta and arch formed from neural crest cells), has an elastin:collagen ratio which is lower than the thoracic aorta (Ailawadi et al., 2003) and is exposed to pulse wave reflections from the aortic bifurcation which increase relative pressure at this site.(Dua and Dalman, 2010) These and other anatomical and structural observations, such as the lack of vasa vasorum and the reduced elastic lamellar density have all been proposed as factors predisposing to aneurysm development in the abdominal portion of the aorta. There are also striking differences between AAA and the thoracic counterpart (TAA) which tend to occur in younger patients with a strong family history (as much as 20%) and no clear male predominance. Clearly these differences require investigation but the

extent to which these factors can be modified is obviously minimal and hence their relative importance in the pathogenesis of aneurysmal disease is, as yet, unclear.

As mentioned, there are a number of clear risk factors for AAA which include smoking, hypertension, hypercholesterolaemia, increasing age and male gender. Of these, smoking has been shown to be the most important risk factor with a greater influence than is seen in either stroke or coronary heart disease.(Lederle et al., 2003) As well as increasing incidence of AAA, cigarette smoke also promotes aneurysmal growth (Brady et al., 2004) and rupture in a dose-dependent manner, with both amount and duration of exposure being important parameters of risk. The mechanism(s) underlying this association are not clear but may include epigenetic modification of genes such as *5-LO* involved in inflammation,(Krishna et al., 2010) effects on the inflammatory cell infiltrate seen in the aneurysmal wall, as well as direct effects of cigarette smoke on VSMC proliferation and survival.

In contrast to the effects of smoking, there is an inverse relationship between the presence of Diabetes Mellitus (DM) and aneurysm development, expansion and rupture; with patients with DM having an odds ratio (OR) of AAA diagnosis of 0.75 in a study of over 3 million individuals.(Kent et al., 2010) Again, the mechanisms behind this relationship are unclear but may include the ability of AGEs to induce protective collagen cross-linking with the aortic media.(Lederle, 2012) By studying populations with significantly increased or decreased AAA risk we may be able to elicit some of the mechanisms involved in pathogenesis but the fact that AAA disease is seen both in patients who have never smoked and in patients with severe diabetes is evidence of the multifactorial nature of this condition. Indeed, despite extensive research, the pathophysiology of aneurysmal disease remains poorly understood and it is becomingly increasingly evident that the factors that initiate aneurysm development may be very different from those that lead to disease progression and eventual rupture.(Thompson et al., 2002)

1.3.2 ECM breakdown and atherosclerosis

Whereas initial theories pointed to atherosclerosis as the causative lesion in aneurysmal disease (because of the almost universal finding of atherosclerosis in the walls of AAA),(Dobrin, 1989) this has not been borne out by recent studies and one current theory regards AAAs as a localised presentation of a systemic disease of the vasculature.(Nordon et al., 2009)

Atherogenesis and aneurysmal disease, although similar, have key differences in terms of risk factors, response to therapy and genetic predisposition.(Newby, 2012) The discrepancy between smoking status and risk of AAA vs athero-occlusive disease has been discussed and clearly the identification of DM as a negative risk

factor for AAA points to a different pathogenic mechanism than that seen in atherosclerosis and strongly suggests that these two conditions are distinct disease entities. Likewise, animal models have demonstrated that therapies effective against atherosclerosis have little or no effect in terms of aneurysm development (Golledge et al., 2010) and that the atherosclerosis seen in aneurysms develops as a consequence of altered flow, rather than occurring prior to dilatation. If atherosclerosis did precede vessel expansion it would be expected that severity of atherosclerosis would correlate with AAA development; this relationship is not seen in large cohort studies and the reverse is also not true, as anatomical sites that are prone to the atherosclerosis (such as the superficial femoral artery (SFA)) are not common sites for aneurysm development.(Norman and Powell, 2010)

Rather than a localised disease, some have suggested that AAA represents a single manifestation of a more generalised pathology (Nordon et al., 2011) with increased MMP-2 levels at remote vascular sites (Goodall et al., 2001) and venous abnormalities including reduced elastin content.(Goodall et al., 2002) Whilst the causes of such systemic pathology are unknown, the histological manifestations of aneurysms are clear. AAAs are characterised by alterations in the arterial media and adventitia that include medial thinning, disruption and loss of elastin,(Campa et al., 1987) a decreased elastin to collagen ratio,(Mesh et al., 1992) disordered ECM remodelling and loss of VSMCs.(Alexander, 2004)

This elastin breakdown or elastolysis may be triggered by a number of factors but is then potentiated by chronic inflammation (predominantly T-cells) resulting in an imbalance between proteolysis and normal proteolytic inhibition.(Knox et al., 1997) Although the initiation of AAA formation is therefore loss of elastin, the arterial dilatation, progression (and subsequent rupture), is thought to occur when collagen deposition (which reinforces the arterial wall)(Berillis, 2013) is outweighed by collagen degradation. Newby has described a “multi-stage initiation and destabilisation paradigm for aneurysm growth and rupture”(Newby, 2012) which we attempt to summarise in Figure 7. Clearly, a greater understanding of this paradigm is required, as is the ability to identify patients at risk of entering, or at the early stages of this process and, crucially, an ability to manipulate this ECM destruction to prevent the vicious cycle of AAA expansion, increased wall stress (Dobrin, 2000) and eventual rupture.

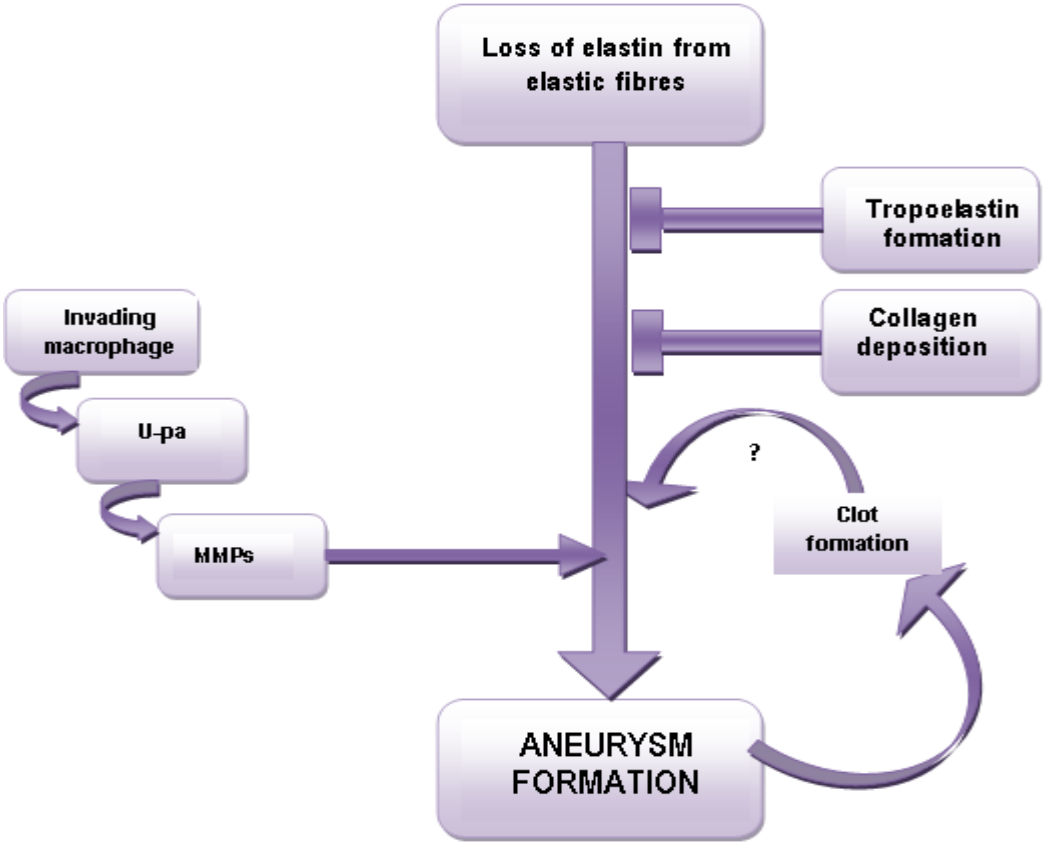

Figure 7. Pathogenesis of AAA

Schematic of AAA pathogenesis emphasising the importance of elastin loss in initiating and potentiating aneurysm development. The cartoon illustrates the crucial role of invading inflammatory cells and matrix metalloproteinases (MMPs) in the breakdown of the extracellular matrix (ECM). Novel tropelastin formation and collagen deposition both occur as a compensatory response to elastin loss and dilatation occurs when collagen degradation exceeds deposition. The role of the intraluminal thrombus (ILT) in aneurysm progression is controversial.
U-pa = urokinase type plasminogen activator

1.3.3 Inflammation and aneurysm pathogenesis

The histology of aneurysmal disease is well characterised and is typified by an intense inflammatory cell infiltrate composed predominantly of macrophages and lymphocytes.(Freestone et al., 1995) Inflammation is therefore reported to be key to aneurysm pathogenesis, although this view is challenged by single reports of rapid aneurysm expansion in immunosuppressed individuals.(Lindeman et al., 2011) Certainly it appears that inflammation is triggered by elastin breakdown (Hance et al., 2002) and that recruited inflammatory cells produce both inflammatory cytokines and ROS (Miller et al., 2002) (thus potentiating an inflammatory cascade) as well as being the source of the MMPs which facilitate further ECM degradation.

In 2010 Wang *et al* showed that monocytes are likely to be a key regulator in the inflammatory process seen in aneurysms. They generated mice with clodronate-depleted monocytes and saw a dramatically reduced incidence, severity and rupture rate of AAA generated using the Angiotensin II (AngII) experimental model.(Wang et al., 2010) Likewise deficiency of certain chemokine receptors (CCR2)(Daugherty et al., 2010, Moran et al., 2013) usually involved in macrophage recruitment, and factors involved in macrophage lineage differentiation (e.g. MyD88)(Owens et al., 2011) have also been shown to reduce aneurysm formation in various murine models.

Xiong *et al* reported that CD4+ T-cells, the most predominant lymphocyte present in aneurysms, are required for AAA development in the calcium chloride ($CaCl_2$) murine model (Xiong et al., 2004) and T-helper subtypes Th1, Th2 and Th17 have all been shown to be increased in human and AngII induced aneurysms (see Dale *et al* (Dale et al., 2015) for a review). Interestingly the role of B-cell lymphocytes has been less well investigated although some authors have hypothesised that AAA development represents an autoimmune process and various auto-antigens (including AAAP-40 and CA1) have been proposed as triggers for lymphocyte activation, stimulation of the complement system and further inflammation.(Zhang and Wang, 2015)

Given that early aneurysms show a relative paucity of inflammatory cells (Freestone et al., 1995) it is likely that those that are present (possibly neutrophils (Tilson, 2005)) are crucially important in aneurysm pathogenesis. Targeting cell recruitment and signalling at this early stage could be a realistic strategy in preventing AAA initiation as, at a later stage, when these cells are present in any significant number, the “tipping point” of AAA development could already have been reached.

In view of the important role of inflammation in aneurysm progression it is unsurprising that several inflammatory chemokines have been reported to be critical

in aneurysm development in both animal experiments and in human studies looking at cytokine levels in aneurysm samples. As previously noted, however, these samples reflect end-stage disease and the extent to which results can be extrapolated to the early phases of AAA development are unclear. Several of the interleukin family members (including IL-1β, and IL-6) have been shown to be increased in aneurysm tissue relative to control (Abdul-Hussien et al., 2010, Harrison et al., 2013) and patients with AAA have increased circulating plasma IL-1β levels.(Juvonen et al., 1997) In a murine elastase model of AAA induction, Johnston *et al* showed that IL-1β depletion (or inhibition of its receptor) prevented aneurysm development.(Johnston et al., 2013)

TNF-α, a key inflammatory chemokine released by T-cell lymphocytes initially and then by macrophages, has also been shown to be upregulated in the plasma of AAA patients (Juvonen et al., 1997) and Xiong *et al* showed that TNF-$\alpha^{-/-}$ mice failed to develop aneurysms in a $CaCl_2$ model and infliximab (a TNF-α antagonist) also blocked formation.(Xiong et al., 2009) Unfortunately infliximab treatment failed to prevent aneurysm development if given *after* the injury model had been undertaken and failed to prevent aneurysm growth once established. These results have also not been replicated in the AngII aneurysm model and hence their relevance to clinical practice is uncertain.

One cytokine that has attracted a lot of interest in the aneurysm field is TGF-β and many leading researchers have attested to the importance of this signalling protein. Wang *et al* (Wang et al., 2013b) summarise the literature with regards TGF-β and AAA but essentially TGF-β is thought to decrease inflammatory cell infiltration (and thus MMP activity and ECM breakdown), decrease VSMC apoptosis and even enhance the production of ECM components by VSMCs and fibroblasts.(Newby, 2012) In animal models TGF-β inhibition has been shown to augment AngII induced AAA (with increased VSMC death and elastin fragmentation),(Wang et al., 2010) whilst overexpression of TGF-β can stabilise pre-existing experimental AAA (Dai et al., 2005) and protect against AAA rupture. Various single nucleotide polymorphisms (SNPs) in genes encoding TGF-β forms and their receptors have been reported in genetic studies of AAA populations, although many of these appear to be important only in concert with other SNPs or in the presence of additional risk factors.(Wang et al., 2013b) TGF-β signalling is downregulated in human AAA (Biros et al., 2012) and hence represents an important potential target for study; both in terms of the downstream effects discussed here but also because of the ability of TGF-β signalling to upregulate TG2 transcription (Ritter and Davies, 1998) (see section 1.4.1) in response to cellular stress.

1.3.4 MMPs and aneurysm pathogenesis

Matrix metalloproteinases, and specifically MMP-2, -9 and -12, have been implicated in the breakdown of the ECM in AAA and are released and activated (via uPA and plasmin) by invading macrophages. As the damaged vessel wall dilates, intraluminal thrombus is laid down which may drive further expansion (although this remains controversial) by aggregating platelets, “trapping” cells and thereby acting as a source of secreted proteases.(Fontaine et al., 2002) Whilst much research has focussed on the inflammatory nature of aneurysmal disease (Duftner et al., 2006) the ability to strengthen elastin and protect it from degradation could prevent the initiating event in the pathway detailed in Figure 7 and thus provide a therapeutic target for aneurysmal disease.

A pathway for the time course of MMP production and activity in aneurysms can be constructed from the literature; with tissue obtained from early aneurysms showing a relative paucity of inflammatory cells and elastin destruction associated with MMP-2 produced from VSMCs.(Freestone et al., 1995) In line with the known mechanism of activation of MMP-2, TIMP-2 and MT1-MMP are also present but MMP-9 is notably absent from AAA samples at this stage of disease. MMP-2 KO mice do not develop $CaCl_2$-induced AAA (Longo et al., 2002) and likewise deficiency of TIMP2 leads to a decrease in AAA formation, probably via a decrease in MMP-2 activation.(Xiong et al., 2006) Transplant of WT macrophages into these mice does not return aneurysm formation to control rates, emphasising that the likely source of MMP-2 is VSMCs rather than inflammatory monocyte/macrophages.(Keeling et al., 2005)

Additional MMPs are then thought to be recruited by a combination of inflammation +/- angiogenesis (Tedesco et al., 2009) and activated MMP-3 and -9 are present in aneurysmal aortas in contrast to non-dilated samples. Silence *et al* reported that MMP-$3^{-/-}$. $ApoE^{-/-}$ double knockout mice show decreased AAA formation but persistent atherogenesis, adding weight to the argument that atherosclerosis and AAA are divergent processes, but also suggesting that MMP-3 may cause medial degeneration, either directly or via activation of MMP-9.(Silence et al., 2001)

MMP-9 expression is increased 12-fold in patients with aneurysms vs. control subjects (Tung et al., 2001) probably due to both increased production by VSMCs and release from infiltrating macrophages, and its use as a potential biomarker has been proposed. Plasma levels of MMP-9 do appear to be elevated in patients with AAA (McMillan and Pearce, 1999) and various authors have shown MMP-9 levels in tissue that correlate with increasing size (McMillan et al., 1997) and/or rupture risk.(Petersen et al., 2002) There is, however, data that conflicts these findings and

certainly no clear indication of how MMP-9 levels could be used clinically either as a marker of risk, progression or to indicate complications post repair. Pyo et al showed that MMP-9 deficient mice have attenuated development of both elastase- and $CaCl_2$ induced aneurysms (Pyo et al., 2000a) and that infusion of WT macrophages was sufficient to remove this attenuation, suggesting that macrophage derived MMP-9 is required for dilatation in these models.

MMP-12 has been localised to the aortic media of aneurysmal samples where it is produced by inflammatory macrophages (Thompson et al., 1995) and binds with high affinity to elastic fibres.(Curci et al., 1998) Transgenic mice deficient in MMP-12 show reduced (but not absent) aortic dilatation with $CaCl_2$ application (26% vs 63% dilatation in WT mice) (Longo et al., 2005) perhaps suggesting that MMP-12 produces dilatation in combination with other MMPs and is involved in the later stages of aneurysm progression.

In a study by Eskandari *et al* (Eskandari et al., 2005) TIMP-KO mice developed larger aneurysms than their WT countertypes suggesting that an imbalance of MMP activity versus inhibition is fundamental to AAA development. In line with this, the pharmacological inhibition of MMP activity has been widely investigated in relation to aneurysm formation, however, with somewhat inconsistent results. Doxycycline, a broad spectrum MMP inhibitor, has been shown to decrease aneurysm formation in both rat (Petrinec et al., 1996, Sho et al., 2004) and mouse (Bartoli et al., 2006) elastase models and in various cellular, murine and human studies has been shown to reduce MMP expression as well as activity (see (Newby, 2012) for further details). It is unclear whether doxycycline reduces inflammation per se, or “just” ECM proteolysis, and if so what the pathogenic significance of each of these scenarios might be. Certainly the clinical trials of doxycycline have as yet been inconclusive and underpowered to assess action on aneurysm size or growth rate (Dodd and Spence, 2011) and a large scale, randomised, clinical trial (Non-Invasive Treatment of AAA Clinical Trial – NCT01756833) is currently underway in the United States to validate the potential use of doxycycline as a therapeutic agent in AAA.

There is now a wealth of evidence implicating MMPs in the pathogenesis of aneurysm disease; further understanding is needed as to how these proteases interact with each other, and with their inhibitors, to effect the ECM breakdown seen in aneurysmal disease and crucially whether their actions can be modified to prevent disease without deleterious side effects.

1.3.5 Genetic basis for AAA

Family history is a strong risk factor for the development of AAA, second only to smoking, and is independent of both atherosclerosis and smoking.(Nordon et al., 2011) A history of a first degree relative with a diagnosed AAA doubles the risk of AAA prevalence (Larsson et al., 2009) and if a family history is present then subjects are also more likely to develop AAA at a younger age. It has been argued that this represents a high-risk population who should be offered screening at an early age.(Moll et al., 2011)

There is also a very high male preponderance of AAA compared to female patients (ratio 6:1) which is higher than the discordance seen in coronary artery disease (ratio 2:1) and is not explained by gender bias in any one known risk factor; again suggesting that aneurysmal disease is distinct from atherosclerotic disease.

The heritability of AAA has been assessed in a number of twin studies with a reported OR of 36 in monozygotic and 5 in dizygotic twins.(Wahlgren et al., 2010) This Swedish study concluded that the heritability of AAA was very high (70%), suggesting that key genetic causative factors are waiting to be discovered. Despite this promise, candidate gene association studies and genome wide linkage studies have thus far produced variable results and have generally been under-powered to draw meaningful conclusions. Many of the problems with these studies stem from the late age of onset of AAA disease, the low post-mortem rates in many countries and the lack of available biological samples from patients with AAA.(Golledge and Kuivaniemi, 2013) Coupled with these issues are the difficulties in classifying study controls which may variably come from the unscreened population (i.e. those not known to have a AAA diagnosis), the screened population (with an ultrasound-proven normal aortic diameter) or those who have undergone aortic surgery for another reason (e.g. aorto-occlusive disease).

The key findings from gene-association studies are summarised in Table 3 however, whilst genome wide association studies (GWAS) may represent the best opportunity for identifying target genes, they require extremely large patient (and control) numbers and rely on collaborations between extensive networks of researchers and clinicians. Others have focussed their efforts on specific genes based on the known likely mechanisms of AAA development and Morris *et al* report on a meta-analysis of all published data related to SNPs within MMP and TIMP genes and their association with AAA.(Morris et al., 2014) Once again, the authors comment on the problems of under-powered studies which incompletely report on other risk parameters, but they do find that the 5A risk allele in the *MMP3* gene is associated with AAA with an OR of 1.48 in a dominant inheritance model. This

deletion polymorphism is associated with an increase in MMP-3 mRNA expression and protein content in aneurysm samples and clearly represents a biologically plausible gene candidate.

Whilst human studies are plagued by a lack of early disease samples, there are a multitude of animal studies, and predominantly genetic mouse models, which have aimed to identify or confirm genes of interest in AAA disease. These range from the “blotchy” mouse (Brophy et al., 1988) – which has defective ECM cross-linking due to impaired copper metabolism and develop thoracic aortic aneurysms – to the ApoE and (low density lipoprotein receptor (LDLR) (Tangirala et al., 1995) knockout mice which develop spontaneous AAA if subjected to a high fat diet. Other transgenic mice models of relevance to this thesis are discussed where appropriate and clearly much can be learnt from these animals, however any findings obtained from murine studies must be confirmed in human patients. It is this ability, to translate preclinical findings to the care of patients, that has, as yet, been absent in the field of AAA research.

Type of Study	Patient Numbers	Key Finding	Proposed Mechanism	Reference
Candidate gene study	2836 cases, 16 732 controls (unscreened)	AAA associated with locus on chromosome 9p21.3 in non-coding RNA gene CDKN2BAS (OR 1.31)	CDKN2BAS thought to regulate cyclin dependent kinase inhibitors CDKN2A and CDKN2B. Cdkn2b$^{-/-}$ mice show increased elastase-induced AAA (?mediated via p53 apoptosis pathways)	(Helgadottir et al., 2008)
GWAS	123 cases, 112 controls (screened)	AAA associated with SNP in contactin-3 gene (OR 1.33)	Not fully understood. Contactin-3 gene encodes a cell adhesion molecule found in aortic wall	(Elmore et al., 2009)
GWAS	1292 cases, 30503 controls (unscreened)	AAA associated with SNP in DAB21P gene (OR 1.21)	DAB21P encodes a protein known to be involved in the downregulation of cell survival and proliferation	(Gretarsdottir et al., 2010)
GWAS	~2000 cases, ~ 5000 controls	AAA associated with SNP in LRP-1 gene (OR 1.15)	LRP-1 gene encodes low density lipoprotein receptor protein-1 which is thought to signal via Smad pathway and may be involved in maintaining normal blood vessel stability	(Bown et al., 2011)

Table 3. Key findings from genetic studies in AAA

The table summarises some of the key genetic associations reported for AAA with the highest level(s) of supporting evidence. None of the GWAS (or candidate gene studies) have reported odds ratios that would be consistent with the high degree of heritability seen in population based epidemiology studies and from screening programmes and registry data.

1.3.6 Newer therapies

The potential of MMP inhibitors as treatments for AAA have been discussed, but there are clearly complex mechanistic networks involved in the pathogenesis of aneurysm disease and any therapeutic agent would have to specifically target some or all of the involved pathways without causing unwanted side effects. Davis *et al* (Davis et al., 2014) outline a number of novel therapies which include anti-hypertensives (ACEi and ARBs which have been linked in animal studies to inhibition of AAA development) and immunosuppressive agents, and emphasise the importance of evidence for therapies which target aneurysm *progression* rather than *initiation*. From a clinical perspective, patients are only diagnosed and identified as having an aneurysm once significant ECM degradation has already occurred. Potential therapies must be able to prevent progression and slow growth through ECM protection and/or regeneration.

One signalling pathway which appears amenable to modification is the c-Jun N-terminal kinase (JNK) pathway which is stimulated by numerous “stress molecules” including Ang-II, TNF-α and IFN-γ, which have all been implicated in aneurysm disease. Yoshimura *et al* (Yoshimura et al., 2005) found that this pathway is upregulated in AAA samples in humans and using two different murine models of AAA showed that inhibition of JNK could both prevent initiation of experimental dilatation and, more importantly, cause regression of established aneurysms.

Micro-RNAs (miRNA or miRs) may represent another mechanism whereby several different cellular processes can be targeted simultaneously in a tissue-specific manner.(Maegdefessel et al., 2013) These small, non-coding RNA molecules can act to silence mRNA and regulate gene expression and have been implicated in numerous disease processes (see Bartel for a review (Bartel, 2004)). In AAA, miR-21,(Maegdefessel et al., 2012a) miR-29b (Maegdefessel et al., 2012b) and miR-712 (Kim et al., 2014) have all been shown to have a role in aneurysm development and manipulation of these molecules can reduce aneurysm formation in the Ang-II infusion aneurysm model. Although miRNA-targeting molecules are currently in pre-clinical development for the treatment of cancer, heart disease and insulin resistance there are numerous challenges with these therapies, including off-target effects and the ability to deliver the drug to the target cells in a therapeutic dose.(Li and Rana, 2014)

Novel therapies for the treatment of AAA are clearly needed to help what is a very high-risk population; currently available interventions are associated with considerable risk and a better understanding of aneurysm pathogenesis is fundamental to the development of effective medical therapies. As yet it is unclear

whether expansion of AAA occurs through the same mechanism as formation, and delineating these two processes will be key to furthering our collective understanding of this potentially fatal disease.

1.3.7 Experimental models of aneurysms

AAA is a major cause of death in the western world yet its pathophysiology remains poorly understood, in part because of the progressive, silent nature of aneurysm development. Surgical AAA repair gives access to only “end-stage” tissue for histological analysis and even this is decreasing in availability due to the increased rate of endovascular repair. There is a lack of age-matched “normal” aortic tissue with which to compare disease samples (with most “control” tissue originating from young deceased patients or elderly vascular patients undergoing surgery for aorto-occlusive disease) and even if available this would not allow for study of disease progression (Tsui, 2010) and/or potential therapeutic interventions.

In vivo models are therefore required and a number of large animal models have been proposed in the literature. Whilst each species has its advantages – sheep have a similar coagulation system to that of humans whilst the swine arterial system is comparable in terms of size and anatomy – and large animal models will undoubtedly be required to study future surgical and technological advancements, mouse models of disease predominate in pathogenesis hypothesis testing because of “their small size…cheapness…ability to compare well documented genetic backgrounds and the ability to delete or overexpress specific genes”.(Daugherty and Cassis, 2004)

Although spontaneously occurring genetic mutations have been shown to lead to aneurysm development (as in the “blotchy” mouse) these animals are limited in their usefulness because of systemic pathology and thus, three key mouse models of aneurysm development have evolved and are discussed below.

1.3.7.1 Angiotensin II model

First described by Daugherty *et al*,(Daugherty et al., 2000) the AngII model of aneurysm formation was discovered as a “by-product” of experiments to identify the role of AngII in atherosclerosis in ApoE deficient (hyperlipidaemic) mice. These mice had AngII infused (at a dose of 500-1000ng/kg/min) for 28 days via a subcutaneous osmotic mini-pump and showed an increased number of new atherosclerotic lesions and (unexpectedly) AAA development in the suprarenal aorta. This dilatation was not related to local atherosclerosis but histologically did show medial breaks and dissections (a feature not commonly seen in human aneurysms), gross inflammation and thrombus formation.

In this model aneurysm formation appears to be independent of changes in blood pressure, cholesterol and triglyceride levels and has a male predisposition as in human disease. However this model has a number of limitations in that WT mice are relatively resistant to AngII aneurysm formation, with much lower incidence than hypercholesterolaemic mice (Daugherty et al., 2011) (meaning that an ApoE deficient or LDLR deficient background is necessary, and adds to the complexity of transgenic experiments), and Ang II induced aneurysms are prone to rupture (Cao et al., 2010) with quoted rates of 10-47% (Chamberlain et al., 2010, Saraff et al., 2003) leading to high rates of mouse mortality. In addition, several studies have shown that ApoE$^{-/-}$ mice have altered immune responses with impaired immunity after bacterial challenge (Roselaar and Daugherty, 1998) and decreased delayed-type hypersensitivity.(Laskowitz et al., 2000) Ang II appears to act through angiotensin 1a (AT1a) receptors to induce aneurysm formation; as shown by the inhibition of aneurysm development by AT1-receptor blockers or by the transgenic knockout of the AT1a receptor completely (causing inhibition of aneurysm development) or in endothelial cells (causing attenuated aneurysm development)(Rateri et al., 2011) however the relevance of this mechanism to human aneurysm formation is yet to be fully elucidated.

1.3.7.2 Elastase model

The elastase model of AAA development was first introduced because of the disrupted nature of elastin observed in human aneurysmal tissue. Initially established in rats (Anidjar et al., 1990) and subsequently adapted by Pyo *et al* (Pyo et al., 2000b) for use in mice, this model involves infusion of type-1 porcine pancreatic elastase (PPE-1) into the infra-renal aorta, after isolation from the rest of the circulation by proximal (distal to the renal arteries) and distal (at the level of the iliac bifurcation) ligatures. The procedure is technically very difficult and results in immediate mechanical dilatation of the vessel that persists for up to a week. This is followed by an inflammatory response with adventitial macrophage infiltration, destruction of the medial elastic lamellae and rapid vessel dilatation. Although this model has been used to study a number of gene targets (Thompson et al., 2006) it should be noted that some authors claim that aneurysm development varies depending on the source of the elastase used,(Carsten et al., 2001, Curci and Thompson, 1999) possibly suggesting a role for “contaminators” found in some commercial preparations. A recent publication by Bhamidipati *et al* (Bhamidipati et al., 2012) has attempted to simplify this model by reporting the development of AAA with *periadventitial* application of elastase. Regardless of route of administration however, the administration of elastase as an experimental model shortcuts the

“trigger factors” for AAA development, focusses solely on the downstream effects of elastolysis and hence is not first choice for our work investigating the potential protective role of TG2.

1.3.7.3 Calcium chloride ($CaCl_2$) model

Intimal calcification is a common feature of vessels displaying atherosclerosis and up to 80% of human AAAs show significant arterial wall calcification.(Maier et al., 2010) First published by Gertz *et al* (Gertz et al., 1988) the $CaCl_2$ aneurysm model was initially described as application of 0.5M $CaCl_2$ on to the *carotid* arteries of rabbits. A 60% increase in diameter was seen after just 3 weeks and crucially, histological examination revealed some of the key features of human aneurysmal tissue; specifically elastin calcification, thinning of elastin and loss of fibre waviness as well as MMP induction, inflammatory cell infiltration and loss of VSMCs.

In 1997 Freestone *et al* (Freestone et al., 1997) adapted the model to induce aneurysms in rabbit aortas (using a combination of $CaCl_2$ and thioglycylate application) but it was not until 2001 that Chiou *et al* (Chiou et al., 2001) reported the use of $CaCl_2$ as a reproducible model of AAA formation in mice. Since then many authors have used the technique of applying $CaCl_2$ directly to the ventral surface of the aorta and “knock-out” and transgenic technologies have been utilised to investigate different aspects of aneurysm formation.

The specifics of the model ($CaCl_2$ concentration, duration of application and time from induction to harvest) differ significantly between research groups and some authors advocate the use of $CaCl_2$ application plus either elastase or collagenase, the combination of which seems to generate larger diameter aneurysms than $CaCl_2$ alone. The ability to accelerate or retard aneurysm development by altering $CaCl_2$ concentration has potential benefits in a novel project such as this where the response to injury is unpredictable, however no matter which protocol is used, the $CaCl_2$ model displays may of the features of human AAAs, as summarised by Wang *et al*.(Wang et al., 2013a) It is also relatively simple to perform, results in minimal bleeding (pilot data) and $CaCl_2$ application can be localised to the infra-renal aorta, the site of 95% of AAA development in humans, thus minimizing the confounding variable of altered blood flow in the renal arteries

Unlike the AngII model, the $CaCl_2$ model does not have a male preponderance and does not require a hyperlipidaemic, pro-atherosclerotic background. As such it can be undertaken in WT mice meaning that subsequent transgenic studies do not require complex, time-consuming breeding strategies. Furthermore the $CaCl_2$ model allows direct comparison between pre- and post-induction vessel diameter

and between adjacent or opposing (ventral vs. dorsal) sections of treated and untreated aorta so that each mouse can act as its own control.

Freestone *et al* (Freestone et al., 1997) and others have reported that $CaCl_2$ application appears to cause aortic wall thickening rather than true dilatation (as observed by an increase in outer vessel diameter (OD) but not inner diameter (ID)) however all studies utilising this model have employed similar techniques of aortic measurement (either analysis of photographs of the exposed vessel or in-vivo analysis by digital callipers, a micrometer, video microscopy or calibrated grids) (Wang et al., 2013a) and it is generally accepted that this model represents the early stages of vascular injury (and aneurysm development) rather than an end-point of gross dilatation.

1.4 Transglutaminases

Transglutaminases (TGs) were first described in 1959 (Clarke et al., 1959) and comprise a family of 8 catalytically active enzymes (and 1 inactive homologue) which have the primary function of introducing intra-chain and inter-chain isopeptide linkages between polypeptide chains. These calcium dependent enzymes catalyse the formation of a covalent bond between a free amine group (for example that found on a protein-bound lysine residue) and the gamma-carboximide group of a protein or peptide bound glutamine residue (see Figure 8). This ε(γ-glutamyl) lysyl bond shows high resistance to proteolytic breakdown and hence transglutaminases have been described as “biological glues”(Griffin et al., 2002) and the process of bond formation likened to “spot-welding”. This section gives an overview of the structure and function of TG2 and FXIII-A, the transglutaminases of interest in this study, and briefly outlines the roles of the other family members, both in terms of their known physiological functions and their contributions to various disease processes. The evidence from mouse models of TG2 and FXIII-A deficiency is summarised in chapter 2, however, where relevant, knock-out models of the other transglutaminases are discussed here.

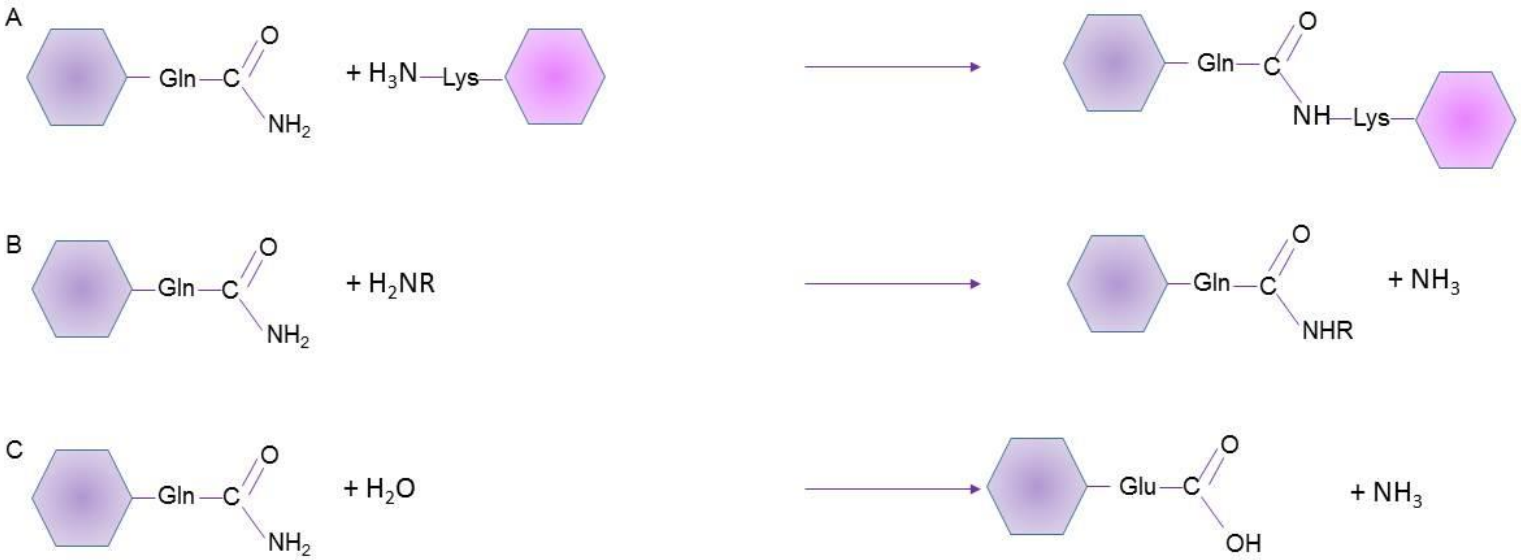

Figure 8. Transamidating role of TG2

Schematic showing the various transamidation reactions catalysed by TG2. In **A)** two proteins are cross-linked through the formation of a covalent bond between the γ-carboxyamide group of a peptide bound glutamine and the ε-amino group of a peptide bound lysine residue. In **B)** a protein modification occurs by reaction with a primary amine. Finally in **C)**, if there is no suitable amine available then a water molecule acts as an acyl acceptor to deaminate a glutamine residue to glutamate. This situation may require the presence of an acidic environment however selective deamidation of certain residues with concurrent transamidation of others has been reported (see text).

1.4.1 Transglutaminase 2 (TG2)

Transglutaminase 2, also known as tissue transglutaminase (tTG), cytosolic- or liver-type transglutaminase, is the most ubiquitous of the transglutaminase family, is found in numerous mammalian tissues (including lung, liver, heart, bone and spleen) and is expressed by almost all cell types including osteoblasts, mesenchymal stem cells, endothelial cells and SMCs; although the level of expression varies considerably with cell type.

Encoded by a gene mapping to human chromosome locus 20q11-12, TG2 is a protein comprising 687 amino acids with a molecular mass of 77.3kDa and four distinct structural domains; an N-terminal β-sandwich domain, a catalytic core and two C-terminal β-barrel domains. As with the other TGs, the most recognised function of TG2 is its ability to transamidate proteins, leading to protein cross-linking, protein modification (by addition of a primary amine) and/or deamidation. These reactions are summarised in Figure 8 and this function is located within the catalytic core of TG2 which contains the “catalytic triad” of cysteine (at position 277), histidine (335) and aspartate (358) residues seen within numerous cysteine proteases.(Gundemir et al., 2012) The transamidating activity of TG2 is calcium dependent and cooperative binding of calcium at (at least) 6 binding sites is thought to give rise to the “open” or active conformation of TG2 (see Figure 9). There is increasing evidence, however, that a rise in calcium concentration alone is not sufficient for activation and that TG2 is probably latent in terms of its transamidation activity in most circumstances and that its non-enzymatic functions are of greater importance than previously recognised.

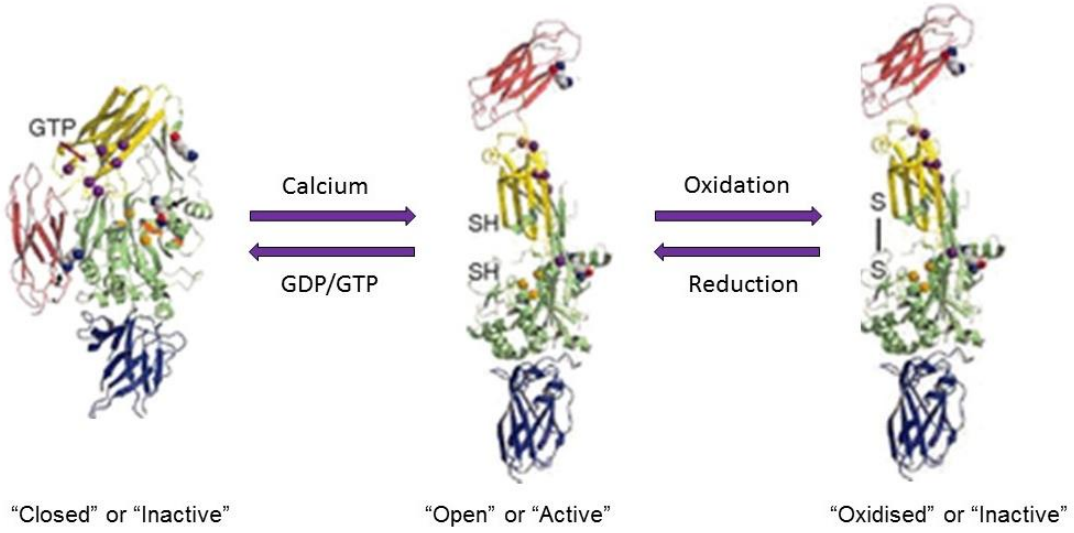

Figure 9. Regulation of TG2 activity

Cartoon depicting the regulation of TG2 transamidating activity. TG2 with bound GDP/GTP is held in a stable compact "closed" structure which is inactive in terms of transamidating function. Binding of calcium promotes an "open" or "active" confirmation whilst oxidation of this protein results in the formation of disulphide bridges within the active site, and catalytic inactivity. Figure re-drawn and modified from Eckert *et al*. (Eckert et al., 2014)

Uniquely amongst the TGs, TG2 can bind guanine nucleotides and hydrolyses GTP to couple adrenoreceptors, thromboxane and oxytocin receptors (amongst others) to phospholipase C in cell-signalling pathways.(Lorand and Graham, 2003) TG2 has also been hypothesised to bind ATP and function as a protein kinase (Mishra and Murphy, 2004) (although this function has not been demonstrated *in vivo*) and it has been shown to have actions as a protein disulphide isomerase and a protein scaffold.(Wang and Griffin, 2012) This multitude of actions has led to TG2 being described as a "molecular Swiss army knife",(Gundemir et al., 2012) a term which highlights the importance of the structural conformation of TG2 in its various functions (see Figure 9). For example; binding of GDP/GTP, which occurs between the catalytic core and the first β-barrel domain,(Jang et al., 2014) stabilises a compact "closed" structural form of TG2 which inhibits its transamidating function. Likewise, calcium binding inhibits GTP binding, thus providing reciprocal regulation of function.(Nakaoka et al., 1994)

Further regulatory mechanisms have been identified which mean it is likely that the enzymatic activity of TG2 is transient in most situations. For example, key cysteine residues can be nitrosylated by reaction with NO (Lai et al., 2001) leading to inactivation of its transamidating function and predominance of other roles. This is hypothesised to be the mechanism which links TG2 to arterial stiffening, whereby decreased NO bioavailability leads to decreased S-nitrosylation and a relative increase in TG2 cross-linking of vascular wall proteins.(Santhanam et al., 2010) Likewise, reduction of TG2 (possibly by thioredoxin)(Jin et al., 2011) reverses the vicinal disulphide bond formation which occurs between cysteine residues (Cys 370 and 371) and which normally render extracellular TG2 catalytically inactive. Finally, the ability of TG2 to act at the cell surface to bind fibronectin, integrins (and other partners) with high affinity, means that it becomes unable to participate in cross-linking reactions. Although much of this data needs confirmation in the *in vivo* setting, it is clear that TG2 regulation is complex and multifactorial and that its primary function at a given time point is influenced by a number of factors.

As well as the *structure* of TG2, it is also apparent from the literature that the *location* of TG2 is critically important in determining activity. TG2 has intracellular roles as well as those within the ECM and at the cell surface and its various functions take precedence depending on its location; for example the protein disulphide isomerase activity of TG2 (Hasegawa et al., 2003) appears to be key in the cytosolic compartment where TG2 can modify mitochondrial proteins to affect ATP homeostasis, whereas the scaffolding function (i.e. its ability to form complexes with fibronectin and integrins) is crucial at the cell surface where it

mediates cell-adhesion and migration. Clearly this location-specific activity adds a layer of complexity when trying to investigate the actions of TG2 and means that *in vitro* data must be appreciated with caution.

Given the importance of TG2's physical location is seems surprising that more is not yet known about how it reaches the extracellular space. The TG2 protein lacks a conventional hydrophobic leader sequence so must be secreted by an alternative mechanism to the conventional Golgi/ER pathway.(Cordell et al., 2010) It had previously been assumed that TG2 was only found extracellularly when cells became damaged or membrane integrity was compromised but Verderio*et al* showed that increased TG2 expression in cultured fibroblasts results in increased extracellular TG2 without the need for conditions of cellular stress.(Verderio et al., 1998) No clear secretion mechanism has as yet been discovered but some authors suggest that TG2 is released via microparticle formation (van den Akker et al., 2012) whilst others report that either an intact structure (Gaudry et al., 1999) or the ability of TG2 to alter its structural confirmation may be a key determinant in its extracellularisation.(Balklava et al., 2002)

The control of TG2 expression is primarily mediated at the transcriptional level and various activators of transcription (and their respective downstream binding sites on the *TGM2* gene) have been identified and include retinoic acid, IL-6, NFκB, hypoxia inducible factor (HIF), TNF-α and TGF-β. Because of these activators, and its upregulation under conditions of tissue injury, TG2 is increasingly recognised as a stress-related protein (Wang and Griffin, 2012) which acts to limit cell damage. Just as cell stress increases TG2 expression, it may also increase nuclear translocation of TG2, thus enabling TG2 to act as a regulator of transcription in its own right. Some of these actions are mediated through transamidation – for example the cross-linking of transcription factor SP1 by TG2 in response to ethanol, downregulates SP1 mediated gene transcription (Tatsukawa et al., 2009a) – whilst the observed TG2 mediated increase in NFκB transcriptional activity occurs by mechanisms which are as yet incompletely understood.

Another means by which protein function may be altered is through the generation of splice variants which may be preferentially expressed in disease states. At least 4 splice variants of TG2 (TG2H, $TG2H_2$, $TG2_{v1}$ and $TG2_{v2}$) have been reported, all of which show alternative C-terminal domains (Phatak et al., 2013) with loss, or impaired, GTP-binding. TG2H is a truncated isoform which shows increased transamidating activity (presumably due to removal of GTP-mediated inhibition) and upregulated levels of TG2H have been reported in the brains of patients with Alzheimer's disease. $TG2H_2$ is also a shortened form of the TG2 protein at only 349

amino acids in length and has been shown to be induced in rat neuronal astrocytes after exposure to inflammatory cytokines; this splice variant has a lower transamidating activity than constitutive TG2, but activation requires lower concentrations of calcium. $TG2_{v1}$ and $TG2_{v2}$ are both generated by alternative splicing events (Lai et al., 2007) and have decreased catalytic activity but the biological significance of these (and other) isoforms is yet to be fully investigated.

One of the most examined roles of TG2 is its association with apoptosis and it has variably been described as having either a primarily pro- or anti-apoptotic phenotype. Certainly, overexpression of TG2 has been linked to increased apoptosis and in response to “stressful” conditions such as UV radiation, TG2 accumulates and is activated by Ca^{2+} release brought about by the same stimuli (Odii and Coussons, 2014) (which may include the production of ROS, or retinoic acid, for example). TG2 can then initiate apoptosis via cross-linking of intracellular proteins and subsequently mediates the clearance of dying cells by a) formation of chemoattractant molecules (which promote macrophage migration), b) the activation of macrophage released TGF-β and c) the release of phosphatidyl serine which increases the recognition of apoptotic cells by macrophages.

When located in the nucleus however, TG2 has anti-apoptotic effects which are independent of its transamidation and cross-linking activity and relate instead to its interaction with nuclear transcription factors. One example of this is the interaction of TG2 with retinoblastoma protein (pRb) which results in the polymerisation of transcription factors (e.g. NFκB), prolongation of activity and the up-regulation of anti-apoptotic genes. Such interactions have been shown in several cancer cell lines (Verma and Mehta, 2007, Kim et al., 2006) and also in breast tumours where levels of TG2 expression correlate with NFκB activity and are related to resistance to doxyrubicin chemotherapy.(Park et al., 2009) In the ECM, TG2 can stabilise ECM-cell binding in cooperation with fibronectin and/or integrins and thus can protect against anoikis (Verderio et al., 2003) (a form of apoptosis occurring when normally anchored cells detach from the ECM) and activate cell survival pathways mediated via FAK and PI3K/Akt (Verma and Mehta, 2007) or Rho/ROCK signalling.(Wang and Griffin, 2012)

TG2 has many other functions which may impact on the cardiovascular system including roles in inflammation and platelet function, however its contribution to apoptosis may prove critical to its role in aneurysm development. TG2 expression shows a close correlation with the occurrence of developmental (Fesus, 1999) and induced (Fesus et al., 1987) apoptosis yet $TG2^{-/-}$ mice show normal development and induced thymocyte apoptosis.(De Laurenzi and Melino, 2001) Some authors

have postulated a direct role of TG2 in programmed cell death (Melino et al., 1994) whilst others emphasise the relationship with the apoptosis regulator BAX (Rodolfo et al., 2004) (leading to mitochondrial pore formation and permeabilisation), and others report that TG2 can induce release of apoptosis inducing factor (AIF) in a caspase-independent apoptosis pathway.(Fok and Mehta, 2007) Certainly the cross-linking function of TG2 may help stabilise dying cells (Fesus and Szondy, 2005) and help to minimise the leakage of intracellular components and the Melino $TG2^{-/-}$ mouse has been reported to have macrophages with impaired ability to engulf and clear apoptotic cells, possibly due to the formation of fewer, less efficient phagocytic portals.(Toth et al., 2009) TG2-null macrophages may also show an altered, pro-inflammatory, cytokine response to apoptotic cells (Falasca et al., 2005) thus potentiating the risk of subsequent inflammation. Whether the pro-apoptotic roles reported are truly due to increased death *in vivo*, or actually, to impaired macrophage clearance of apoptotic cells warrants further study.

In contrast to its pro-apoptotic function, many authors report a protective effect of TG2 against apoptosis, primarily due to its role in adhesion dependent survival signalling (Fesus and Szondy, 2005, Kotsakis and Griffin, 2007) thus it is possible that TG2 may promote survival of “damaged” cells, and hence inflammation and tissue damage, in aneurysm development rather than affording protection. Gundemir *et al* (Gundemir et al., 2012) hypothesise that “overall TG2 is upregulated in response to stress…however if the insult is excessive…TG2 may also facilitate cell death”.

Aside from its role in cancer through its anti-apoptotic function, TG2 has been postulated to have roles in numerous other disease processes, the best studied of which is gluten mediated enteropathy or Coeliac Disease (CD). This autoimmune condition affects up to 2% of the general population, is characterised by intestinal villous atrophy and inflammation, manifesting as chronic diarrhoea and malabsorption and is triggered by dietary exposure to gluten. TG2 has a dual role in CD in that it deamidates glutamine residues within protease-resistant gluten peptides prior to their uptake by antigen presenting cells (thus stimulating the T-cell mediated adaptive immune response), and it forms complexes with gluten proteins +/- collagen which act as triggers for B-cell production of TG2-specific antibodies (thus stimulating the humoral immune response).(Iismaa et al., 2009) Anti-TG2 autoantibodies can be detected on serological testing or patients and NICE guidelines recommend IgA tissue transglutaminase testing as first-line investigation in anyone suspected of having CD.(NICE, 2015)

TG2 has also been implicated in the pathogenesis of cataracts (through cross-linking of lens proteins), Huntington's disease (by promoting the formation of neurotoxic insoluble aggregates of the huntingtin protein within the striatum and cerebral cortex) and Alzheimer's Disease (via TG2 mediated formation of angiotensin-II (AT_2) receptor oligomers). Within the cardiovascular system TG2 has been reported to be involved in cardiac hypertrophy,(Small et al., 1999) arterial remodelling,(Bakker et al., 2005) atherosclerosis,(Haroon et al., 2001) coronary artery disease (Sumi et al., 2002) and arterial calcification (Faverman et al., 2008) although reports are conflicting with (for example) work from our group showing no difference in buried plaque formation in ApoE.$^{-/-}$TG2$^{-/-}$ mice when compared with ApoE$^{-/-}$ mice.(Williams et al., 2010) Much of the controversy regarding TG2 arises from the theoretical ability of FXIII-A to compensate for TG2 deficiency, highlighting the potential value of the TG2$^{-/-}$.FXIII-A$^{-/-}$ double knockout (DKO) mice in teasing out the roles of TG2 in health and disease.

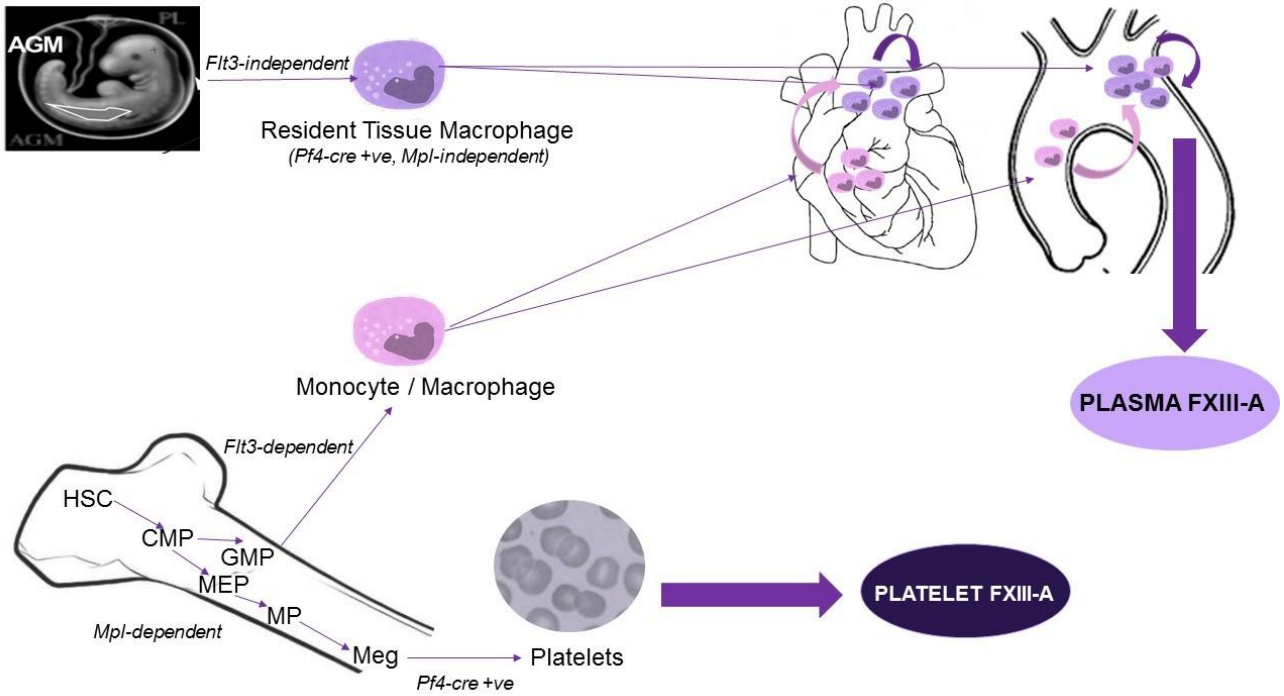

Figure 10. Cellular source of plasma FXIII-A

Diagram summarising the work from our group undertaken through a BHF Programme Grant (PG/03/080/15731). Using two different thrombocytopenic mouse lines and cre-lox fingerprinting we have generated evidence to disprove the historical theory that platelets are the source of plasma FXIII-A. We instead hypothesise that the cellular source of plasma FXIII-A is a population of resident tissue cells, most likely macrophages, which are located in the heart and aorta. These cells are generated from primitive (flt-3-independent) yolk-sac haematopoiesis and migrate early to the dorsal aorta. We believe that the cells are primed to produce FXIII-A in foetal and adult life, and may act as a source of FXIII-A to facilitate tissue repair after injury. These cells can replace themselves autonomously or can be displaced by bone-marrow derived macrophages generated via definitive (flt-3-dependent) haematopoiesis. Full publication in preparation; Characterisation of the cellular source of plasma FXIII-A using a novel FXIII-A floxed mouse – Griffin, Simpson & Beckers *et al*.(Griffin et al., 2015)

HSC = haematopoietic stem cell, CMP = common myeloid progenitor, GMP = granulocyte/macrophage progenitor, MEP = megakaryocyte/erythrocyte progenitor, MP = megakaryocyte precursor, Meg = megakaryocyte, AGM = aorto-gonadal mesonephros, Pf4 = Platelet factor-4, Mpl = thrombopoietin receptor, flt-3 = Fms-like tyrosine kinase-3.

1.4.2 Factor XIII-A (FXIII-A)

Factor XIII is a pro-transglutaminase found in plasma – complexed as a heterotetrameric structure (A_2B_2 or pFXIII-A) consisting of two globular active "A" subunits and two strand-like inactive, carrier "B" subunits – and in cellular form (as A_2 or cFXIII-A) in megakaryocytes, chondrocytes, osteoblasts and certain macrophage populations. FXIII-A is the only transglutaminase which is known to exist in dimeric form and consists of two polypeptides of mass 83kDa which each contains an N-terminal β-sandwich domain, a central core domain for catalysis (containing the Cys/His/Asp triad) and two β-barrel domains as are seen in other TGs. FXIII-A also possesses a 34-residue N-terminal activation peptide which is cleaved during FXIII-A activation enabling access to the active site cysteine residue.

FXIII-B is a monomeric protein of ~80kDa mass which is encoded by the *F13B* gene on human chromosome 1 and which consists of 10 short "sushi" repeat domains. FXIII-B, which is synthesised in, and secreted from hepatocytes, does not contain the catalytic triad, has no transglutaminase activity and is thought to act primarily to carry FXIII-A and protect it in the circulation. In agreement with this role, homozygous deficiency of *F13B* leads to markedly reduced pFXIII-A protein and activity levels,(Souri et al., 2008a) however, FXIII-B is also thought to have a regulatory role in the thrombin activation of pFXIII-A (see Figure 11) and mediates the binding of the A_2B_2 structure to fibrinogen. FXIII-B is present in excess in the circulation with up to 50% found in a non-complexed state,(Komaromi et al., 2011) meaning that newly secreted FXIII-A can be rapidly and efficiently bound.

Similarly to TG2, FXIII-A lacks an identifiable hydrophobic leader sequence and secretion could not be observed under conditions where interleukin-1β (a non-classically secreted protein) could be demonstrated.(Cordell et al., 2010) The cellular source of the plasma pool of FXIII-A is also, as yet unknown, although historically bone marrow transplant experiments have been interpreted as showing that the likely source is platelets or platelet precursors of the megakaryocytic lineage.(Poon et al., 1989) Experiments conducted by our group however, have previously demonstrated that pFXIIIA levels are normal in two thrombocytopenic mouse lines; the Bcl-x^{plt20} mouse, which shows rapid platelet turnover and clearance and the $Mpl^{-/-}$ mouse, which has a targeted mutation of the thrombopoietin receptor.(Cordell et al., 2010)

A programme of work has subsequently shown that in fact, the likely source of pFXIII-A is a subset of resident aortic macrophages which are generated early in embryonic development and are variably replaced and repopulated by circulating

monocyte/macrophages. This work has relied on the use of lineage specific deletion of FXIII-A using the FXIII-A floxed mouse (described in section 2.1) and mice expressing cre-recombinase driven by the following promoters; Pf4, Cd11b, LysM and Flt-3 which would be expected to cause gene deletion in megakaryocytic cells, macrophages – CD11b and LysM cre are both (differentially) expressed in macrophage populations – and bone marrow derived cells respectively. We have compared the effects of –cre deletion on both pFXIII-A and cellular FXIII-A mRNA and by this "fingerprinting" approach have shown that the profile of depletion of pFXIII-A closely resembles that of FXIII-A mRNA in the aorta, suggesting that aortic resident macrophages and/or cells closely related to them, maintain pFXIII-A. The dorsal aorta is a site to which primitive haematopoietic cells migrate early in development, raising the possibility that location within this aortic niche "primes" macrophages to secrete pFXIII-A into the circulation. Heidt *et al* (Heidt et al., 2014) have shown that occupation of certain tissue niches is associated with conformational and cytoskeletal changes (as in the heart where resident macrophages become elongated and spindle shaped) and it may be that similar structural changes are ultimately required for pFXIII-A secretion. A summary of this work can be seen in Figure 10 and further details obtained in (Griffin et al., 2015).

The primary function of pFXIII-A is haemostasis and its roles in fibrin-matrix stabilisation and platelet activation are well established.(Muszbek et al., 1999) Although FXIII-A does not impact clotting-time, it cross-links monomers within the fibrin mesh of the developing thrombus and thus increases the stiffness of the fibrin clot 5-fold. FXIII-A cross-linking also incorporates α2-plasmin inhibitor (α2-PI) into the clot and reduces plasminogen-fibrin binding thus increasing the resistance of the clot to lysis. The activation of FXIII-A in the circulation is shown in Figure 11 and is maximally efficient in the presence of both thrombin and calcium (although activation can proceed in a non-thrombin dependent pathway) and is enhanced in the presence of fibrin.(Komaromi et al., 2011) Intracellular activation of FXIII-A also requires calcium binding to elicit a conformational change, exposing the catalytic site, but this requires only a small increase in calcium concentration in comparison to that seen in the coagulation cascade. In contrast to its activation, FXIII inactivation is less well studied but appears to occur through oxidation (Robinson et al., 2000) and to a lesser extent via proteolytic inactivation by non-specific proteases such as MMP-9 and elastase.(Muszbek et al., 2011b)

Unsurprisingly, patients with FXIII-A deficiency show prolonged bleeding time with weaker clots that are easier to lyse. The bleeding phenotype seen in these patients can vary markedly but spontaneous haemorrhage, haemarthroses and recurrent

miscarriage are all features of deficiency.(Muszbek et al., 2011a) It should be noted however that only ~5% plasma activity of FXIII-A is required to control bleeding in humans and heterozygous FXIII-A deficiency in humans (with resulting 50% plasma activity) is usually asymptomatic.

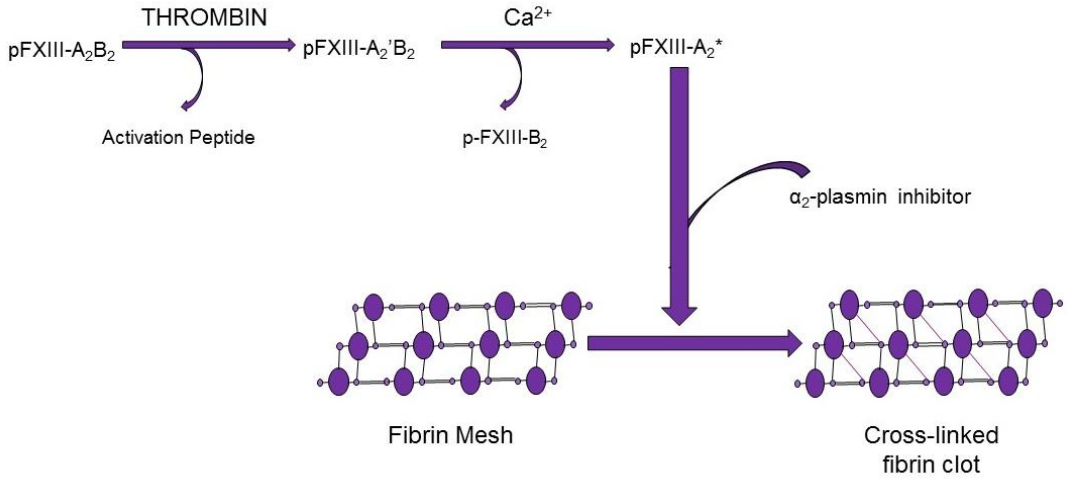

Figure 11. Activation of clotting Factor XIII

Schematic showing activation of clotting factor XIII and its role in the production of a cross-linked fibrin clot. Plasma FXIII is activated in a thrombin-mediated pathway by cleavage of a 34-residue activation peptide. Following calcium binding, the carrier B-subunits are released to generate activated clotting FXIII-A. This enzyme, via its transglutaminase activity, is able to cross-link fibrin fibres in the developing thrombus as well as incorporating protease inhibitors (such as α-2-plasmin inhibitor) and thus contributes to the generation of a stable clot that is resistant to lysis. For further details see text.

Multiple polymorphisms of the *F13A* gene have been reported with 5 (Val34Leu, Tyr204Phe, Pro564Leu, Val650Ile, Glu651Gln) being the most common. Of these polymorphisms, the change from valine to leucine at position 34 (Mikkola et al., 1994) is the most well studied and frequent, occurring in up to 25% of Caucasians and with less frequency amongst African populations. The Val34Leu site is close to the cleavage site for thrombin and the Leu polymorphism accelerates the release of the activation peptide from pFXIII-A by 2.5-fold. The Tyr204Phe and Pro564Leu polymorphisms have been shown to decrease FXIII-A activity, consistent with their location within the catalytic core of the enzyme, and although FXIII-A polymorphisms have variably been reported to be related to risk of myocardial infarction (MI), deep vein thrombosis (DVT) and arterial thrombosis (amongst other pathologies) these claims have not been supported by evidence from GWAS studies.

As yet, FXIII has not been shown to have the pleiotropic actions of TG2 however there is significant evidence of protein disulphide isomerase activity (Lahav et al., 2009) and certainly the transglutaminase actions of FXIII-A are not limited to fibrin cross-linking. Additional substrates of FXIII-A catalysis include other fibrinolytic proteins (e.g. plasminogen and thrombin activatable fibrinolysis inhibitor (TAFI)), ECM proteins (including fibronectin, osteopontin and vitronectin), cytoskeletal proteins (including actin and myosin) and others such as the AT_1 receptor and α-2-macroglobulin.(Muszbek et al., 2011b)

Although many of the non-clotting functions of FXIIIA remain controversial, there is a significant body of evidence supporting its role in wound healing, inflammation and angiogenesis. Patients with FXIII deficiency may show impaired wound healing – an observation first made in 1961 (Beck et al., 1961) – however not all patients show impairment with rates reported at 14-36% (Muszbek et al., 2011b) depending on study population and inclusion criteria. Certainly, FXIII-A deficient mice show decreased wound healing, delayed re-epithelialisation and abnormal scar formation (Lauer et al., 2002, Inbal et al., 2005) and there is evidence of the involvement of FXIII-A in chronic venous leg ulceration.(Zamboni and Gemmati, 2007) The potential mechanisms by which pFXIII-A exerts its action on wound healing are multiple and include a role in fibroblast and monocyte proliferation, migration and survival (Soendergaard et al., 2013) as well as pro-angiogenic effects via endothelial cells, downregulation of thrombospondin-1 (TSP-1, an inhibitor of angiogenesis) and vascular endothelial growth factor (VEGF) receptor-2 mediated signalling.(Dardik et al., 2006) Cellular FXIII-A may also be in involved in wound healing; its expression is increased in activated macrophages (Torocsik et al.,

2005) and it has been shown by one group to cross-link AT_1 receptors in monocytes leading to enhanced G-protein signalling and increased phagocytosis of apoptotic cells and cellular debris (although this has not been replicated by other investigators). The actions of pFXIII-A and cFXIII-A in response to tissue injury are summarised succinctly in (Muszbek et al., 2011b) and are clearly worthy of further study to determine their importance in clinical practice.

FXIII-A has numerous other postulated roles in addition to its clotting function which include the cross-linking of platelet proteins (facilitating platelet spreading and clot retraction) and the induction of hypertrophic differentiation in chondrocytes and osteoblasts.(Nurminskaya and Kaartinen, 2006) This function is not well characterised although some authors have hypothesised a cooperative role of TG2 and FXIII-A in this potentially pathological process (hypertrophy is characteristic of osteoarthritis) which can be induced by IL1-β and TGF-β.(Johnson et al., 2001, Johnson et al., 2008b) Given that DKO mice do not show any skeletal pathology it seems unlikely that either enzyme has an essential role in bone development and calcification (Cordell et al., 2015) although further studies may yet uncover a role in healing and repair.

In the cardiovascular system FXIII-A has been shown to be expressed at the site of myocardial infarction, has been implicated in hypertension induced endothelial dysfunction and arterial remodelling (Taherzadeh et al., 2010) and may have a role in the maintenance of normal vascular permeability (Wozniak et al., 2001, Noll et al., 1999a) through cross-linking of ECM proteins such as fibronectin in the intracellular clefts between endothelial cells.(Muszbek et al., 2011b) In 2006 Nahrendorf *et al* undertook experiments examining the role of FXIII-A in cardiac remodelling, utilising a murine coronary ligation model of MI and comparing FXIII-A deficient mice with WT animals and with deficient animals given exogenous FXIII-A supplementation. They showed that both heterozygous ($FXIII\text{-}A^{+/-}$) and homozygous ($FXIII\text{-}A^{-/-}$) mice suffer from infarct expansion, left ventricular rupture and death within 5 days of surgery, whereas the WT, sham operated and reconstituted animals had much lower mortality rates (~40% at 10 days). The authors conclude that the findings can be explained by an impaired inflammatory response – with decreased neutrophil and macrophage recruitment – and an imbalance in matrix turnover (with decreased collagen and increased MMP-9 seen in FXIII-A deficient animals). Although mortality rates were returned to normal by FXIII-A supplementation there were still physiological and histological differences seen in these animals in comparison with controls, supporting an additional role for cFXIII-A in cardiac remodelling post-infarct.

Interestingly, Souri *et al* (Souri et al., 2008b) have reported that older male mice with FXIII-A deficiency show spontaneous cardiac fibrosis with widespread haemosiderin deposition seen on histology. This gender-specific pathology resulted in high mortality rates (50% at 10 months) due at least in part to intrathoracic haemorrhage. Although the authors hypothesis that the “fighting behaviours” of male mice may explain the gender bias in these findings, this has not been proven and clearly warrants further study to determine whether cardiac fibrosis is secondary to impaired vascular barrier function or to impaired repair post-injury, or both.

Taken as a whole, the above evidence suggests that FXIII-A may have a role in cardiovascular stability and repair, which may overlap with that of TG2. A greater understanding of this is critical, both in our study of aneurysm development but also to investigate the suitability of FXIII-A inhibitors which have been proposed as therapeutic strategies for thrombosis (Lorand, 2000b) and arterial calcification.(Matlung et al., 2009)

1.4.3 TG1, 3 and 5: The “keratinocyte-type” transglutaminases

TG1, 3 and 5 are collectively known as the keratinocyte transglutaminases and are primarily found within the spinous and granular layers of the skin epidermis. Each enzyme is secreted as an inactive zymogen and all three have transglutaminase cross-linking actions which are involved in the formation of the cornified cell envelope (CE) in both hair follicle and epidermal development.

Transglutaminase 1 is encoded by the *TGM1* gene at human chromosome locus 14q11.2 and is predominant in the epidermis where its expression is progressively increased in keratinocytes as they migrate towards the surface of the epidermis and terminally differentiate into corneocytes. TG1 is also expressed in epithelial cells in a variety of organs and has been reported in the endothelium of the cardiac microvasculature (Baumgartner et al., 2004) however, experimental TG1 deficiency reveals that the primary function of TG1 is in the formation of the lipid and protein cell envelope of the skin.

$TG1^{+/-}$ mice are phenotypically normal, however knockout of TG1 leads to impairment of normal skin development, rapid dehydration and death within a few hours of birth. In humans, lamellar ichthyosis occurs as a result of defects in TG1 activity and X-linked ichthyosis is due to excess cholesterol sulphate inhibiting the cross-linking ability of TG1. As with all ichthyoses, these conditions manifest as thickened, scaly skin which is excessively keratinised and which is thought to be a secondary response to try to prevent water loss through an inadequate/absent cell envelope.

TG5 is also found in the spinous and granular layers of the skin epidermis and is thought to stabilise the junction between the stratum granulosum and the stratum corneum (the “outermost” layer of the skin that is continuously shed and regenerated). A loss-of-function mutation (G113C) within the catalytic core of TG5 has been shown to be responsible for the autosomal recessive clinical condition Acral Peeling Skin Syndrome (APSS) (Cassidy et al., 2005) which presents with spontaneous, painless, peeling of the superficial skin of the palms and soles of the feet, however no mouse model of TG5 deficiency has as yet been reported.

TG3 is secreted as an inactive 77kDa zymogen and following activation (by cathepsin) is able to cross-link proteins such as loricrin and involucrin during CE formation in the upper granular skin layer and within the inner root of hair follicles. Although no human disease resulting from TG3 defect or deficiency has been discovered, there are conference reports of $TG3^{-/-}$ mice showing curled fur and whiskers,(Iismaa et al., 2009) possibly due to a deficiency of crosslinking of the hair structural protein trichohyalin. TG3, like TG2, possesses a GTP binding domain and has been shown to be expressed at high levels in the amygdala region of human brain samples (Kim et al., 1999) but further work is needed to determine the roles of TG3 in normal physiology as well as its potential function in disease states.

1.4.4 Transglutaminases 4, 6, 7 and band 4.2

The remaining transglutaminase (TG4, 6, 7 and band 4.2) are considerably less well understood, in part due to the absence of murine models of deficiency of these proteins and/or the lack of a clear role in human disease.

TG4 or prostatic transglutaminase is a 73kDa protein present in the prostate gland, prostatic fluid and seminal plasma of male rodents and humans.(Eckert et al., 2014) Rat studies have shown that this enzyme is regulated by androgen levels,(Dubbink et al., 1998) and deficiencies in TG4 cross-linking function lead to defective copulatory plug formation and decreased fertility in rats and mice. Although initial studies about the role of TG4 in prostate cancer were conflicting, it now seems likely that TG4 expression correlates with the “aggressiveness” of prostate tumour cells and an increased ability to migrate and invade.(Jiang and Ablin, 2011) Davies *et al* have shown that TG4 is expressed in a prostate cancer cell line and knocking down transglutaminase function reduced invasive potential in these cells.(Davies et al., 2007) Differential expression of several splice variants of TG4 in prostate cancer versus benign prostatic hypertrophy has also been cited as potential marker of disease (Cho et al., 2010) but this has not been borne out thus far; clearly a better understanding of the role of TG4 in this common, often chronic, malignant process may lead to earlier diagnosis and more targeted therapies in the future.

TG6 is poorly characterised in terms of structure and function. Recent molecular modelling studies suggest that TG6 requires proteolytic cleavage to generate the catalytically active form of the protein, and, like TG2, likely has GTP-binding (intracellular) functions as well as (extracellular) cross-linking roles.(Thomas et al., 2013) Expression of TG6 is highest in the brain, although transcripts are also seen in the testes and lung, and TG6 has been implicated in a number of neurological conditions including gluten ataxia (Hadjivassiliou et al., 2008a) and spinocerebellar ataxia type-35.(Guo et al., 2014) Gluten ataxia is a cerebellar disorder presenting with loss of coordination, gait abnormality and disorders of eye movement and is the result of the production of TG6 autoantibodies to the cerebellum of affected gluten-sensitive (coeliac disease) patients.(Hadjivassiliou et al., 2008b) TG6 autoantibodies can be present in patients with or without neurological symptoms and recently have also been implicated in a sub-type of Amyotrophic Lateral Sclerosis (ALS) or motor neurone disease.(Gadoth et al., 2015) Although TG6 function in health and development is poorly understood, mutations in the *TGM6* gene result in the autosomal dominant spinocerebellar ataxia type-35 (SCA35), a progressive neurological disorder seen within families in China.(Guo et al., 2014) No mouse model of TG6 is currently available however the development of such a knockout could provide vitally important insights into these devastating conditions.

TG7 is the least well studied of the transglutaminases and no genetic KO models of this enzyme exist. TG7 appears to be ubiquitously expressed although high levels have been reported in testicular and lung tissue specifically.(Eckert et al., 2014) Despite this, the function of TG7 is as yet unknown and no specific role in human disease pathogenesis has been reported although there is a single observational study from Jiang *et al* (Jiang et al., 2003) suggesting that TG7 expression is increased in breast tumour samples as compared to normal breast tissue. Whether this represents compensatory upregulation following loss of another transglutaminase or a similar role of TG7 to that of TG2 in tumour metastasis remains to be seen.

Band 4.2, a 72kDa protein found on the cell membrane of red blood cells, is the only catalytically inactive member of the transglutaminase family,(Iismaa et al., 2009) due to the active site substitution of alanine for cysteine,(Korsgren et al., 1990) but it is able to bind ATP and has role in maintaining erythrocyte shape and membrane stability.(Eckert et al., 2014) Band 4.2 appears to act by regulating the association of band 3 (also known as anion exchanger 1 (AIE-1)) with Ankyrin (band 2.1), a protein that facilitates attachment of membrane proteins to the structural cytoskeleton. Mutations encoding band 4.2 are rare but account for an

atypical form of hereditary spherocytosis in humans (primarily seen in Japanese patients) giving rise to haemolytic anaemia, jaundice and splenomegaly. In mice, deficiency of band 4.2 (Peters et al., 1999) gives rise to dehydrated red blood cells (RBCs) that are smaller and spheroid in shape. These mice are phenotypically normal with only mild anaemia and show no changes in the rhesus protein complex, which is altered in human deficiency, thus highlighting the importance of recognising differences in phenotype (and severity) between human disease and transgenic mouse models and the potentials dangers of extrapolating from one to the other.

1.4.5 TG2 and FXIII-A inhibitors

Transglutaminase 2 inhibitors have been proposed as potential therapeutic targets for a number of pathological conditions including pulmonary (Olsen et al., 2011b) and liver fibrosis,(Daneshpour et al., 2011) as well as neurological diseases such as Alzheimer's (Johnson et al., 1997) and Huntington's Disease.(Prime, 2011) It has been hypothesised that selective inhibition of FXIII-A may be a viable therapeutic approach to thrombosis,(Lorand, 2000a, Leidy et al., 1990) atherosclerosis (Lorand, 2000a) and in limiting the complications of indwelling central venous catheters.(Daneshpour et al., 2013) These theoretical therapeutic agents would function to inhibit the enzymatic activity of the TGs, i.e. their cross-linking ability, and relies on the assumption that the role of TGs in these disease processes is based on their TG function, rather than on the other described roles of TG2 and (to a lesser extent) FXIII-A. As further knowledge is acquired about the multitude of functions undertaken by TG2/FXIII-A and their roles in important cellular signalling, it may be that inhibition is deemed more or less favourable but certainly, TG inhibitors in general suffer from a lack of specificity; both in terms of specificity of inhibition of enzymatic activity and with regards specificity of inhibition of one TG over another.

Reported TG inhibitors can be classified as either irreversible (the majority of which target the active site cysteine residue) or reversible, of which there are competitive and non-competitive sub-types. Irreversible inhibitors, also known as suicide inhibitors, prevent substrate binding by covalently modifying the enzyme and include halomethyly carbonyls (such as iodoacetamide), the Michael acceptors and sulfonium inhibitors which are negatively charged at physiological pH and hence have been proposed as a viable target to the extracellular pool of TG2.(Keillor et al., 2015) These irreversible inhibitors all contain an electrophilic "warhead" which can react with the catalytic cysteine residue (Siegel and Khosla, 2007) and a number of these agents have been used in *in vivo* studies, for example in a murine model of

diabetic nephropathy (Huang et al., 2009) where irreversible TG2 inhibition with NTU281 (a sulfonium) was shown to reduce collagen accumulation and improve the disease parameters of serum creatinine and albuminuria.

Competitive inhibitors of TGs are those which act as an enzyme substrate themselves and hence compete with the natural amine substrates in the cross-linking reaction. These drugs include the widely used monodansylcadaverine (MDC) and in general are widely available (and hence widely used), stable and non-toxic.(Siegel and Khosla, 2007) Cystamine also acts as a competitive inhibitor of TG2 and has been used in a number of models (both cellular and animal) of neurodegenerative disease, (Junn et al., 2003, de Cristofaro et al., 1999, Karpuj et al., 2002) however this molecule also *inactivates* TG2 over time, possibly via the oxidation of the disulphide bond within the active site. The competitive TG inhibitors are non-specific and will inhibit all TGs and although useful *in vitro* they pose a theoretical risk of generating aminated proteins *in vivo* which could promote an autoimmune response similar to that seen in CD.

The non-competitive reversible inhibitors are a group of compounds which prevent TG activity but do not covalently modify the enzyme, and include GDP/GTP analogues (which, on binding, promote the “closed” conformation of the enzyme and thus prevent access to the active site), zinc ions (which compete with the calcium binding site(s) to prevent activity) and others. It should be noted however that TG3 and TG5 also bind GTP, and all the TGs are calcium dependent and hence these agents will still have potential problems with specificity.(Badarau et al., 2013)

Recent advances in the design and development of TG inhibitors has included the use of high throughput screening to identify small molecules which have the potential to inhibit enzyme activity. One such study by Yakubov *et al* (Yakubov et al., 2014) targeted the binding of fibronectin to TG2 (because of the known role of this interaction in facilitating β-integrin mediated cell adhesion), and found that inhibition of this binding site could block cell migration, invasion and proliferation without affecting TG2 enzyme activity. Given that TG2 is increasingly implicated in numerous signalling pathways it may be that target of its binding partners may prove to be a mechanism by which inhibition can be localised to (for example) areas of high cell activity in cancer. Work from our group has utilised molecular modelling to modify the known binding of the natural compound cerulenin (produced by a rice fungus) to FXIII-A to try to generate novel FXIII-A inhibitors.(Avery et al., 2015) Although the resulting compound was selective when

compared to cathepsin S, it was still not able to differentiate between FXIII-A and TG2, again highlighting the challenges of drug design in this field.

Clearly the ability to inhibit TG function has potential therapeutic benefits in a number of conditions and the speed of discovery in this area has increased dramatically in recent years however it is important that we continue to investigate the role of TGs and their mechanisms of action, particularly in terms of arterial protection and response to injury. This understanding may help to mitigate the cardiovascular side effects of treatment with TG2 inhibitors or, if TG2 activity is found to have a detrimental effect in arterial injury, may identify a new condition in which TG2 inhibition is desirable.

Chapter 2: TG2 and FXIII-A Deficiency

Chapter 2: TG2 and FXIII-A Deficiency

Animal studies allow the "integrated actions of proteins to be evaluated in the setting of diverse cellular contexts and inputs",(Iismaa et al., 2009) and murine models are increasingly used in basic scientific research because of their advantages in terms of small size, relative inexpensiveness and the ability to manipulate specific genes either by modification, addition or deletion. This chapter introduces the three mouse lines utilised in this work; the TG2-deficient mouse ($TG2^{-/-}$), the FXIII-A deficient mouse ($FXIII\text{-}A^{-/-}$) and the double deficient mouse ($TG2^{-/-}$.$FXIII\text{-}A^{-/-}$ or DKO).

2.1 TG2 and FXIII-A deficient mouse lines

Given the multiple ascribed roles of TG2, it would seem likely that knockout of the *TGM2* gene would prove lethal or at least generate severe phenotypic abnormalities. This has not been observed in either of the two widely used $TG2^{-/-}$ mouse lines, leading to suggestions that upregulation of, and compensation by, other transglutaminases occurs. Numerous authors have hypothesised that compensation may occur between TG2 and FXIII-A, however evidence for this is lacking and Ismaa *et al* (Iismaa et al., 2009) have called for use of a double-knockout mouse model to dissect the "overlapping or opposing roles" of these two enzymes. The published literature relating to these mice is summarised (where available) and background data from our previously established collaboration with the Bristol Heart Institute is provided as context to the results from this thesis.

2.1.1 The Graham TG2-deficient mouse

Mice derived by Prof Graham at the Victor Chang Institute in Sydney (Nanda et al., 2001) (and utilised by us in this work) are produced by cre-lox recombination,(Sauer and Henderson, 1988) whereby lox-P sites are inserted into introns 5 and 8 of the *TGM2* gene (flanking the catalytic core domain). These "floxed" mice are crossed with transgenic mice expressing cre-recombinase in the germline (under the control of the ubiquitous CMV-promoter) to generate $TG2^{-/-}$ mice (Figure 12). These $TG2^{-/-}$ mice show no gross phenotypic abnormality and are born at normal size and weight and with expected Mendelian frequency. Specifically, Nanda *et al* report that developmental apoptosis is not impaired,(Nanda et al., 2001) although dexamethasone induced apoptosis of thymocytes revealed an increased susceptibility to death and increased clearance of dead cells. Mearns *et al* have shown that these $TG2^{-/-}$ mice do show some

deficiencies in dermal healing (Mearns et al., 2002) with a reported role of TG2 in promoting cell proliferation and stabilising collagen fibrils.

Professor Graham and his collaborators have gone to considerable lengths to show that TG2 is not involved in glucose homeostasis and have challenged the views of others who suggest that TG2 is a candidate gene for maturity-onset diabetes of the young (MODY). They report that TG2 deficiency on both a C57Bl/6 and a 129T2/SvlmsJ background is not associated with any difference in fasting blood glucose or serum insulin level (compared to WT mice from the same congenic background) or in the response to either oral or intra-peritoneal (IP) glucose challenge.(Iismaa et al., 2013) Furthermore, they show that constitutive activation of the transamidase activity of TG2 (via generation of the $TG2^{R579A}$ mouse) does not result in any change in glucose homeostasis. They (and others)(Leiter, 2002) advocate the use of >2 strains of unrelated mice when confirming metabolic phenotype, as it is clear that susceptibility to DM is influenced by components of parental genetic background in ways that are as yet undefined.

Similar strain differences have been described in the response of $TG2^{-/-}$ mice to hepatic injury with both protective and pathological roles of TG2 reported,(Nardacci et al., 2003, Sarang et al., 2005, Tatsukawa et al., 2009b, Strnad et al., 2007) highlighting the importance of accurate reporting of strain background data and emphasizing the need for sequential back-crossing to achieve a known genetic background.(Wong, 2002, Lambert, 2007)

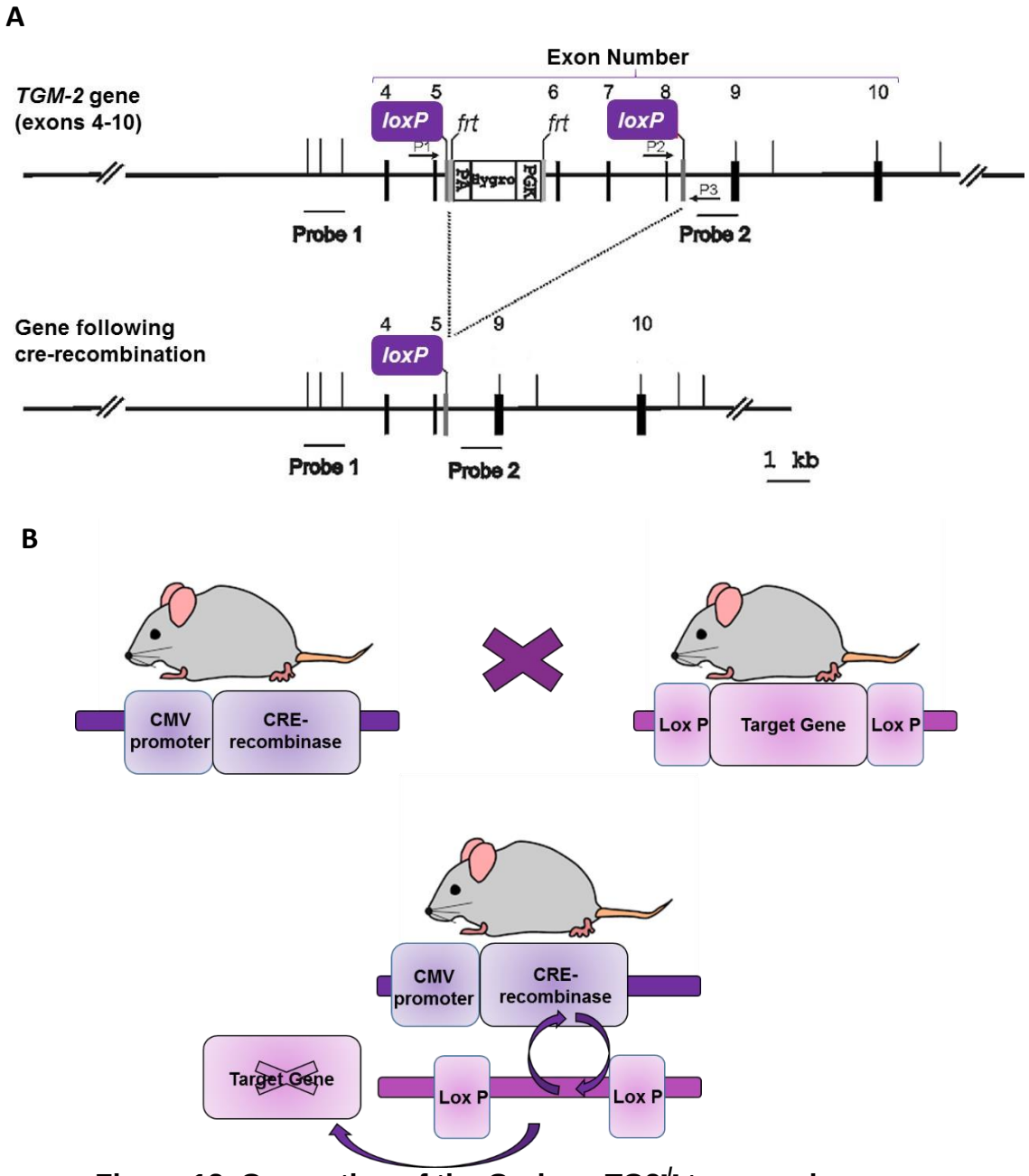

Figure 12. Generation of the Graham TG2$^{-/-}$ transgenic mouse

Panel A depicts a schematic of the cre-lox strategy used by Nanda *et al* (Nanda et al., 2001) whereby loxP sites are inserted within introns 5 and 8 of the *TGM2* gene, flanking the catalytic core domain. Panel B shows that "floxed" (flanked by loxP) mice are then crossed with mice expressing cre-recombinase in the germline (under the control of the ubiquitous CMV-promoter). Recombination occurs between the loxP sites in all cells and the *TGM2* gene is no longer expressed, generating TG2$^{-/-}$ offspring.

2.1.2 The Melino TG2-deficient mouse

Mice generated by homologous recombination by Melino *et al* (De Laurenzi and Melino, 2001) have replacement of 1.2kbp of the *TGM2* gene with a neomycin resistance gene. These mice show loss of the TG2 protein however demonstrate some residual TGase activity despite the replacement of exon 6 which contains the enzymatic active site of TG2; this residual activity is hypothesised to be due to TG1 function. These knockout mice (on a mixed background) show no phenotypic, developmental or reproductive abnormality and show normal induction of apoptosis in both thymocytes and mouse embryonal fibroblasts (MEFs). Szondy *et al* demonstrated, however, that these mice show marked suppression of macrophage uptake of apoptotic cells as well as features of autoimmunity.(Szondy et al., 2003)

This transgenic line has been utilised in numerous studies and has highlighted potential roles of TG2 in sepsis,(Bijli et al., 2014) in the development of post-injury intimal hyperplasia (Min et al., 2014) and, as discussed above, in glucose homeostasis. Bernassola *et al* reported in 2002 that these TG2-deficient mice were glucose intolerant and hyperglycaemic due to impaired insulin secretion, a situation analogous to that seen in MODY.(Bernassola et al., 2002) In contrast to these results, a hypoglycaemic response was observed following exogenous insulin challenge, which, the authors hypothesise, is due to a compensatory increased insulin sensitivity in peripheral tissues. This situation is not recapitulated in the MODY population, and has not been observed in the Graham mouse and hence its relevance to human disease is unclear. Given the more severe phenotype of the Melino $TG2^{-/-}$ mouse, and the fact that there is no universally accepted TG2-deficient mouse model, we elected to use the Graham TG2-deficient mouse in our work. This mouse was kindly provided by Professor Bob Graham and was imported on a known C57Bl/6 background, eliminating the highlighted issues of mixed strain backgrounds and their variable phenotypes.

2.1.3 The Dickneite FXIII-A-deficient mouse

Dickneite and colleagues produced a FXIII-A-deficient mouse line (on a mixed 129Ola/CBACa background) by homologous recombination, with replacement of exon 8 (coding exon 7) by a neomycin phosphotransferase selectable cassette.(Lauer et al., 2002) Heterozygote offspring ($FXIII\text{-}A^{+/-}$) have plasma activity that is 50% reduced when compared with WT and show no obvious phenotype, whilst the KO mice have absent plasma FXIII-A activity and show increased tail-tip bleeding with decreased clot stability and rapid clot degradation. Subsequent studies have shown that these FXIII-A deficient mice show no differences in the number of pregnancies achieved, however parturition rates are decreased, with a

higher occurrence of miscarriage, maternal bleeding events (including subcutaneous bleeding, haemothorax and haemoperitoneum),(Koseki-Kuno et al., 2003) and maternal death. As mentioned earlier, male FXIII-A deficient mice produced by this technique show a gender-specific decreased survival rate thought to be related to cardiac haemosiderin deposition and subsequent fibrosis. These pathological changes were found in male mice that had died spontaneously as well as those sacrificed at 10 months of age despite apparently normal cardiac function *in vivo*.(Souri et al., 2008b)

Recent work from Myeni *et al* has implicated FXIII-A in pre-adipocyte proliferation and differentiation (Myneni et al., 2014) and has suggested that the transglutaminase activity of FXIII-A leads to crosslinking of fibronectin and matrix assembly. This in turn provides a framework on which pre-adipocytes can proliferate more readily (in response to insulin) and thus these cells differentiate at a lower rate, resulting in less lipid accumulation. This work, combined with findings of increased circulating FXIII-A levels in patients with type 2 diabetes (Mansfield et al., 2000) and associations of *F13A* gene SNPs with obesity in GWAS studies (Naukkarinen et al., 2010) have prompted suggestions that FXIII-A may play a key inhibitory role in the development of obesity. Crucially, there have been no reports of obesity in the Dickneite FXIII-A-deficient mouse, and obesity and/or metabolic dysfunction are not recognised phenotypes of patients with FXIII-A deficiency. Further evidence to support or refute this purported role of FXIII-A has been called for (Mosher, 2014) and would obviously be extremely important given the current, and increasing, global obesity epidemic.

Personal communication from the facilities manager at Harlan laboratories (and confirmed by our collaborators in Bristol) revealed that the Dickneite transgenic line underwent a phenotypic shift with continued breeding. In contrast to the reports of Koseki-Kuno,(Koseki-Kuno et al., 2003) pregnancy and delivery was achieved in homozygous KO females (on a mixed background) without any increase in bleeding or mortality. This shift occurred with no concurrent change in the impaired clotting phenotype and unstable thrombi that were more liable to embolisation were observed on intravital microscopy. This observation lends weight to the hypothesis that FXIII-A plays a role in (placental) vessel integrity and that this role is distinct from its crosslinking function in coagulation.

To enable us to produce cell-type-specific FXIII-A KO animals for a programme of work investigating the cellular source of pFXIII-A (see section 1.4.2), and in light of concerns about the stability of the vascular phenotype, we chose not to utilise the Dickneite mouse, instead commissioning the generation of a novel floxed FXIII-A

mouse from GenOway (Lyon, France). Details of the cre-lox strategy utilised in the generation of this mouse are shown in Figure 13 and results from the characterisation of this mouse are discussed in Chapter 5.

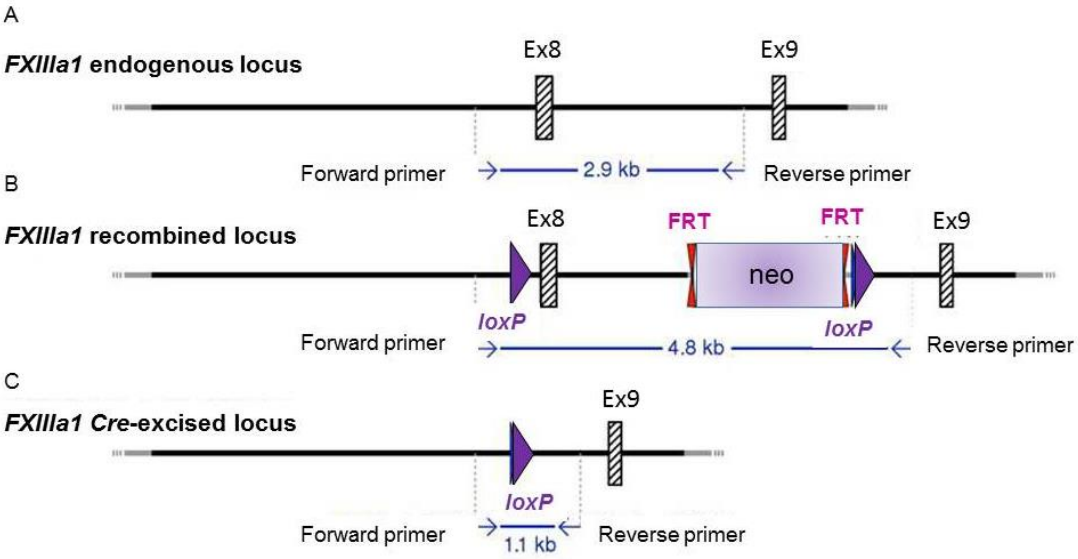

Figure 13. Generation of the FXIII-A$^{-/-}$ transgenic mouse

Schematic of the cre-lox strategy used by GenOway in the generation of our novel floxed FXIII-A mouse. The endogenous gene locus is shown **(A)** as is the locus with the addition of LoxP sites which were inserted adjacent to exon 8 of the *FXIIIa1* gene **(B)**. A neomycin cassette flanked by FRT sites is utilised for selection of embryonic stem cells. This neomycin cassette was later excised by flp-recombination to generate FXIII-A floxed mice **(C)** that can be used for breeding of conditional KO lines. We crossed this (mixed background) mice with mice expressing cre-recombinase under the control of the ubiquitous CMV promoter to generate a constitutive FXIII-A KO line. Back-crossing to >95% C57Bl/6 background was undertaken to eliminate issues with mixed-strain backgrounds.

2.2 TG2 and FXIII-A double knockout mouse line (DKO)

2.2.1 Rationale for generation of DKO

It has been widely suggested that some of the pleiotropic functions of FXIII-A and TG2 may overlap as they often co-localise intracellularly and both perform intra- and extra-cellular cross-linking.(Iismaa et al., 2009) There is also significant substrate overlap between the two enzymes (e.g. fibrin, vimentin, osteopontin, type III collagen, α-2-antiplasmin and PAI-2 are all crosslinked by both TG2 and FXIII-A) and both transglutaminases are expressed and activated in response to tissue injury.

Specifically, overlapping roles for TG2 and FXIII-A have been proposed in the cardiovascular system and in the skeletal system during epiphyseal growth plate maturation. Expression of TG2 has previously been shown to correlate with chondrocyte differentiation and matrix mineralisation (Aeschlimann et al., 1993, Nurminskaya et al., 1998) and in 2009, Tarantino *et al* reported that expression of FXIII-A was increased 5-fold in the distal femoral epiphysis of newborn $TG2^{-/-}$ mice which they cite as evidence of functional compensation between the two enzymes.(Tarantino et al., 2009) Certainly cultured osteoblasts show a lack of mineralisation in the presence of the relatively non-specific TGase inhibitor cystamine (Nakano et al., 2007) but this may not reflect the situation *in vivo* and transglutaminase-independent pathways of mineralisation have also been reported.(Johnson et al., 2003a)

Arterial calcification is thought to occur through a process analogous to that in the skeletal system and staining for both TG2 and FXIII-A is seen in calcified atherosclerotic plaques.(Matlung et al., 2009) Van Herck *et al* reported that TG2-deficient mice have a more vulnerable plaque structure but show no difference in the number of buried plaques (a surrogate for plaque rupture).(Van Herck et al., 2010) They hypothesise that this is due to compensation by FXIII-A which is expressed within the atherosclerotic plaque and possibly released by infiltrating macrophages. Similar overlapping roles have also been proposed in the formation of coated platelets (Jobe et al., 2005) since platelet lysates from FXIII-A deficient mice show an increased transamidase activity, suggesting that TG2 may compensate for a lack of cross-linking activity in this process.

The most convincing evidence for compensation is from Bakker *et al* (Bakker et al., 2006) who showed that $TG2^{-/-}$ mice demonstrate delayed flow-dependent inward remodelling. This was associated with an increase in arterial expression of FXIII-A and significant transglutaminase activity at the site of injury. Administration of liposome-encapulsated clodronate to remove monocyte/macrophages reduced this

FXIII-A expression and abolished the delayed remodelling, suggesting that macrophage-associated FXIII-A is compensating for a lack of TG2.

Given the above evidence, it is a clear that a mouse deficient in both TG2 and FXIII-A (if viable and lacking any severe phenotype) would eliminate the confounding effects of compensation observed in single KO mice and would enable the investigation of the functions of these enzymes in the cardiovascular and skeletal systems as well as revealing other, potentially unexpected, roles.

2.2.3 ApoE/TG2/FXIII-A triple knockout (TKO) mouse

Work performed previously by us and in collaboration with the University of Bristol has utilised a triple knockout mouse line with "knockout" of both TG2 and FXIII-A on an Apo-$E^{-/-}$ background These mice were found to be viable, fertile, and grossly normal in appearance with no apparent deficiencies in growth or skeletal development (Cordell et al., 2015) and normal survival up to the age of 6 months. Specifically this work showed no evidence of compensatory upregulation of other transglutaminases to WT levels and there was no observed difference in terms of atherosclerotic plaque area or stability, as per previous work from our group (Williams et al., 2010) although a difference in plaque composition was seen.

Crucially, Newell *et al* have observed spontaneous cardiac fibrosis within the hearts of $ApoE^{-/-}$.$FXIII\text{-}A^{-/-}$ male mice, which correlates with haemosiderin deposition, possibly due to the extravasation of blood from "leaky" cardiac vessels (Newell et al, in preparation). This effect is exacerbated by the additional absence of TG2 however no cardiac fibrosis was observed in the $ApoE^{-/-}$.$TG2^{-/-}$ cohort, suggesting that TG2 compensates for FXIII-A deficiency, but that dual deficiency leads to impaired vessel integrity. Although cause of death data was not collated in this study there was a significantly increased observed mortality in the $ApoE^{-/-}$.$FXIII\text{-}A^{-/-}$ and TKO groups when the mice were subject to a 12-week period of high-fat feeding (mortality rate: $ApoE^{-/-}$ 2.0%, $ApoE^{-/-}$.$FXIII\text{-}A^{-/-}$ 13.2% ($p<0.05$), $ApoE^{-/-}$.$TG2^{-/-}$ 2.2%, TKO 20.5% ($p<0.01$)). The confounding $ApoE^{-/-}$ background utilised in this work (designed primarily to investigate atherosclerosis) may obviously explain some of these findings and ApoE may have anti-oxidant and anti-proliferative effects (Zadelaar et al., 2007) (which could contribute to its protective role in atherosclerosis), as well as immunomodulatory effects.(Laskowitz et al., 2000, Tenger and Zhou, 2003).

Some authors have suggested that $ApoE^{-/-}$ deficiency can lead to increased permeability in the blood-brain-barrier (BBB) of KO mice (Methia et al., 2001, Hafezi-Moghadam et al., 2007) with implications for the pathobiology of Alzheimer's disease and other neurodegenerative conditions. Although Methia et al did not

observe increased permeability in the systemic vasculature, others have reported increased Evans Blue leakage in atherogenesis-prone areas (in the aorta and carotid) in $ApoE^{-/-}$ mice.(Lundeberg et al., 2015, Phinikaridou et al., 2012) The ability to investigate the overlapping roles of TG2 and FXIII-A without the $ApoE^{-/-}$ background is obviously critical in my project and in future work pertaining to cardiac fibrosis.

As part of the work undertaken by Newell *et al*, a carotid artery ligation model was utilised to stimulate local vascular remodelling, with thrombosis and neointimal formation typically seen in wild-type mice. The results of this work are currently in preparation for publication and are summarised in Figure 14. Unexpectedly the TKO mice displayed vessel damage with frequent elastic lamellar breaks and ultimate vessel rupture. Such a finding could be explained by decreased vessel stability (due to TG2 deficiency) combined with an increased bleeding tendency (due to FXIII-A deficiency) or alternatively could be due to a dual effect of both TGs on arterial structure. The carotid ligation model does not allow for differentiation between these two hypotheses, in contrast to the tunable $CaCl_2$ injury model. It should be noted however, that similar breaks were also seen in operated TG2-deficient mice and even in sham-operated triple knockouts (although without rupture) indicating that TG2 confers vessel wall stability, but that both transglutaminases can contribute to maintaining arterial integrity under basal conditions.

Elastic lamellar flattening - a feature preceding aneurysm development - was also seen in the triple knockout mice and dilatation of the carotid artery was observed in the ApoE/TG2 double knockout mice, thus adding weight to the hypothesis that FXIII-A and TG2 have overlapping structural roles and one (likely TG2) or both may be implicated in aneurysm formation. The use of a targeted, modifiable injury model to tease out the roles of TG2 and FXIII-A (without a ApoE-deficient background) in vessel stability, repair and aneurysm formation is an obvious “next step” to the work presented here and I am grateful to Drs Newell and Jackson for their advice and guidance in the early stages of this project.

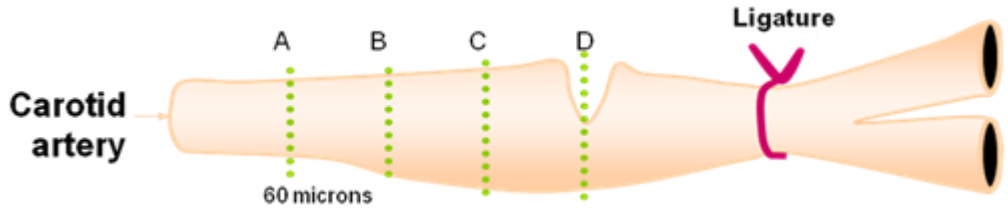

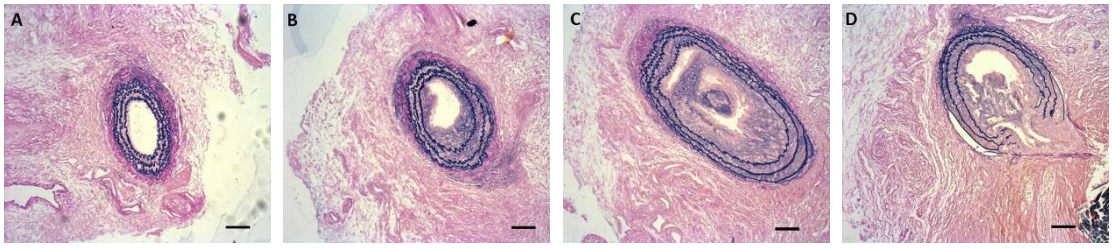

	ApoE$^{-/-}$.FXIII-A$^{-/-}$	ApoE$^{-/-}$.TG2$^{-/-}$	ApoE$^{-/-}$.TG2$^{-/-}$.FXIII-A$^{-/-}$
Vessel Dilatation	0	↑↑	(Died)
Vessel Wall Breaks	0	↑↑↑	(Died)
Vessel Rupture	0	0	↑↑↑

0/26

6/12

p<0.01

Figure 14. Carotid artery ligation model – summary

Schematic showing carotid artery model. **Panels A-D** show representative histology at each of points A-D from the ligated carotid artery in the triple knockout mouse. **Panel C** demonstrates the characteristic flattening of the elastic lamellae and vessel dilatation whilst **D** shows elastin breaks and vessel rupture. The table summarises the results from this work with TG2-deficient mice showing vessel wall breaks and increased medial area (vessel dilatation) as in early aneurysm formation. The triple knockout mice showed a severe phenotype with vessel rupture and a significantly increased mortality rate when compared to either of the single-transglutaminase deficient mouse lines. Scale bars represent 100µm. All images and data received from L. Newell with thanks.

Chapter 3: Hypothesis and Aims

Chapter 3: Hypothesis and Aims

3.1 Hypothesis

Under basal conditions both TG2 and FXIII-A contribute to the maintenance of arterial integrity. TG2 appears to be more important for stability under conditions of stress or injury and hence would determine the response to aneurysm induction. TG2 can compensate for FXIII-A deficiency and therefore FXIII-A does not play an essential role under conditions where TG2 is expressed and can be considered as an anti-thrombotic target.

3.2 Aims

1. Generate and characterise mice deficient in TG2, FXIII-A and both TG2 and FXIII-A on a C57Bl/6 background
2. Elucidate the roles of TG2 and FXIII-A in basal vessel structure and function, and investigate the evidence for upregulation of other transglutaminases to compensate for single/dual deficiency.
3. Establish the murine calcium chloride model of abdominal aortic aneurysms in our Institute
4. Investigate the roles of TG2 and FXIII-A in aneurysm induction and progression using the above model.

Chapter 4: Materials and Methods

Chapter 4: Materials and Methods

4.1 Mouse breeding & husbandry

All animals were conventionally housed at the University of Leeds. Animal housing, husbandry, care and procedures were conducted in accordance with guidelines and regulations of the CBS unit of the University of Leeds and of the United Kingdom Home Office (Project license holder: Dr Stephen Wheatcroft – Nos. 40/3523 and 70/8115, Personal license holder: Miss Kathryn Griffin – No. 40/10367). All mice had *ad libitum* access to food (standard chow diet) and water throughout the duration of all studies unless specifically outlined.

4.1.1 Breeding strategy

TG2 heterozygote founder mice on a C57Bl/6 background were obtained from Professor Graham in Australia, housed in the CBS unit of the University of Leeds and crossed to generate $TG2^{-/-}$ progeny. Breeding was closely controlled to obtain true littermates and to regulate the availability of mice for experimental work.

To obtain FXIII-$A^{-/-}$ mice, mice floxed in the *F13A* gene (Figure 13) were crossed (by GenOway) with transgenic mice expressing cre-recombinase under the control of the ubiquitous CMV-promoter. These commercially obtained heterozygous mice were genotyped as detailed below and then bred to homozygosity with back-crossing (to >95% C57Bl/6) to eliminate strain differences. Double knockout mice were obtained following the strategy detailed in Figure 15. In brief, $TG2^{-/-}$ mice were crossed with FXIII-$A^{-/-}$ mice to generate double heterozygote ($TG2^{+/-}$FXIII-$A^{+/-}$) offspring. Further breeding with $TG2^{-/-}$ mice increased Bl6 background percentage at each generation whilst ultimately generating $TG2^{-/-}$FXIII-$A^{+/-}$ mice for eventual sib-cross breeding.

Although we undertook a trial breeding programme utilising FXIII-$A^{-/-}$ females (results outlined in chapter 5), KO pups were routinely obtained from heterozygous female breeding i.e. FXIII-$A^{-/-}$ male x FXIII-$A^{+/-}$ female.

4.1.2 Breeding and frequency calculation

To assess the impact of TG2 and FXIII-A deficiency on mouse fertility and breeding we analysed litter size and offspring genotype from the following breeding pairs (and trios where appropriate).

1. $TG2^{+/-}$ male x $TG2^{+/-}$ female
2. FXIII-$A^{WT/flox}$ male x FXIII-$A^{WT/flox}$ female

3. FXIII-$A^{-/-}$ male x FXIII-$A^{+/-}$ female
4. $TG2^{-/-}$.FXIII-$A^{-/-}$ male x $TG2^{-/-}$.FXIII-$A^{+/-}$ female

The average litter size was compared across these breeding pairs/trios and analysed by Kruksall Wallis testing. Observed genotype frequencies were compared to those expected by Mendelian inheritance and the chi-squared statistic used to assess statistical significance of any differences found.

4.1.3 Weighing

Groups of mice were weighed weekly to characterise any phenotypic differences between the transgenic lines and all mice subject to surgical procedures were weighed at regular intervals post-operatively to establish animal well-being (standard protocol; day 1, 2, 5, 7 and weekly thereafter). Animals were also routinely weighed prior to any study being undertaken to confirm “fitness” to undergo the procedure. Any animal showing >15-20% weight loss following any procedure was culled as per Home Office guidelines using an approved Schedule 1 method.

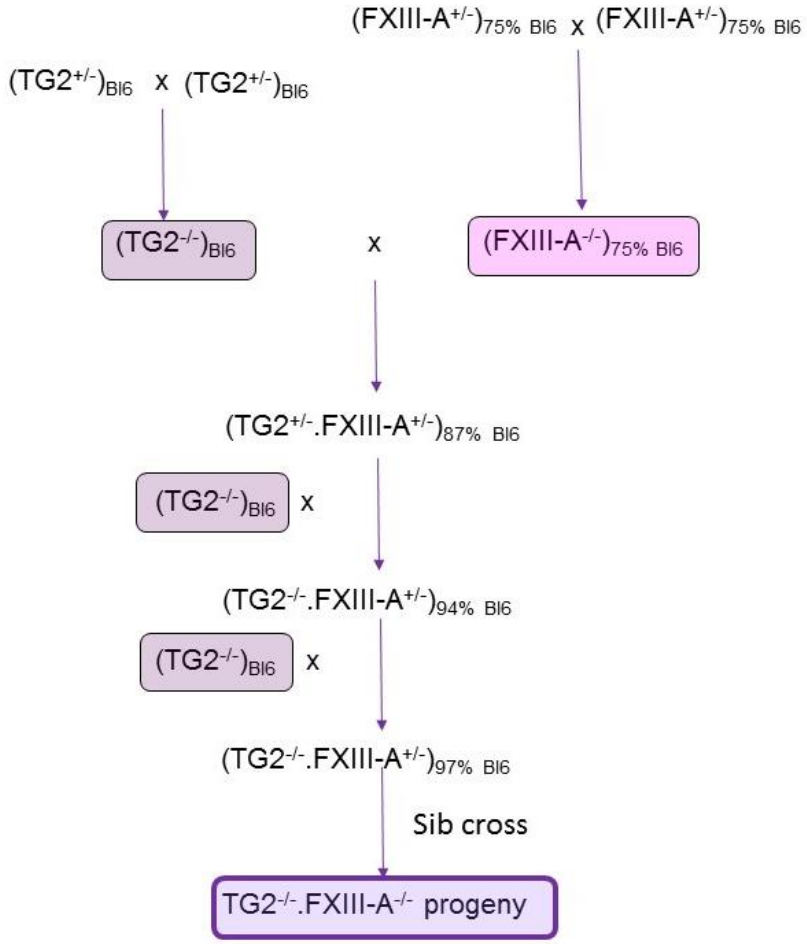

Figure 15. Breeding strategy to generate DKO offspring

Schematic outlining the breeding strategy implemented to generate pups deficient in both TG2 and FXIII-A for further experimental work. $TG2^{-/-}$ mice obtained from heterozygous founders were crossed with $FXIII\text{-}A^{-/-}$ mice to generate double heterozygote ($TG2^{+/-}FXIII\text{-}A^{+/-}$) offspring. Further breeding with $TG2^{-/-}$ mice increased Bl/6 background percentage at each generation whilst ultimately generating $TG2^{-/-}FXIII\text{-}A^{+/-}$ mice for eventual sib-cross breeding

4.2 Genotyping

4.2.1 DNA extraction

Mouse ear notch samples were obtained from newly weaned pups by CBS unit staff. These notches are used as both an identification system (see Appendix A: Murine ear code identification system) and as samples for DNA genotyping. DNA was extracted by placing the ear clippings in a PCR tube and adding 100µl of 25mM NaOH / 0.2mM EDTA. The sample was then heated in a Thermo cycler (Harlow Scientific, UK) to 95ºC for 20 minutes. 100µl of 40mM Tris-HCl was then added and the sample vortexed for a few seconds. After nano-drop (NanoDrop™ 1000 Spectrophotometer, ThermoScientific, UK) analysis to assess the DNA concentration and purity, samples were frozen at -20ºC prior to PCR.

4.2.2 Standard PCR and primer details

Standard PCR was used to determine the genotype of each sample (Figure 16). The PCR methods for each of the two genes of interest are described below with full details of the primer sequences (all from Sigma, UK) and amplicon sizes shown in Table 4. The TG2 primers were already in use in the lab and had previously been designed by Dr Richard Pease (University of Leeds) whereas de novo FXIII-A primers were designed specifically for this project.

4.2.2.1 TG2 PCR

Each reaction mixture was prepared using 0.5µL Taq polymerase (ThermoScientific, UK), 0.2 µL primer 1 *(RPmouP1L)* (amplifies knockout allele-specific sequence), 0.4µL primer2 *(RPmouP2L)* (amplifies wild-type allele-specific sequence), 0.4 µL primer 3 *(RPmouP3L*) (amplifies sequence common to both wild-type and knockout alleles), 0.5 µL dNTPs (Thermoscientific, UK), 2.5 µL of PCR buffer solution (ThermoScientific, UK), 17.3µL nuclease-free water and 2 µL 1:10 diluted DNA. Reaction mixtures were overlaid with 15 µL mineral oil (Sigma, UK) prior to PCR to prevent evaporation. PCR cycle details are as follows:

1. 94ºC for 2 minutes
2. 94ºC for 15s
3. 64ºC for 20s
4. 72ºC for 45s
5. Repeat steps 2-4 another 29 times
6. 72ºC for 5 minutes
7. Cool at 4ºC

Products were resolved on an agarose gel consisting of 2% w/v agarose (Bioline, UK), 150ml 1X TAE, and 15µl ethidium bromide. A molecular ladder (ThermoScientific, UK) was used to estimate amplicon size and the bands were visualised under UV light (G:Box scanner, Syngene, UK) after electrophoresis at 100V for 60 minutes.

4.2.2.2 FXIII-A PCR

Each reaction mixture was prepared using 0.5µL Taq polymerase (Thermoscientific, UK), 0.4 µL primer 1 *(13 intron8FL)* (amplifies knockout allele-specific sequence), 0.4µL primer 2 *(13i8R2)* (amplifies wild-type allele-specific sequence), 0.4 µL primer 3 *(13i9R2)* (amplifies sequence common to both wild-type and knockout alleles), 0.5 µL dNTPs (Thermoscientific, UK), 2.5 µL of PCR buffer solution (ThermoScientific, UK), 17.1µL nuclease-free water and 2 µL 1:10 diluted DNA. Reaction mixtures were overlaid with 15 µL mineral oil (Sigma, UK) prior to PCR to prevent evaporation. PCR cycle details are as follows:

1. 94ºC for 2 minutes
2. 94ºC for 15s
3. 62ºC for 20s
4. 72ºC for 45s
5. Repeat steps 2-4 another 29 times
6. 72ºC for 5 minutes
7. Cool at 4ºC

Products were resolved on an agarose gel consisting of 2% w/v agarose (Bioline, UK), 150ml 1X TAE, and 15µl ethidium bromide. A molecular ladder (ThermoScientific, UK) was used to estimate amplicon size and the bands were visualised under UV light (G:Box scanner, Syngene, UK) after electrophoresis at 100V for 90 minutes.

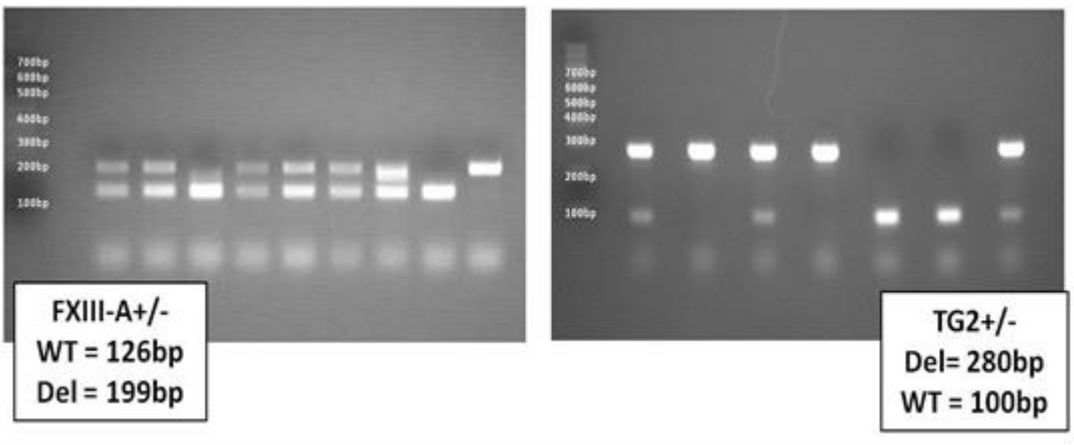

Figure 16. Genotyping of TG2 and FXIII-A deficient mouse lines

Images showing representative gels from the PCR genotyping of ear notches obtained from newly weaned pups. Panel A shows genotyping of nine samples from FXIII-A breeding with WT ($^{+/+}$) pups showing a single band of 126bp size, KO ($^{-/-}$) pups showing a single band of 199bp size and heterozygous offspring ($^{+/-}$) displaying both bands. Panel B shows genotyping of 7 samples from TG2 breeding with WT ($^{+/+}$) pups showing a single band of 100bp size, KO ($^{-/-}$) pups showing a single band of 280bp size and heterozygous offspring ($^{+/-}$) displaying both bands.

Gene	Target Allele	Sequence
TG2	KNOCK-OUT (280bp)	GGAGCACACAGGCCTTATGAGCTGAAG
TG2	WILD TYPE (100bp)	GCACAGATAGGGATACAAGAAGCATTGAAG
TG2	COMMON	GTCCTCGGATGACAAGGTGACAGAGCA
FXIII-A	KNOCK-OUT (199bp)	TCTGGGCCAAACCAAGTACCTGG
FXIII-A	WILD TYPE (126bp)	CAAGACCAGACTGTGCAAAGGG
FXIII-A	COMMON	GGGGCATTGCTCCCATGTAAA

Table 4. PCR primer details; amplicon length and target sequence

4.3 Metabolic testing

4.3.1 Glucose tolerance testing

Mice of 10 or 40 weeks of age were subject to an overnight fast (~16 hours) prior to weighing and measurement of baseline fasting glucose level. An intra-peritoneal (IP) injection of 200mg/ml glucose solution was then administered at a dosage of 1mg/g body weight and blood glucose measurements (in mmol/l) recorded at 30, 60, 90 and 120 minutes. All samples were obtained from a single tail bleed where possible and analysed using the Accu-chek® Aviva glucometer and test strips (Roche, UK). Mice were monitored for signs of distress throughout the study and food supply was restored immediately after the test had been completed. ANOVA testing was used to analyse group average values at each time point as well as summary area-under-the-curve data for the tolerance test as a whole.

4.3.2 Insulin tolerance testing

Mice of 10 or 40 weeks of age were subject to a 4 hour fast prior to weighing and measurement of baseline fasting glucose level. An IP injection of diluted Actrapid insulin (Novo Nordisk, UK) solution (0.2 iU/ml) was then administered at a dosage of 0.75 iU/kg body weight and blood glucose measurements (in mmol/l) recorded at 30, 60, 90 and 120 minutes, All samples were obtained from a single tail bleed where possible and analysed using the Accu-chek® Aviva glucometer and test strips (Roche, UK). Mice were monitored closely for signs of hypoglycaemia (irritability, lethargy and coma) and if present were given a “rescue” injection of glucose. ANOVA testing was used to analyse group average values at each time point as well as summary area-under-the-curve data for the tolerance test as a whole.

4.4 Tissue harvesting

4.4.1 IVC blood sampling

To obtain blood samples for FXIII-A activity, 8-10 week old mice were anaesthetised with isoflurane and blood was collected under direct vision from the inferior *vena cava* into syringes containing the anticoagulant CTAD (BD Biosciences, UK) using a 23 Ga needle. Blood to CTAD ratios (by weight) were recorded for later calculation and samples were placed on ice. Plasma was separated by centrifugation at 10000g for 10 minutes and then samples were stored at -20ºC prior to assay.

4.4.2 Organ harvesting

Tissue samples for analysis were obtained by standard operative techniques following perfusion exsanguination (with 5ml PBS) via the left ventricle under isoflurane general anaesthesia. Aortas were dissected free of surrounding tissue and samples from descending aorta (beyond aortic arch) to iliac bifurcation were extracted and snap frozen in liquid nitrogen prior to storage at -80ºC. Where required, carotids, hearts, livers, and spleens were also harvested, snap frozen and stored.

4.5 FXIII-A activity assay

FXIII-A activity was determined with a microtiter assay using fibrinogen and 5-(biotinamido)pentylamine as substrates, based on a method described by Song *et al*.(Song et al., 1994) Nunc Immuno Maxisorp 96-well microtiter plates (Nunc A/S, UK) were coated with 100µL per well of fibrinogen (Calbiochem, UK) at 40µg/mL in Tris buffered saline (TBS) (pH 8.3) and incubated at room temperature for 40 minutes, or overnight at 4ºC.

The microtiter plate was emptied and washed 3 times with 300µl per well of TBS (pH 8.3). To each well, 300µL of 1% BSA in TBS (pH 8.3) was added and the plate was incubated at 37°C for a minimum of 90 minutes before washing with 4 x 300µl per well of TBS (pH 8.3).

10µl of citrated mouse plasma samples, diluted 1 in 100, 1 in 200 or 1 in 400 (to give the equivalent of 0.1, 0.05 or 0.025µl neat plasma respectively) in TBS, was added in 3 duplicates to the wells, and the cross-linking reaction was started by addition of 150µL of the reaction mixture (see Appendix B).

After incubation at room temperature, the reaction was stopped at 7.5 minutes by addition of 200µL of 200mM EDTA. Wells were washed 4 times with 300 µL TBS1/0.1% Tween20 and incubated with 100µL of 10µg/mL streptavidin–alkaline phosphatase (Sigma, UK) in 1% BSA/TBS1 /0.1% Tween20 for 1 hour at 37°C.

After 4 washes with 300µL of TBS1/0.1% Tween20, colour was developed by incubation with 100µL of 1 mg/mL *p*-nitrophenyl phosphate (Sigma, UK) in 1 mol/L diethanolamine/0.5mmol/L $MgCl_2$ (pH 9.8), for 1 hour at 30ºC. Absorbance was measured at 405nm on a Labtek plate reader (ThermoScientific, UK) with readings taken every minute for the hour long incubation period.

4.6 Rotational thomboelastometry

Coagulation analysis of murine whole blood was undertaken by rotational thromboelastometry using the ROTEM® system (Tem Ltd, UK) which is an established viscoelastic method for haemostasis testing. Briefly, IVC blood samples were obtained as above and kept on ice prior to rapid transfer to the ROTEM® analyser. Each sample was analysed under three conditions designed to replicate either activation of clotting by 1) the extrinsic coagulation pathway or 2) the intrinsic coagulation pathway or 3) the fibrinolysis of the formed clot. In each case, a disposable pin is suspended in the whole blood sample (150µl) and rotated slowly back and forth to mimic venous blood flow. Changes in elasticity in the developing and resolving blood clot are then transmitted using an optical detector system, and are displayed graphically. Measures of clotting time (CT, time until the sample starts to clot), clot formation time (CFT, time taken to reach a clot firmness of 20mm), alpha angle (a surrogate of CFT), maximum clot firmness (MCF, reflecting the absolute clot strength) and lysis index (LI30, the % of the remaining clot stability in relation to maximum clot firmness at 30 minutes) were recorded and analysed by ANOVA with Bonferroni correction for multiple testing.

A.

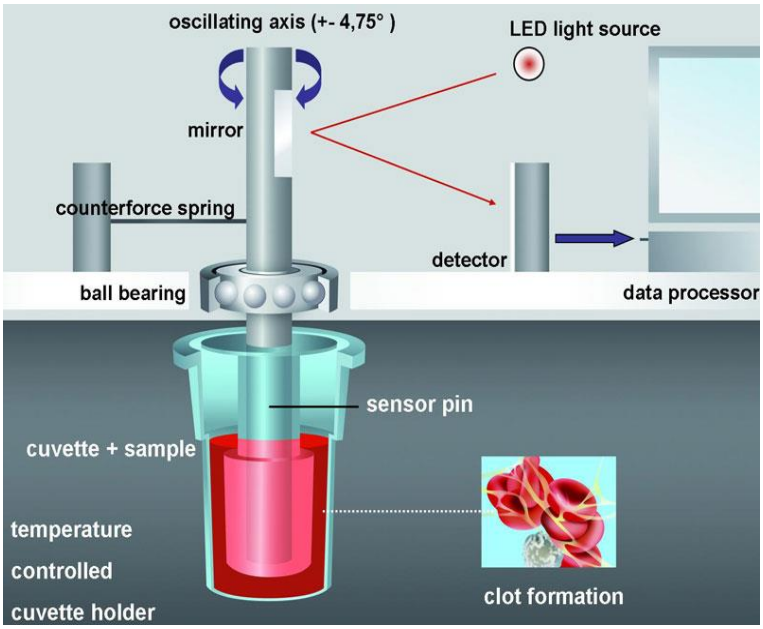

B.

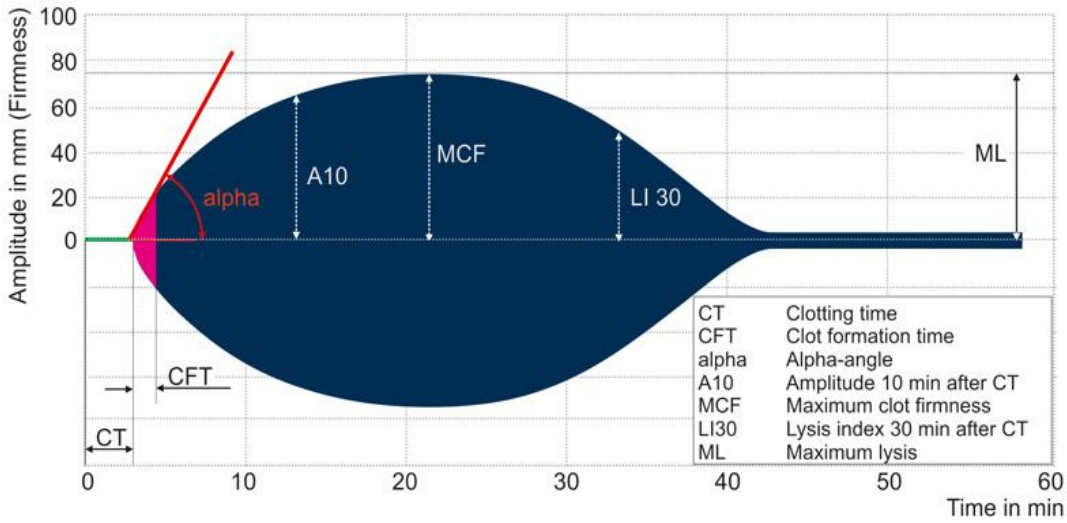

Figure 17. ROTEM® – experimental set up and representative trace

Panel A illustrates the experimental set up for the ROTEM® system whereby a suspended pin is rotated within the whole blood sample. As a clot is formed the movement of the pin is impeded and this resistance is transmitted by the optical detection system resulting in a graphical output. **Panel B** demonstrates a typical trace from the ROTEM® system and highlights the key measured parameters of clotting time (CT), clot formation time (CFT), alpha angle, maximum clot firmness (MCF) and lysis index (LI30). Both images are freely available downloads from the ROTEM® page of the TEM group (Basel, Switzerland) product website accessed June 2016 (https://www.rotem.de/en/products/rotem-delta/)

4.7 Quantitative RT-PCR

4.7.1 RNA extraction

RNA was extracted from snap-frozen tissues using the TRIzol method, whereby 1ml of TRIzol reagent (Life Technologies, UK) was added per 100mg of lysed tissue. Phase separation was undertaken by addition of 100µl of bromochloropropane (per ml of TRIzol), incubation, and centrifugation at 12000g for 15 minutes at 4ºC. The aqueous phase was then retained and precipitated with 10µl of glycogen and 0.5ml of ice-cold isopropanol. After centrifugation, the supernatant was removed and the pellet repeatedly washed with 75% ethanol and centrifuged (at 7500g for 5 minutes at 4ºC). The pellet was then re-suspended in RNAse-free water and either stored at -80ºC or DNA contamination was removed immediately using the Turbo^{TM} DNAse kit (Ambion, Life Technologies, UK). RNA concentration and purity was analysed using the NanoDrop^{TM} 1000 Spectrophotometer (ThermoScientific, UK) and if required, ethanol precipitation was performed to concentrate and de-salt preparations.

4.7.2 Reverse transcription

Reverse transcription was performed using the Applied Biosystems High capacity cDNA reverse transcription kit (Life Technologies, UK). Samples were placed in a thermal cycler under optimised conditions (25ºC for 10 minutes, 37ºC for 2 hours, 85ºC for 5 minutes, 4ºC to cool) and the resultant cDNA diluted 1 in 10 to give a 10ng/µl solution for real-time PCR.

4.7.3 Reference gene determination

Personal experience from our lab and pilot data from this thesis revealed that standard reference or “housekeeping genes” such as GAPDH may show considerable variation in expression in different mouse tissues; several authors have suggested that reference genes should be selected for each experimental model used and/or that multiple reference genes used in combination may provide a better reference than any one gene in isolation.(Barber et al., 2005, Szabo et al., 2004, Hruz et al., 2011)

A combination of literature searching, personal communication (from the Baxter group, Nebraska, USA) and use of the “Refgenes” online tool (Hruz et al., 2011) (available from http://www.refgenes.org/rg/) revealed that both β-actin (a cytoskeletal actin involved in cell motility, structure and integrity) and Rpl-32 (a ribosomal protein component of the 60S subunit) have been suggested as suitable reference genes for use in studies of arterial gene expression. Testing with qPCR of

aortic samples (addition of presumptively similar amounts of DNA) across the different experimental genotypes revealed some minor variation in the expression of β-actin with relative stability of expression of Rpl-32. This data is shown below (Figure 18). For all further qPCR we used both β-actin and Rpl-32 as reference genes, standardising to the arithmetic mean of the Ct values obtained from each assay.

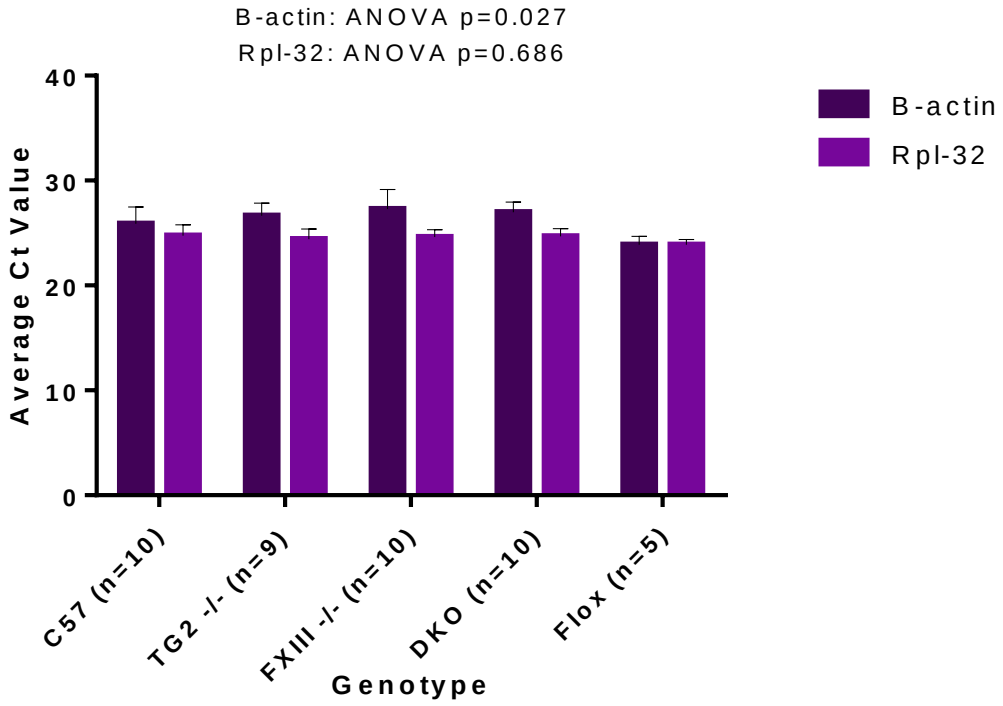

Figure 18. Reference gene determination

qPCR of aortic samples was undertaken to assess variability of gene expression of two potential reference genes; β-actin and Rpl-32. Average Ct ("crossing threshold") values are shown with 95% confidence intervals. ANOVA testing revealed no statistically significant difference in Rpl-32 expression (p=0.686), but some variation in β-actin expression (p=0.027) across experimental genotypes.

4.7.4 Quantitative RT-PCR (qPCR)

All quantification of gene transcript expression was performed using quantitative real-time PCR using the Roche LightCycler 480-II (Roche Diagnostics, UK). Reactions were performed in duplicate with 20ng of cDNA added to 15µl of a master mix containing DNA primer pairs, water, Taq DNA polymerase and SYBR green I dye (Roche). Primer sequences are listed in Appendix E: Quantitative real time PCR primer sequences

Optimised thermal cycling settings were used (95ºC for 10 minutes, 45 cycles of (95ºC for 15 seconds then 60ºC for 60 seconds)) and raw threshold cycle (Ct) data extracted. The averaged Ct of the reference genes (β-actin and Rpl-32) was then subtracted to determine relative gene expression (ΔCt) and duplicate sample ΔCt values were averaged. Mean ΔCts were calculated per mouse genotype group for each experimental condition and inserted into the standard formula ($2^{-\Delta Ct}$) to calculate the relative change in amount of gene product (compared to the reference). The value for each gene product was then compared to that seen in the wild type e.g. for elastin in the $TG2^{-/-}$ mouse:

Change in elastin expression = ($2^{-\Delta Ct}$ of $Elastin_{TG2^{-/-}}$) / (($2^{-\Delta Ct}$ of $Elastin_{WT}$)

and this was compared across mouse genotypes to give a relative fold-change for each gene of interest. All statistical analysis was performed on raw ∆Ct values rather than transformed data.

4.8 Basal vessel biochemistry

Prior to biochemical analysis, snap frozen aorta samples were dehydrated under vacuum for 1 hour (which in testing resulted in no further weight change) and then weighed. Samples were lysed for a minimum of 48 hours at 4ºC in 750µl of lysis buffer (50mM NaH_2PO_4, 50mM NaCl, 1% Triton, 0.1% SDS) and then centrifuged at 14000rpm for 10 minutes at 4ºC. The lysate was used for determination of LDH, DNA and solubilised protein and the pellet for analysis of either elastin or collagen.

4.8.1 LDH quantification

Following the lysis step described above, LDH content was determined using a modification of the CytoTox 96 LDH assay (Promega, UK). Samples (50µl) and a positive control (supplied) were transferred in triplicate to a 96-well plate (ThermoScientific, UK) and incubated with an equal volume of substrate mix (supplied) for 30 minutes at room temperature. The enzymatic reaction generated is the reduction of NAD^+ to NADH, which is catalysed by cellular LDH. A red formazan product is then generated by NADH reduction of a tetrazolium salt and hence

formazan production is proportional to LDH concentration. Reactions were stopped at 30 minutes by addition of a “stop solution” (supplied) and the absorbance was read using the Labtek plate reader (ThermoScientific, UK) at a wavelength of 490nm. Adjusted absorbance was then calculated by subtracting the absorbance of the reagent blank (50µl substrate mix) and this was normalised to solubilised protein content.

4.8.2 DNA quantification

Following the lysis step described above, double stranded DNA content was quantified using a modification of the protocol described by Leggate et al in 2006.(Leggate et al., 2006) In summary, 200µl of assay buffer (50mM NaH_2PO_4, 2M NaCl, pH 7.4) containing SYBR green dye at a concentration of 1:20000 was added to 10µl of each sample in a 96-well plate and incubated in the dark, at room temperature, for 2 hours. Fluorescence was read using the Varioskan fluorometric plate reader (ThermoScientific, UK) with a 494/530nm excitation/emission filter set with a band width of 12nm. DNA content was then quantified using a standard reference curve (0-1000ng) and normalised to solubilised protein content.

4.8.3 Solubilised protein quantification

Following the lysis step described above, solubilised protein content was quantified using the Pierce BCA Protein Assay Kit (Thermofisher, UK). This colorimetric assay involves the reduction of Cu^{2+} ions to Cu^{1+} by proteins and the binding of Cu^{1+} ions to bicinchonic acid to generate a purple reaction product. Samples (25µl) and albumin standards (in the range 0-2000µg/ml) were transferred in triplicate to a 96-well plate and 200µl of working reagent (supplied) added before thorough mixing and incubation for 30 minutes at 37ºC. Absorbance was read using the Labtek plate reader (ThermoScientific, UK) at a wavelength of 562nm and adjusted absorbance calculated. Solubilised protein content was determined using a reference standard curve.

4.8.4 Elastin quantification

Elastin content was determined per milligram of dry tissue using the Fastin™ (Bicolor Ltd) elastin assay. Briefly, alpha-elastin was extracted by heating for three one-hour periods with 0.25M oxalic acid. After pooling of the extracts, Elastin Precipitating Reagent (supplied) was added and samples were vortexed and left to allow complete precipitation. An elastin-dye complex was formed by addition of the Dye Reagent (supplied) which was observed as a reddish-brown deposit after centrifugation and removal of unbound dye. Dye Dissociation Reagent (supplied) was then added and samples were transferred to a 96-well plate and absorbance

read using the Labtek plate reader (ThermoScientific, UK) at a wavelength of 490nm. Adjusted absorbance was then calculated by subtracting the absorbance of the reagent blank (0.25M oxalic acid), elastin content was determined using a reference standard curve and this was then normalised to solubilised protein content.

4.8.5 Collagen quantification

Collagen content was determined per milligram of dry tissue using the Sircol^{TM} (Biocolor Ltd) soluble collagen assay. Briefly, Sircol Dye Reagent (supplied) was added and samples were mechanically mixed for 40 minutes to allow precipitation of a collagen-dye complex. Samples were then centrifuged and any unbound dye removed by washing with Acid-Salt Wash Reagent (supplied) and further centrifugation. The collagen bound dye was released by addition of Alkali Reagent (supplied), samples were transferred to a 96-well plate and absorbance was read using the Labtek plate reader at a wavelength of 555nm. Adjusted absorbance was then calculated by subtracting the absorbance of the reagent blank (100µl de-ionised water), collagen content was determined using a reference standard curve and this was then normalised to solubilised protein content.

4.9 MMP assay

To generate conditioned media for zymography, non-operated and experimental aortas were harvested into 1ml of PBS on ice before transfer to a 96-well plate under sterile conditions. Vessels were submerged in 100µl of OptiMEM (Thermofisher, UK) culture media supplemented with penicillin and streptomycin. Samples were incubated for 48 hours at 37ºC, 5% CO_2 and then 25µl aliquots snap frozen in liquid nitrogen and stored at -80ºC. Gelatin (for MMP-2 and -9) and casein (for MMP-12) zymography was undertaken using pre-cast gels from Invitrogen (Thermofisher, UK). A lane marker and positive control was included in each experimental run and 10µl of each sample was loaded per well in 1:1 ratio with loading buffer (0.2g SDS (2%), 0.01g bromophenol blue (0.1%) in 5ml stacking buffer (6.06g Tris-HCl (0.5M) and 0.05g Sodium Azide in 100ml water, pH 6.8) and 5ml 40% glycerol). Gels were run in 1X SDS running buffer (10X solution - 30.2g Tris-HCl, 144g Glycine, 10g SDS in 1l water, pH 8.3) at 125V for 60-90 minutes. Gels were then washed (for 3 x 20 minutes) in 2.5% Triton X-100 before incubating at 37ºC for 3-7 days in developing buffer (7.5g Tris base (50mM), 11.7g NaCl (200mM), 0.7g $ZnCl_2$, 0.74g $CaCl_2.2H_2O$ (5mM), Triton X-100 (2%), Brij-35 (0.05%), 0.2g NaN_3 (0.02%) in 900ml water, pH 7.4). After staining for 1 hour (1g coomassie

blue in 500ml methanol, 200ml acetic acid and 300ml water), gels were de-stained (300ml methanol, 693ml water, 7ml formic acid) for a minimum of 2 hours before imaging under UV light (G:box scanner, Syngene, UK).

4.10 Endothelial permeability

Vascular permeability within the aorta was determined using a method similar to that described by Orr *et al*. (Orr et al., 2007) Briefly, 8-12 week old mice were anaesthetised using inhaled isoflurane, and were then warmed and restrained to allow injection of 0.1ml of 1% Evans Blue into the tail vein. Mice were recovered and then 30 minutes later were re-anaesthetised and euthanized by perfusion with 10mls of 4% paraformaldehyde (PFA) (see Appendix) via cardiac puncture into the left ventricle. The whole aorta (from descending aorta to iliac bifurcation) was dissected and excised and samples were immediately dried in a vacuum oven for 1 hour before weighing. After determination of weight, samples were incubated in 1ml of formamide for 24 hours at 60ºC. An Evans Blue concentration curve was constructed in the range 0-1000ng/ml and transferred to a 96-well plate along with the extracted samples. Absorbance was read using the Labtek plate reader (ThermoScientific, UK) at 620nm and adjusted absorbance calculated by subtracting absorbance of the reagent blank (formamide). Evans Blue content of each sample was calculated from the concentration curve and then normalised to sample weight.

4.11 Wire Myography

Wire myography studies were set up and optimised following a standardised experimental protocol and further assays were carried out in conjunction with Dr Lih Cheah. A summary protocol diagram is shown in Figure 19 but briefly; mice aged 8-12 weeks old from each experimental genotype (n=4) were killed (as per Home Office Schedule 1 guidelines) and the abdominal aorta dissected in cold Hanks solution (see Appendix C: Wire myography solutions).

Aortic rings (2 per sample) of 1mm length were then mounted in a myograph (610 M, Danish Myograph Technology), left to equilibrate for 30 minutes, and then placed under normalised tension in a bath of pre-warmed (to 37ºC), and gassed (with 5% CO_2) Krebs solution.

Contractile function of the vessel was assessed by the addition of 1) high concentration potassium (60mM K^+ in Krebs solution), and then 2) phenylephrine (PE, 1µM), to the organ bath. A concentration response curve of % contraction vs.

PE dose was then constructed by the step-wise addition of 0.03, 0.1, 0.3, 1.0, 3.0 and 10.0µM PE. Each concentration was applied and then contraction response recorded; when a steady state was reached, the next concentration was administered.

Finally, the relaxation response to carbachol (CCh, 1µM) was observed following an induced vessel contraction with 1µM PE. A relaxation response to CCh - which occurs via NO release - confirms the presence of an intact endothelial layer and this step was performed as a control mechanism to ensure that the endothelium had not been damaged during dissection or mounting.

EC_{50} values (the concentration of PE required to produce 50% maximal response) were calculated by non-linear regression analysis using Origin® software (OriginLab Corp., USA) and these, as well as area-under-the-curve data and force differences (maximum-minimum contraction), were compared across genotypes using ANOVA testing (with Bonferroni correction) or Kruksal-Wallis testing (with Dunn’s correction) as appropriate.

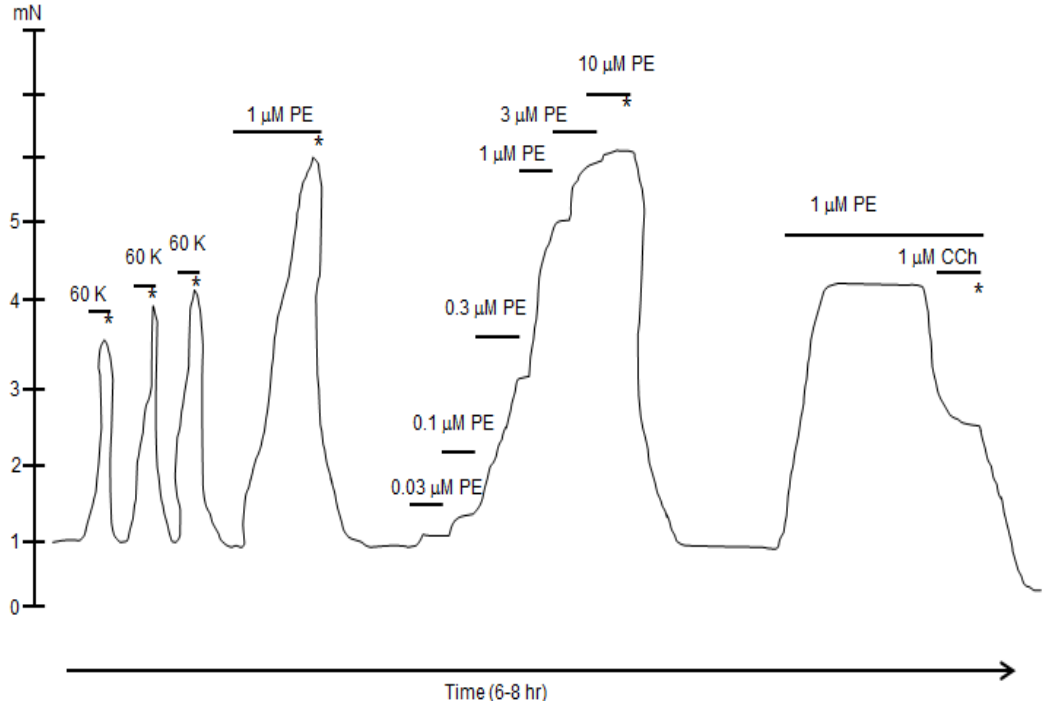

Figure 19. Myography experimental protocol

Schematic showing myography experimental protocol. 60K=Krebs solution containing 60mM K^+, PE=phenylephrine, CCh=carbachol, * denotes points at which the solution bathing the vessel was exchanged three times with fresh pre-warmed, gassed, Krebs solution.

4.12 Carotid ligation model

The carotid ligation model was undertaken as previously carried out by Newell *et al* in Bristol; mice aged 8-12 weeks were weighed, anaesthetised with inhaled isoflurane and restrained on a warmed operating surface. A midline neck incision was performed and the right common carotid artery located and exposed using a combination of blunt and sharp dissection. The vessel was slung using a small strip of silicone and photographed using the OPMI-PICO video system (Carl Zeiss AG) to allow baseline vessel diameter measurements (below the carotid bifurcation) to be taken post-operatively. The common carotid artery was then ligated using a 3/0 silk suture and the wound washed out with 0.9% sterile saline and closed using continuous 6/0 vicryl sutures. Operated mice were recovered in a warmed clean cage, returned to their cages and were given a soaked diet for 24-48 hours to facilitate adequate nutrition

After 28 days mice were re-anaesthetised and arterial perfusion-exsanguination performed via the left ventricle using 5mls PBS (outflow via the transected IVC) followed by 10mls 4% PBS-buffered PFA. The right carotid artery was then dissected from surrounding tissue and removed for histological processing and analysis.

A.

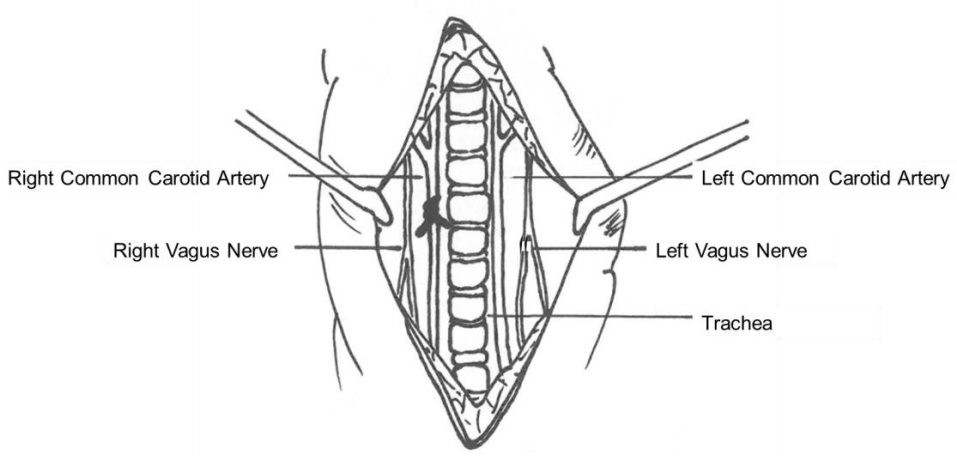

B.

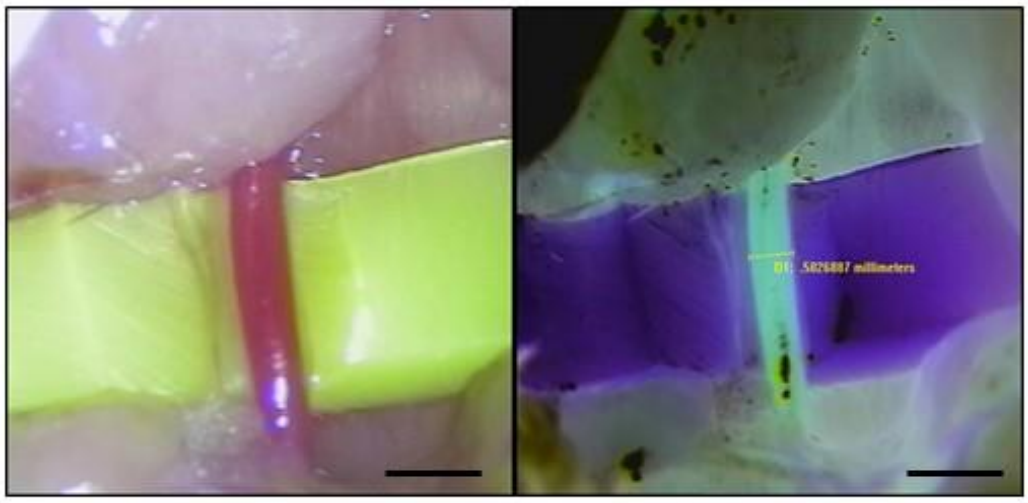

Figure 20. Carotid artery ligation model

Panel A depicts a simplified diagram of the anatomy of the neck in the mouse when in a supine position. The right common carotid artery is identified and isolated (using a small piece of silicone) as shown in **Panel B**. The vessel is then photographed and can be measured (if required) at a later time, using the “invert contrast” function in Image Pro. After imaging, the vessel is ligated using a 3/0 silk suture to completely occlude blood flow and the wound is closed and the animal recovered. Scale bar = 1 millimetre

4.13 Calcium chloride (CaCl2) model

The protocol for the $CaCl_2$ model is summarised in Figure 21. Mice aged 8-12 weeks were weighed, anaesthetised with inhaled isoflurane and restrained on a warmed operating surface. The abdomen was then shaved, epilated and cleaned with ethanol for laparotomy. In each case the abdominal aorta was exposed and isolated from the surrounding retroperitoneal structures using blunt dissection. Photographs of the abdominal aorta were captured using the OPMI-PICO video system (Carl Zeiss AG) and base-line vessel diameter measurements (midway between the left renal artery origin and the iliac bifurcation) were taken post-operatively.

After image capture, 0.25M or 0.5M $CaCl_2$ was applied to the external surface of the aorta using a cotton gauze applicator. NaCl (0.9%) was substituted for $CaCl_2$ in sham operated mice. After 7 minutes the applicator was replaced with a second solution-soaked applicator and after a further 7 minutes the aorta was rinsed with 0.9% sterile saline and the incision was closed in layers using 8/0 and 6/0 vicryl. Buprenorphine in the form of Vetergesic® (Reckitt Benckiser) was administered as an intra-peritoneal injection (dose 0.5mg/kg) to minimise post-operative pain and then mice were recovered in a warmed clean cage and were returned to their cages when deemed fully recovered. Operated mice were given a soaked diet for 24-48 hours to facilitate adequate nutrition.

Either six weeks or six months later (depending on study group) the mice underwent re-laparotomy and dissection. Images were captured at the same location in the mid-infra-renal aorta. Aortas were then either harvested fresh (for myography), snap frozen in liquid nitrogen (for mRNA, biochemical and zymography studies) or perfusion-fixed with 4% PBS-buffered PFA and harvested for histological analysis.

Vessel measurements pre-and post-injury were calculated from the calibrated captured images using Image-Pro software (MediaCybernetics). In all cases measurements were made in agreement by two investigators after processing the images using the “invert contrast” function to allow better visualisation of the vessel walls. An anatomical landmark (e.g. branch vessel point) was sought for pre-injury diameter measurement; for post-injury diameters, measurements were taken at the point of maximal dilatation.

In a subset of mice, the $CaCl_2$ model was applied to the common carotid artery rather than the abdominal aorta. In these mice the carotid was approached and exposed as per the carotid ligation model (see section 4.11), the vessel was then isolated from surrounding tissue using a small strip of silicone (Eddington’s Ltd.,

UK) and photographed. Using a small cotton applicator, 0.5M $CaCl_2$ was applied to the artery for 2 x 7 minutes as detailed above, the area was then washed with saline and the neck wound closed in a single layer with 6/0 vicryl sutures before recovery.

Data were analysed by calculation of the % change in infra-renal aortic diameter and comparison across groups with Student's t-test (for 2 groups) or one-way ANOVA testing with Bonferroni correction (for >2 groups). The proportion of mice that developed an aneurysm was generated by count of mice exhibiting a greater than 50% increase in aortic diameter; these data were analysed using Fisher's exact test (of proportions).

A

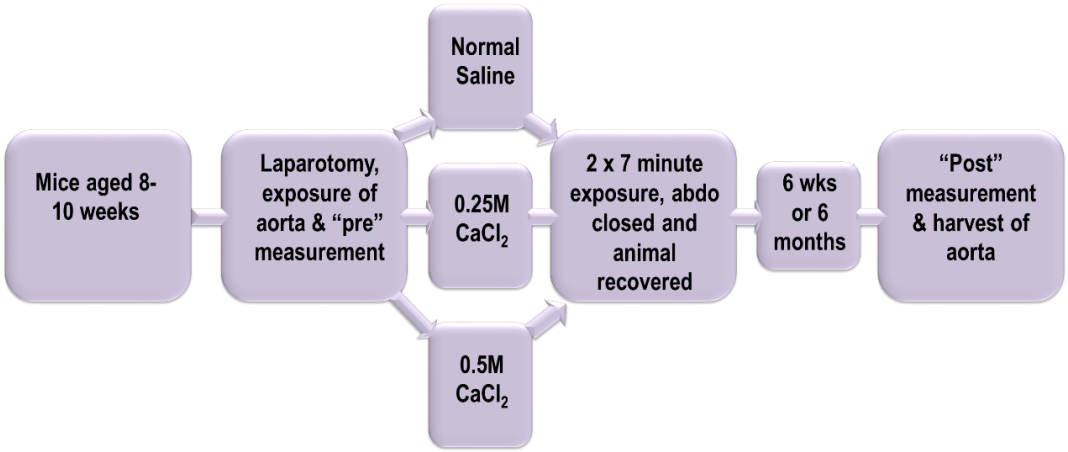

B i) **ii)** **iii)**

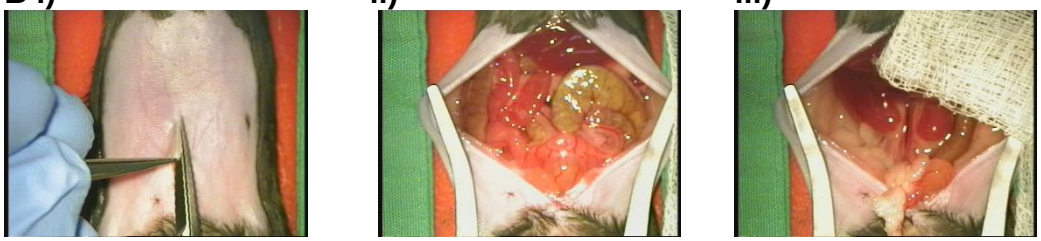

iv) **v)** **vi)**

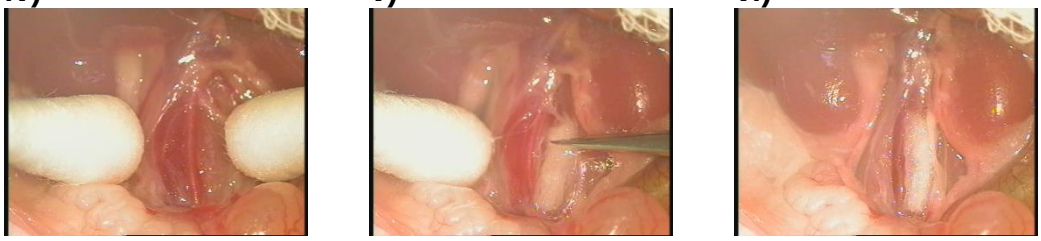

vii) **viii)** **ix)**

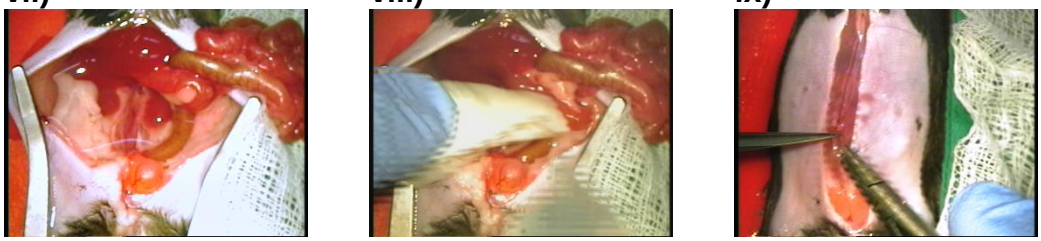

x) **xi)** **xii)**

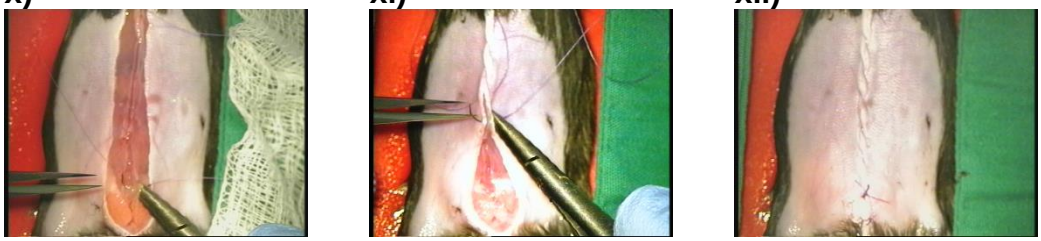

Figure 21. $CaCl_2$ aortic injury model

Panel A details the overall experimental protocol for the $CaCl_2$ aortic injury model. **Panel B** shows details of the operative procedure; i) laparotomy is performed with retraction of the skin edges (ii) and exposure of the aorta (iv). Blunt dissection is used to free the aorta from surrounding fascia (iv) and then $CaCl_2$ is applied using cotton gauze (v and vi). Following 2 x 7 minute applications of $CaCl_2$, the site is washed with normal saline (vii), dried (viii) and the wound closed in two layers (ix to xii).

4.14 Histology

4.14.1 Processing

Perfusion-fixed samples were stored in 4% PFA for a minimum of 48 hours and then dehydrated using the Leica TP1020 tissue processing carousel (Leica Microsystems) before paraffin embedding. All samples were subject to a 17 hour processing programme as detailed in Appendix D: Histology – additional methodological detail. Immediately after processing the tissue samples were placed into plastic moulds and embedded with liquid paraffin (Sigma-Aldrich, UK) which was then hardened by cooling.

4.14.2 Sectioning

All microscopy slides were pre-coated prior to use (see Appendix D). Either representative sectioning (at random intervals) or serial sectioning of vessel samples (from left renal artery to iliac bifurcation) was undertaken on the Leica RM2125 microtome (Leica Microsystems, UK) at a section thickness of 5μm. Slides were left to dry at 37ºC overnight and then stored.

4.14.3 Haematoxylin and eosin

Histological slides were de-waxed and rehydrated with xylene and stepwise ethanol before washing in distilled water. Slides were then stained in Harris' haematoxylin solution (Sigma, UK) for approximately 10 minutes prior to washing and differentiating in 1% acid-alcohol (1% HCl in 70% EtOH). After washing, slides were allowed to "blue" in 0.2% ammonia water before washing with tap water and rinsing in 70% ethanol. Counterstaining with eosin Y stain (Sigma, UK) was undertaken for ~30 seconds and then stains were dehydrated with ethanol and xylene. Coverslips were applied with DPX mountant (Sigma Aldrich, UK)

4.14.4 Miller Van Gieson (for elastin)

Histological slides were de-waxed and rehydrated with xylene and stepwise ethanol immersion and were then washed and dried. Slides were then sequentially placed in 0.5% potassium permanganate solution, 2% oxalic acid solution, distilled water and ethanol (to rinse) before staining with Miller stain (Cell Path, UK) for 1 hour. Excess stain was removed with ethanol, and then slides were stained with Van Gieson stain (100ml of saturated aqueous solution of picric acid added to 5ml of 1% aqueous solution of acid fuschin) for 15 minutes, prior to rinsing and incubation at 70ºC for ~10 minutes until completely dry. Dehydration with xylene was then undertaken and coverslips were applied with DPX mountant.

4.14.5 Sirius Red (for collagen)

After de-waxing and rehydration, slides were stained with Weigert's haematoxylin (Atom Scientific, UK) for 10 minutes prior to thorough washing (for at least 5 minutes) in tap water. Slides were then placed in 1% acid-alcohol to reduce background and then incubated in Picro-sirius red solution for 1 hour and washed twice in clean acidified water. Excess water was removed by vigorous shaking and then dehydration with 100% ethanol was undertaken prior to the application of coverslips wiih DPX mountant.

4.14.6 Alizarin Red (for calcium)

Histological slides were de-waxed and rehydrated with xylene and stepwise ethanol immersion. Slides were then stained with Alizarin Red Solution (see Appendix D) for ~2 minutes or until red-orange staining was observed microscopically. Excess stain was removed by blotting and then slides were dehydrated sequentially in 100% acetone and then 1:1 acetone-xylene solution. Coverslips were then applied with DPX mountant.

4.14.7 Perl's Prussian Blue (for haemosiderin)

Histological slides were de-waxed and rehydrated with xylene and stepwise ethanol immersion. Slides were then incubated with potassium ferrocyanide solution (see Appendix D) for 10 minutes before dehydration in histological grade alcohol and xylene. Coverslips were then applied with DPX mountant.

4.14.8 Vessel morphometry analysis

Maximum elastic lamellae number was quantified in un-operated (n=2 per genotype) and sham operated (n=2 per genotype) aortic samples. After perfusion-fixation, processing and embedding, vessel samples were sectioned with 2 x 5µm sections cut at 200µm intervals throughout the area of injury. Maximum lamellae number was recorded for each section and then the mean maximum number calculated for each vessel and compared across genotypes using Kruksal-Wallis testing with Dunn's correction.

Elastin damage was quantified in the aneurysm model using an adaptation of the method reported by Watanabe *et al*.(Watanabe et al., 2012) Briefly, n=6 short-term aneurysms per group were fixed, processed, embedded and serial sectioned (if more than 6 samples were available for analysis then those closest to the average diameter change for the group were selected for study). The area of injury was identified (either at the time of harvest or on sectioning) and 20 x 5µm sections analysed from the central 100µm of injury. The vessel circumference was

measured on each section and elastin damage expressed as a proportion (%) of total circumference. Elastin fibres were classified by an investigator blind to genotype as either 1) healthy, 2) damaged but intact or 3) damaged and broken. A similar protocol was followed for examination of un-operated (n=2) and sham-operated (n=2) aortas and of those injured with $CaCl_2$ and harvested at 6 months (n=6).

Collagen distribution and density was examined using multiphoton microscopy after the serial sectioning and sampling protocol as above and staining with Sirius Red stain. Slides were scanned at 10X magnification with the Zeiss 710 muliphoton microsope to detect the collagen second harmonic generation (SHG) signal at excitation wavelength 800-860nm. On each image three areas of interest were identified corresponding to healthy elastin, damaged (but intact) elastin and broken elastin fibres. Within each area a 10x10 (arbitrary units^2) square was drawn and the integrated density of the collagen signal was measured using ImageJ software (nih.gov, USA). A similar protocol was followed for examination of aortas exposed to $CaCl_2$ and harvested at 6 months (n=6).

4.14.9 Cardiac fibrosis analysis

Quantification of cardiac fibrosis was performed on 3-5 paraffin sections from n=10-27 mice from each genotype at 8 weeks (baseline) and at 21 weeks. Briefly, analysis was performed using ImageJ software (nih.gov, USA) and involved calculation of the mean % area of fibrosis (collagen deposition, stained red with Sirius Red and manually defined) relative to the total myocardial area. Haemosiderin deposition was quantified in a similar way (relative to total area) after staining with Perl's Prussian Blue stain. Data were analysed using Kruksall Wallis testing with Dunn's test for multiple groups.

4.14.10 Immunohistochemistry

Histological slides were de-waxed with xylene (2 x 5 minutes) and then immersed in 100% ethanol (2 x 5 minutes). Endogenous peroxidase activity was blocked using 1:100 methanol:hydrogen peroxide and then slides were rehydrated in stepwise ethanol. Microwave antigen retrieval was performed with sodium citrate buffer (10mM trisodium citrate buffer, 0.05% Tween 20, pH6) before slides were cooled and washed in PBS. Cells were permeabilised with 0.1% Triton X100 and then slides washed prior to blocking with 4% BSA for 30 minutes at room temperature. Primary antibody incubation was carried out at room temperature for one hour at the following concentrations; anti-SMA (ab184675, mouse) – 10ug/ml, anti-MMP-12 (ab200410, rabbit) – 2.5ug/ml (all antibodies from Abcam Plc, UK. After

washing, slides were incubated with an equal volume of Polyview® anti-mouse horseradish peroxidase (HRP) and anti-rabbit alkaline phosphatase (AP) (ADI-950-112, Enzo Life Sciences, UK) for 20 minutes. Slides were then washed, incubated with DAB and then HighDef red stain (for AP) (Enzo Life Sciences, UK) before mounting, drying and application of a coverslip with Shandon mount medium (ThermoSciences, UK).

4.15 Statistics

Unless explicitly stated, all data is presented as mean ± standard deviation. All values were analysed using Prism 7 (GraphPad Software, San Diego, CA, USA). Each data set is presented with details of the statistical analysis used, however, in summary; data were analysed for normality with Shapiro-Wilks testing. Non-normal data and those with unequal variances across groups were analysed using non-parametric methods (Mann-Whitney for two-group comparisons and Kruskal-Wallis with Dunn's correction for multiple groups). Data that were normally distributed were analysed using Student's unpaired t-test for two-group comparisons (with Welch's correction for unequal variance if required) and one-way ANOVA for multiple groups (with Bonferroni's post-test correction). Discontinuous data (breeding outcomes) were analysed using a Chi-squared (χ^2) test and contingency data (aneurysm development) using Fisher's exact test of proportions. In all cases significance was accepted where the two-tailed probability was less than $p=0.05$.

Chapter 5: Results – Characterisation of Mouse Lines

Chapter 5: Results – Characterisation of Mouse Lines

Using the transgenic methods, breeding programme and genotyping strategy as outlined, we were able to generate TG2$^{-/-}$, FXIII-A$^{-/-}$ and TG2$^{-/-}$.FXIII-A$^{-/-}$ (DKO) offspring on a defined C57Bl/6 background for use in further experiments. The DKO mice generated by this project are the first reported mice which lack both transglutaminases, without coexistent ApoE deficiency, and as such are an important tool for the investigation of the distinct and overlapping roles of TG2 and FXIII-A. This chapter will outline the results from the characterisation of the various transgenic lines in terms of their gross phenotype, growth, glucose homeostasis, and coagulation function.

5.1 Maternal FXIII-A$^{-/-}$ phenotype

As discussed in the methods section, we recognised that there were potential concerns related to breeding from FXIII-A deficient female mice given the observations from Koseki-Kuno *et al* (Koseki-Kuno et al., 2003) of overt genital bleeding at day 10 of gestation and increased maternal mortality. However, we felt it was important to confirm the maternal phenotype of our novel FXIII-A$^{-/-}$ mouse. A trial breeding programme was established whereby female FXIII-A$^{-/-}$ mice (with ~75% C57Bl/6 background) were crossed with either male C57Bl/6 mice or male FXIII-A$^{-/-}$ mice. Unfortunately this breeding was unsuccessful, with recapitulation of the expected phenotype. Following this, all subsequent breeding (to generate both FXIII-A$^{-/-}$ and TG2$^{-/-}$.FXIII-A$^{-/-}$ offspring) was carried out using female mice heterozygous for FXIII-A KO.

	Details of Pregnancy / Complications
#1	Found dead; obviously pregnant with evidence of bleeding in the cage
#2	Uneventful pregnancy, found dead after delivery of two (non-viable) pups
#3	Found dead; not obviously pregnant, no evidence of haemorrhage

Table 5. Results from trial breeding with FXIII-A$^{-/-}$ females

5.2 Frequency of breeding

During the course of our breeding programme we observed what appeared to be a decreased frequency of FXIII-A$^{-/-}$ offspring in comparison to the numbers expected by Mendelian frequency. To assess the impact of TG2 and FXIII-A deficiency on

mouse fertility and breeding we analysed litter size and offspring genotype from the following breeding pairs (and trios where appropriate).

1. $TG2^{+/-}$ male x $TG2^{+/-}$ female
2. FXIII-$A^{WT/flox}$ male x FXIII-$A^{WT/flox}$ female
3. FXIII-$A^{-/-}$ male x FXIII-$A^{+/-}$ female
4. $TG2^{-/-}$.FXIII-$A^{-/-}$ male x $TG2^{-/-}$.FXIII-$A^{+/-}$ female

Breeding of FXIII-$A^{-/-}$ male with FXIII-$A^{+/-}$ females generated numbers of offspring that were significantly different from expected values with 226 KO pups observed vs. the 325 KO expected (p=0.001). Likewise, DKO offspring were generated at a significantly lower rate than that predicted by Mendelian frequency (265 observed vs. 355 predicted, p=0.005). Heterozygous flox breeding generated 52 FXIII-$A^{flox/flox}$ offspring, compared to an expected 66 pups, and likewise, heterozygous TG2 breeding generated 80 knockout pups, when 88 were predicted by Mendelian frequency. Neither of these differences was statistically significant.

The normal litter size from C57Bl/6 breeding is 6.2 pups per litter (Nagasawa et al., 1973) and was 6.8 in our hands. There was no significant difference in average litter size between this and either the TG2 breeding (6.3 pups/litter) or the Flox breeding (6.9 pups/litter), however the FXIII-A breeding resulted in an average of only 5.4 pups/litter which was significantly different from Flox (p=0.023) and our C57Bl/6 (p=0.015) breeding. Likewise the DKO breeding resulted in smaller litter sizes (5.7 pups/litter). Female mice will release 6-10 oocytes per oestrus (Pinkert, 2012) and a proportion will not survive due to failure of fertilisation, implantation or subsequent embryogenesis. Given that the frequency of FXIII-$A^{+/-}$ offspring did not differ from that predicted (388 observed vs. 399 expected, p=NS) it seems likely that it is FXIII-A deficiency in the oocyte that is the cause of an increased “failure to survive” of these cells. This is obviously an interesting observation and one worthy of future study.

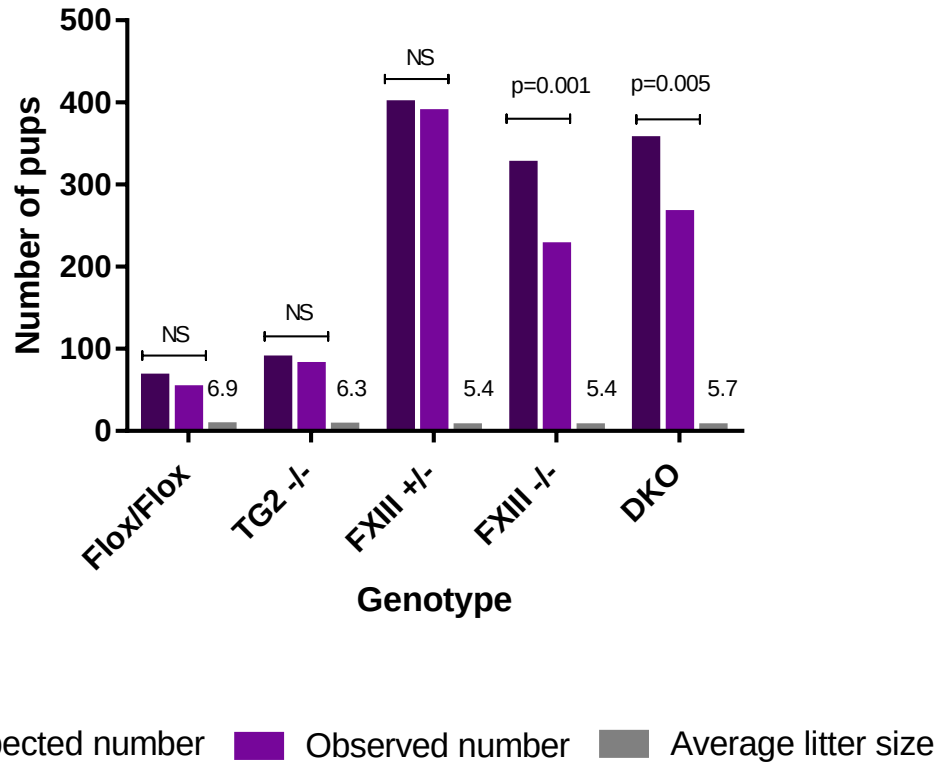

Figure 22. Breeding frequency by genotype

Frequency of genotype was retrospectively analysed for each heterozygous breeding pair/trio and the observed number of pups compared with the number expected by Mendelian frequency using the chi-squared statistic. Average litter size for each breeding line was also recorded and Kruksall Wallis test applied to assess difference from WT or Flox mice. *** p=0.001, ** p=0.005

5.3 Growth

None of the transgenic mouse lines exhibited any gross phenotypic change and specifically no obvious defects in skeletal or vascular development were observed. Weekly weights were monitored in a subset of mice of each genotype (n=8, m:f=1:1) and no significant difference (on AUC AVOVA testing) between groups was seen to 16 weeks of age. Mice were also weighed prior to any intervention and a summary graph of all data is shown in Figure 23. A sub-group of mice (n=4-8 male mice per genotype) were weighed weekly to 40 weeks of age. There was no statistically significant difference in weight between groups at 40 weeks (weight (g) ± SD; C57 28.13 ± 5.91, $TG2^{-/-}$ 34.18 ± 7.32, $FXIII\text{-}A^{-/-}$ 33.01 ± 6.54, DKO 31.22 ± 2.29, p=0.477)

5.4 Blood pressure

As part of an allied but separate study undertaken by our group, mice aged 24 weeks (n=7-11 per group) were subject to right ventricular catheterisation and assessment of cardiac function via pressure-volume loop recording. Baseline (anaesthetised) systolic blood pressure (BP) measurements were recorded to enable comparison between the genotypes and these data were kindly provided by Dr Mark Drinkhill and are summarised in Figure 24. There was no difference in systolic blood pressure between the groups on ANOVA testing(mean BP (mmHg) ± SD; C57 73.67 ± 7.19, $TG2^{-/-}$ 73.73 ± 2.14, $FXIII\text{-}A^{-/-}$ 72.28 ± 10.93, DKO 73.36± 10.72, p=0.984).

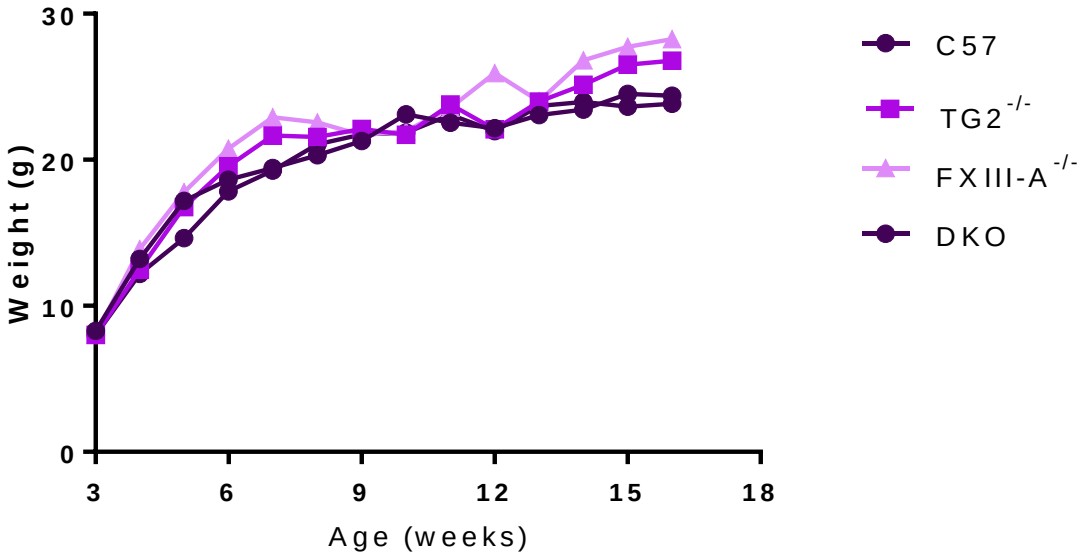

Figure 23. Growth of transgenic mice

Figure shows average weight gain over time for each transgenic mouse line (n=>4 at each time point). Data are only shown for mice that had not undergone any prior intervention or operative procedure. There is no statistical difference in weight gain between the experimental groups to 16 weeks of age and no statistical difference between genotypic groups in those mice investigated at specific later time points.

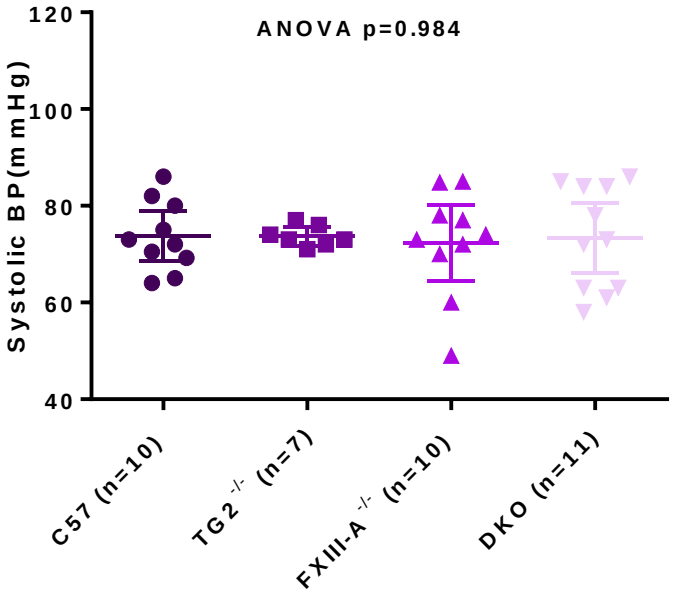

Figure 24. Systolic blood pressure

Figure shows mean systolic (anaesthetised) blood pressure (with 95% CI) for each transgenic mouse line (n=7-11 per group). There is no statistical difference between the groups on ANOVA testing, p=0.984.

5.4 FXIII-A activity

Plasma FXIII-A activity (velocity) was determined from murine plasma samples for n=10-18 mice per genotype. Each plate was run with one control WT sample and one human sample for which FXIII-A activity had previously been quantified. In each case the human sample was seen to have FXIII-A activity of 15% (± 5%) of that seen in the WT sample.

For the purpose of comparison, the average activity in each experimental genotype was compared to the plasma activity of the FXIII-A "floxed" mouse (FXIII-$A^{Flox/Flox}$) group to give a measure of relative FXIII-A activity (Figure 25). Data were analysed with one-way ANOVA testing with Bonferroni correction. The floxed mouse was taken as control because of an observed small decrease in FXIII-A activity in the floxed mouse (mean activity (AU) ± SD; C57 2691 ± 558, Flox 2195 ± 632; 81.6% relative to C57Bl/6, p=0.013) which may be related to altered efficiency of gene splicing or subtle changes in gene expression.

There was no statistically significant difference in plasma FXIII-A activity between the FXIII-$A^{Flox/Flox}$ mice and the $TG2^{-/-}$ mice, however heterozygosity for the FXIII-A gene decreased plasma activity levels to 74.3% of control (± 7.2%) and FXIII-A gene knockout resulted in a complete lack of plasma FXIII-A activity, as expected in both the FXIII-$A^{-/-}$ and DKO groups (***, $p<0.0001$). There was no statistically significant difference between FXIII-$A^{-/-}$ mice and the DKO mice group ($p>0.99$).

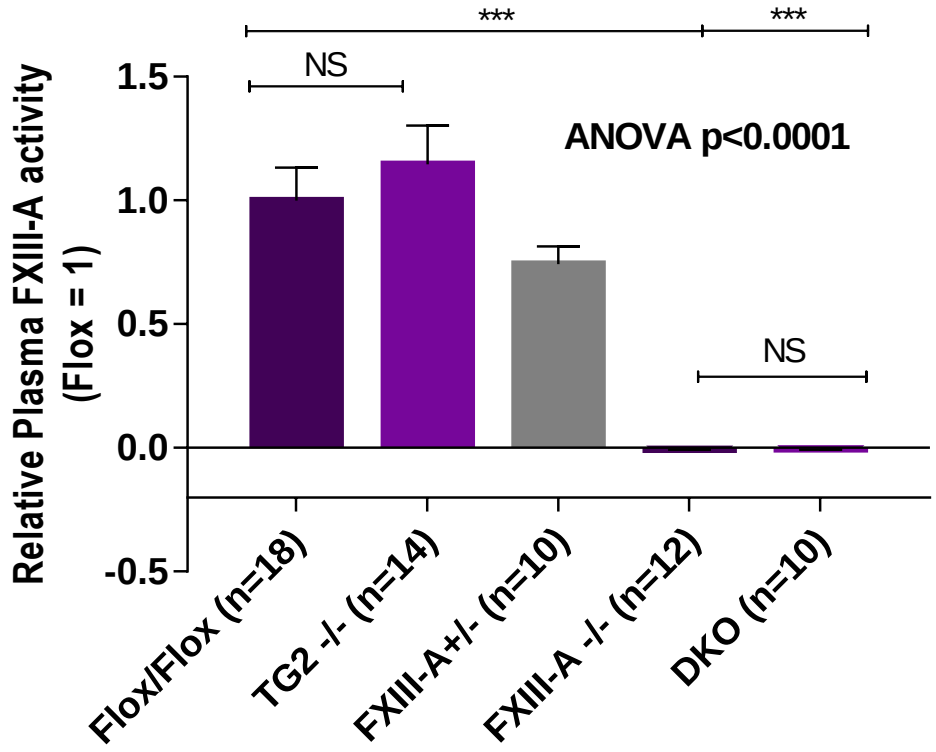

Figure 25. Relative plasma FXIII-A activity

Plasma FXIII-A activity was determined from murine plasma samples for n=10-18 mice per genotype. Each genotype was compared to the control ($FXIII\text{-}A^{Flox/Flox}$) group to give a measure of relative FXIII-A activity which is shown above with 95% confidence intervals. NS = not significant, *** p<0.001

5.5 Metabolic testing

TG2 has been reported to be involved in glucose homeostasis in a number of *in vitro* studies (Sener et al., 1985, Bungay et al., 1986) and Bernassola et al have published evidence of glucose intolerance, hyperglycaemia and impaired insulin secretion in their TG2$^{-/-}$ mouse line.(Bernassola et al., 2002) They also report a *TGM2* gene mutation (Asn333Ser) located within the active site region of the gene which was present in 2 members of a family with MODY. No putative mechanism is given as to how this mutation causes hyperglycaemia and, as discussed in section 2.1, these murine observations have not been recapitulated in the Graham TG2$^{-/-}$ mouse. However given the conflicting evidence in the literature, we sought to characterise our own TG2$^{-/-}$ line (generated from heterozygous founders provided by Prof Graham but back-crossed to a defined background) as well as the FXIII-A$^{-/-}$ and DKO lines in terms of their response to exogenous glucose or insulin challenge. The characterisation of the metabolic phenotype of the FXIII-A$^{-/-}$ mouse is vital in light of recent reports that FXIII-A has a role in adipogenesis (Myneni et al., 2014) and the development of obesity.

There is some evidence to support an age-related decrease in insulin tolerance in laboratory mice (Lavine et al., 1971, Bailey and Flatt, 1982) and hence metabolic experiments were conducted in both young (10-12 week old) and aged (40-42 week old) mice.

5.5.1 Glucose tolerance

Glucose tolerance testing performed in 10-12 week old mice revealed no significant difference in glucose tolerance at any time point (Figure 26). Area-under-the-curve (AUC) analysis also showed no difference, either between the transgenic lines or when compared with the C57Bl/6 mice (C57 940.1 ± 133.4, TG2$^{-/-}$ 867.9 ± 97.2, FXIII$^{-/-}$ 1040.1 ± 254.2, DKO 919.9 ± 161.2; p=0.24). Likewise, glucose tolerance testing in old (40-42 week old) mice revealed no significant difference in blood glucose levels at any time point (Figure 28). AUC analysis was not significantly different between groups (C57 867.9 ± 97.2, TG2$^{-/-}$ 979.2 ± 299.0, FXIII$^{-/-}$ 834.3 ± 97.0, DKO 1003.9 ± 128.1; p=0.29) with these results providing evidence that our lines are normoglycaemic and supporting the view that TG2 is *not* involved in glucose homeostasis.

5.5.2 Insulin tolerance

Insulin tolerance testing (ITT) measures the change in blood glucose level in response to an exogenous insulin challenge. ITTs performed in 10-12 week old mice revealed no significant difference in insulin tolerance at any time point (Figure

27). AUC analysis also showed no significant difference between groups in insulin tolerance across the whole 2-hour protocol (C57 631.7 ± 196.2, $TG2^{-/-}$ 497.8 ±203.2, $FXIII^{-/-}$ 760.1 ± 162.4, DKO 638.3 ± 197.6; p=0.06). In contrast, ITTs in 40-42 week old mice (Figure 29) revealed a significant difference in blood glucose levels across the whole protocol (AUC: C57 810.3 ± 70.6, $TG2^{-/-}$ 743.6 ± 57.4, $FXIII^{-/-}$ 527.6 ± 129.0, DKO 645.7 ± 159.4; p=0.0044) with the FXIII-$A^{-/-}$ mice have significantly lower AUC than the C57Bl/6 mice (p=0.0066). In this aged group of FXIII-$A^{-/-}$ mice, insulin sensitivity appeared to be increased (with a trend towards lower blood glucose levels seen at each time point). We had limited availability of aged FXIII-A mice because of reduced breeding numbers and hence we feel these results reflect insufficient mouse numbers (i.e. under-powering) rather than a true difference in glucose homeostasis.

There was no significant difference in AUC analysis for ITTs, between 10-week old and 40-week old mice (all genotypes combined; p=0.623) (data not shown) hence our mice did not show any evidence of impaired insulin tolerance with increasing age, up to 40 weeks.

A

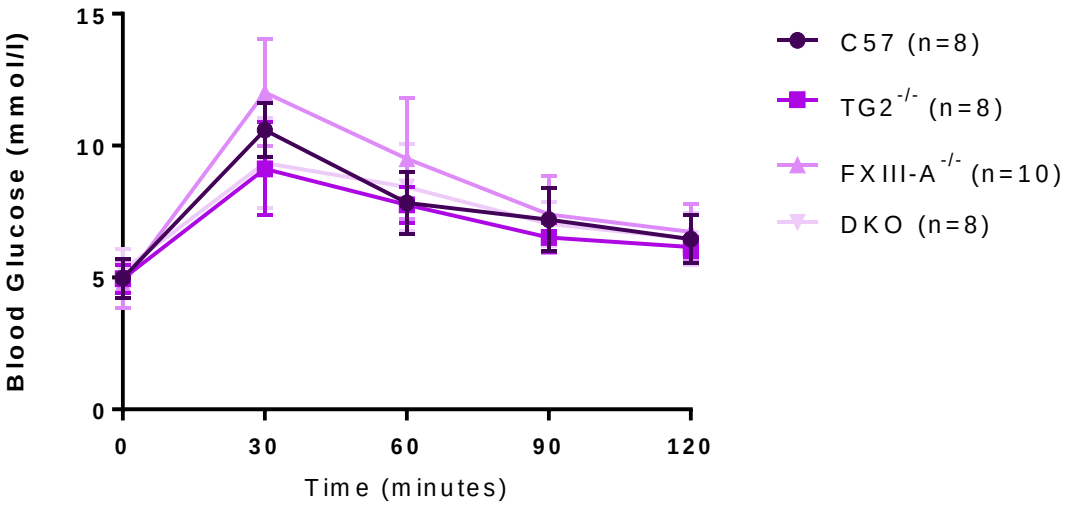

B

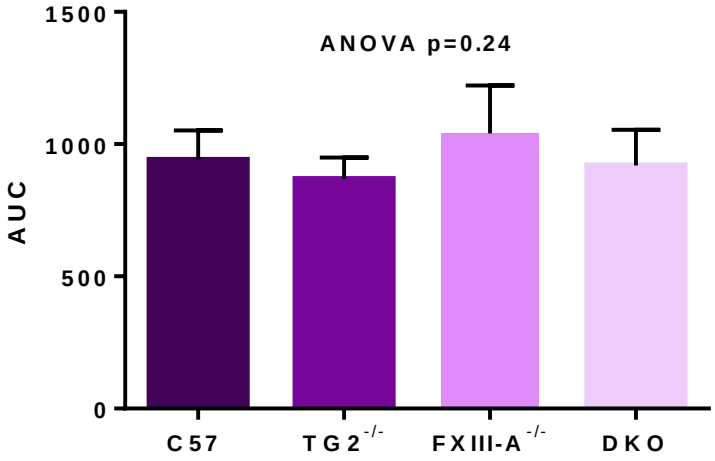

Figure 26. Glucose tolerance testing – young mice

Mice (n=8-10 per genotype) aged 10-12 weeks underwent glucose tolerance testing as described in the text. Average (mean ± 95% CI) blood glucose tracings across the duration of the test are shown in **panel A**. ANOVA analysis of area-under-the-curve (AUC) data (**panel B**) revealed no statistically significant difference in glucose tolerance between the four experimental genotypes in "young" mice. AUC data is presented as mean ± 95% confidence intervals.

A

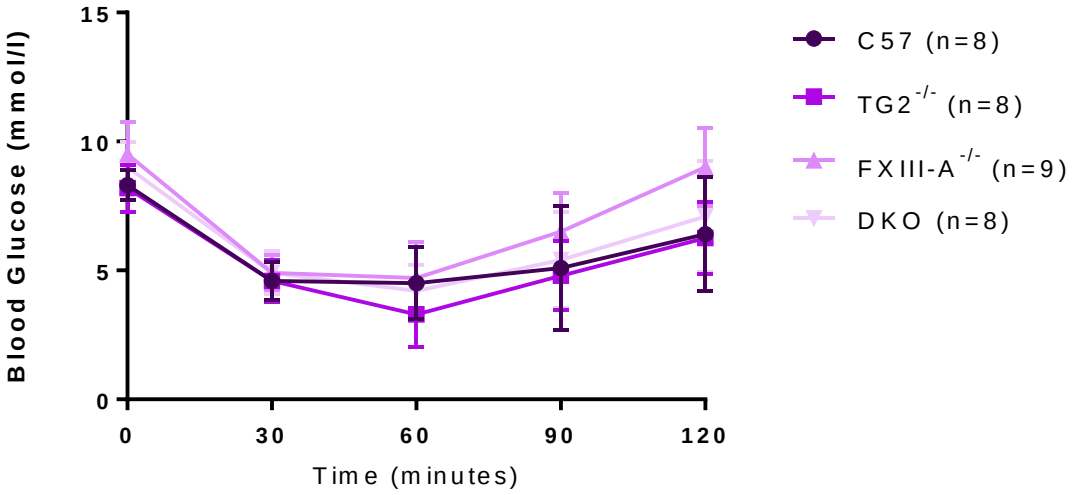

B

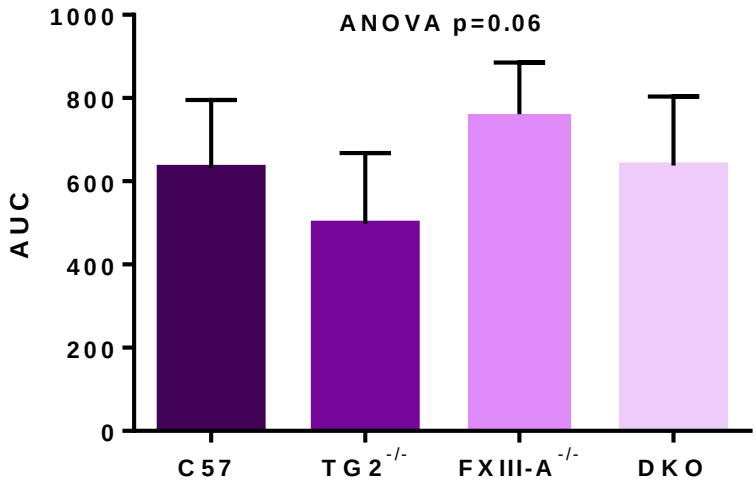

Figure 27. Insulin tolerance testing – young mice

Mice (n=8-9 per genotype) aged 10-12 weeks underwent insulin tolerance testing as described in the text. Average (mean ± 95% CI) blood glucose tracings across the duration of the test are shown in **panel A**. ANOVA analysis of area-under-the-curve (AUC) data (**panel B**) revealed no statistically significant difference in insulin tolerance between the four experimental genotypes in "young" mice. AUC data is presented as mean ± 95% confidence intervals.

A

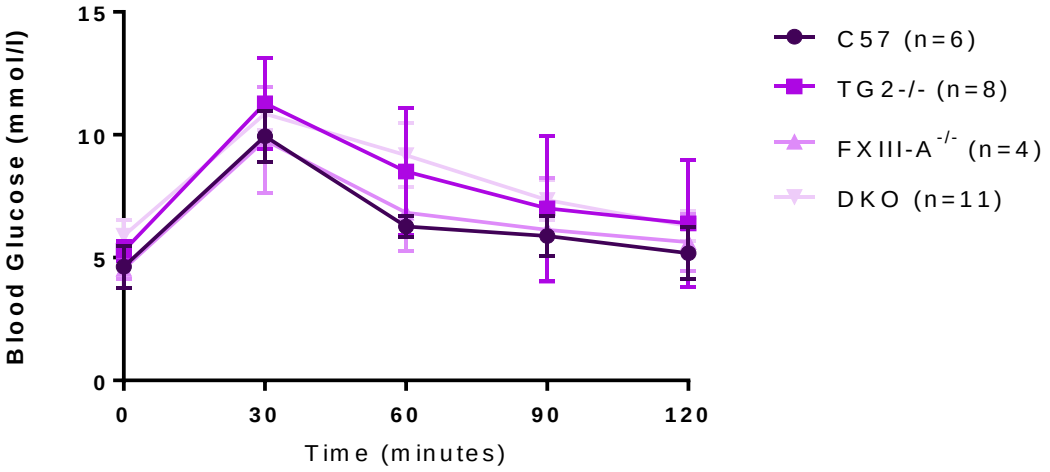

B

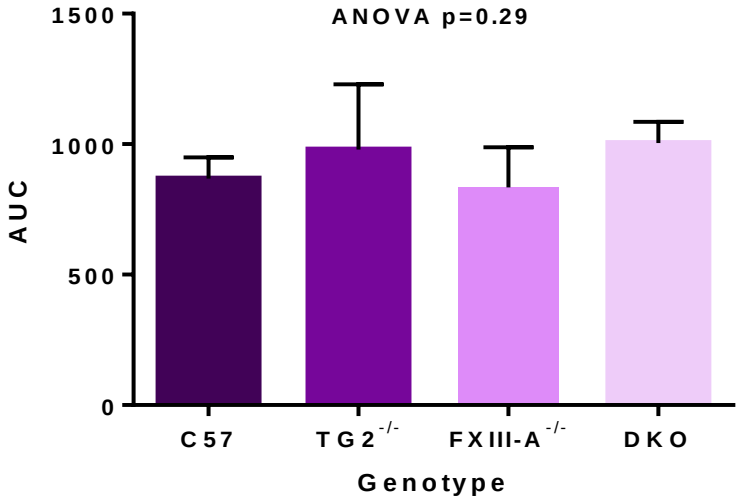

Figure 28. Glucose tolerance testing – old mice

Mice (n=4-11 per genotype) aged 40-42 weeks underwent glucose tolerance testing as described in the text. Average (mean ± 95% CI) blood glucose tracings across the duration of the test are shown in **panel A**. ANOVA analysis of area-under-the-curve (AUC) data (**panel B**) revealed no statistically significant difference in glucose tolerance between the four experimental genotypes in “old” mice. AUC data is presented as mean ± 95% confidence intervals.

A

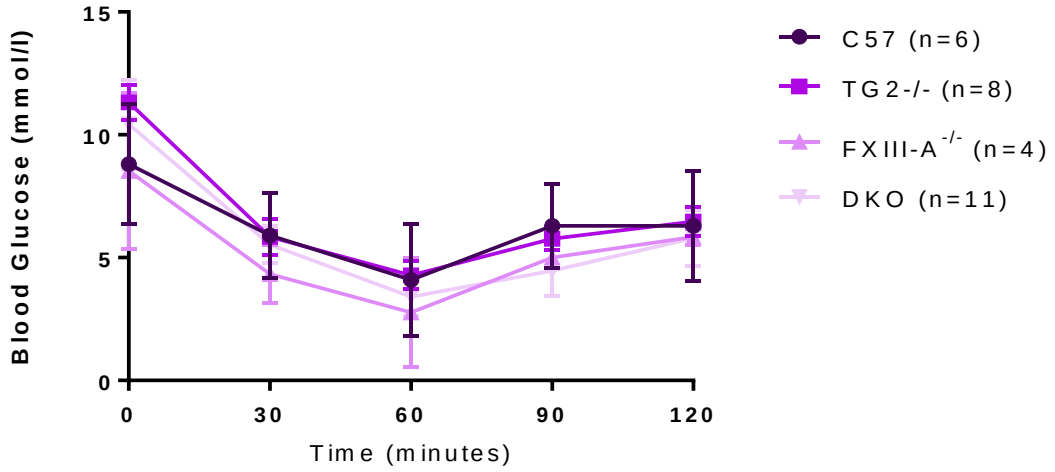

B

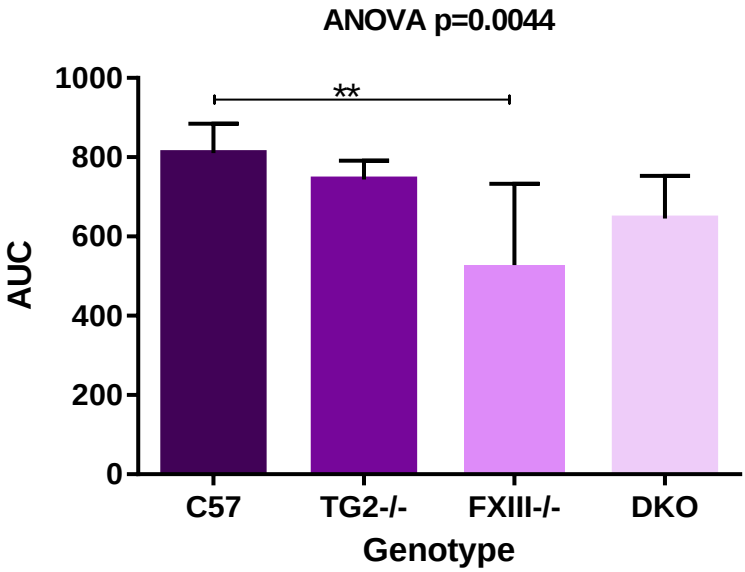

Figure 29. Insulin tolerance testing – old mice

Mice (n=4-11 per genotype) aged 40-42 weeks underwent insulin tolerance testing as described in the text. Average (mean ± 95% CI) blood glucose tracings across the duration of the test are shown in **panel A**. ANOVA analysis of area-under-the-curve (AUC) data (**panel B**) revealed a statistically significant difference in insulin tolerance between the four experimental genotypes "old" mice. AUC data is presented as mean ± 95% confidence intervals.

5.6 Coagulation function

ROTEM® analysis was performed on murine whole blood samples as a measure of overall coagulation function of the various experimental mouse lines. Each sample was analysed under conditions designed to replicate either the extrinsic (“extem”) or intrinsic (“intem”) coagulation pathway but results were not statistically different between conditions (data not shown) and hence only “extem” data is shown in Figure 30. Data were analysed by one-way ANOVA testing with Bonferroni correction.

As expected from the known fibrin-crosslinking function of FXIII-A, samples from mice deficient in FXIII-A - both the FXIII-$A^{-/-}$ and the $TG2^{-/-}$.FXIII-$A^{-/-}$ double deficient mice - form clots more slowly than those from other genotypes (α-angle (degrees); C57 74.8 ± 5.5, $TG2^{-/-}$ 70.3 ± 3.1, FXIII-$A^{+/-}$ 66.3 ± 4.7, FXIII-$A^{-/-}$ 43.0 ± 8.0, DKO 44.2 ± 6.9, $p<0.0001$) and produce weaker blood clots (maximum clot firmness (MCF) (mm); C57 56.5 ± 2.4, $TG2^{-/-}$ 52.0 ± 7.0, FXIII-$A^{+/-}$ 51.0 ± 4.6, FXIII-$A^{-/-}$ 19.0 ± 4.0, DKO 15.2 ± 4.5, $p<0.0001$) which are easier to lyse (lysis index at 30 minutes (%); C57 100.0 ± 0.0, $TG2^{-/-}$ 100.0 ± 0.0, FXIII-$A^{+/-}$ 100.0 ± 0.0, FXIII-$A^{-/-}$ 50.0 ± 8.3, DKO 51.7 ± 7.5, $p<0.0001$).

TG2 deficiency alone had no impact on clot formation time, clot strength or resistance to lysis and TG2 deficiency in addition to FXIII-A deficiency did not worsen the clotting abnormalities observed. Heterozygosity for the FXIII-A gene was not sufficient to result in a change in clot characteristics.

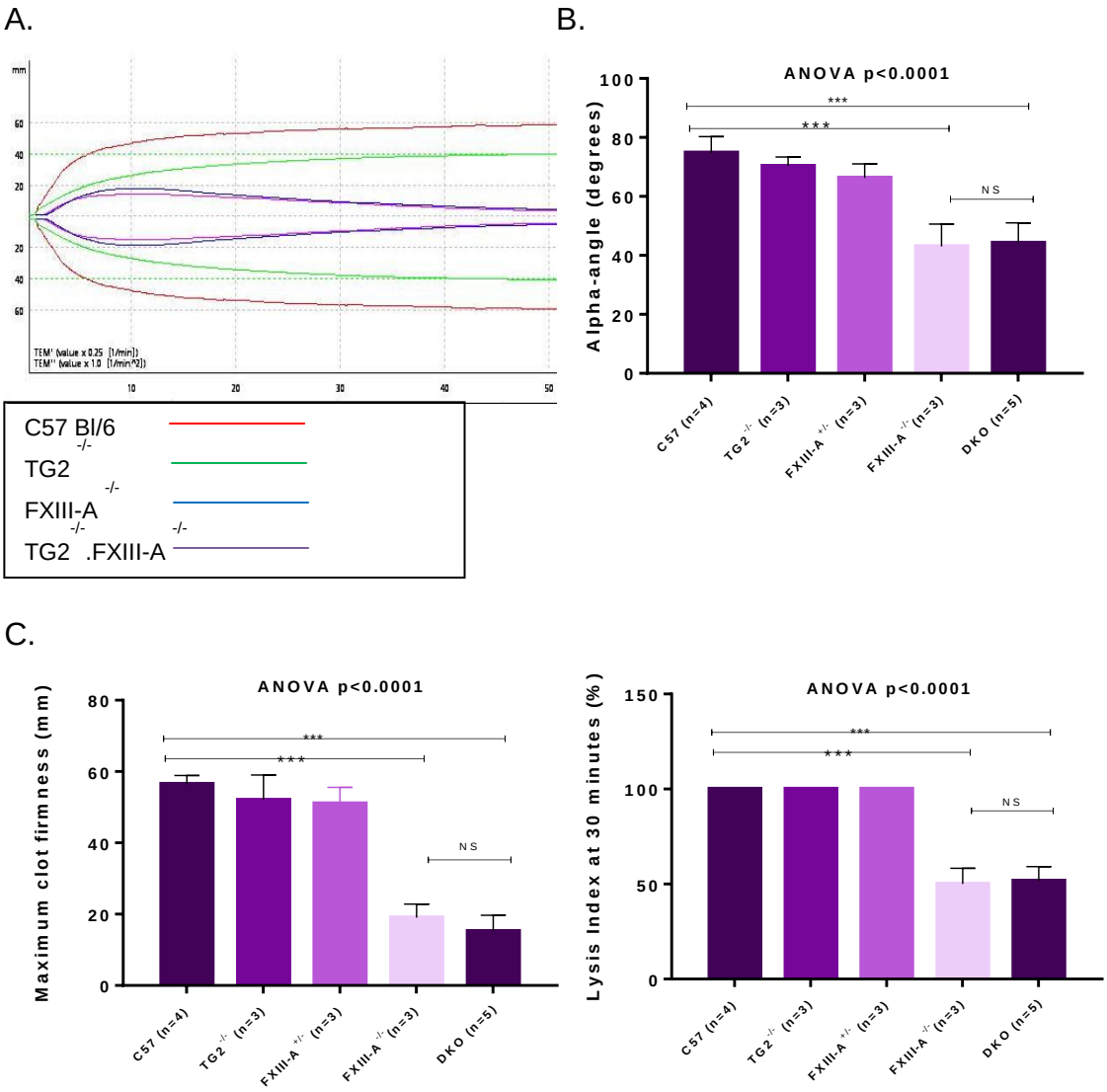

Figure 30. ROTEM analysis of murine whole blood samples

Murine whole blood samples for each genotype (n=3-5) were analysed by rotational thromboelastography. **Panel A** shows representative traced from the four transgenic mouse lines. **Panel B** showsresults for α-angle (a surrogate of clot formation time) with larger values representing a longer time to form a clot of 20mm firmness. **Panel C** shows results for the maximum clot firmness (in mm) reached over the two-hour study period and **panel D** demonstrates the clot lysis index (% of the remaining clot stability in relation to maximum clot firmness, at 30 minutes). Data were analysed by ANOVA for multiple groups with Bonferroni correction for multiple testing.

5.7 Cardiac fibrosis

As part of the characterisation of our mice and, in an attempt to verify the results seen by Newell *et al* in Bristol, we sought to investigate the potential role of TG2 and FXIII-A in the development of cardiac fibrosis. This analysis of this work was carried out in conjunction with Dr Cora Beckers and is summarised in Figure 31. Myocardial fibrosis was determined by % collagen content from Sirius Red staining at 8 weeks of age (baseline, n=10-14) and at 21-weeks of age after feeding with chow diet (n=18-27). Figure 31 shows representative images from the three transgenic lines and Figure 32 presents data compared to the results seen in FXIII-$A^{-/-}$ mice at 21 weeks. Data were analysed by Kruksal-Wallis testing with Dunn's correction.

Cardiac sections from C57Bl/6 and $TG2^{-/-}$ mice showed no evidence of myocardial fibrosis at either baseline or at 21-weeks. In contrast, the FXIII-$A^{-/-}$ group showed small amounts of fibrosis at baseline (0.80 ± 0.51%) which was significantly different from WT ($p=0.0001$) and which had increased by 21-weeks (2.39 ± 2.25%), again to a level significantly different from WT or $TG2^{-/-}$ mice ($p<0.0001$). The DKO group showed significantly higher levels of fibrosis at baseline (3.25 ± 5.14%) when compared to either the C57Bl/6 or $TG2^{-/-}$ ($p<0.0001$) groups and by 21-weeks showed obvious fibrotic change (14.0 ± 8.25%) which was significantly different from C57Bl/6 and $TG2^{-/-}$ mice ($p<0.0001$) but not from FXIII-$A^{-/-}$ mice ($p=0.456$) at the same time-point.

Haemosiderin deposition was quantified in adjacent paraffin sections using % Prussian Blue staining and results are presented in Figure 32. At 21-weeks of age, hearts from WT mice showed 0.14% haemosiderin content (SD 0.53%), as compared to 0.12 ± 0.28% in $TG2^{-/-}$ mice, 0.10 ± 0.26% in FXIII-$A^{-/-}$ mice and 0.76% ± 0.35% in DKO mice. Haemosiderin deposition was significantly different across groups with the DKO mice showing more deposition when compared to that seen in WT (Dunn's, $p<0.001$), $TG2^{-/-}$ ($p=0.002$) and FXIII-$A^{-/-}$ ($p<0.001$) mice.. Despite the obvious overall similarity in the above results with the DKO mice showing greater amounts of both fibrosis and haemosiderin deposition, there was only minimal correlation between these two parameters when either DKO alone, or all genotypes, were examined.

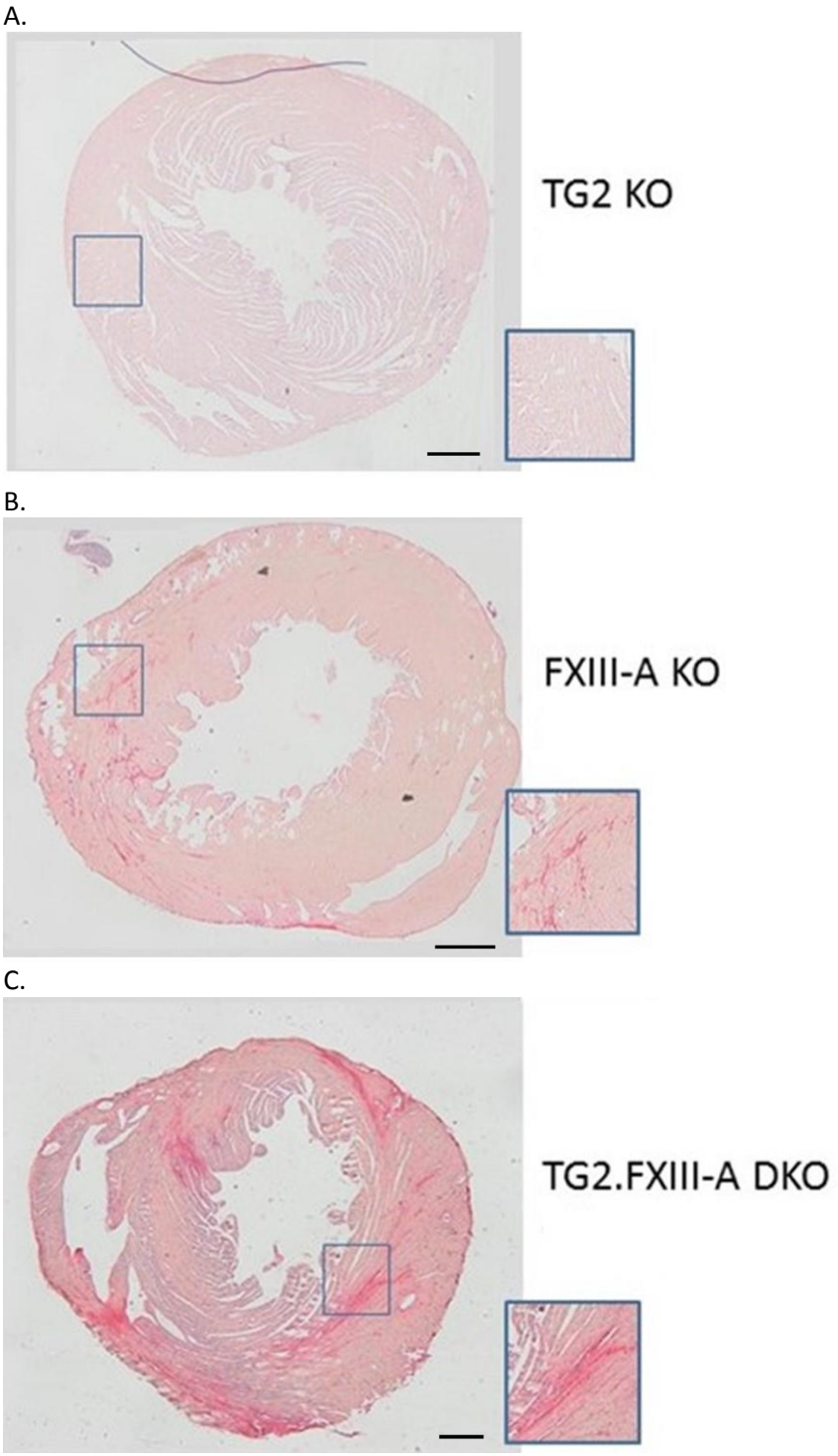

Figure 31. Representative images – myocardial fibrosis

Panel A shows a representative cardiac section (with Sirius Red staining) from a $TG2^{-/-}$ mouse. **Panel B** is from a $FXIII\text{-}A^{-/-}$ mouse and shows sparse areas of fibrosis and **panel C** is from a DKO animal and shows definite strands of fibrosis within the myocardium. Collagen is stained red / dark pink.Scale bars represent 500µm in each image.

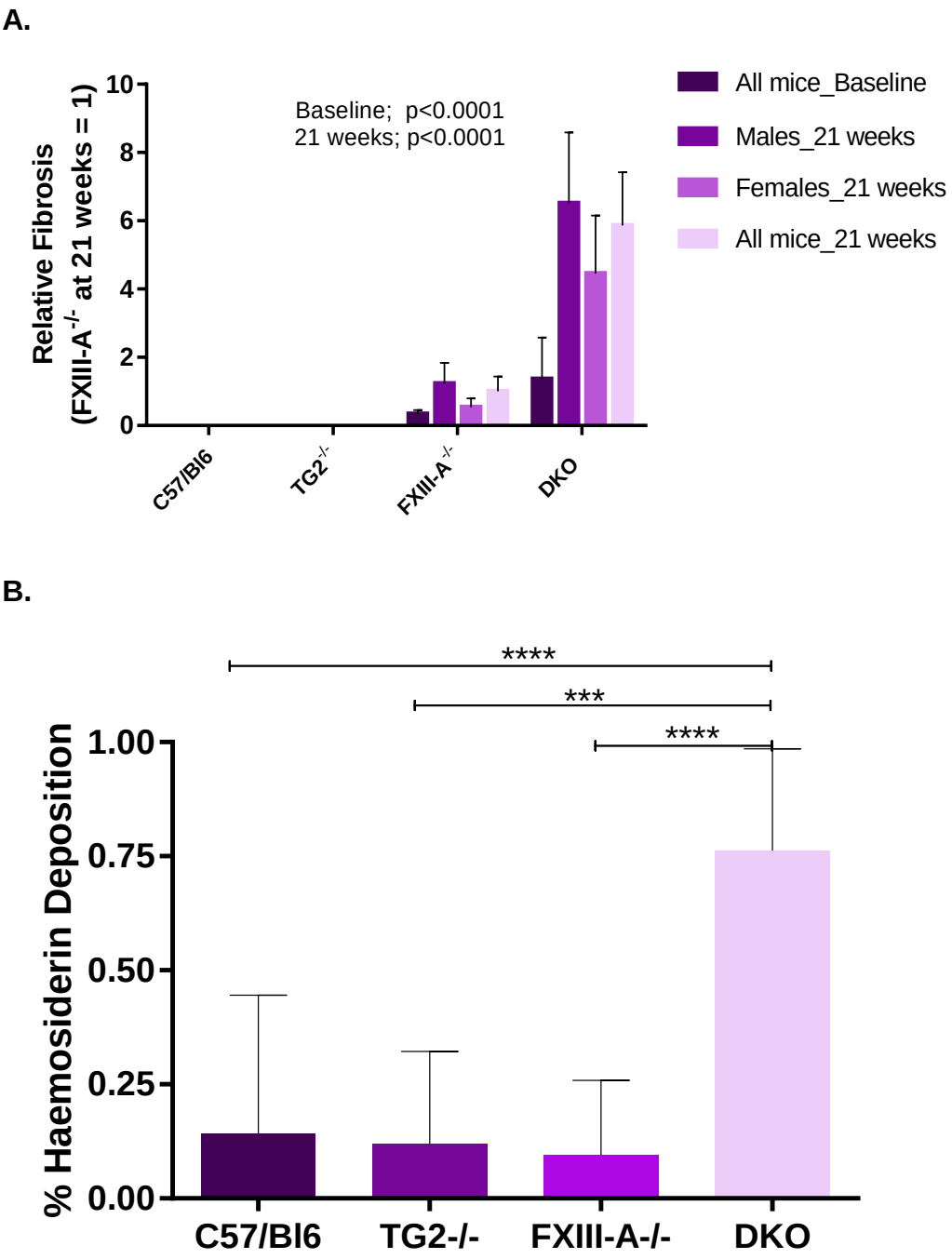

Figure 32. Myocardial fibrosis and haemosiderin deposition

Panel A summarises relative fibrosis in each of the experimental mouse groups at baseline and after 21 weeks chow diet and are presented as relative fibrosis compared to that seen in the FXIII-A$^{-/-}$ mice at 21 weeks. P-values shown are for Kruksall Wallis testing (with Dunn's correction) of all groups at baseline and 21-weeks. Further statistical detail is provided in the main text. **Panel B** shows data for % haemosiderin deposition in cardiac sections from mice in each of the experimental groups at 21 weeks. Results are presented as mean ± 95% confidence intervals

Phenotypic Characteristic	**TG2$^{-/-}$**	**FXIII-A$^{-/-}$**	**DKO**
Breeding	No phenotypic change observed	Unable to breed from FXIII-A$^{-/-}$ KO females ↓ litter size ↓ no. of KO offspring	Unable to breed from TG2$^{-/-}$.FXIII-A$^{-/-}$ KO females ↓ litter size ↓ no. of KO offspring
Growth	Normal	Normal	Normal
Skeletal Development	No phenotypic change observed	No phenotypic change observed	No phenotypic change observed
Glucose homeostasis	Normal	? ↑ insulin sensitivity with age (requires confirmation)	Normal
FXIII-A activity	Normal	Absent	Absent
Clotting	Normal	Clots; -take longer to form -are less stable -more easily lysed	Clots; -take longer to form -are less stable -more easily lysed (no different from FXIII-A$^{-/-}$ KO)
Cardiac Fibrosis	None observed	↑ at baseline ↑↑ at 21 weeks	↑↑ at baseline ↑↑↑ at 21 weeks

Table 6. Summary results – characterisation of transgenic mouse lines

The above table summarises the results presented in this chapter pertaining to the phenotypic characterisation of the three transgenic mouse lines utilised in this thesis. Where a characteristic is described as “normal”, we found no statistically significant difference in phenotype between the transgenic and the WT line.

5.8 Discussion

This chapter presents results (summarised in Table 6) from the characterisation of the three transgenic mouse lines used in this thesis; the Graham TG2$^{-/-}$ mouse, which is a well-established model of TG2 deficiency (Nanda et al., 2001) that has been previously characterised on various strain backgrounds but which was utilised by us, in this work, on a known C57Bl/6 background; a FXIII-A$^{-/-}$ mouse line, generated from a novel "floxed" mouse using cre-lox recombination technology, again on a C57Bl/6 background, and finally; a double-deficient TG2$^{-/-}$.FXIII-A$^{-/-}$ or DKO mouse line which is previously unreported and allows for investigation of the distinct and/or overlapping roles of TG2 and FXIII-A without the confounding influence of ApoE deficiency.

As expected, our TG2$^{-/-}$ mice were viable, fertile and showed no gross phenotypic abnormality. The mice lacking FXIII-A also showed normal fertility (i.e. FXIII-A is not required for conception) but as in the human situation – where patients with FXIII-A deficiency experience recurrent 1st trimester losses – we were unable to breed from homozygote female mice due to bleeding and maternal death. This phenotype is as reported by Koseki-Kuno *et al* in 2003 (Koseki-Kuno et al., 2003) which was hypothesised to be due to rupture of placental vessels, but we have also seen reduced numbers of FXIII-A$^{-/-}$ offspring (from both FXIII-A$^{-/-}$ and DKO breeding) in the setting of smaller litter size.

Various roles have been proposed for FXIII-A in the maintenance of a viable pregnancy and FXIII-A has been reported in histiocytes and macrophages within uterine implantation tissue and within the developing placenta.(Adany and Muszbek, 1989, Asahina et al., 2000) Muszbek *et al* (Muszbek et al., 2011b) report that ECM cross-linking by plasma FXIII-A is key to development of the Nitabuch's fibrin layer within the placenta, which has an "immunological barrier" function (Schneider and Moser, 2016) as well as being crucial to placental integrity. Whilst maternal FXIII-A activity is of key importance in pregnancy; our results, which show reduced FXIII-A$^{-/-}$ offspring with no evidence of pregnancy-associated bleeding or foetal loss, suggest that *embryonic* FXIII-A may also play a role in embryo survival or implantation. The significance of this is as yet unknown and clearly worthy of future study.

Despite this breeding deficiency, FXIII-A$^{-/-}$ and DKO mice develop normally and, like the TG2$^{-/-}$ mice, show no impairment in terms of growth or gross skeletal development. This is in contrast to the work of Al Jallad *et al* (Al Jallad et al., 2006) and Tarantino *et al*,(Tarantino et al., 2009) who have suggested that there is

functional redundancy between FXIII-A and TG2 with regards bone deposition and mineralisation, and instead supports work from our group,(Cordell et al., 2015) which showed no gross deficit in bone mineralisation (on x-ray or DEXA scanning) in TG2$^{-/-}$.FXIII-A$^{-/-}$ double knockout mice on an ApoE-deficient background. These findings highlight the caution that is required when extrapolating *in vitro* culture results to the *in vivo* situation.

Hyperglycaemia (induced by streptozotocin injection) has been reported to limit aneurysm development in both the elastase and AngII aneurysm models.(Miyama et al., 2010) Although these findings have not been reported in the $CaCl_2$ model, it is clear that any large differences in glucose homeostasis observed in the transgenic mouse lines would potentially complicate the results obtained from aortic injury. In line with the work of Iismaa *et al* (Iismaa et al., 2013) we have found no significant differences in glucose homeostasis in the mice deficient in TG2 in either “young”, or “aged” mice at 40-weeks of age. Likewise, despite analogous claims that FXIII-A is involved in the proliferation of pre-adipocytes (rather than their differentiation and deposition as fat),(Myneni et al., 2014) our FXIII-A$^{-/-}$ and DKO mice were not obese, demonstrated normal weight gain and had esssentially normal glucose homeostasis. We saw no evidence of increased fat deposition in these mice during organ harvest, or at the time of aortic injury and hence have found no evidence of gross metabolic phenotype in any of these experimental mice that could potentially influence the response to vascular injury.

Our anticipated findings were confirmed using a FXIII-A activity assay which showed that gene knockout resulted in a complete absence of plasma enzyme activity in the FXIII-A$^{-/-}$ and DKO mice. FXIII-A activity was reduced to approx. 75% of control in mice heterozygous for FXIII-A gene knockout and activity was (as expected) not affected by TG2 gene deficiency. These changes in FXIII-A activity had predictable effects on clot formation with FXIII-A$^{-/-}$ and DKO mice producing clots that took longer to form, were less stable and were more easily lysed than the clots formed by WT mice. TG2 deficiency has not been reported to affect clotting parameters and this was confirmed in our mice.

Souri *et al* (Souri et al., 2008b) have previously reported on the development of spontaneous cardiac fibrosis in the hearts of older male mice with FXIII-A deficiency, leading to an increased mortality rate by 10 months of age. Likewise, Newell and colleagues in Bristol (in preparation) have shown cardiac fibrosis in both FXIII-A$^{-/-}$ and TG2$^{-/-}$.FIII-A$^{-/-}$ male mice on an ApoE deficient background, subject to a high fat diet. In this work, and as part of ongoing studies into the role of FXIII-A in vessel stability and repair, we have shown that FXIII-A$^{-/-}$ mice of both sexes, subject

to a normal chow diet, develop spontaneous myocardial fibrosis by 21 weeks of age. This fibrotic change is exacerbated in mice which have concomitant TG2 deficient and appears to be present as early as 8 weeks of age. Although male mice showed more fibrosis than female mice (in both FXIII-$A^{-/-}$ and DKO groups) this was not statistically significant hence we cannot comment on specific gender differences in predilection to fibrosis in this study.

Cardiac fibrosis has also been reported in the hearts of mice lacking tissue factor (TF) and Factor VII in the work of Pawlinski *et al*.(Pawlinski et al., 2002) They, like Newell *et al*, and recapitulated by us, show deposition of haemosiderin at sites of fibrosis and conclude that fibrosis occurs as a response to impaired haemostasis and haemorrhage from cardiac vessels. The alternative theory, to one of impaired haemostasis, is that FXIII-A in this context is playing a role in vascular integrity and that impairment of this function leads to vessel "leakiness", bleeding and haemosiderin deposition, and subsequent fibrosis. The role of FXIIII-A in the maintenance of endothelial barrier function has been discussed and it is feasible that TG2 activity could mitigate cardiac damage, either by compensating for FXIII-A in terms of vessel stability or by instigating tissue repair and thus limiting the fibrosis seen in FXIII-A single deficient mice. In DKO mice however, vessel integrity is either further compromised, or tissue damage goes unchecked, and hence fibrosis can proceed to the levels seen in our samples.

We have observed increased haemosiderin deposition in the hearts of our DKO animals, which is localised to the areas of fibrotic change. We have not shown any correlation between haemosiderin and collagen content, however non-fibrotic hearts did not show any evidence of haemosiderin staining using the robust Perl's Prussian Blue method. In many ways this result is unsurprising as there is likely to be a considerable time differential required between red blood cell leakage, macrophage uptake and production of haemosiderin (the presumed trigger for fibrosis) and the development of fibrosis itself.

Further work is ongoing to assess whether the fibrosis observed at a histological level in our mice has an impact at the physiological level in terms of cardiac function and/or mortality. Certainly baseline investigations show that there is no difference in anaesthetised (unstressed) systolic blood pressure between the genotypes. If histological fibrosis is observed without significant myocardial impairment this would represent a useful, spontaneously occurring, model of fibrosis which could be utilised in future work to investigate the potential therapeutic role of FXIII-A.

Chapter 6: Results – TG2 and FXIII-A in Normal Vessel Structure and Function

Chapter 6: Results – TG2 and FXIII-A in Normal Vessel Structure and Function

6.1 Aim

We aim to elucidate the roles of TG2 and FXIII-A in basal vessel structure and function, and investigate the evidence for upregulation of other transglutaminases to compensate for single/dual deficiency.

6.2 Transglutaminase compensation

It has been suggested in the literature that TG2 and FXIII-A overlap functionally and that they can compensate for each other under conditions of deficiency. A full discussion of the arguments for and against this theory is given in section 2.2, however we sought to investigate whether there is upregulation of any of the transglutaminases in the aorta with single ($TG2^{-/-}$ or $FXIII\text{-}A^{-/-}$) or double ($TG2^{-/-}$.$FXIII\text{-}A^{-/-}$) gene deficiency. Levels of aortic mRNA were determined by qPCR. The expression levels of each transglutaminase are given relative to the level of that particular transglutaminase in C57Bl/6 control tissue and statistical significance of the change of expression was calculated using one-way ANOVA with Bonferroni correction for multiple testing. Statistical analysis was performed on raw ΔCt values rather than transformed ($2^{-\Delta Ct}$) data and significance was assumed where $p<0.05$.

Transglutaminase 2 is the most abundant transglutaminase expressed in the aorta (Figure 33, panel A) and expression levels of the other transglutaminases are low (FXIII-A and TG3) or negligible (TG1, TG4, TG5, TG6, TG7) in comparison. Absence of TG2 and/or FXIII-A does not significantly increase the expression of any of the other transglutaminases (Figure 33, panel B) and specifically, TG2 or FXIII-A deficiency does not appear to induce compensatory upregulation of mRNA expression of the reciprocal enzyme.

Relative to WT mice, $FXIII\text{-}A^{-/-}$ mice actually showed a reduced level of mRNA expression of TG2 (approx. 3-fold reduction in expression; $p<0.045$); the reverse of what would be expected if reciprocal compensation was occurring in aortic tissue. There was a statistically significant difference in TG3 mRNA expression across the experimental groups ($p=0.029$) with both the $TG2^{-/-}$ and DKO experimental groups exhibiting reduced aortic expression of TG3 mRNA relative to WT (C57 vs $TG2^{-/-}$ $p=0.037$, C57 vs DKO $p=0.031$), a trend also shown by the $FXIII\text{-}A^{-/-}$ group (C57 vs $FXIII\text{-}A^{-/-}$ $p=0.053$). However, the absolute expression of TG3 in our WT samples

was extremely low and therefore it is unlikely that TG3 contributes to the overall TGase activity in the aorta and that these decreases are biologically relevant.

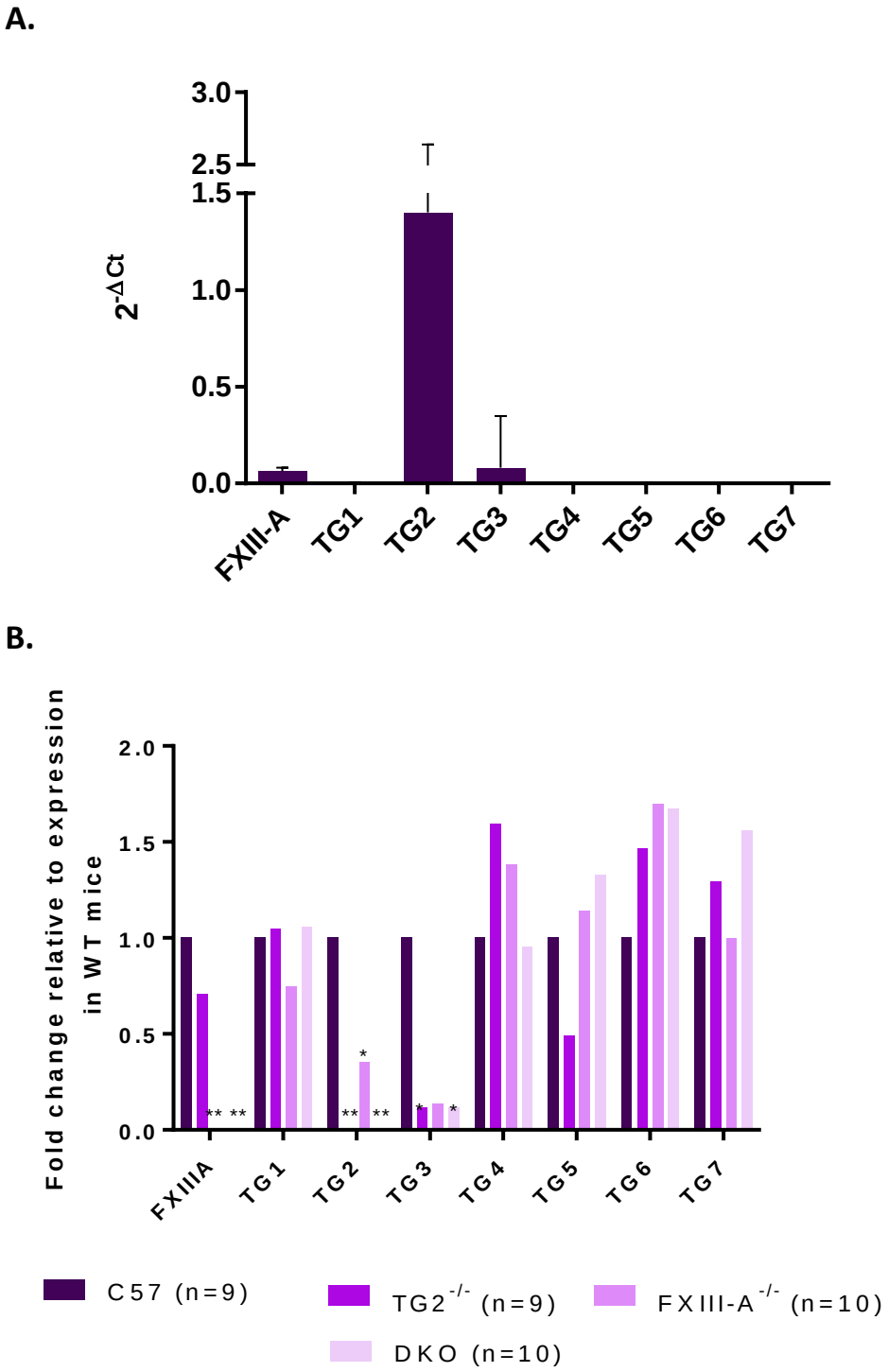

Figure 33. Expression levels of the transglutaminases in the aorta

Panel A. Transglutaminase 2 is the most abundant transglutaminase expressed in the aorta. Expression levels of the other TGs are low (FXIII-A and TG3) or negligible (TG1, TG4, TG5, TG6, TG7). Values shown are TG expression ($2^{-\Delta Ct}$) in C57Bl/6 control aortic tissue (Mean ± 95%CI). **Panel B**. Absence of TG2, and/or FXIII-A does not significantly *increase* the expression of the other TGs, however the FXIII-A$^{-/-}$ mice showed a reduced expression of TG2. Both the TG2$^{-/-}$ and DKO mice showed significantly reduced aortic expression of TG3 relative to WT. All values are expressed as fold change relative to the expression level of that particular transglutaminase in C57Bl/6 control aortic tissue. * = $p<0.05$, ** = $p<0.001$

6.3 Baseline biochemistry

In order to identify any differences in the experimental genotypes in terms of vessel composition we sought to analyse baseline vessel biochemistry prior to injury in a cohort of mice. Important parameters were deemed to be elastin and collagen content as well as a measure of cellularity in the form of LDH and/or DNA levels (relative to protein content). The oxalic-acid extraction required for elastin quantification is not compatible with collagen extraction and hence it was not possible to quantify both elastin and collagen in the same sample. Given that the insoluble fraction was utilised for elastin *or* collagen measurement, LDH and DNA levels were instead compared to solubilised protein content, with a decrease in LDH:protein or DNA:protein ratio indicating a relative loss of cellularity.

Data are summarised in Figure 34 and Figure 35 and are from n=25-28 mice per genotype for LDH and DNA measurements and from n=8-12 mice for elastin and collagen measurements . Statistical analysis was performed using one-way ANOVA with Bonferroni correction for multiple comparison. As elastin:collagen ratios are calculated from average elastin content per group compared to average collagen content per group and do *not* come from elastin and collagen data from the *same* sample, it is not straightforward to present an estimate of the error of these data and hence mean ratio data are presented. More sophisticated statistical options may be available and are being investigated for future work.

Determination of LDH:solubilised protein ratios revealed a statistically significant difference between groups (mean ± SD) (C57 0.013 ± 0.005, $TG2^{-/-}$ 0.013 ± 0.006, FXIII-$A^{-/-}$ 0.011 ± 0.005, DKO 0.009 ± 0.004; p= 0.012) with the DKO group showing a decreased LDH:solubilised protein ratio (p=0.027), indicative of decreased cellularity. Quantification of DNA content was also undertaken with a statistically significant difference found between groups (mean ± SD) (C57 0.0030 ± 0.0014, $TG2^{-/-}$ 0.0028 ± 0.0010, FXIII-$A^{-/-}$ 0.0023 ± 0.0009, DKO 0.0022 ± 0.0006; p<0.0001). Both the FXIII-$A^{-/-}$ and DKO mice had lower DNA:solubilised protein ratios when compared to WT mice (p<0.001 in both cases) although there was no difference between those mice with single FXIII-A gene deficiency and the DKO group. Again, these findings would be in keeping with basal differences in biochemical composition between the genotypes with decreased cellularity in the aortas of mice lacking FXIII-A.

Elastin content was determined using the Fastin^{TM} assay and standardised to solubilised protein and where sufficient sample available, also to LDH content. There was no significant difference in standardised elastin content between genotypes on ANOVA testing (Elastin:solubilised protein, p=0.872, Elastin:LDH

p=0.507). Collagen content was determined using the Sircol^{TM} assay and again standardised to solubilised protein +/- LDH. The DKO mice had a higher mean standardised collagen content than the other genotypes when standardised to solubilised protein content (C57 0.0135 ± 0.006, TG2$^{-/-}$ 0.0118 8 ± 0.006, FXIII-A$^{-/-}$ 0.0133 ± 0.008, DKO 0.0171 ± 0.009, p=0.341) or to LDH content (C57 1.16 ± 0.48, TG2$^{-/-}$ 1.21 ± 0.67, FXIII-A$^{-/-}$ 1.48 ± 0.73, DKO 1.89 ± 1.23, p=0.176) however this was not statistically significant.

Summary data for elastin:collagen ratios for each of the methodologies (solubilised protein: C57 25.1, TG2$^{-/-}$ 24.5, FXIII-A$^{-/-}$ 22.5, DKO 15.8; LDH: C57 20.2, TG2$^{-/-}$ 18.2, FXIII-A$^{-/-}$ 18.3, DKO 15.8) are presented in Figure 35 and clearly show a trend towards a decreased ratio in the DKO group. This finding could either reflect a decreased vessel elastin content, which is not seen, or indicates a relative collagen increase i.e. fibrotic change within the aorta.

A.

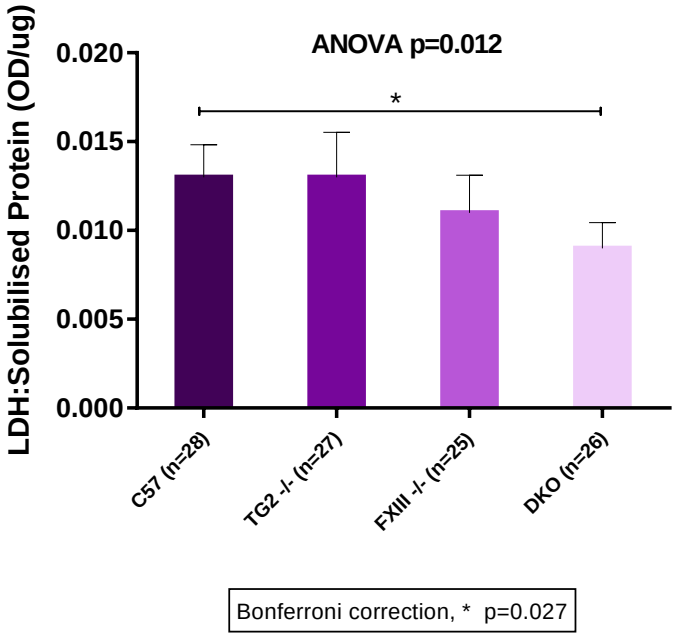

B.

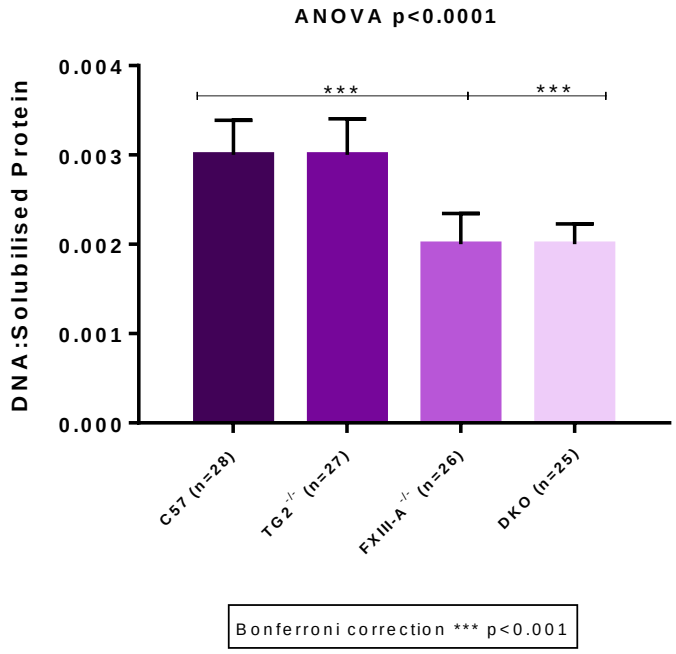

Figure 34. Baseline biochemical characteristics of un-operated aortas
Data shown as mean ± 95% confidence intervals, n=25-28 in each group. **Panel A.** shows LDH levels in un-operated aortas, standardised to solubilised protein content. ANOVA testing revealed a statistically significant difference between groups with DKO aortas having a lower LDH:solubilised protein ratio than the other genotypes. **Panel B.** shows DNA content in un-operated aortas, standardised to solubilised protein content. ANOVA testing revealed a highly statistically significant difference between groups with FXIII-A$^{-/-}$ and DKO aortas having a lower DNA:solubilised protein ratio than the other genotypes. See text for further details.

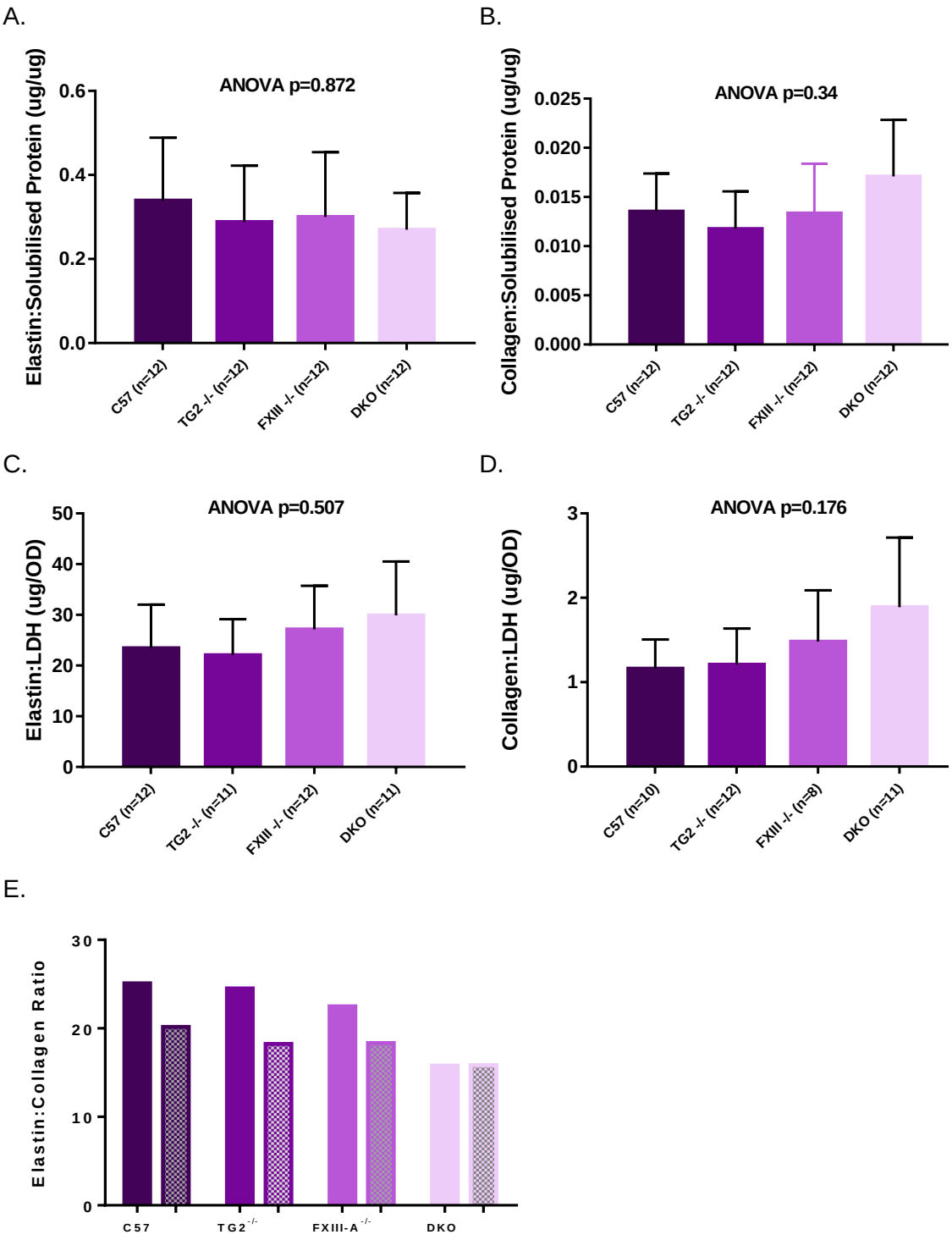

Figure 35. Elastin and collagen content of un-operated aortas

All results are presented as mean ± 95% confidence intervals, n=8-12 in each group. **Panel A**. shows elastin content in un-operated aortas, standardised to solubilised protein content. Panel B shows collagen content (standardised to solubilised protein). **Panels C and D** respectively show elastin and collagen content standardised to LDH content. Elastin:collagen ratios (mean elastin content / mean collagen content for each group) are presented in **Panel E**. with results from the solubilised protein methodology shown in filled bars and the results from the LDH methodology shown in patterned bars.

6.4 Expression data

Given the role of TG2 as a cross-linking enzyme and its multiple “structural” protein substrates (including tropoelastin and fibrillin) we sought to investigate whether TG2 deficiency (and/or FXIII-A deficiency) altered the mRNA expression of various structural proteins within the mouse aorta. Levels of mRNA expression were determined by qPCR and statistical analysis was performed on raw ΔCt data (i.e. $Ct_{gene\ of\ interest} - (0.5*(Ct_{\beta actin}+Ct_{Rpl32}))$. Experimental groups were compared using one-way ANOVA with Bonferroni correction for multiple testing. As well as structural proteins, a number of other gene transcripts were investigated, including CD163 (an M2 macrophage marker), tPA and uPA (serine proteases which catalyse plasminogen activation and ECM breakdown), perilipin (a protein found on the surface of lipid droplets), PAI-1 (due to its role as an inhibitor of tPA and uPA) and TGF-β. These results are summarised in Figure 36.

There was no statistically significant difference in expression of any of the “structural” proteins investigated across the experimental groups. Specifically there was no statistically significant difference in the expression of elastin in the $TG2^{-/-}$ group, despite levels being approximately 17% of that seen in the C57Bl/6 mouse aortas.

Perilipin expression differed significantly across groups (p=0.0023) and expression was lower in both the $TG2^{-/-}$ (p=0.022) and FXIII-$A^{-/-}$ groups (p=0.001), although not significantly different from WT in the DKO group (p=0.373). Given that perilipin is associated with lipid droplet formation it may be that these results reflect a difference in the amount of fat collected at the time of aortic harvest, rather than a true difference in expression subsequent to gene deficiency. Certainly there was no marked increase in perilipin expression in FXIII-A deficient mice, despite claims that FXIII-A inhibits adipogenesis in culture. There was also no statistically significant, or systematic, difference in expression of PAI-1, uPA, tPA, or CD163, thus providing no evidence of differences in local inflammation between genotypes, at an mRNA level.

Expression of TGF-β was significantly different across the groups (p=0.0044) due to a higher level of expression in the FXIII-$A^{-/-}$ group only (levels >2-fold increased compared to WT; p=0.002). Aortic expression levels of the other gene transcripts of interest were not significantly different in the transgenic mice compared with the WT group.

A.

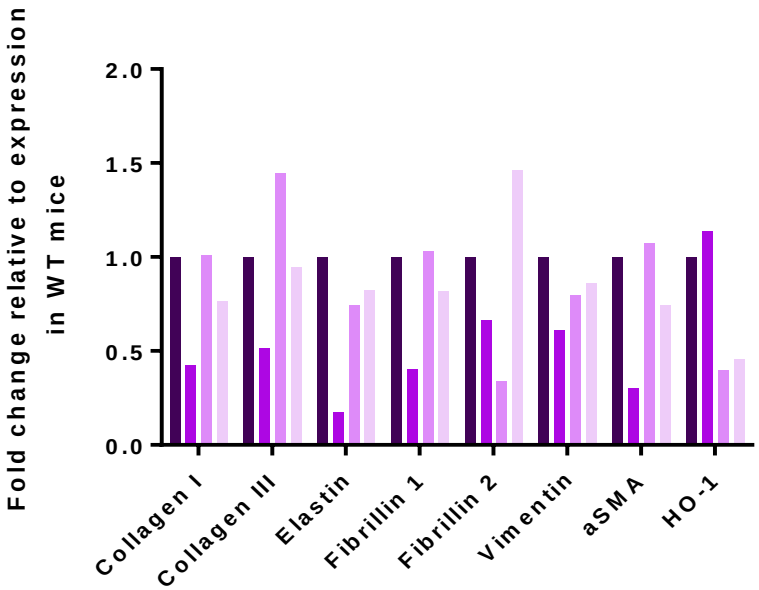

B.

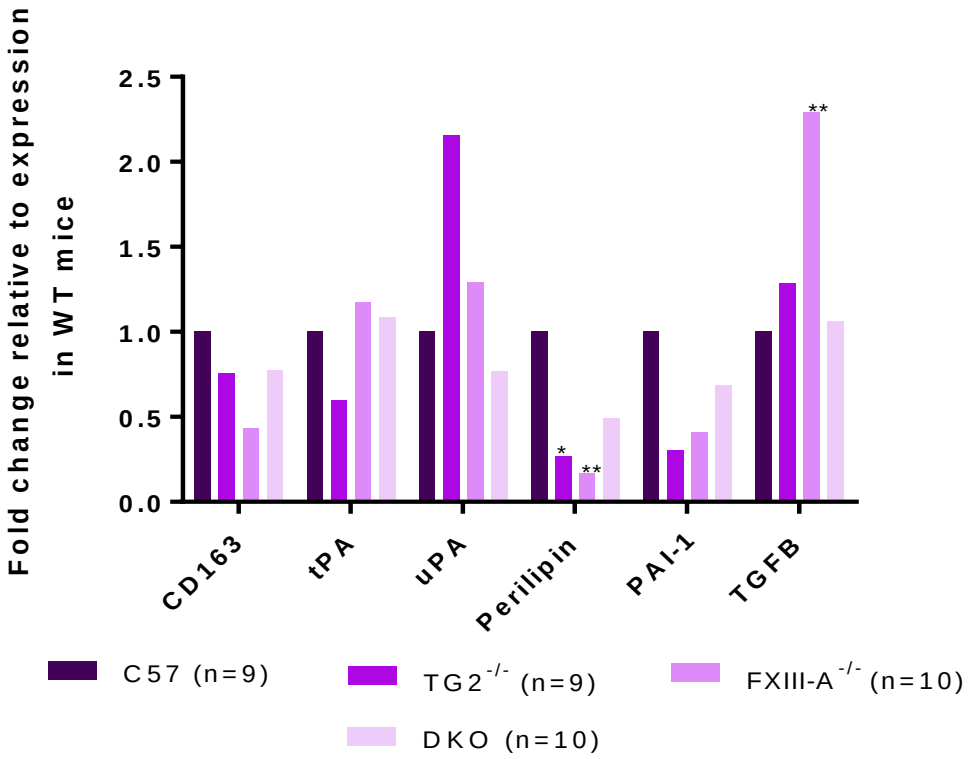

Figure 36. Gene transcript expression levels in the un-operated aorta
Data is expressed as fold change relative to the expression level of that particular gene transcript C57Bl/6 control aortic tissue. **Panel A.** shows mRNA expression of various "structural" proteins in the un-operated aorta with no significant differences between experimental groups. **Panel B.** shows expression of a number of other genes of interest. Statistical analysis was performed using one-way ANOVA with Bonferroni correction. * = $p<0.05$. ** = $p<0.01$

6.5 MMPs

Quantitative real-time PCR was performed to investigate the mRNA expression of various MMPs in aortic tissue from each of the experimental genotypes. In view of their reported importance in aneurysm development, we chose to look at MMP-2, -9, -12, -14 (MT1-MMP), as well as TIMPs -1 and -2. These results are summarised in Figure 37 and data were analysed using ANOVA and Bonferroni testing.

MMP-2 and TIMP-2 showed the highest levels of expression in the un-operated WT aorta (Figure 37, panel A), with very low levels of MMP-9, MT-MMP-1 and TIMP-2. There was no detectable expression of MMP-12 in the un-operated aorta in the C57Bl/6 group, as expected from its known release from macrophages in response to injury.

Only expression of MMP-9 ($p=0.025$) and TIMP-1 ($p=0.035$) differed significantly across the experimental groups. Aortas from the $TG2^{-/-}$ mice had lower levels of MMP-9 expression (approx. 40% of WT expression, $p=0.034$), however given the very low expression of this gene transcript under normal circumstances, this additional decrease is unlikely to be biologically relevant.

TIMP-1 expression was increased in aortas taken from $FXIII\text{-}A^{-/-}$ mice (nearly 3-fold increase compared to WT, $p=0.013$), a difference not seen in either the $TG2^{-/-}$ or DKO groups. All three transgenic groups showed detectable MMP-12 mRNA by q-PCR however there was no statistically significant difference in MMP-12 expression between the WT mice and any of the transgenic mouse aortas on ANOVA testing.

Attempts were made to validate the findings from qPCR using enzyme zymography with methodology as outlined in section 4, and currently in use in our lab utilising cell lysates. Unfortunately, we were unable to optimise this assay sufficiently to obtain useful data. Conditioned media from cultured HT-1080 cells (kindly supplied by Dr Emily Clarke on behalf of Dr Karen Porter) was successfully assayed as a control sample (see gel in Figure 38), and hence we proceeded to assess the optimum conditions to produce conditioned media from our aortic samples. Although we were able to assay “fresh” conditioned media from our un-operated aorta samples (see Figure 38. panel B), subsequent samples, from both operated and non-operated vessels, generated absent or unclear digestion bands which we were unable to quantify meaningfully. We felt that at least some of the issues with this protocol may have been explained by the freezing of these media samples prior to subsequent assay in “batches” of samples. This was done for logistical reasons but may have impacted on enzyme activity in the small amount of aortic tissue harvested from each mouse. A trial zymography assay was undertaken in freshly

harvested operated aortic tissue but again we were unable to identify the presence of either pro- or activated forms of MMP-2 or -9 in gelatin zymography or MMP-12 with casein zymography. We hypothesise that we are seeing proteolytic degradation of our samples and hence will need to extract the MMPs in an appropriate protease inhibitor, such as that used by Eliason *et al*,(Eliason et al., 2005b) which would spare the zinc-dependent MMPs. Further work is planned to optimise this technique to enable quantification of differential MMP content and activity in un-operated vs. operated samples and across the experimental genotypes.

A.

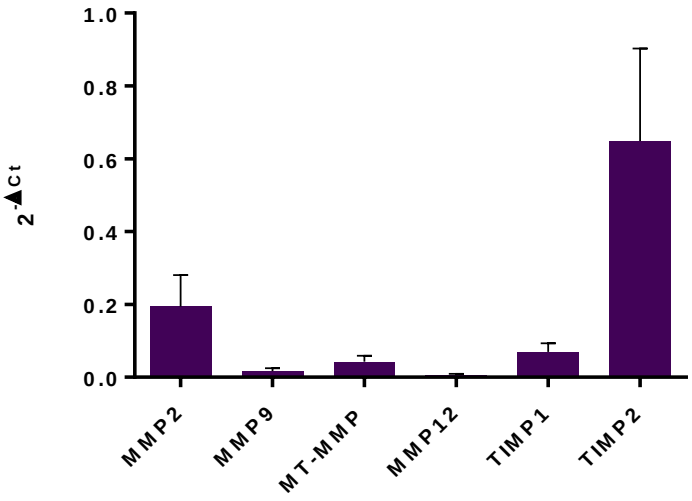

B.

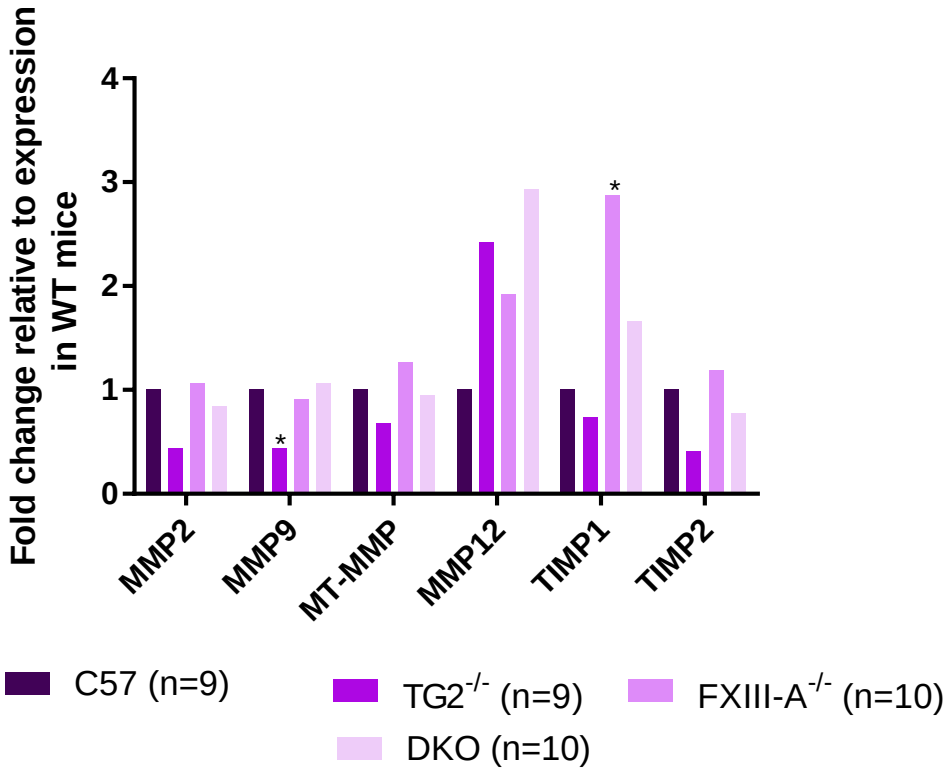

Figure 37. Expression levels of the MMPs in the un-operated aorta
Panel A. Values shown are MMP expression ($2^{-\Delta Ct}$) in C57Bl/6 control aortic tissue (Mean ± SD). MMP-2 is the most abundant MMP expressed in the aorta, and TIMP-2 the most abundant TIMP of those investigated. Expression levels of the other MMP/TIMPs are low (MMP-9, MT-MMP-1, TIMP-1) or absent (MMP-12). **Panel B.** TG2-deficient mice showed a decrease in MMP-9 and FXIII-A mice an increase in TIMP-1 expression. MMP-12 expression was detectable in control aortas from all of the transgenic mouse lines. All values are expressed as fold change relative to the expression level of that particular transglutaminase in C57Bl/6 control aortic tissue. * = $p<0.05$.

A.

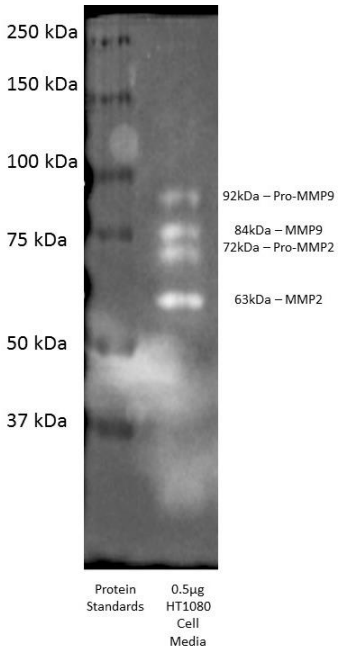

B.

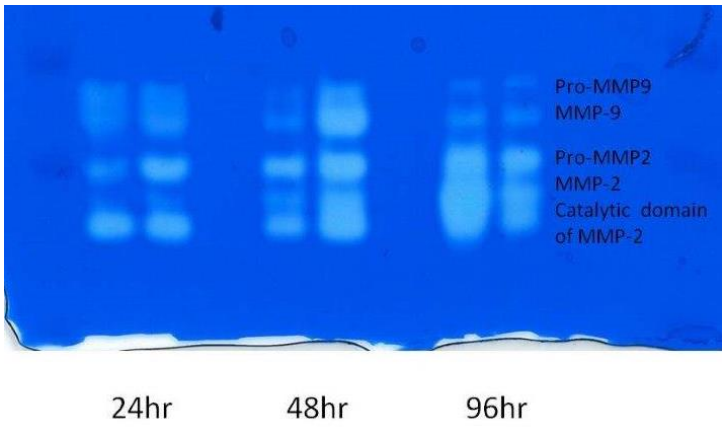

Figure 38. MMP gelatin zymography

Panel A. Gelatin zymography of conditioned media from cultured HT1080 cells. Gel clearly shows bands of enzymatic digestion at sizes consistent with both the pro- and active forms of both MMP-2 and MMP-9. **Panel B.** is a representative gel from a trial assay whereby un-operated WT aortic samples were incubated in reduced serum media for either 24-, 48-, or 96-hours prior to zymography. Although digested bands are visible they are unclear and difficult to quantify using densitometry. See text for more details.

6.6 Endothelial permeability

Transglutaminases (and specifically FXIII-A) have been implicated in the maintenance of endothelial barrier function,(Sane et al., 2007) the loss of which plays a role in the early development of atherosclerosis and fibrosis. FXIII-A is thought to modify paracellular transport in endothelial cell culture (Noll et al., 1999b) and acquired, relative FXIII-A deficiency may contribute to the myocardial and pleural oedema seen after cardiopulmonary bypass.(Wozniak et al., 2001) The role of TG2 in endothelial barrier function is less well understood. To investigate this further we used a method described by Orr *et al* (Orr et al., 2007) to assess aortic vessel permeability in each of the four experimental genotypes (n=10-12). Data was analysed using one-way ANOVA testing with Bonferroni's correction.

Figure 39 summarises this data and shows mean Evans Blue concentration (amount (ng) per mg dry weight of aorta) for each of the genotypes. Account needs to be taken for the variation in this technique, however despite this we obtained results similar to Orr *et al*. Our C57Bl/6 mice showed low levels of Evans Blue (mean ± SD; 17.7 ± 10.6 ng/mg), indicating minimal leakage of dye into the aorta and "normal" vessel permeability.

The $TG2^{-/-}$ group (7.7 ± 5.6 ng/mg, p=NS) was not significantly different from WT, whereas the $FXIII\text{-}A^{-/-}$ and DKO groups both showed increased Evans Blue concentration (34.9 ± 20.8 (p=0.045) and 34.6 ±14.9 (p=0.051) ng/mg respectively). There was no significant difference in Evans Blue concentration between the $FXIII\text{-}A^{-/-}$ and DKO (p>0.99) indicating that it is FXIII-A that contributes to endothelial permeability and that additional TG2 loss does not worsen the observed deficit in barrier function.

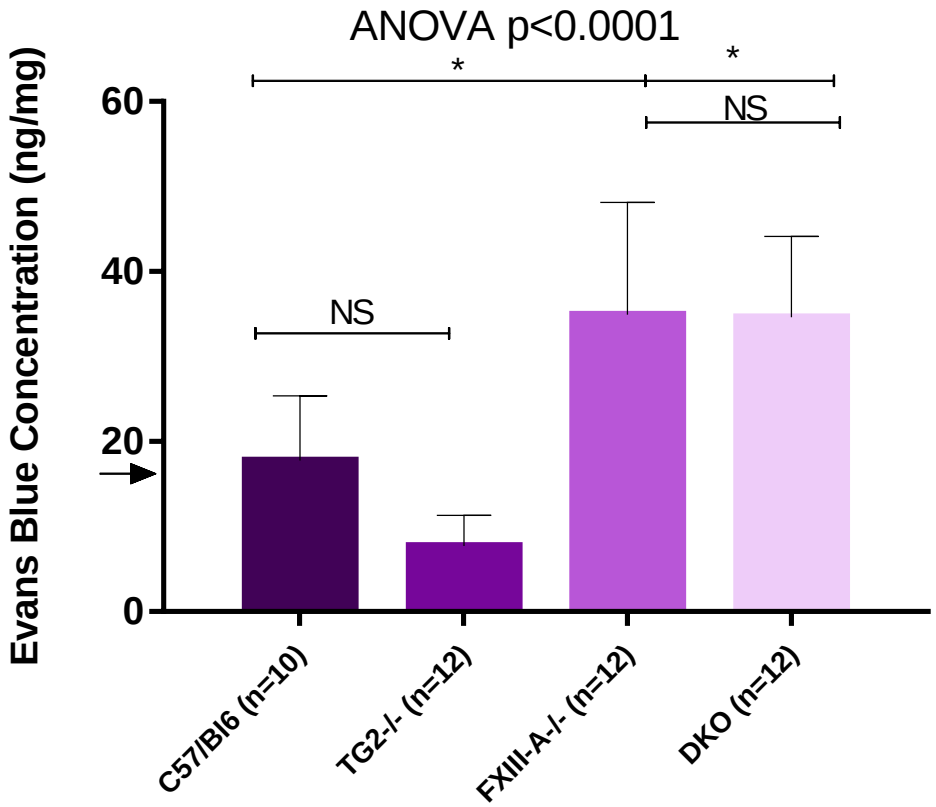

Figure 39. Aortic endothelial permeability

Data shown are mean Evans Blue concentration (amount by aorta weight (ng/mg)) with 95% CI. Evans Blue concentration is significantly increased in the FXIII-A$^{-/-}$ and DKO groups compared to wildtype (*, $p<0.05$) indicating an increased endothelial permeability in these mice. There was no significant difference on ANOVA testing between C57Bl/6 mice and those with TG2 deficiency, or between the FXIII-A$^{-/-}$ and DKO groups. Arrow indicates mean result (18 ± 4 ng/mg) obtained by Orr *et al* in (Orr et al., 2007).

6.7 Wire myography

Biochemical assays on the DKO arteries at baseline indicate that they have an increased collagen:elastin ratio. Our initial results also suggest that the DKO vessels (and possibly also the FXIII-$A^{-/-}$ vessels) are less cellular, possibly due to a loss of aortic VSMCs. Wire myography provides a means of measuring aortic tension and contractility under controlled conditions and allows us to investigate the expected differences between the genotypes. This myography assay was established and optimised following the advice of Prof David Beech and then individual experiments were performed by Dr Lih Cheah - I would like to acknowledge her skill and time with regards the generation of these data.

The infrarenal aorta (n=4 per genotype) was harvested into cold Hanks solution and aortic rings (2 per sample) of 1mm length were mounted in a myography. The rings were then placed under normalised tension by increasing the separation distance of the mounting wires. The force (mN) generated at each separation distance (µm) was recorded and is shown graphically in panel B of Figure 40. This process provided initial evidence that the DKO vessels were different from those from other genotypes as they generated less force at each separation distance than vessels from mice of other genotypes, i.e. they have intrinsically lower vessel tension. After equilibration and assessment of contractile function to high concentration K^+ and phenylephrine (PE) a concentration response curve of contraction (mN) vs. log [PE] was constructed.

Mean dose-response curves for each genotype group are shown in panel D of Figure 40 along with calculated EC_{50} values (the concentration of PE required to produce 50% maximal response) in panel C. The EC_{50} values were not statistically different on Kruksal-Wallis testing across the groups (mean concentration (µM) ± SD; C57 0.125 ± 0.049, $TG2^{-/-}$ 0.179 ± 0.040, FXIII-$A^{-/-}$ 0.120 ± 0.052, DKO 0.158 ± 0.061, p=0.129) and the maximum force generated was also not statistically different between groups although this value was lower in the DKO vessels (mean maximum force (mN) ± SD; C57 3.99 ± 1.95, $TG2^{-/-}$ 3.66 ± 1.61, FXIII-$A^{-/-}$ 3.50 ± 1.96, DKO 2.58 ± 0.91, p=0.439). To attempt to assess tension as a whole – which appeared to be lower in the DKO vessels (mean curve shifted downwards and to the right) – we performed area-under-the-curve (AUC) analysis which has been advocated by some to be the most reliable metric to assess dose-response curves (Huang and Pang). DKO vessels showed a trend towards lower AUC values than control vessels (mean AUC ± SD C57 11.55 ± 3.65, $TG2^{-/-}$ 10.65 ± 3.91, FXIII-$A^{-/-}$ 10.16 ± 5.49, DKO 6.55 ± 2.09, p=0.118) however this did not reach statistical significance (p=0.072) and requires further investigation.

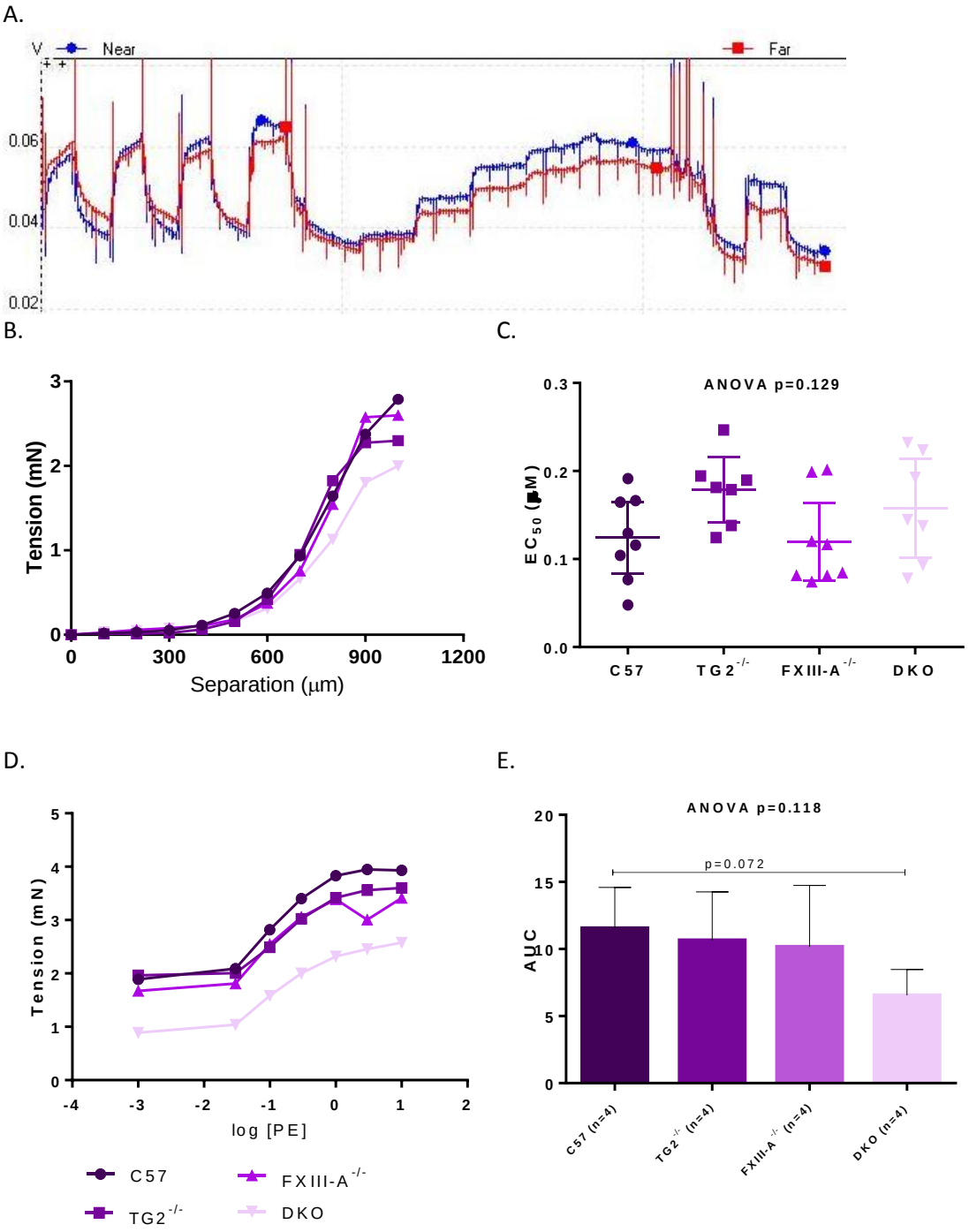

Figure 40. Wire myography – un-operated aorta

Panel A. is a representative myography trace from a WT mouse. For details of the full protocol see section 4.11. **Panel B** .shows the average force generated by the initial wire separation during myography set-up and highlights that the DKO vessels generated less force for each separation distance. Mean dose-response curves (n=4 per genotype with 2 repeats per vessel) showing the contraction response (force in mN) to increasing concentrations of PE are shown in **panel D**. with EC_{50} data (presented as mean ± 95%CI) in **panel C.** Summary data for this dose-response is presented in **panel E**. as AUC analysis with ANOVA testing, p=0.118.

6.8 Histology

Normal, un-injured, aortas (n=2 per genotype) were harvested into 4% PFA and 2 x 5µm sections cut at 200µm intervals throughout the vessel. Sections were stained with haematoxylin and eosin and imaged to assess any obvious histological differences in vessel structure between the four experimental genotypes. Representative images from each of the genotype groups are shown in Figure 41. No obvious differences were seen between the groups, however Newell *et al* (publication in preparation) reported histological differences between carotid arteries of $ApoE^{-/-}$ and $ApoE^{-/-}.TG2^{-/-}.FXIII^{-/-}$mice subject to sham operation. The TKO cohort showed increased elastic lamellae number and a higher frequency of elastic breaks than the control animals.

In light of these findings, the same sectioning protocol as above was undertaken in both un-operated (n=2 per group) and sham operated (NaCl application, n=2 per group) followed by staining with Miller Van Gieson to highlight elastin fibres (shown as purple in the image in Figure 41). The maximum lamellae number was recorded for each section and then the mean maximum number calculated for each vessel and compared across genotypes. These results are tabulated in panel E of figure 39; there was no difference between the experimental groups in terms of lamellae number under either un-operated or sham-operated conditions. Likewise sham operation (the application of NaCl) had no effect on lamellae number in any of the experimental groups i.e sham-operation does not induce an increase in lamellae number, unlike the changes seen in the ligation protocol. No broken elastic fibres were observed in aortic sections from any of the genotypes at baseline, nor after sham-operation.

A.

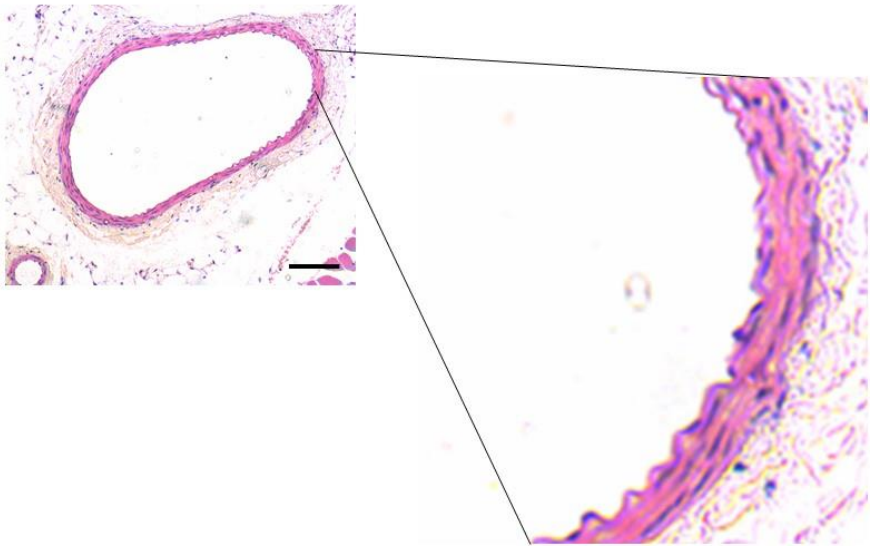

B.

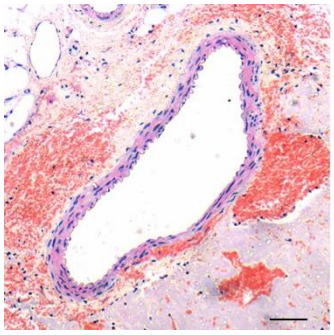

C.

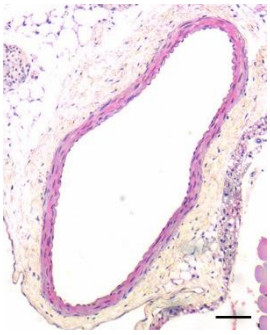

D.

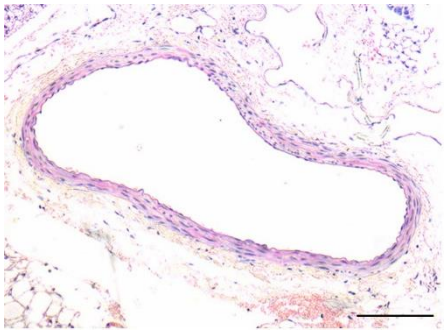

E.	C57Bl/6	TG2$^{-/-}$	FXIII-A$^{-/-}$	DKO
Normal "un-operated" vessels	4.82 ± 0.51	4.45 ± 0.51	4.55 ± 0.51	4.66 ± 0.55
Sham (NaCl) operated vessels	4.70 ± 0.56	4.31 ± 0.47	4.64 ± 0.49	4.62 ± 0.55

Figure 41. Effect of TG2 and/or FXIII-A deficiency on "normal" aortic histology

Panels A shows a representative section from a "normal" un-operated aorta from a C57Bl/6 mouse with inset to show lamellar structure. **Panels B, C and D** show representative sections from "normal", un-operated vessels from a TG2$^{-/-}$, FXIII-A$^{-/-}$ and DKO mouse respectively. All images are from haematoxylin and eosin stained 5µm sections imaged at 10X magnification. Scale bar represents 100µm in each image. **Panel E.** shows lamellar number (mean ± SD) for normal and sham operated aortas (n=2 per genotype) Statistical analysis was perfomed using Kruksall Wallis testing and showed no differences between genotype groups.

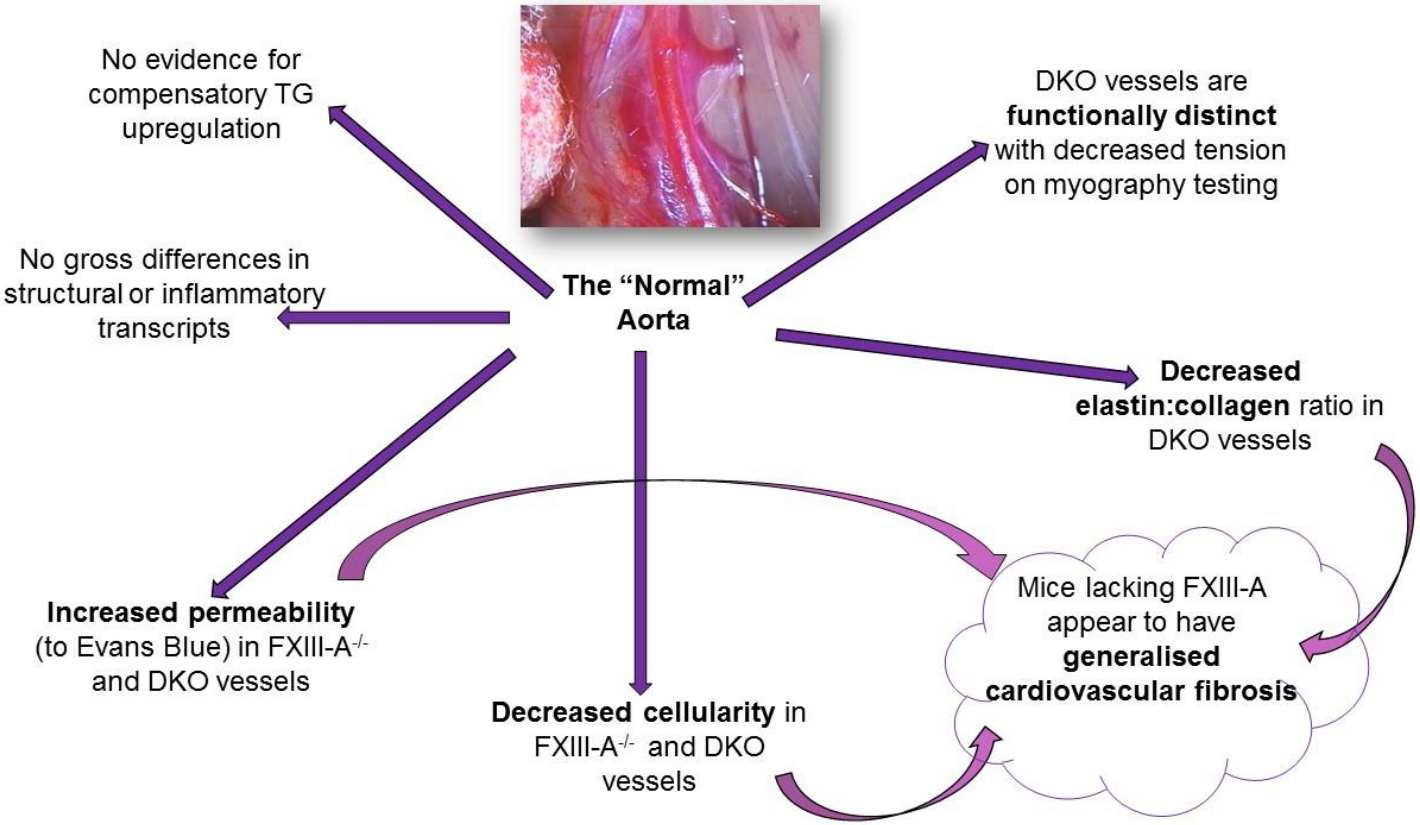

Figure 42. Summary diagram - the normal aorta

This figure summarises the main findings from Chapter 6 pertaining to the structure and function of the the "normal" un-operated aorta in each of the transgenic mouse lines. Dark purple arrows highlight findings from this thesis whilst light purple arrows illustrate those findings that may be related to the overall conclusion that mice lacking FXIII_A appear to have generalised (aortic) cariovascular fibrosis. These results are discussed in full in section 6.9.

6.9 Discussion

In this chapter we investigate the roles of TG2 and FXIII-A in basal structure and function and present the evidence for upregulation of other transglutaminases to compensate for single or double gene deficiency. These findings are summarised in Figure 42 and ultimately lead to the conclusion that mice lacking FXIII-A exhibit generalised cardiovascular fibrosis, which (we hypothesise) is secondary to increased vessel “leakiness”.

Using qPCR we determined that (as previously shown by Cordell *et al* in cardiac tissue)(Cordell et al., 2015) TG2 is the most abundantly expressed transglutaminase in the mouse aorta. Similar levels of transglutaminase mRNA gene expression were seen in aortas harvested from the transgenic lines (with complete absence of TG2 in the $TG2^{-/-}$ line, FXIII-A in the $FXIII\text{-}A^{-/-}$ line and both TG2 and FXIII-A in the DKO line as expected). We found no evidence of a compensatory increase in mRNA expression of any of the other transglutaminases in the setting of gene deficiency and, specifically, there was no evidence of a compensatory increase in mRNA of the alternative enzyme in either the TG2 or FXIII-A KO animals.

One obvious limitation of qPCR and the analysis of transcription levels of mRNA is that these levels do not necessarily correlate to enzyme activity within the tissue examined. Transcription may be increased, yet changes in translation or post-translational modification may mean that protein levels are unchanged or even decreased. Likewise, changes in enzyme inhibition or activation may mean that increased amounts of a particular transglutaminase do not equate to increased activity. Even if a particular mRNA transcript (and subsequent protein product) is increased we are unable to predict the effect that this could have on the complex signalling networks and cascades that exist within the aorta. For example, a small rise in MMP expression could effect multiple targets, leading to cell infiltration, growth factor release and proteolytic degradation, or alternatively could be rapidly neutralised by already present inhibitors. Real-time PCR results must therefore be interpreted whilst taking account of the limits of the methodology, but they still provide an important means of identifying potential candidates for follow-up protein studies.

If, as is reported, TG2 and FXIII-A are predominantly found in an inactive or latent state with regards their transamidating function, it may be that conditions that result in their activation (such as a rise in calcium concentration or reduction via thioredoxin) may be more important in functional compensation than upregulation

per se. Confirmation of this hypothesis would require in situ assay of isozyme-specific transglutaminase activity in the aorta which could be undertaken using the methodology of Itoh *et al* who utilised fluorescence-labelled substrate peptides to localise TG2-ase activity in whole body sections from mice.(Itoh et al., 2011) However, certainly at an mRNA level, there is no evidence of reciprocal compensation between FXIII-A and TG2 in the aorta.

We found no gross differences in levels of mRNA for various "structural" gene transcripts and no evidence of differences between the groups in those transcripts known to be involved in inflammation and proteolysis. Alpha-SMA was expressed at the highest levels in the aorta (far in excess of the levels of any of the other transcripts) and reflects the presence of VSMCs; collagen, elastin and vimentin were also expressed at high levels, although again, did not vary significantly between groups. A knowledge of transcription levels in the "normal" or WT tissue under study is obviously important when interpreting fold changes, for example TGF-β levels were 2-fold higher in FXIII-$A^{-/-}$ samples, a statistically significant change, however one which was not seen in DKO samples and correlates to a very small *actual* level of expression.

Investigation of MMP mRNA levels revealed that MMP-2 levels were highest in the baseline WT aorta and that these were unchanged in the transgenic lines. MMP-12 expression could not be detected (below the threshold of Ct=40) in the WT samples which was as expected given the known release of this enzyme from infiltrating macrophages in response to injury. In contrast, we were able to detect MMP-12 expression in the aortas of $TG2^{-/-}$, FXIII-$A^{-/-}$ and DKO mice which may be reflective of low level vascular damage in these experimental animals.

Of particular interest, in light of the cardiac fibrosis exhibited by our FXIII-$A^{-/-}$ and DKO animals, was the finding that aortas from these animals also showed evidence of decreased LDH (in DKO mice) and DNA (in FXIII-$A^{-/-}$ and DKO mice) content relative to solubilised protein levels. These results are indicative of decreased cellularity, perhaps indicating a loss of VSMCs in these vessels. Coupled with this is an observed increase in collagen content seen in the vessels of the DKO animals. This result suggests a degree of fibrotic change in the aortas of the DKO mice at baseline and is important when interpreting any subsequent differences in response to injury in these animals.

Just as the myocardial sections of the mice with cardiac fibrosis also showed increased haemosiderin deposition (suggesting increased vessel "leakiness") we have shown that the FXIII-$A^{-/-}$ and DKO aortas showed increased Evans Blue content reflecting an increased large vessel permeability. No significant difference

was observed between WT and TG2$^{-/-}$ mice or between FXIII-A$^{-/-}$ and DKO mice in this assay implying that it is FXIII-A that contributes to endothelial permeability and that additional TG2 deficiency does not worsen the observed deficit. We hypothesise that FXIII-A$^{-/-}$ mice have increased vessel "leakiness", allowing extravasation of RBCs, and the production of haemosiderin by inflammatory macrophages. This persistent inflammatory stimulus prompts attempts at vessel repair (by TG2) which are partially successful in FXIII-A$^{-/-}$ mice (hence the reduced cardiac fibrosis and relatively "normal" aortic biochemistry) but are lacking in DKO mice giving rise to generalised cardiovascular fibrosis.

Wire myography (with vessels held under isometric conditions) allows the examination of basic vessel properties such as length-tension relationships and vascular smooth muscle function whilst also providing a system for assessment of pharmacological reactivity. Although pressure myography (with vessels held under isobaric conditions) is felt by some to be more "physiological", similar results for passive relationships can be obtained with both techniques (Buus et al., 1994) and agonist responses can be adequately compared between vessels when using either methodology. Although there is a theoretical risk of endothelial surface damage with the wire mounting, we screened for this by assessing vessel response to carbachol and this was not an issue in our hands. The wire myography protocol has been fully optimised by the Beech group in our Institute and we are grateful to Professor Beech for his input to this work.

Using the wire myography protocol we have identified that the DKO aortas are functionally distinct from those in the other genotype groups. Less tension was developed in these vessels during the initial normalisation procedure, i.e for every µm of "stretch" applied to the vessel a lower force was recorded. Contractility as measured by dose-response to phenylephrine was not significantly different in the DKO aortas with equivalent EC_{50} and force range (maximum force – minimum force) values achieved across all genotypes. The reasons for the observed decreased vessel tension are not immediately obvious although these data could suggest that elastin function is in some way comprised in the DKO aorta. We have not seen evidence for a loss of elastin in these vessels (either biochemically or histologically) and no elastin breaks were observed in un-operated aortas. We hypothesise that the decreased vessel tension is a function of impaired elastin cross-linking (?by TG2) in the media; the fact that deficit is only seen in the DKO vessels implies that either 1) both TG2 and FXIII-A contribute to elastin x-linking basally and that function is only compromised with loss of both enzymes, 2) TG2 cross-links elastin basally but deficit is compensated by FXIII-A activity or 3) loss of

TG2 cross-linking coupled with impaired vessel integrity (due to FXIII-A action on endothelial barrier function) is sufficient to cause functional impairment. Further work is required to elicit which of these possible mechanisms is physiologically relevant *in vivo* however (tropo)elastin has not previously been reported to be a substrate for FXIII-A .

Chapter 7: Results – TG2 and FXIII-A in Aneurysm Induction and Progression

Chapter 7: Results – TG2 and FXIII-A in Aneurysm Induction and Progression

7.1 Aims

We aim to establish the murine $CaCl_2$ model of abdominal aortic aneurysms in our Institute and optimise the experimental conditions for its use. We then aim to investigate the roles of TG2 and FXIII-A in aneurysm induction and progression using the above experimental model.

7.2 Carotid ligation model

7.2.1 Survival and histology

Carotid ligation has been widely used as a model of neointimal formation and inward vessel remodelling however, in $ApoE^{-/-}.TG2^{-/-}.FXIII\text{-}A^{-/-}$ (TKO) mice carotid ligation has been shown to result in elastin damage, vessel dilatation and rupture. To verify the results obtained by Drs Newell and Jackson in Bristol without the presence of a confounding $ApoE^{-/-}$ background, we carried out carotid ligation in a cohort of C57Bl/6 and DKO mice. Mice (n=10 per genotype) underwent right common carotid artery ligation under anaesthesia, were recovered, and harvested at 28 days. All C57Bl/6 mice (M:F=1:1) survived to harvest with no post-operative complications. Of the 10 DKO mice operated (M:F=3:2), one (female) mouse was found dead at 24 days post-op. A post-mortem analysis was carried out, which revealed findings consistent with vessel rupture with a large amount of blood and clots in the neck. There was no other gross pathology evident.

In many ways these results replicate what was seen by Newell *et al*, in that WT mice tolerated the procedure well, with no associated morbidity or mortality. The only death in our hands occurred in the DKO group and was indicative of vessel rupture, however this mortality occurred much later than the deaths observed in the TKO mice (which occurred at 5-7 days) and at a much lower rate. This suggests that the additional $ApoE^{-/-}$ gene deficiency may influence outcome after surgery by means that are as yet unknown.

Representative histology from these procedures (as shown in Figure 43) was obtained in n=2 mice per group with Miller van Gieson staining undertaken to show elastin fibres. The C57Bl/6 mice appeared to show elastin flattening but no clear evidence of either inward remodelling or elastin fibre breakage. In contrast, the DKO mice showed an increased lamellae number (as was seen in the TKO sham

operated group) but without elastin disruption. Further work is needed to fully characterise this model in our DKO mice but clearly the additional ApoE gene deficiency is detrimental to vessel integrity either before or following carotid ligation .

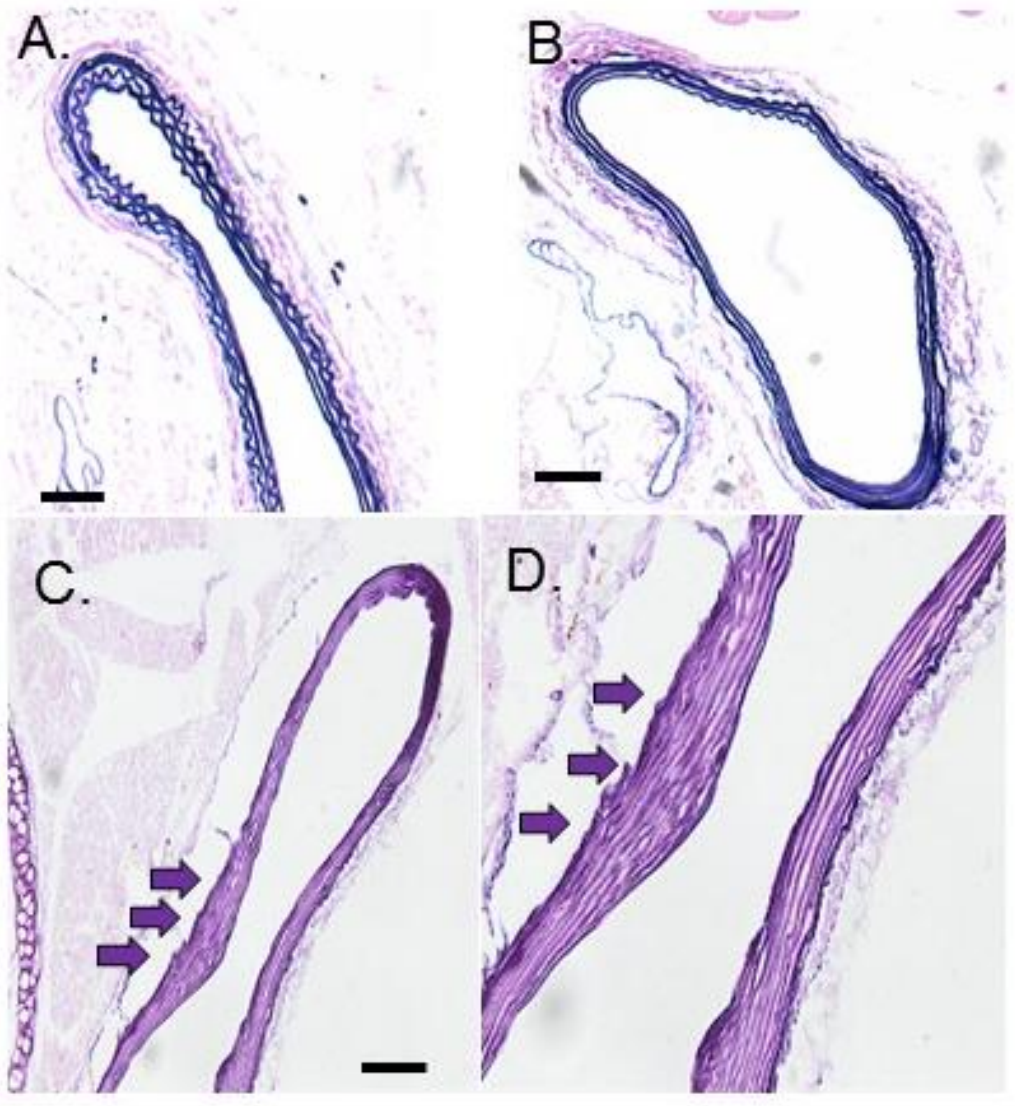

Figure 43. Representative histology – carotid ligation model

Images are captured at 10x magnification from 5µm sections of mouse carotid arteries. All panels show staining with Miller staining to highlight vessel elastin fibres and scale bar represents 100µm in each image; **panels A and B** are co-stained with Van Gieson stain whilst **panel** C is co-stained with Picosirius Red. **Panel A** is representative of a “normal”, unoperated C57Bl/6 carotid artery with typical wavy fibres and 3-5 clearly defined elastic lamellae. **Panel B** is from a C57Bl/6 mouse subjected to carotid artery ligation. Elastin flattening is seen in these vessels but with no loss of integrity. **Panel C** showd a DKO mouse carotid artery following ligation. Again, there is no evidence of elastic fibre disruption but an increased lamellae number was clearly observed (filled arrows) which is shown magnifid in **panel D**

7.3 CaCl2 aneurysm model

7.3.1 Safety and feasibility of the model

The $CaCl_2$ model, as communicated by the Baxter lab at the University of Nebraska, was established in our Institute and piloted in a trial group of C57Bl/6 mice. The model was found to be reproducible with obvious gross differences between the vessels of those mice treated with NaCl and those treated with $CaCl_2$ (see Figure 44).

Operations carried out in the first two months (n=21) after initiating the Nebraska protocol were undertaken in a mean of 38.4 ± 7.5 minutes, which is far below the duration of isofluorane anaesthesia deemed safe.(Szczesny et al., 2004) Those undertaken in the second two months (n=47) were undertaken in a mean of 32.6 ± 3.0 minutes, which was not significantly different from the overall mean operating time (31.6 ± 3.9 minutes; p=0.09). This suggests that there is an initial learning curve to the model, during which operation time can be reduced, and beyond which operation time cannot be reduced further. Pilot work also revealed that laparotomy and aortic exposure could be achieved without significant intra-operative bleeding and that there were no obvious problems with wound healing.

7.3.2 Effect of increasing $CaCl_2$ concentration

The specifics of the $CaCl_2$ model (concentration of calcium, exposure time, time to harvest) vary between investigators.(Wang et al., 2013a) To determine the optimal concentration of $CaCl_2$ to utilise in this work we undertook injury using NaCl (sham-operated), 0.25M $CaCl_2$ and 0.5M $CaCl_2$ in C57Bl/6 mice before harvest at 6 weeks. Aggregated data from all control mice utilised in the data to be presented below is shown in Figure 44.

Aortas treated with NaCl (n=4), showed no gross changes at 6 weeks with minimal inflammation, scarring or dilatation (% change in aortic diameter; 2.2 ± 6.1). In contrast, those exposed to 0.25M $CaCl_2$ showed superficial inflammation with only mild dilatation (28.7 ± 17.5%) whereas exposure to 0.5M $CaCl_2$ resulted in gross inflammation, scarring (with formation of adhesions) and obvious focal dilatation (60.0 ± 36.3%). The observed change in aortic diameter was significantly different between experimental conditions (p=0.0014) with differences observed between NaCl and 0.5M $CaCl_2$ application (p=0.0047) and between 0.25M and 0.5M $CaCl_2$ application (p=0.0416). Similar results have been observed in $TG2^{-/-}$ mice (data not shown).

Serial sectioning of harvested vessels (n=2 for C57Bl/6 and $TG2^{-/-}$) was performed to assess the histological changes seen with increasing calcium concentration.

Representative images seen with each experimental condition are shown in Figure 45. Sham operated vessels showed no obvious damage, with intact elastin fibres and minimal inflammation, whereas vessels injured with 0.25M $CaCl_2$ exhibited early signs of aneurysm development with loss of elastin fibre waviness. The area of injury on the ventral aorta was clearly distinguishable from the normal, unexposed, dorsal vessel. Aortas subject to injury with 0.5M $CaCl2_2$ showed evidence of severe damage with elastin fibre loss and breakage. Again, the damaged and uninjured parts of the vessel were easily identified, confirming that each mouse could act as its own histological control if required.

In our hands, the $CaCl_2$ model represents a reproducible experimental protocol to induce vascular injury in the infra-renal aorta. This targeted and tuneable insult causes arterial damage and provides a mechanism by which the actions of transglutaminases in aneurysm development and arterial protection can be studied. $CaCl_2$ concentrations ranging from 0.15 to 1.0M have been described, however strain specific differences in response have been reported (personal communication and (Wang et al., 2013a). Our preliminary images were reviewed by Dr Wanfen Xiong (University of Nebraska) who confirmed that they were what would be expected from the technique they developed. We therefore decided to use a $CaCl_2$ concentration of 0.5M for all future experiments as this consistently resulted in gross inflammatory changes after exposure in our WT control animals.

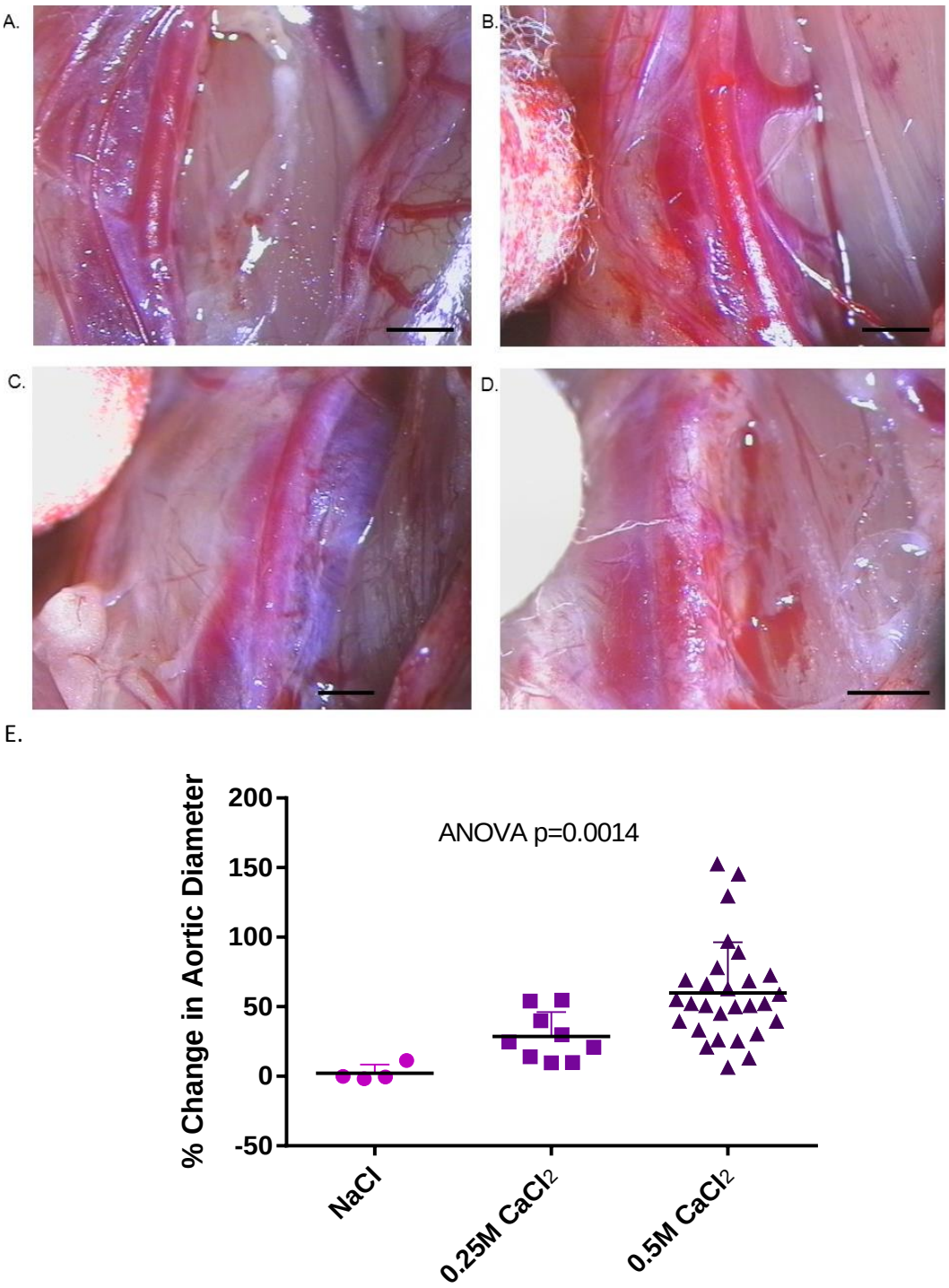

Figure 44. Effect of increasing calcium concentration

All images and data are from C57Bl/6 mice and scale bar represents 1mm in all images.. **Panel A** shows a representative image from a non-operated aorta (i.e. a "pre-op" image). **Panel B** shows the same aorta after application of NaCl and harvest at 6 weeks. **Panel C** shows a representative image of the infra-renal aorta after exposure to 0.25M $CaCl_2$ and harvest at 6 weeks and displays superficial inflammation but only very mild dilatation. **Panel D** is representative of the changes seen at 6 weeks after application of 0.5M $CaCl_2$ and highlights the gross inflammation and focal vessel dilatation seen with this injury model. **Panel E** summarises the change in aortic diameter (given as % change from baseline) seen with each experimental condition.

A.

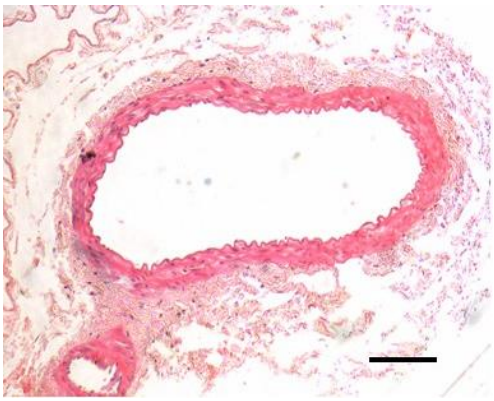

B.

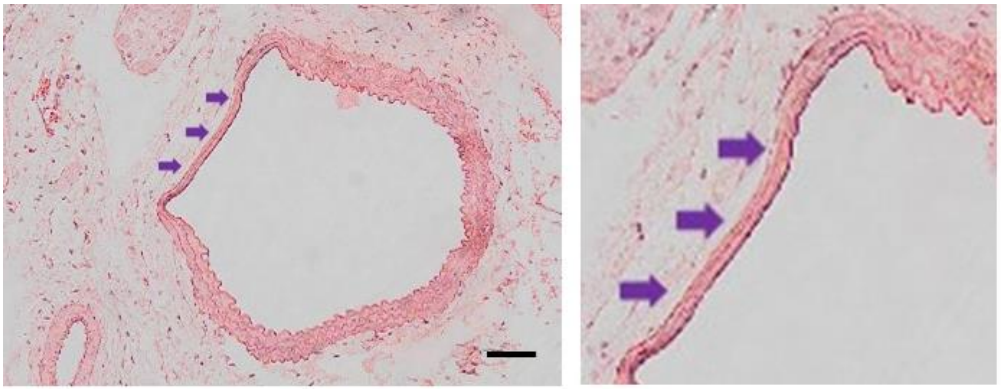

C.

Figure 45. Representative images – sham-operated and injured aortas

All images are from haematoxylin and eosin stained 5µm sections imaged at 10X magnification. Scale bar represents 100µm in each case. **Panel A** is representative of images obtained after NaCl application (sham operation) in a C57Bl/6 mouse. **Panel B** shows a representative image following 0.25M $CaCl_2$ injury in a $TG2^{-/-}$ mouse and clearly shows elastin flattening (filled arrows and inset). **Panel C** shows a typical image following 0.5M $CaCl_2$ exposure and harvest at 6 weeks (image from a C57Bl/6 mouse). There is an obvious distinction between the un-injured (dorsal) aorta (open arrows) vs. the injured (ventral) aorta (filled arrows) which displays characteristic elastin damage, breakage and fibre loss.

7.4 Short term aneurysms

7.4.1 Survival and growth in operated mice

The $CaCl_2$ aneurysm model involves an anaesthetic time of ~30 minutes, a laparotomy, exposure of the aorta (through blunt dissection) and insult to the main vessel of the abdomen. Although initial pilot work had not shown any significant problems with the $CaCl_2$ model in terms of bleeding, wound healing, abdominal complications or mortality, the majority of this work was undertaken in C57Bl/6 and $TG2^{-/-}$ mice because of delays in breeding the FXIII-$A^{-/-}$ and DKO transgenic mice. As further experiments were undertaken it became apparent that mice lacking FXIII-A had an obviously decreased survival rate following apparently normal recovery from the injury procedure.

In general, the mice appeared to recover normally but were then either found dead in the subsequent 1-5 days, or failed to gain weight post-operatively, became increasingly ill and were terminated (by a Schedule-1 approved method) as per Home Office guidelines. Overall the mortality rate for all operations (from which the mouse was recovered from anaesthetic) was 8.6% in the C57Bl/6 group, 6.8% in the $TG2^{-/-}$ group, 41.1% in the FXIII-$A^{-/-}$ group ($p<0.0001$) and 62.3% ($p<0.0001$) in the DKO mice.

In response to this unexpected high mortality rate, we initiated closer monitoring of the post-op animals, held a low threshold for termination if there was evidence of suffering and undertook detailed recording of cause of death and post-mortem findings where possible. Table 7 outlines operating numbers, mortality rates and causes of death for the 6 week $CaCl_2$ injury model and highlights that there is a low level of mortality (8.6%) associated with this model in C57Bl/6 mice. The causes of death in these mice included bleeding problems (presumably from unidentified injury at the time of dissection which resulted in continued bleeding) and bowel ischaemia (due to torsion of bowel loops on return to the abdominal cavity) as well as one case of post-op fighting. A similar mortality rate was seen in the $TG2^{-/-}$ mice (6.8%). It should be noted that the majority of these deaths occurred within the first few months of setting up the model and hence may reflect the initial “learning curve” of this technique.

The FXIII-$A^{-/-}$ and DKO mice exhibited very different appearances post-mortem to those animals with normal FXIII-A gene function. These mice showed more episodes of bleeding (which might be expected from their impaired clot function) but also, a significant number of mice (approximately 30-40% of post-op deaths), showed features of cardiac pathology (with blackened, thrombus filled atria) as well as multiple, discrete areas of focal necrosis (for example in the bowel, spleen and

liver). This bowel ischaemia showed a different pattern to that seen with simple bowel torsion/injury and examples of the post-mortem pathology seen are shown in Figure 46. Although it is obviously difficult to conclusively determine cause of death in these mice, we hypothesise that these animals, deficient in FXIII-A, could be forming non-stable clots which are embolised to visceral arteries. The source of these clots may be the site of aortic injury (although this is unlikely given the observed sites of embolisation) or more likely the heart, secondary to some undetermined cardiac pathology. We have not seen additional deaths in our aged, un-operated FXIII-A and DKO mice when compared to WT, hence suggesting that the physiological stress of surgery is required to "trigger" this pathology. Deaths were also seen in sham operated DKO animals (but not in FXIII-$A^{-/-}$ sham operated mice) possibly hinting at a more severe phenotype in this group.

Post-operative weight was measured in all animals as an adjunct to close monitoring of appearance and behaviour in the assessment of animal welfare. As can be seen from Figure 47, the FXIII-$A^{-/-}$ and DKO mice had a lower average weight over the 6 weeks between operation and harvest (AUC data; C57 871.4 ± 235.2, $TG2^{-/-}$ 892.9 ± 239.1, FXIII-$A^{-/-}$ 576.2 ± 413.1, DKO 456.3 ± 408.7) which is attributable to a greater weight loss in the immediate post-op period. When only data from those animals that survived to harvest were analysed (panel C) there was no significant difference in weight between genotypes ($p=0.265$), suggesting that weight loss is a surrogate for probability of survival. Panel D shows the weight loss in the first 7-days after surgery in DKO mice, sub-grouped into surviving and non-surviving animals. It is clear that as early as day 2, weight loss can be used to identify mice that are unlikely to survive and hence, in the future, we would suggest that weight loss on day 2 of >12% is an indication for termination by a Schedule 1 approved method.

Genotype	Operations	Deaths	Mortality Rate	Causes of Death
C57Bl/6	Sham – 4 0.25M – 9 0.5M – 60 **Total – 70**	Sham – 0 0.25M – 0 0.5M – 6 (5M, 1 F) **Total – 6**	**8.6%**	- Bowel Ischaemia - Bleeding - Fighting post-op
TG2 $^{-/-}$	Sham – 4 0.25M – 29 0.5M – 55 **Total – 88**	Sham – 0 0.25M – 4 (1M, 3F) 0.5M – 2 (2M) **Total – 6**	**6.8%**	- Bowel Ischaemia - Bleeding

FXIII-A $^{-/-}$	Sham – 2
	0.25M – 5
	0.5M – 49
	Total – 56
		Sham – 0
		0.25M – 4 (1M, 3F)
		0.5M – 19 (9M, 10F)
		Total - 23
			41.1%	- Bleeding **9%**
				- Cardiac +/- Ischaemia **35%**
				- Other
				  - Bowel Ischaemia
				  - Wound Complication
				  - Unknown

DKO	Sham – 4
	0.25M – 6
	0.5M – 67
	Total – 77
		Sham – 2 (1M, 1F)
		0.25M – 3 (1M, 2F)
		0.5M – 42 (18M, 24F)
		Total - 47
			62.3%	- Bleeding **26%**
				  - Including late ? bleeding events
				- Cardiac +/- Ischaemia **34%**
				- Other
				  - Bowel Ischaemia
				  - Wound Complication
				  - Renal mass? cause
				  - Fighting post-op
				  - Unknown

Table 7. Mortality Rates – $CaCl_2$ Injury

Table outlines operating numbers, mortality rates and causes of death for the $CaCl_2$ injury model. The mortality rate for all operations (from which the mouse was recovered from anaesthetic) was 8.6% in the C57Bl/6 group, 6.8% in the $TG2^{-/-}$ group, 41.1% in the FXIII-$A^{-/-}$ group and 62.3% in the DKO mice. Causes of death are listed in the table and are discussed in detail in the main text.

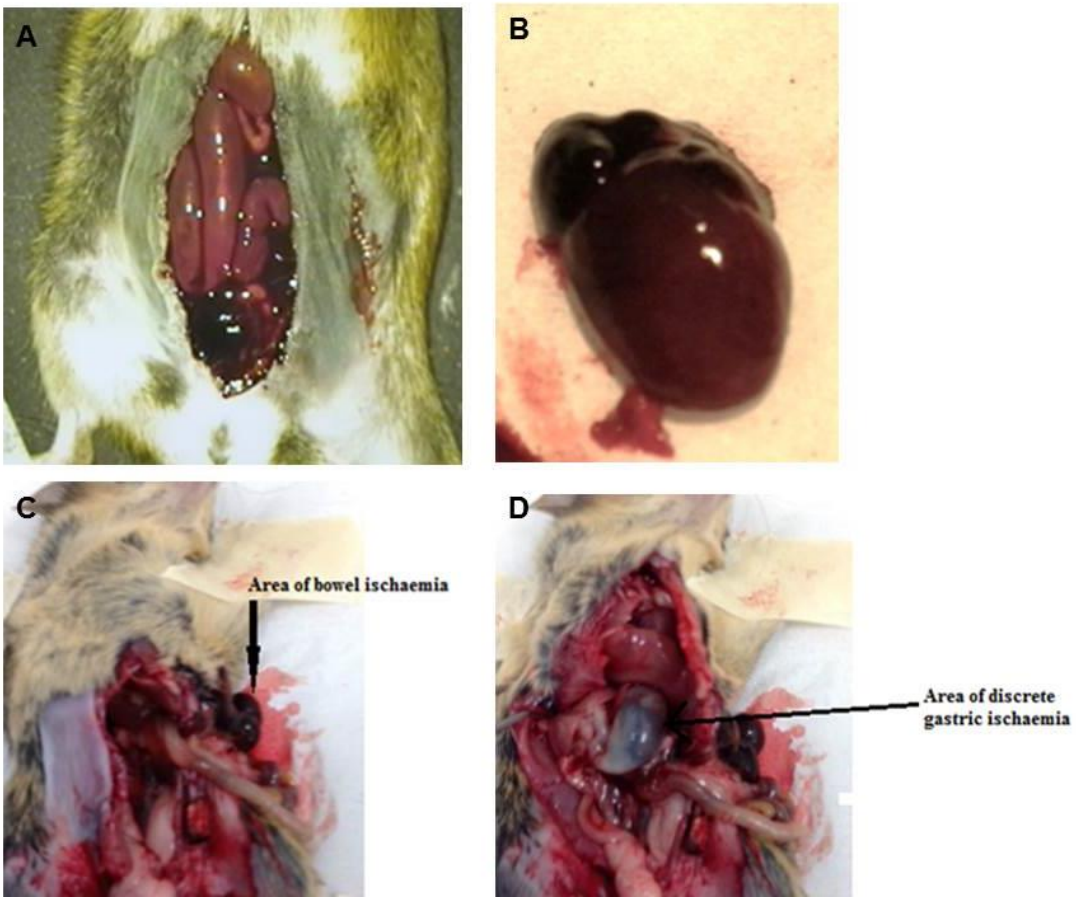

Figure 46. Post-mortem pathology in DKO mice

Representative images from post-mortem examination of DKO mice. **Panel A.** shows a DKO mouse found dead on day 5 post op and is typical of the appearances seen with post-op bleeding. There is bruising to the abdomen with blood and clots found in the abdomen and pelvis. The most common site of bleeding was from the pelvic vessels or along the posterolateral aspect of the aorta. **Panel B.** shows the heart of a DKO mouse that underwent sham operation and was found dead on day 2 post-op. There were no problems with the wound and no evidence of bleeding into the abdomen. Blood stained serous fluid was found in the thoracic cavity and the heart appeared as shown here with a black, clot filled atrium and dusky appearance to the anterior surface. **Panels C and D** are images taken of a DKO mouse found dead at day 5 post-op. Again, there was no evidence of bleeding however the abdominal contents had patchy areas of necrosis with discrete ischaemia shown here in the bowel **(C)** and stomach **(D).**

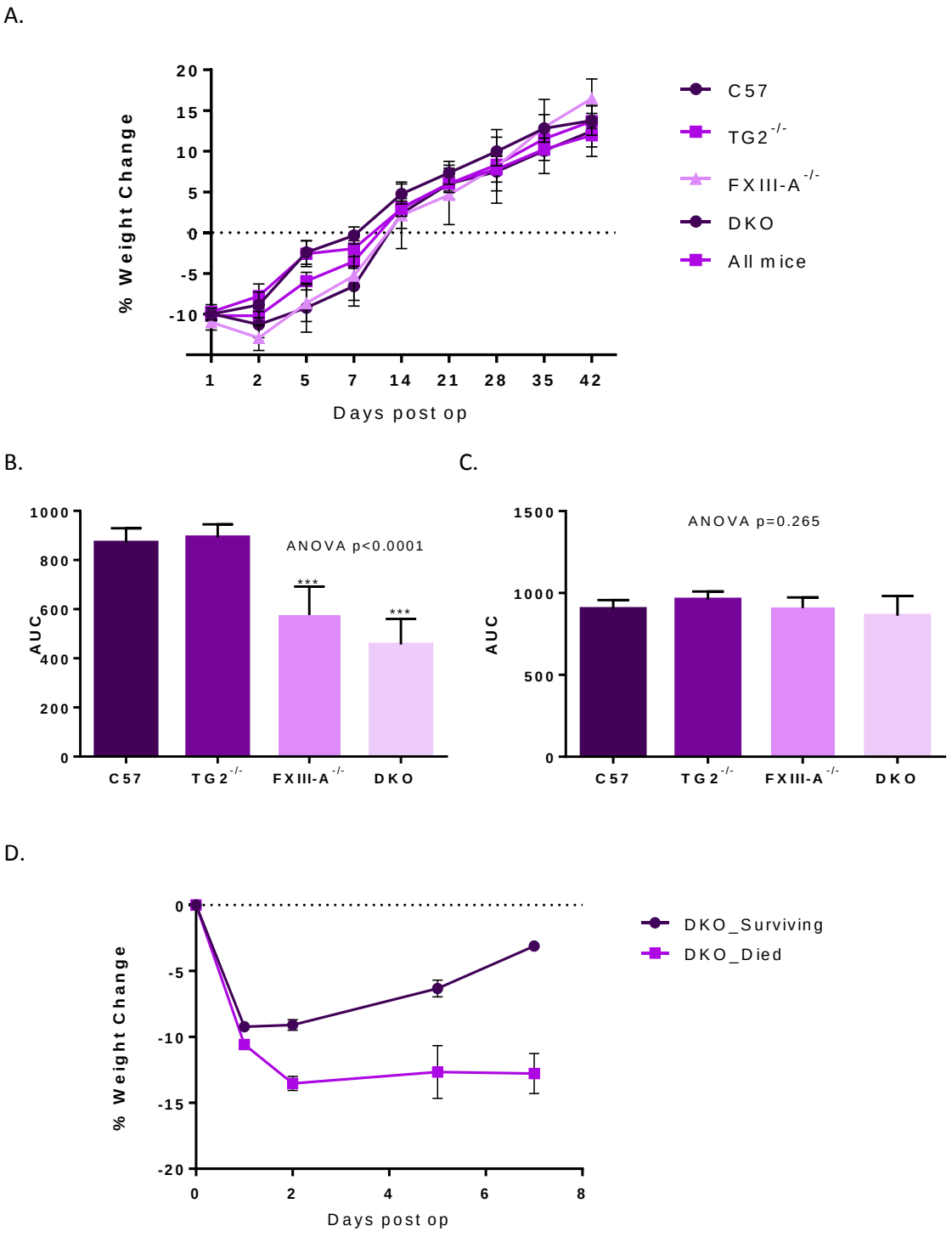

Figure 47. Weight change in mice post-injury

All data is shown as mean % weight change (from pre-op) with 95% confidence intervals. **Panel A** shows weight change in all operated mice after 0.5M $CaCl_2$ injury. **Panel B** shows AUC data for the curves in panel A. One-way ANOVA testing revealed a significant difference in weight between groups ($p<0.0001$) due to lower weights in the FXIII-A$^{-/-}$ and DKO groups, however, when mice that died post-operatively are excluded from analysis **(C),** there is no difference between groups ($p=0.265$). **Panel D** plots weight change in the first 7-days in surviving vs non-surviving DKO mice and shows that by post-op day 2, weight loss can be used to predict survival.

7.4.2 Diameter change and aneurysm proportions

Mice from each genotype (n=19-28) were subject to 0.5M $CaCl_2$ injury to the ventral surface of the aorta as outlined (Figure 21). Aortas were harvested at 6 weeks and the % change in infra-renal aortic diameter calculated from images captured *in vivo* pre-and post-injury. Each experimental group showed a mean % increase in aortic diameter (mean % ± SD; C57 60.0 ± 36.3, $TG2^{-/-}$ 67.5 ± 30.2, FXIII-$A^{-/-}$ 59.4 ± 32.9, DKO 43.1 ± 27.5) although the DKO mice appeared to show smaller % changes in aortic diameter than the other groups. There was, however, a wide variation in response and no statistically significant difference was found between groups (p=0.097).

In conjunction with this observed variation in results it also became apparent that vessels *either* appeared to be grossly dilated *or* showed a lack of obvious inflammation and evidence of injury. To investigate this further we used a 50% increase in diameter as a "cut-off" between those vessels classified as developing an "aneurysm" and those classified as not developing an "aneurysm". This methodology has been utilised by other groups and is equivalent to the 3cm diameter cut-off in the national aneurysm screening programme which represents an increase in 50% from an average aortic diameter of 2cm.

These results are summarised in Figure 49 and it can be seen that 17/28 (60.7%) mice developed an aneurysm in the C57Bl/6 group as compared with 20/27 (74.1%) in the $TG2^{-/-}$ group, 16/26 (61.5%) in the FXIII-$A^{-/-}$ group and 7/19 (36.8%) in the DKO group. Fisher's exact testing showed no significant different in outcome between groups when compared with WT however the DKO mice did develop a significantly lower proportion of aneurysms than the $TG2^{-/-}$ group (p=0.016).

The data from Figure 48 are re-presented in panel C of Figure 49 with sub-group analysis of each genotype group into i) those mice that did reach >50% increase in diameter (developed an "aneurysm") (mean % ± SD; C57 79.4 ± 33.1, $TG2^{-/-}$ 76.5 ± 29.9, FXIII-$A^{-/-}$ 79.11 ± 23.88, DKO 70.0 ± 17.8) and ii) those that did not (C57 30.0 ± 13.4, $TG2^{-/-}$ 41.8 ± 8.4, FXIII-$A^{-/-}$ 27.9 ± 15.9, DKO 27.4 ± 18.3). Kruksal-Wallis testing of these sub-groups (with Dunn's correction) again revealed no differences in % change in aortic diameter across the genotypes in either in those that did (p=0.814) or did not (p=0.160) develop an aneurysm. Overall this data suggests that the DKO mice have a lower propensity to aneurysm development (i.e. initiation is affected) rather than that they develop smaller aneurysms overall.

A.

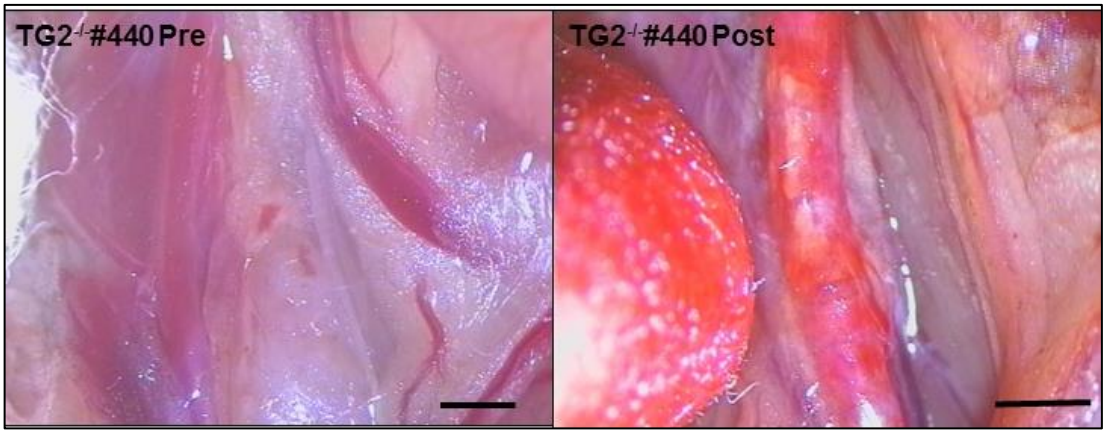

B.

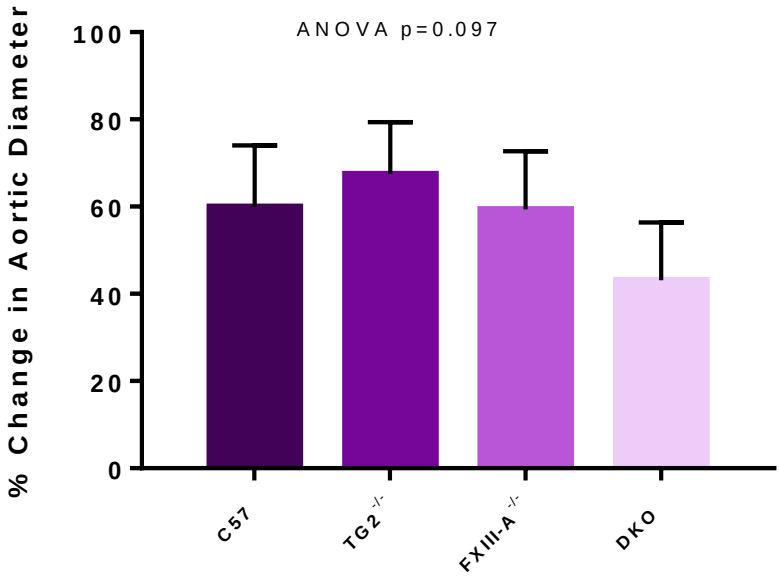

Figure 48. Summary results from the short-term $CaCl_2$ injury model – % change in diameter

Panel A. shows representative images from a $TG2^{-/-}$ mouse pre- and post- injury with 0.5M $CaCl_2$. Scale bar represents 1mm in each image. This vessel increased in size by 70.7% in the 6 week study period. **Panel B.** shows summary data from all four genotypes with results shown as % change in infra-renal aortic diameter (mean ± 95% confidence intervals) from baseline. There was no statistically significant difference seen between groups (ANOVA, p=0.097).

A.

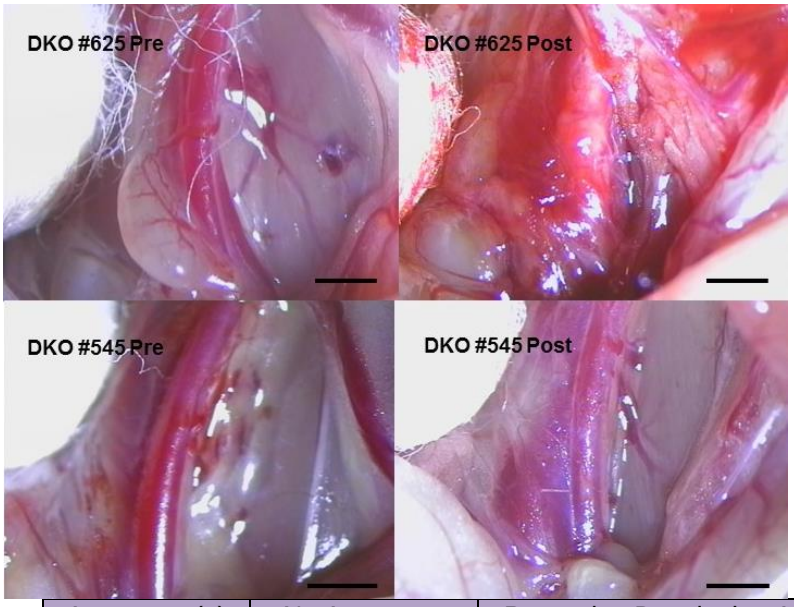

B.

	Aneurysm (n)	No Aneurysm (n)	Proportion Developing AAA (%)
C57Bl/6	17	11	60.7
TG2$^{-/-}$	20	7	74.1
FXIII-A$^{-/-}$	16	11	61.5
DKO	7	12	36.8

C.

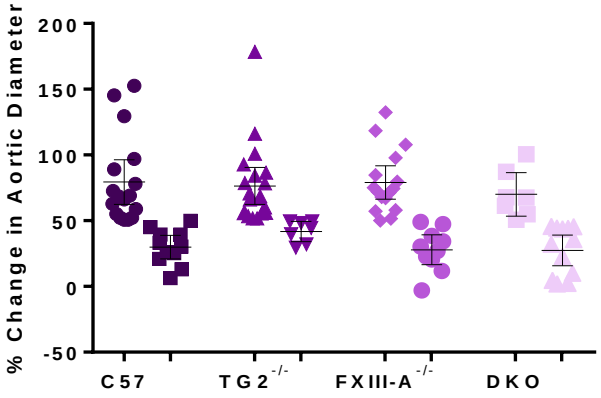

Figure 49. Summary results from the short-term $CaCl_2$ injury model – proportion developing an aneurysm

Panel A shows representative images from two DKO mice; the top images are from a DKO aorta which shows clear inflammation and dilatation (by 87.3%) after 0.5M $CaCl_2$ exposure whilst the bottom images are from a DKO aorta showing very minimal inflammation and no dilatation (1.60%) following the same insult. Scale bar represents 1mm in all images. **Panel B**. shows summary data from all four genotypes with results shown as proportion (%) of mice developing an AAA (i.e. >50% increase in diameter). Fisher's Exact testing revealed no difference between groups when compared to wildtype, however TG2$^{-/-}$ and DKO groups did differ significantly (p=0.016). **Panel C**. shows the data from the previous figure but with each genotype split into those mice that did reach >50% increase in aortic diameter and those that did not. There was no difference in % diameter change between genotypes when these subgroups where analysed separately.

7.4.3 Histology

7.4.3.1 Elastin damage

For each group (n=6) injured aortas were harvested, fixed, processed and sectioned. Slides were stained using the Miller Van Gieson protocol to enable visualisation of elastic fibres. The midpoint of the area of injury was identified and taken as the “zero-point”. Ten serial sections from this point and 5 each from 50µm proximal and 50µm distal to this zero-point were analysed for elastin damage. Each section was analysed blind and elastin fibres classified as either healthy, damaged but intact (i.e. showing mild degradation with flattening and thinning of fibres) or damaged and fragmented. This classification is based on that used by Watanabe *et al* in 2012 (Watanabe et al., 2012) (and shown in Figure 51). The proportion of each degree of damage was calculated relative to the whole vessel circumference and is given as a %. From this analysis we were also able to assess the correlation between outer aortic diameter (as measured from intra-operative photographs) and average inner circumference (as measured on histological sections). The results of this analysis are presented in Figure 50 and show that these two measures are reasonably well correlated (R^2=0.522).

Elastin damage data are shown in Figure 51. One-way ANOVA testing for each degree of elastin damage revealed no significant difference between groups in terms of proportion of healthy fibres (p=0.824), or in proportion of broken fibres (p=0.192) however the groups did vary significantly with regards the proportion of damaged but intact fibres present (p=0.028) with the DKO group showing a significantly higher proportion of damaged/intact fibres when compared with WT mice (p=0.028).

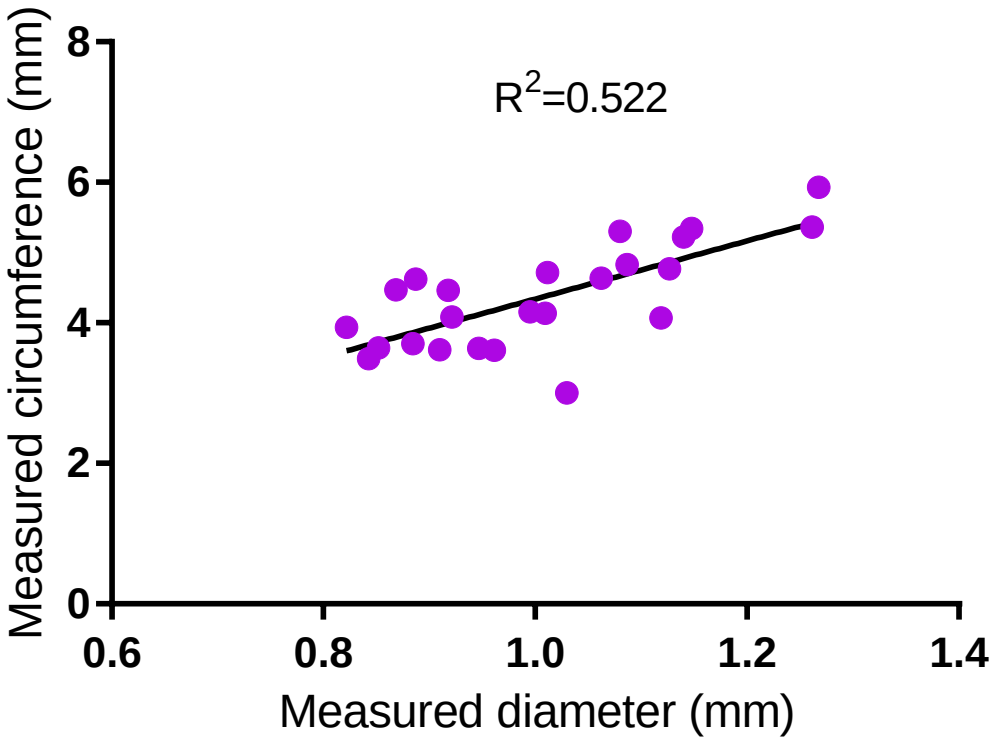

Figure 50. Correlation between "outer" diameter and "inner" circumference

Figure shows the relationship between the post-operative “outer” aortic diameter (n=24), measured from photographs captured *in vivo* at the time of harvest (at 6 weeks) and the “inner” vessel circumference measured from histological sections from the area of injury (mean of 10 sections per vessel, n=24). The coefficient of determination (R^2) is 0.522 with regression equation y=4.143x + 0.1975.

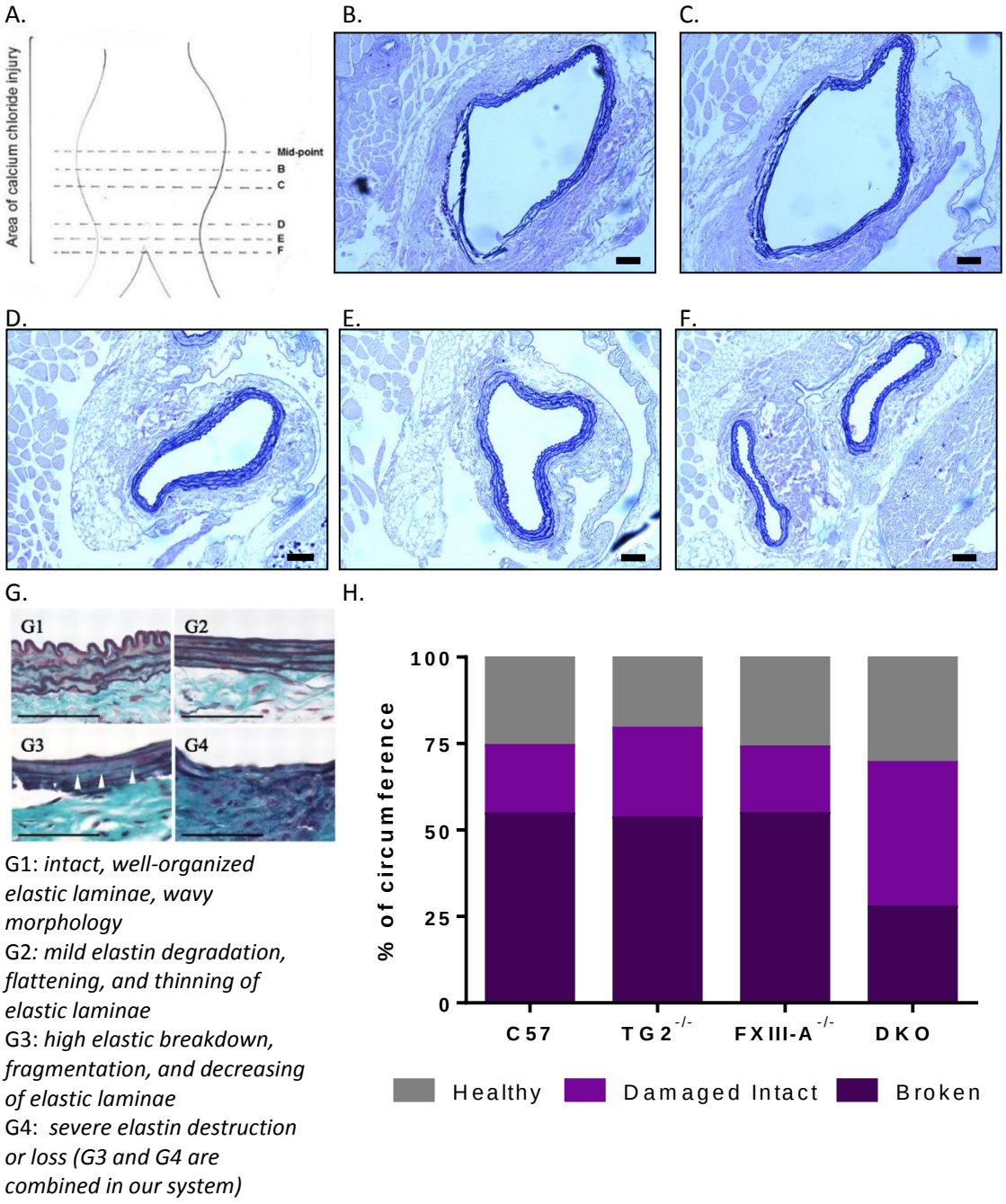

G1: *intact, well-organized elastic laminae, wavy morphology*
G2*: mild elastin degradation, flattening, and thinning of elastic laminae*
G3: *high elastic breakdown, fragmentation, and decreasing of elastic laminae*
G4: *severe elastin destruction or loss (G3 and G4 are combined in our system)*

Figure 51. Elastin damage in the short-term $CaCl_2$ injury model

Panels A-F show representative sections of elastin damage from a DKO mouse aorta exposed to 0.5M $CaCl_2$ and harvested at 6 weeks. Scale bar represents 100µm in each case. **Panel A** is a schematic of the area of injury and highlights the location of panels B-F. **Panels B and C** show areas of gross elastin damage and breakage whilst elastin flattening and loss of fibre waviness are apparent in **D** and **E**. **Panel F** shows the iliac bifurcation with relatively normal elastin fibre appearance seen in both vessels. **Panel G** is taken from (Watanabe et al., 2012) and shows the grading system utilised for classification of elastin damage. Scale bar represents 50µm in these images. **Panel H** summarises the findings in the four experimental genotypes (n=6 mice, 20 sections/vessel) with the mean proportion of healthy, damaged/intact and broken elastin fibres expressed as a % of the total circumference.

7.4.3.2 Collagen density

For each group, (n=6) injured aortas were harvested, fixed, processed and serial sectioned. Every 10th slide was stained using the Sirius Red protocol and then imaged using the multiphoton microscope to enable visualisation of fibrillar collagen. Representative sections from each of the genotypes are shown in Figure 52 and clearly show that collagen density is reduced at sites of elastin damage. Although total collagen content was not quantified, Figure 53 shows collagen density (as measured by Image J software) for each of the genotypes as it relates to the degree of elastin damage. Again, a clear relationship between these two parameters can be seen, with higher collagen densities present adjacent to areas of healthy medial elastin and more sparse fibrillar collagen at sites of elastin damage and breakage. No statistical differences was seen between genotype groups for each degree of elastin damage however when all groups were combined ANOVA testing revealed a statistically significant diffence in collagen density between sites of healthy elastin and sites of *either* damaged or broken elastin ($p<0.001$).

7.4.3.3 Calcification

For each group (n=6) injured aortas were harvested, fixed, processed and serial sectioned. Every 10th slide was stained using the Alizarin Red protocol to enable visualisation of calcification. In a subgroup of mice (n=2 per genotype) vessels were harvested 24 hours after injury and were handled as above.

Analysis of calcification in the 6 week samples revealed that Alizarin Red staining was specifically localised to the site of injured and/or broken elastin fibres in each of the genotypes. Representative images are shown in Figure 54 and clearly demonstrate the correlation between elastin damage and calcification. No calcification was observed in vessels without elastin damage, although in areas where new, disorganised, elastin fibres were visible, calcification was also clearly present. Vessels harvested at 24-hours showed no Alizarin staining and hence no evidence of calcium deposition, thus indicating that the calcium applied to the aorta does not simply remain in situ but is removed and it is the injury and subsequent inflammation that induces calcification at sites of damage.

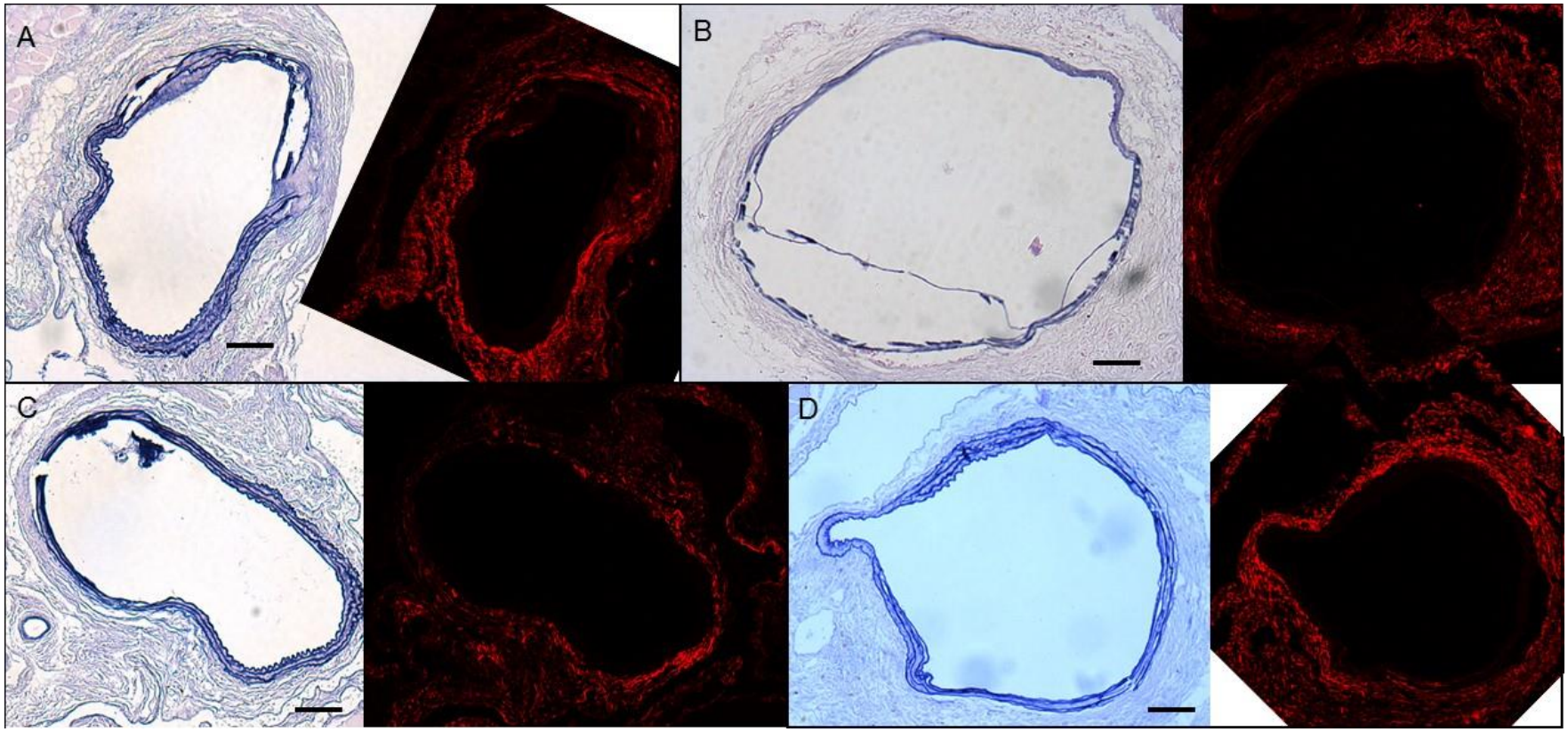

Figure 52. Collagen distribution in the short-term $CaCl_2$ model

Panels A-D show representative matched sections stained with Miller Van Gieson stain (for elastin) on the left or stained with Sirius Red and scanned with the muliphoton microscope (for fibrillar collagen) on the right. Images are from 5µm sections, captured at 2.5x magnification and imaged at 10x magnification. Scale bars represent 100µm in each case. Samples are from each of the genotypes (**A**=C57Bl/6, **B**=$TG2^{-/-}$, **C**=$FXIII\text{-}A^{-/-}$ and **D**=DKO) and clearly show that collagen density is reduced at areas of elastin damage.

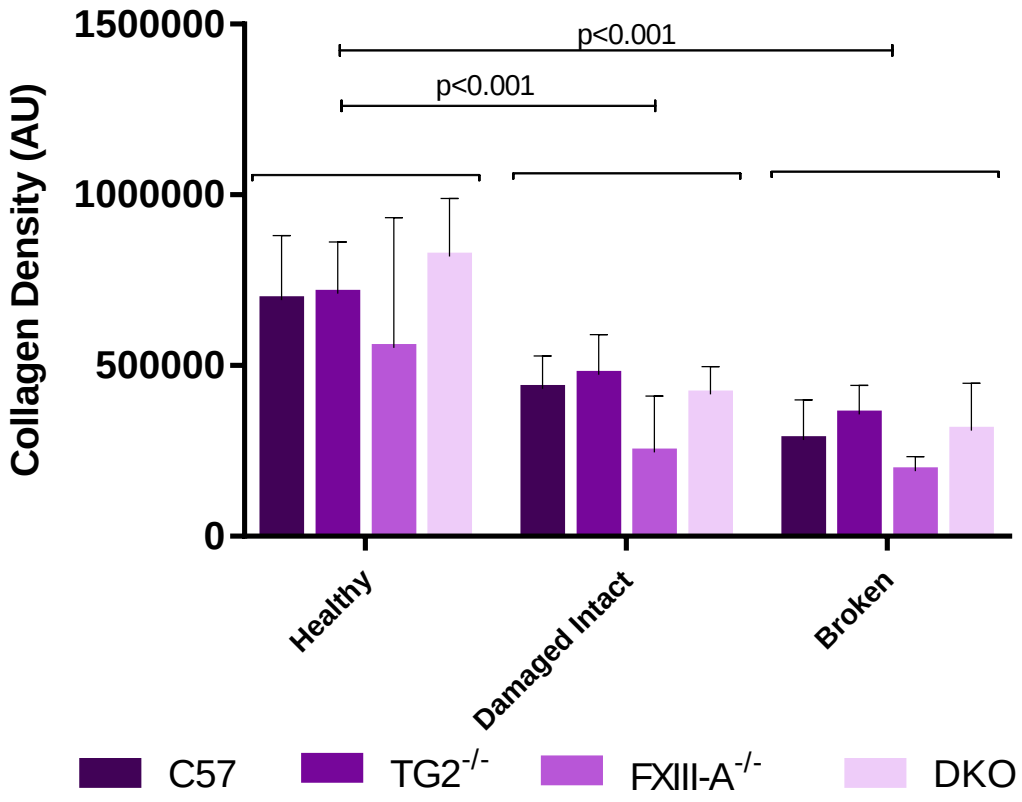

Figure 53. Collagen density in the short term CaCl2 model

Sites of 1) healthy elastin, 2) damaged but intact elastin and 3) broken elastin were identified on n=20 sections per vessel for n=6 vessels per genotype. At each site a 10x10 (AU^2) area was analysed using ImageJ software to measure collagen density. No difference in collagen density was found between genotype groups within each degree of elastin damage. When all groups were combined ANOVA testing revealed a statistically significant diffence in collagen density between sites of healthy elastin and sites of *either* damaged or broken elastin ($p<0.001$). AU = Arbitrary units

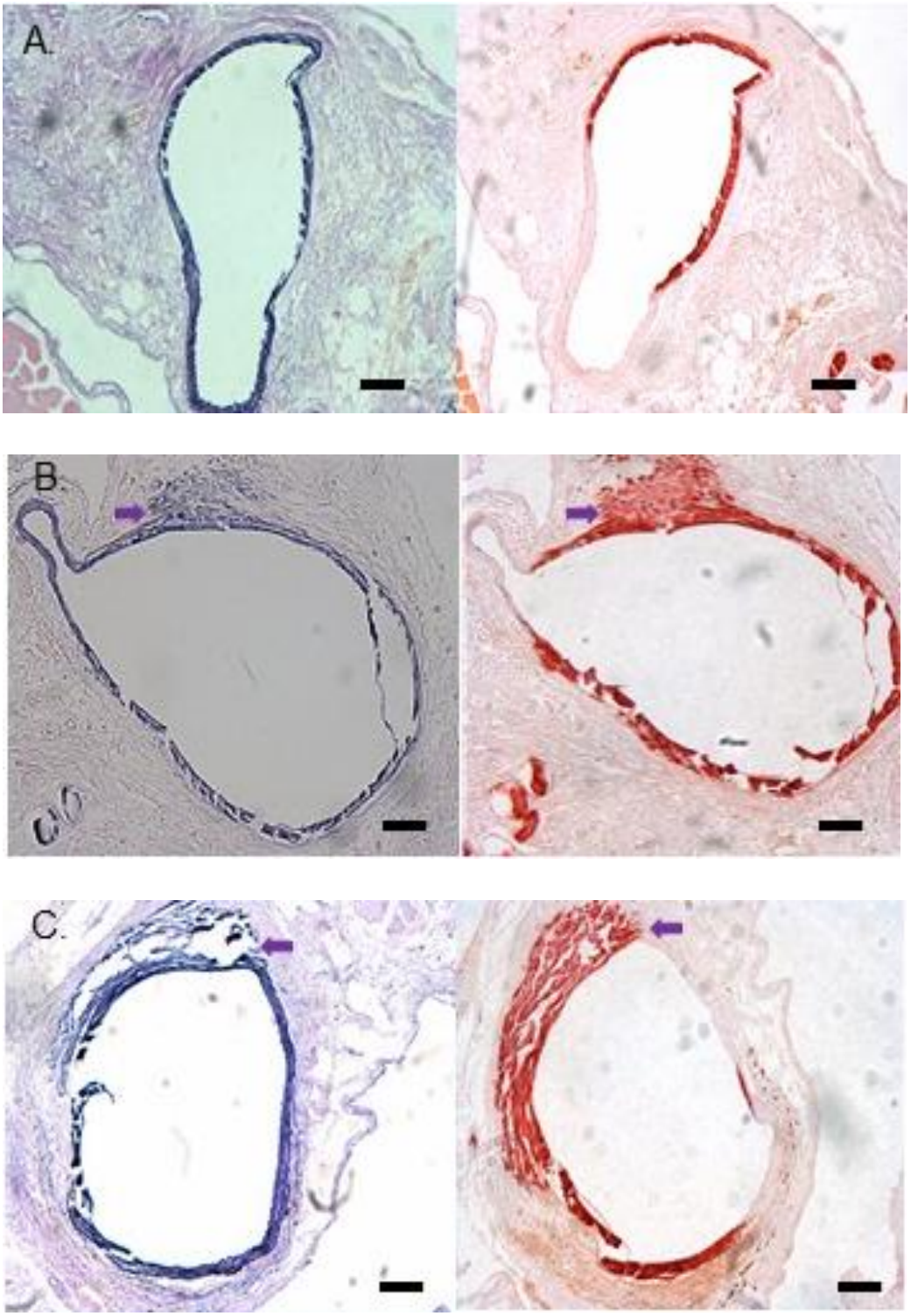
A.
B.
C.

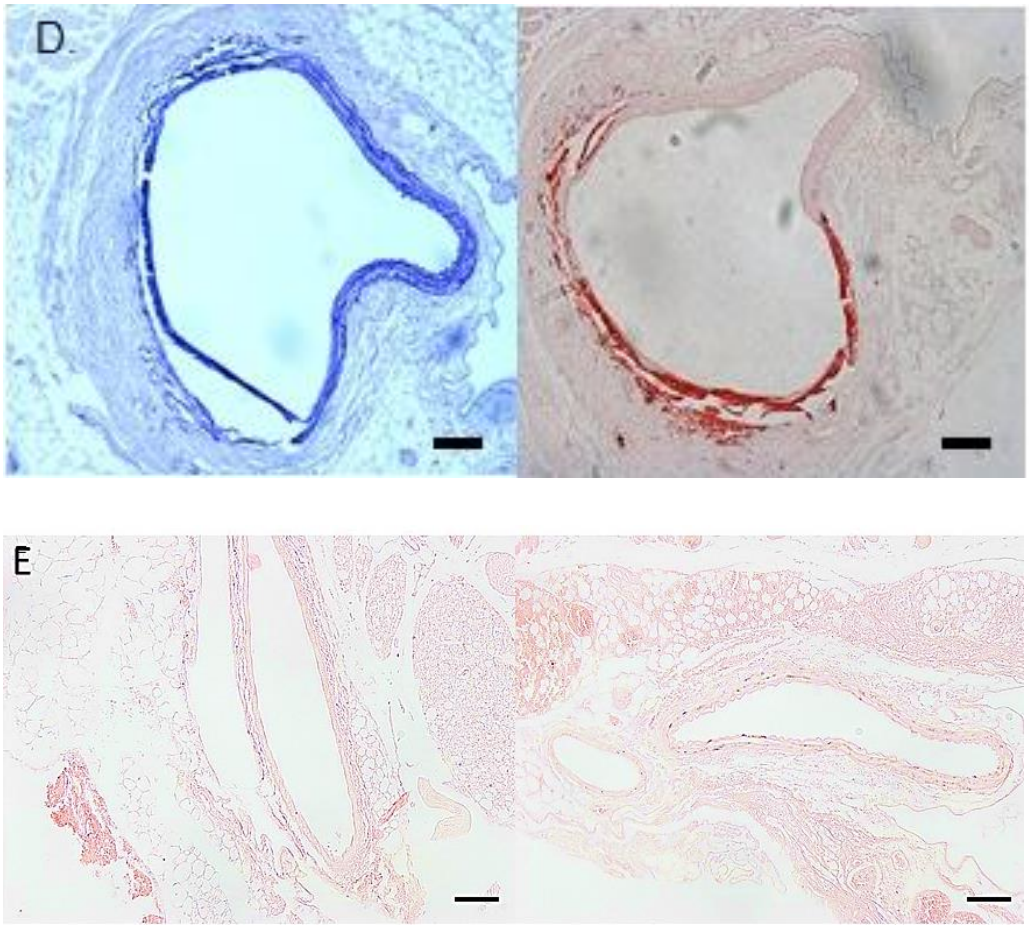

Figure 54. Calcification in the short-term $CaCl_2$ injury model

Panels A-D show representative adjacent sections stained with either Miller Van Gieson stain (for elastin) on the left or Alizarin Red stain (for calcium) on the right. Images are from 5µm sections, captured at 2.5x magnification and imaged at 10x magnification. Samples are from each of the genotypes (**A**=C57Bl/6, **B**=$TG2^{-/-}$, **C**=$FXIII\text{-}A^{-/-}$ and **D**=DKO) and clearly show that calcification (red) is localised specifically to areas of elastin damage and breakage. Panels **B** and **C** appear to show attempts at new elastin deposition (outside the elastic media) but these fibres are disorganised and also show associated calcification (filled arrows). Panel **E** shows representative images from injured aortas (C67Bl/6 (left) and DKO (right) mice) harvested at 24 hours post-op. No calcification was observed in any of these samples (n=2 per genotype). Scale bars represent 100µm in each image

7.4.4 Transglutaminase compensation

Although we found no evidence of upregulation of any of the transglutaminases in the aorta secondary to single ($TG2^{-/-}$ or $FXIII\text{-}A^{-/-}$) or double ($TG2^{-/-}.FXIII\text{-}A^{-/-}$) gene deficiency, we sought to investigate whether injury in the form of the $CaCl_2$ aneurysm model was sufficient to cause compensatory upregulation. Levels of aortic mRNA were determined by qPCR in samples harvested into liquid nitrogen 6 weeks after $CaCl_2$ injury (n=9-10 per genotype). Actual expression levels ($2^{-\Delta Ct}$) in both un-operated and operated vessels from C57Bl/6 mice are shown (Figure 55), as well as expression levels relative to the level of that particular transglutaminase in C57Bl/6 operated tissue. Relative expression levels in un-operated vessels (compared to WT) are shown for comparison and a reference line representing a 4-fold increase in expression is shown across all graphs to enable appraisal between panels. Statistical analysis was performed on raw ΔCt values and significance of change of expression was analysed using one-way ANOVA with Bonferroni correction for multiple testing.

As in the un-operated vessels, TG2 is the most abundant transglutaminase expressed in the WT injured aorta and there is a small but non-significant increase in TG2 levels between un-operated and operated samples (mean with 95% CI; un-operated TG2 expression 1.40 (0.74-2.64), operated TG2 expression 1.77 (1.11-2.82), p=0.602). Expression levels of the other transglutaminases are low (FXIII-A and TG3) or negligible. Therefore $CaCl_2$ injury does not significantly change the expression of any of the transglutaminases in the WT aorta.

Statistically significant differences in transglutaminase expression were seen in operated aortas across the four transgenic lines, however absence of TG2 and/or FXIII-A did not induce compensatory upregulation of mRNA expression of the reciprocal enzyme. TG1 expression was higher in DKO vessels relative to WT (p=0.0055) as was TG4 (p=0.0172) and TG7 (p=0.0017) expression. The $FXIII\text{-}A^{-/-}$ groups also showed a significantly increased TG7 expression (p=0.0021) and TG5 expression was increased in DKO mice relative to either of the single KO groups but was not significantly different from in the WT condition. Despite these differences between groups, no transglutaminase was expressed at a level comparable to that of TG2 in WT tissue hence these increases are unlikely to provide any functional compensation for the absence of TG2 and FXIII-A in the setting of vessel injury.

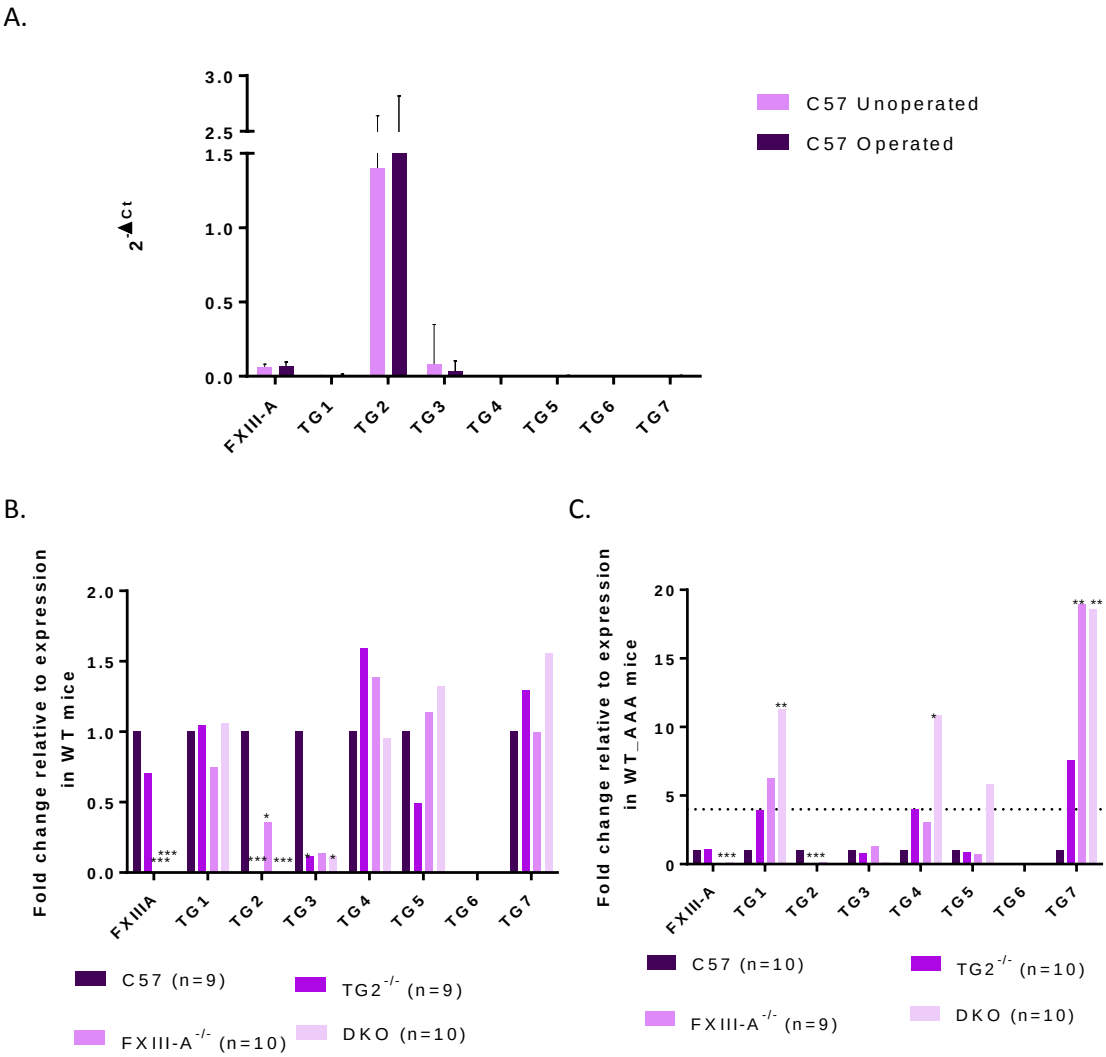

Figure 55. Expression levels of the transglutaminases in the injured aorta

Panel A. Transglutaminase 2 is the most abundant transglutaminase expressed in both the un-operated and operated aorta. Expression levels of the other TGs are low (FXIII-A and TG3) or negligible. Vessel injury does not significantly change the expression of any of the TGs in the WT situation. Values shown are TG expression ($2^{-\Delta Ct}$) in C57Bl/6 un-operated and operated aortic tissue (Mean ± 95%CI). **Panel B**. Expression of TGs in un-operated vessels for comparison. All values are expressed as fold change relative to the expression level of that particular transglutaminase in C57Bl/6 control aortic tissue. **Panel C.** Transglutaminase mRNA expression in operated aortic tissue. All values are expressed as fold change relative to the expression level of that particular transglutaminase in C57Bl/6 operated aortic tissue. Significant differences were seen in TG1, TG4 and TG7 expression however increases were not systematic and were not to the level of TG2 expression and are therefore not likely to be sufficient for functional compensation. Dotted line reflects a 4-fold increase in expression relative to WT * = p<0.05, ** = p<0.01, ***p<0.001.

7.4.5 Expression data

We investigated whether aortic injury via the $CaCl_2$ model resulted in significant up- or down-regulation of a number of gene transcripts of interest. These included various structural proteins including collagen (types I and III), elastin and vimentin, as well as gene transcripts known to be involved in inflammation and proteolysis. Levels of mRNA expression were determined by qPCR and, as previously, statistical analysis was performed on raw ΔCt values with either Student's t-test or ANOVA and Bonferroni testing applied to the data. Expression levels were compared between the un-operated and operated conditions in WT aortic tissue (actual expression levels ($2^{-\Delta Ct}$) shown) and then across the four experimental genotypes after $CaCl_2$ injury (expression is shown relative to levels in WT operated vessels).

Of the gene transcripts investigated, α-SMA was the most predominant in the WT control aorta with expression levels 7-8 times that of the next most highly expressed transcript (vimentin and collagen I). Only PAI-1 expression was significantly different in operated vs un-operated WT aortic tissue with mean expression ~2.5 fold lower in vessels subject to $CaCl_2$ injury ($p=0.0022$).

Our results showed considerable variability between samples as well as a number of statistically "significant" results which are unlikely to represent biologically relevant findings. Despite these caveats, there were a number of key results from these data. Expression of fibrillin-2 varied greatly between experimental genotypes; FXIII-$A^{-/-}$ samples demonstrated a 6-fold increase in fibrillin-2 expression ($p=0.0045$) and levels were 7-fold increased ($p=0.0014$) in operated DKO aortas in comparison with those from C57Bl/6 mice. Likewise, uPA expression and expression of haem oxygenase-1 ((HO-1), an inducible isoform of the haem degradation enzyme which is produced in response to oxidative stress) were also greatly increased in operated samples from the transgenic mice groups when compared to those from the WT group. Expression of uPA showed a trend towards increase in $TG2^{-/-}$mice (3-fold greater, $p=0.079$), was 4-fold greater in FXIII-$A^{-/-}$ mice ($p=0.023$) and approximately 5.5-fold greater in DKO mice ($p<0.001$). Expression of HO-1 was also increased 11-fold in DKO mice compared to WT ($p=0.045$).

In addition to the decreased expression of α-SMA seen in WT operated samples (vs. un-operated aortas) we saw a further decrease in expression levels in the DKO mice (~85-fold decrease, $p<0.0001$). There was no difference between α-SMA expression in FXIII-$A^{-/-}$ or $TG2^{-/-}$ mice as compared to the operated vessels from WT mice. A similar pattern of results was seen with expression of PAI-1 (with

decreased levels in operated vs un-operated WT vessels and further decreases in expression seen in DKO mice (>6-fold decrease, p=0.004)) and vimentin (~3.5-fold decrease in DKO operated vessels compared to WT operated, p=0.009).

A.

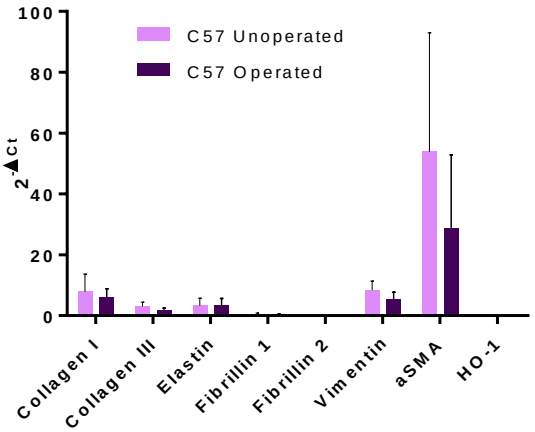
C57 Unoperated
C57 Operated
2-ΔCt
Collagen I
Collagen III
Elastin
Fibrillin 1
Fibrillin 2
Vimentin
aSMA
HO-1

B.

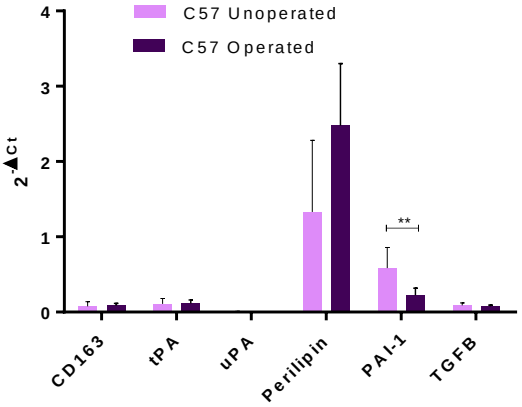
C57 Unoperated
C57 Operated
2-ΔCt
**
CD163
tPA
uPA
Perilipin
PAI-1
TGFB

C.

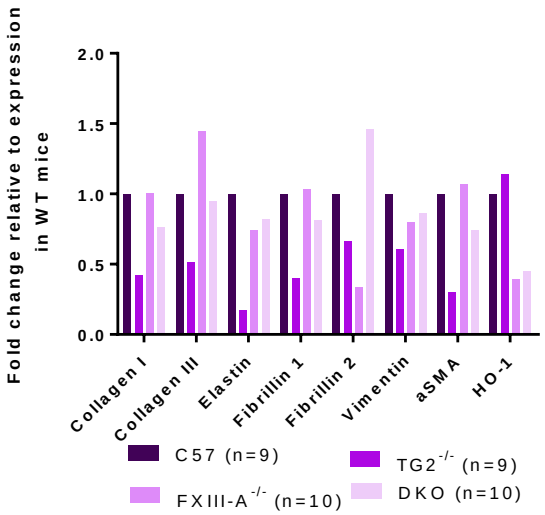
Fold change relative to expression in WT mice
Collagen I
Collagen III
Elastin
Fibrillin 1
Fibrillin 2
Vimentin
aSMA
HO-1
C57 (n=9)
FXIII-A-/- (n=10)
TG2-/- (n=9)
DKO (n=10)

D.

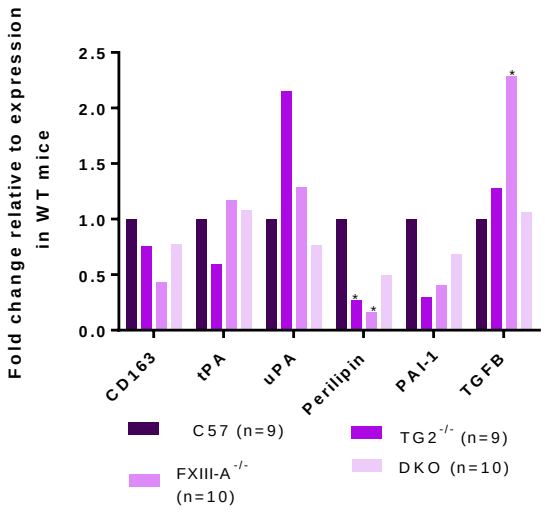
Fold change relative to expression in WT mice
CD163
tPA
uPA
Perilipin
PAI-1
TGFB
C57 (n=9)
FXIII-A-/- (n=10)
TG2-/- (n=9)
DKO (n=10)

E.

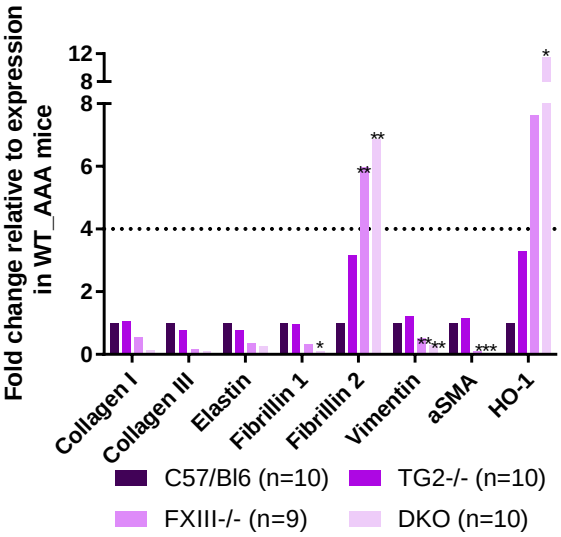
Fold change relative to expression in WT_AAA mice
Collagen I
Collagen III
Elastin
Fibrillin 1
Fibrillin 2
Vimentin
aSMA
HO-1
C57/Bl6 (n=10)
FXIII-/- (n=9)
TG2-/- (n=10)
DKO (n=10)

F.

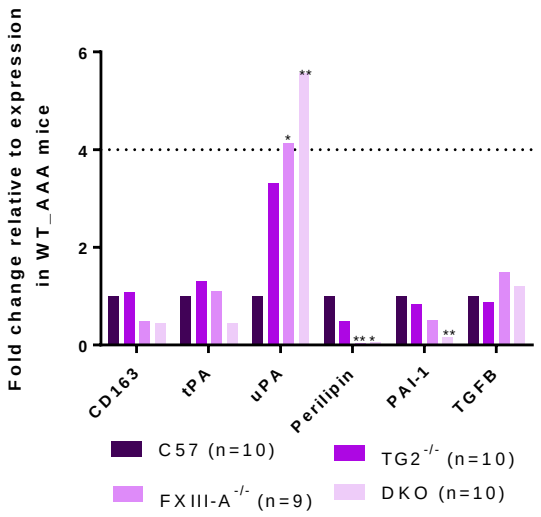
Fold change relative to expression in WT_AAA mice
CD163
tPA
uPA
Perilipin
PAI-1
TGFB
C57 (n=10)
FXIII-A-/- (n=9)
TG2-/- (n=10)
DKO (n=10)

Figure 56. Gene transcript expression levels in the injured aorta

Panels A and B show expression levels in un-operated (n=9) and operated (n=10) vessels from WT mice. Data is presented as $2^{-\Delta Ct}$ values (mean with 95% CI) and highlights that only PAI-1 expression was significantly altered following 0.5M $CaCl_2$ injury and harvest after 6 weeks. **Panels C and D** are provided for reference and show mRNA expression of various gene transcripts in the un-operated aorta (n=9-10) across the experimental genotypes (for interpretation of this data see section 6.3). **Panels E and F** show expression levels of the same transcripts in operated samples (n=9-10 per genotype) with data presented as fold change relative to the expression level of that particular gene transcript in operated vessels from WT mice. Statistical analysis was performed using Student's t-test (for 2 groups) or one-way ANOVA with Bonferroni correction (for multiple groups). Dotted line reflects a 4-fold increase in expression relative to WT. * = $p<0.05$. ** = $p<0.01$, *** = $p<0.001$

7.4.6 MMPs

Quantitative real-time PCR was performed to investigate the mRNA expression of various MMPs in aortic tissue from mice (n=9-10) from each of the experimental genotypes subject to 0.5M $CaCl_2$ exposure and harvested at 6 weeks. These data are shown in Figure 57. Panel A reflects expression levels (as $2^{-\Delta Ct}$ values) of MMPs in un-operated and operated tissue from C57Bl/6 mice. A 17-fold increase in MMP-12 expression was seen in operated vessels relative to baseline (Student's t-test, $p<0.001$) and TIMP-1 expression was increased by 2-fold ($p=0.0047$). None of the other MMPs investigated were differentially expressed in WT vessels following injury.

Comparison was made across the four experimental genotypes after $CaCl_2$ injury (expression is shown relative to levels in WT operated vessels). The only MMP transcript to increase significantly across all genotypes was MMP-12. In addition to the 17-fold increase from basal to operated (in WT), levels showed a further 4.5-fold increase between operated WT and $TG2^{-/-}$ vessels ($p=0.0127$), a 13-fold increase between operated WT and FXIII-$A^{-/-}$ vessels ($p<0.0001$) and an 8-fold increase between operated WT and DKO vessels ($p=0.0004$). This equates to a huge upregulation of MMP-12 of >140-fold when comparing basal WT vessels to those harvested from DKO animals following $CaCl_2$ injury.

TIMP-1 expression was also found to be increased in FXIII-$A^{-/-}$ operated samples (~3-fold increase, $p=0.0475$) and MT-MMP expression was increased in both FXIII-$A^{-/-}$ and DKO samples (5-fold increase, $p=0.0004$ and 4-fold increase, $p=0.002$ respectively). TIMP-2 expression was decreased in DKO operated vessels (to approximately 17% of WT operated levels, $p=0.0042$) but similar decreases were not seen in either of the other transgenic groups. No significant changes were seen in mRNA expression levels of either MMP-2 or MMP-9, either between basal and operated conditions in WT mice, or between genotypes following operation

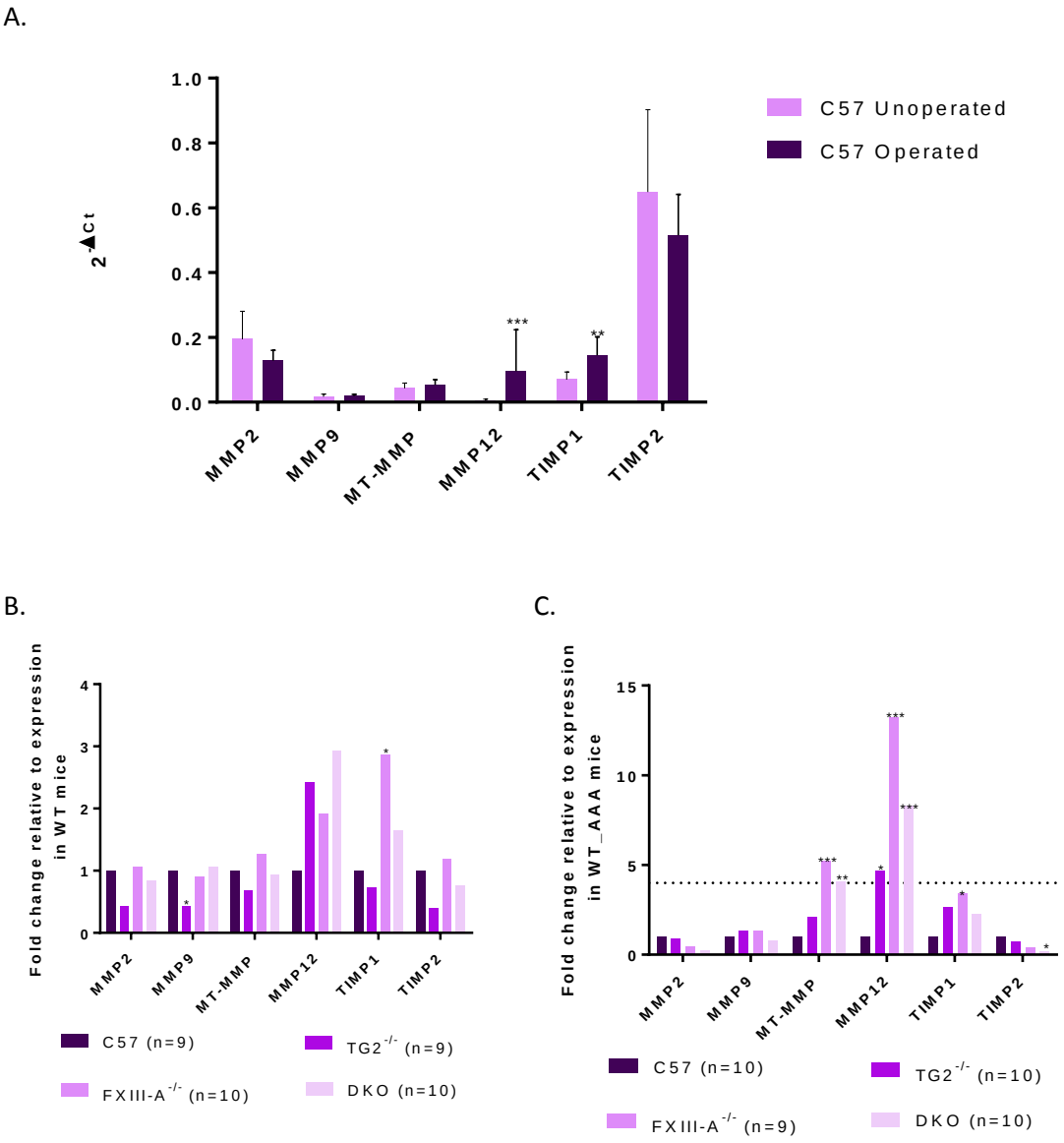

Figure 57. Expression levels of the MMPs in the injured aorta

Panel A. shows expression levels in un-operated (n=9) and operated (n=10) vessels from WT mice. Data is presented as $2^{-\Delta Ct}$ values (mean with 95% CI) and highlights that only MMP-12 and TIMP-1 expression were significantly altered following 0.5M $CaCl_2$ injury and harvest after 6 weeks. **Panel B.** is provided for reference and shows mRNA expression of MMP gene transcripts in the un-operated aorta (n=9-10) across the experimental genotypes (for interpretation of this data see section 6.4). **Panel C** shows expression levels of the same transcripts in operated samples (n=9-10 per genotype) with data presented as fold change relative to the expression level of that particular MMP gene transcript in operated vessels from WT mice. Statistical analysis was performed using Student's t-test (for 2 groups) or one-way ANOVA with Bonferroni correction (for multiple groups). Dotted line reflects a 4-fold increase in expression relative to WT. *, $p<0.05$, **, $p<0.01$, ***, $p<0.001$

7.4.7 Immunohistochemistry

Immunohistochemical staining of selected aortic sections from injured vessels from each genotype (n=6 per group) was undertaken to assay for the presence of αSMA (a specific marker of smooth muscle cells) and MMP-12 in our samples.

Anti-SMA antibody (ab184675, Abcam Plc, UK) was used for staining of αSMA, a highly conserved cytoskeletal protein which is expressed in all eukaryotic cells. This antibody is known to react with rat protein and is predicted to strongly cross-react with a variety of mammalian species including murine samples. The antibody has been tested in SV40LT-SMC cells which are rat aortic smooth muscle cells transfected with simian virus 40 large T antigen. These cells have been shown to main SMC characteristics over >200 population doublings by Reilly (Reilly, 1990) and have been utilised extensively in the literature as a model of SMC phenotype.

Anti-MMP-12 antibody (ab200410, Abcam Plc, UK) was used for staiing of MMP-12. This antibody has been raised against a synthetic peptide corresponding to the last 20 amino acids of the human protein but is predicted to react with both mouse and rat species. The antibody has been tested in the A549 cell line which is derived from human alveolar (lung) adenocarcinoma and in our work murine lung samples were used as a positive control for MMP-12 staining.

Quantification of this work has not yet been undertaken however representative images are shown in Figure 58 and highlight the intense expression of αSMA around damaged and broken elastin fibres. MMP-12 staining appeared to differ between the genotypes and from preliminary analysis is more prevalent in vessels from DKO mice. All the sections examined showed MMP-12 within the adventitia and surrounding inflammatory tissue rather than in the media itself.

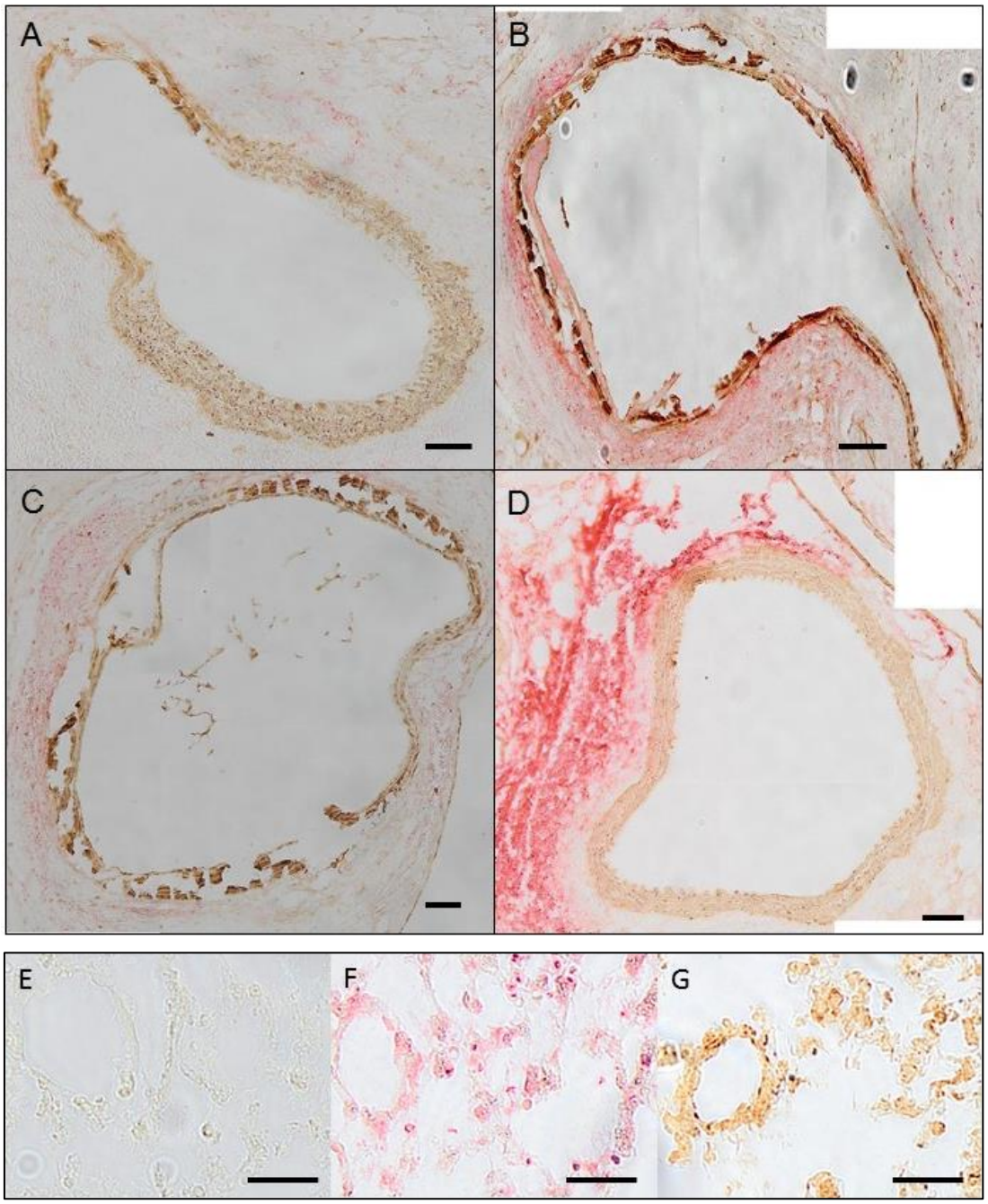

Figure 58. Representative sections – MMP-12 immunohistochemistry

Representative sections (10X magnification) from operated aorta from each of a **A**. C57Bl/6, **B.** TG2$^{-/-}$, **C.** FXIII-A$^{-/-}$ and **D.** DKO mouse. Scale bar represents 100µm in these images. Immunohistochemistry was performed as outlined in methods to stain α-SMA (brown) and MMP-12 (pink). The vessel wall clearly demonstrates α-SMA staining in each case, with intense staining around sites of broken/damaged elastin. MMP-12 staining is variable between genotypes but appears to be strongest in DKO vessels and is located in the surrounding adventitia and inflammatory tissue rather than in the elastic media itself. Panels E, F and G show murine lung tissue and represent our negative (E) control and positive control for MMP-12 (F) and α-SMA (G) staining. Scale bar represents 50µm in these images.

7.5 Long term aneurysms

Many authors have reported a difference between experimental aneurysm initiation and progression and work from our group suggests a role for TG2 in vascular repair. Therefore, we decided to investigate whether there were any longer-term effects of TG2 deficiency in the setting of the $CaCl_2$ aneurysm model. The other experimental genotypes were not investigated under these conditions because of a) ethical considerations regarding the high post-op mortality in these mice and b) the lack of strong evidence for the involvement of FXIII-A in vascular repair.

7.6.1 Diameter change and aneurysm proportions

Mice from C57Bl/6 (n=19) and $TG2^{-/-}$ (n=17) genotype groups were subject to 0.5M $CaCl_2$ injury to the ventral surface of the aorta and results are summarised in Figure 59. Aortas were harvested at 6 months and the % change in infra-renal aortic diameter calculated from images captured *in vivo* pre-and post-injury. Each experimental group showed a mean % increase in aortic diameter (C57 64.1 ± 30.7, $TG2^{-/-}$ 89.5 ± 34.5) with the TG2-deficient mice showing a statistically significant larger increase in diameter over the 6 month period (p=0.025).

Comparison was also made between changes in diameter observed between genotypes at 6 weeks vs. those seen at 6 months. The C57Bl/6 group at 6 weeks showed a change in diameter of 60.0 ± 36.3% which was not statistically different from that seen at 6 months (64.1 ± 30.7), suggesting that these mice were able to halt aneurysm progression (or attempt vascular repair) following the initial injury. In contrast, the $TG2^{-/-}$ mice showed a change in diameter of 67.5 ± 30.2% at 6 weeks, which was significantly different (smaller) than that seen at 6 months (89.5 ± 34.5, p=0.031). This would indicate that the injury has continued to progress unchecked and that the $TG2^{-/-}$ mice are unable to halt aneurysm progression once it has been initiated, perhaps due to a failure of vascular repair.

Vessels were classified as either “aneurysmal” (demonstrating a % change in diameter of >50%) or “non-aneurysmal”. Under conditions of long-term $CaCl_2$ exposure, 10/19 (52.6%) of C57Bl/6 mice studied developed an aneurysm as compared with 16/17 (94.1%) of $TG2^{-/-}$ mice subject to the same experimental conditions. This was statistically significant on analysis with Fisher’s Exact Test (p=0.0084). These data suggest that aneurysm initiation and progression are distinct processes and that TG2 may have a role in the latter, possibly through its arterial repair function.

A.

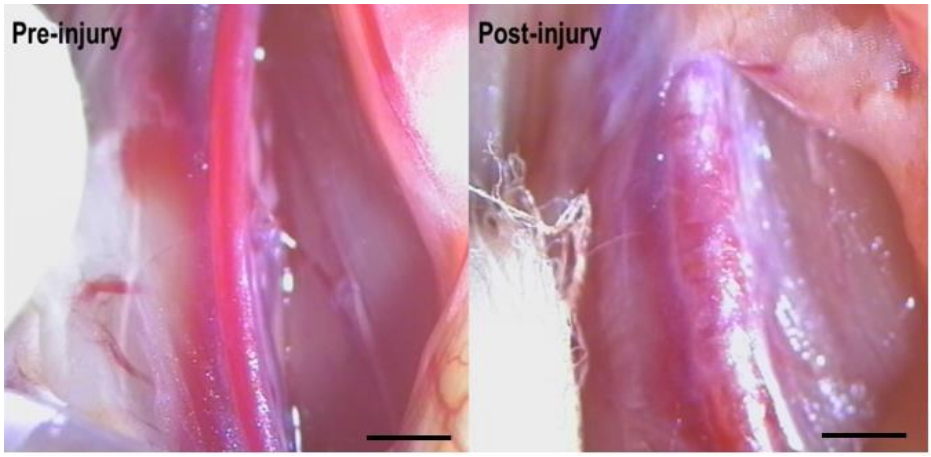

B.

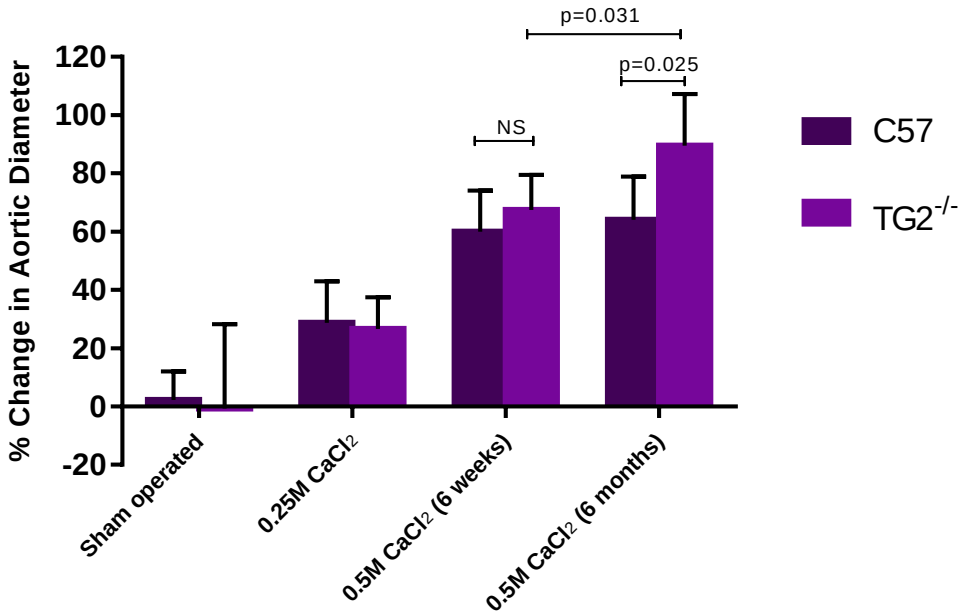

C.

	Aneurysm (n)	No Aneurysm (n)	Proportion Developing AAA (%)
C57Bl/6	10	9	52.6
TG2$^{-/-}$	16	1	94.1

Figure 59. Summary Results – long-term $CaCl_2$ injury model

Panel A. Representative images from "long-term" injury model from a C57B/l6 mouse showing pre- and post-injury appearances. Scale bar represents 1mm. **Panel B.** Summary results from the aneurysm model in C57Bl/6 and TG2 mice under conditions of NaCl application (sham-operated), 0.25M $CaCl_2$ application and 0.5M $CaCl_2$ application with harvest at either 6 weeks or 6 months. Data is shown as mean % change in aortic diameter (from baseline) with 95% confidence intervals. **Panel C**. summarises the proportion of mice of each genotype that develop and "aneurysm" (% diameter change >50%). Data were analysed using Fishers Exact Test (of proportions), p=0.0084

7.6.2 Histology

7.6.2.1 Elastin damage

For each group (n=6) elastin damage was classified as either healthy, damaged but intact or broken, as previously. Data are averaged for each aorta from analysis of 20 sections from the middle 100µm of the area of injury, and then presented as an average for each genotype (either C57Bl/6 or $TG2^{-/-}$). The proportion of each degree of damage was calculated relative to the whole vessel circumference and is given as a %. Results are shown in Figure 60. Student's t-testing for each degree of elastin damage revealed no significant difference between C57Bl/6 and $TG2^{-/-}$ mice in terms of proportion of healthy fibres (p=0.304), damaged but intact fibres (p=0.734) or in the proportion of broken fibres (p=0.570).

7.6.2.2 Collagen density

Long-term injured aortas (n=6 per group) were processed, stained and imaged to enable visualisation of fibrillar collagen. Results similar to those obtained with the short-term protocol were seen, with collagen density clearly reduced with increasing degree of elastin damage (p=0.0012 when data from both genotypes combined) . Figure 61 shows data relating to collagen density (arbitrary units) for each genotype, classified by the degree of elastin damage present at that site. Where elastin was classified as either "healthy" or "damaged but intact", the $TG2^{-/-}$ vessels had a lower collagen density than those from WT mice (p=0.042 and p=0.026 respectively).

7.6.2.3 Calcification

For each group (n=6) injured aortas were harvested, fixed, processed and serial sectioned. Every 10^{th} slide was stained using the Alizarin Red protocol to enable visualisation of calcification.

As seen in the 6 week samples, analysis of calcification revealed that Alizarin Red staining was specifically localised to the site of injured and/or broken elastin fibres in each of the genotypes. Representative images are shown in Figure 62.

A.

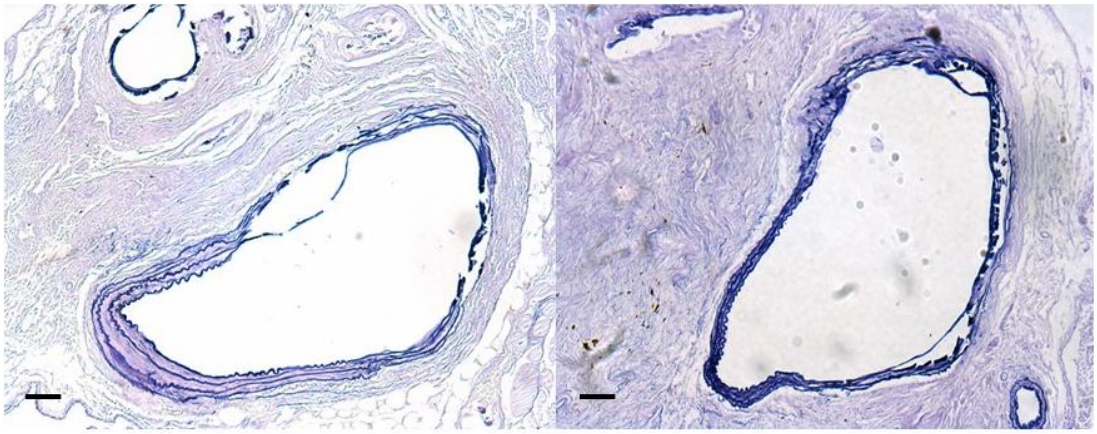

B.

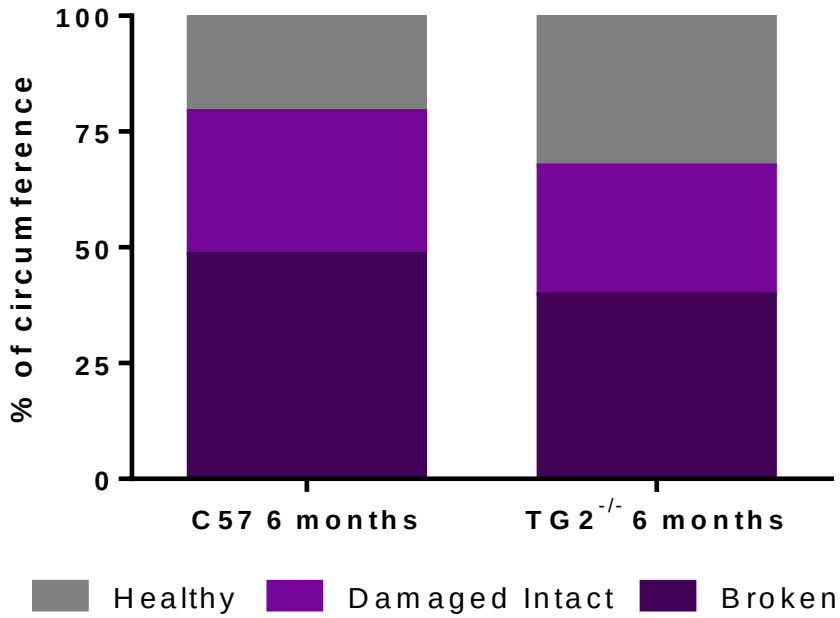

Figure 60. Elastin damage in the long-term $CaCl_2$ injury model

Panel A shows representative sections of elastin damage from a C57Bl/6 and a $TG2^{-/-}$ mouse aorta exposed to 0.5M $CaCl_2$ and harvested at 6 months. Scale bar represents 100µm. **Panel B.** summarises the findings in the two long-term experimental genotypes (n=6 mice, 20 sections/vessel) with the mean proportion of healthy, damaged/intact and broken elastin fibres expressed as a % of the total circumference. Student's t-testing revealed no statistically significant differences between the 2 groups in any of the "degrees of elastin damage".

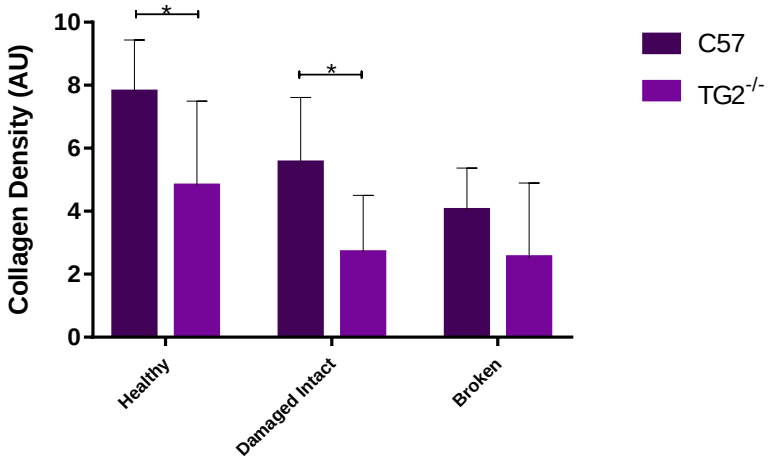

Figure 61. Collagen density in the long-term CaCl2 injury model

Collagen density was measured as described with areas of "healthy" elastin, "damaged but intact" elastin or "broken" elastin assessed separately. In both C57Bl/6 and $TG2^{-/-}$ mice, collagen density was reduced as the severity of elastin damage increased (ANOVA of combined data from both genotypes, p=0.0012). Pairwise Student's t-testing (with Welch's correction) revealed that the C57Bl/6 vessels had increased collagen density when compared to $TG2^{-/-}$ vessels at sites of healthy elastin (*, p=0.042) and where fibres were damaged but intact (*, p=0.026)

A.

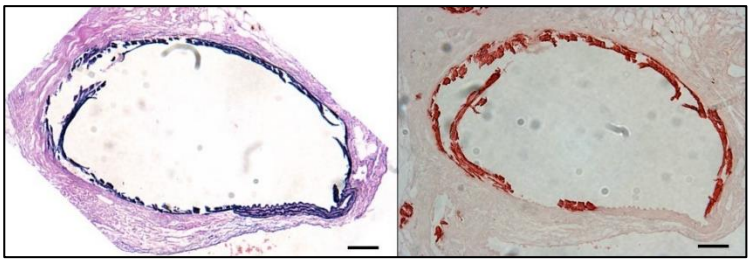

B.

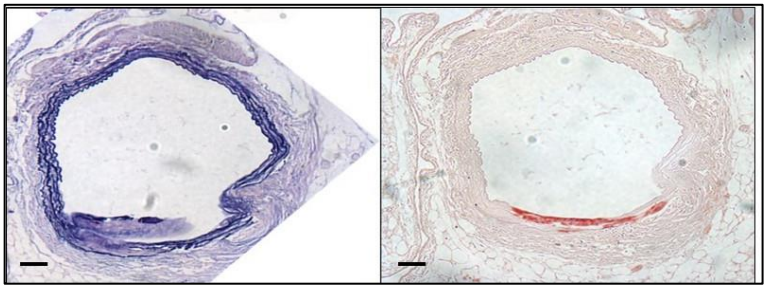

Figure 62. Calcification in the long-term $CaCl_2$ injury model

Panel A. shows representative images from a C57Bl/6 mouse aorta, harvested at 6 months post calcium injury. Images are from 5µm sections, captured at 2.5X magnification and imaged at 10X magnification. Correlation between elastin fibre damage/breakage and calcification is clearly seen. **Panel B.** shows the same findings but are taken from a $TG2^{-/-}$ mouse aorta. Scale bars represent 100µm in all images.

7.6.3 Expression data

Real-time PCR was performed to investigate mRNA expression of the transglutaminases as well as various other gene transcripts in aortic tissue harvested from WT (n=3) and $TG2^{-/-}$ (n=3) mice subject to 0.5M $CaCl_2$ exposure and harvested after 6 months. These results are summarised in Figure 63 and Figure 64 and in both cases show actual expression levels ($2^{-\Delta Ct}$) in un-operated, "short-term" operated and "long-term" operated vessels from C57Bl/6 mice. Statistical analysis was performed on raw delta Ct values. Due to the small number of samples per group normality could not be reliably assessed and hence significance of change of expression was analysed using Mann-Whitney testing (for two groups) and Kruksal-Wallis testing with Dunn's correction for multiple groups.

There was no evidence of substantive transglutaminase upregulation in the long-term $CaCl_2$ model. In WT tissue there was a significant *decrease* in TG2 expression between aortas from the short-term model vs. those subject to the long-term model (p=0.020). A similarly decreased FXIII-A expression was also observed in aortas from WT mice harvested after 6 months (p=0.0129) vs those harvested from the 6 week model. Expression of both TG1 and TG7 was increased in WT aortas from the 6 month model in comparison to those from the un-operated group (p=0.0074 and p=0.0098 respectively). The expression level of TG1 was not significantly higher than that of TG2 (mean $2^{-\Delta Ct}$ with 95% CI; TG1 0.24 (0.09-0.66), TG2 0.11 (0.04-0.30), p=0.70) and despite a >80-fold increase on basal TG1 levels still did not reach the levels of TG2 expression seen in basal tissue samples (1.40 (0.74-2.64)). Similarly, TG7 expression levels (0.18 (0.04-0.75)) were >200-fold increased compared to baseline levels but were not statistically greater than TG2 expression levels in either baseline or operated samples.

When comparing expression between WT and $TG2^{-/-}$ samples the only gene transcript that varied significantly in this model was TG2 itself. No statistically significant differences were seen between expression levels of any of the other transglutaminases compared to expression in WT vessels subject to the same conditions. In terms of the gene transcripts investigated that are known to be involved in inflammation or are components of vessel structure, there was no significant difference between the two experimental genotypes with this model. Expression levels of α-SMA were dramatically decreased in WT aortas harvested at 6 months (>13-fold decrease in expression compared to basal tissue levels, p=0.008) similar to the changes observed in the 6 week model, however α-SMA

expression was not different between WT and $TG2^{-/-}$ samples. Expression levels of many of the other “structural” transcripts were also decreased in the long-term model. Collagen I (11-fold decrease, p=0.0143), collagen III (33-fold decrease, p=0.0057), fibrillin I (8-fold decrease, p=0.0031), and vimentin (4-fold decrease, p=0.0074) expression levels were all decreased relative to basal levels.

Although we did not observe significant differences in expression levels between WT and $TG2^{-/-}$ aortic samples, the long-term model did appear to affect expression levels of fibrillin II (26 fold increase, p=0.0475), HO-1 (14-fold increase, p=0.015), uPA (7-fold increase, p=0.0039) and PAI-1 (35-fold decrease, p=0.0092) when compared to baseline, un-operated, values. Of note, these are the transcripts that varied in the DKO transgenic mouse line in the 6week model, and each result showed the same trend (i.e. either increase or decrease) perhaps suggesting that the loss of FXIII-A *and* TG2 is an “injurious stimulus” similar to that of long term $CaCl_2$ injury in $WT/TG2^{-/-}$ mice.

A.

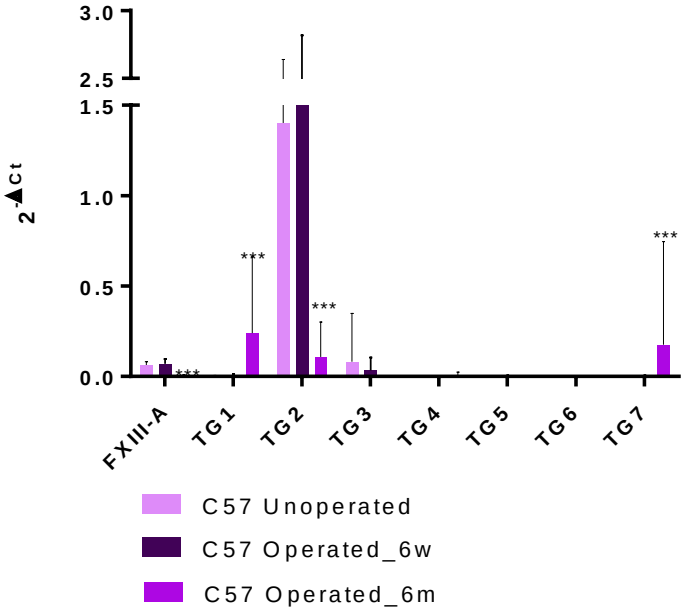

B.

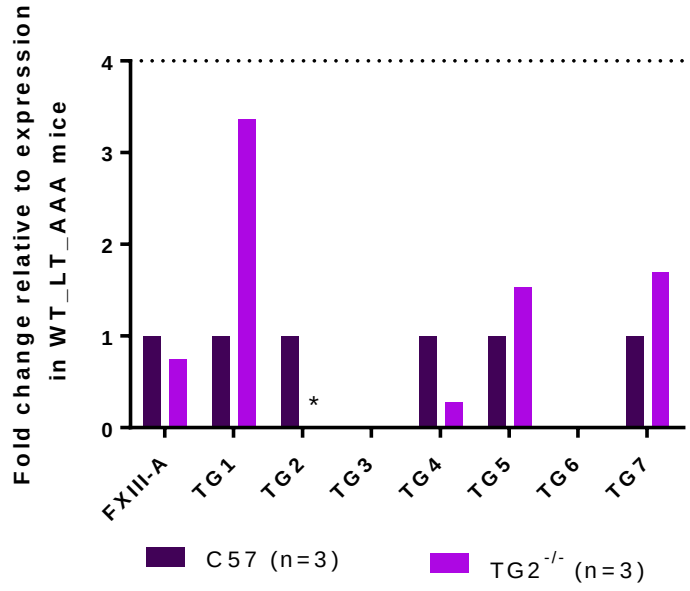

Figure 63. Expression levels of the transglutaminases in the long-term $CaCl_2$ injury model

Panel A. Absolute expression levels (mean $2^{-\Delta Ct}$ values ± 95% CI) of the transglutaminases in un-operated (n=9), "short-term" operated (n=9) and "long-term" operated (n=10) vessels from C57Bl/6 mice TG2 expression is reduced in the long-term model and both TG1 and TG7 expression is increased, but not to the levels of TG2 seen in basal tissue. **Panel B**. Transglutaminase mRNA expression in the 6 month operated aortic samples from C57Bl/6 (n=3) and $TG2^{-/-}$ (n=3) mice. All values are expressed as fold change relative to the expression level of that particular transglutaminase in C57Bl/6 6 month operated aortic tissue. Only TG2 expression was significantly difference between groups. Dotted line reflects a 4-fold increase in expression relative to WT * = $p<0.05$, ** = $p<0.01$, ***$p<0.001$.

A.

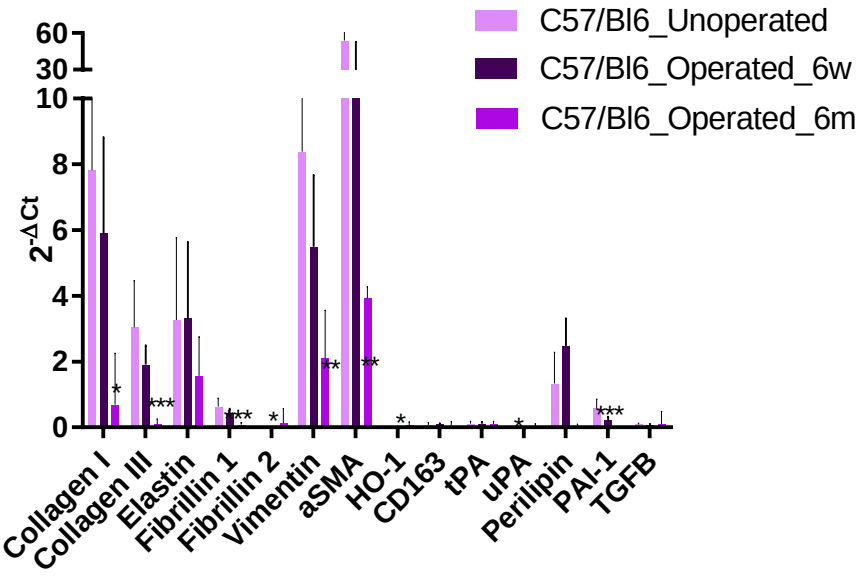

B.

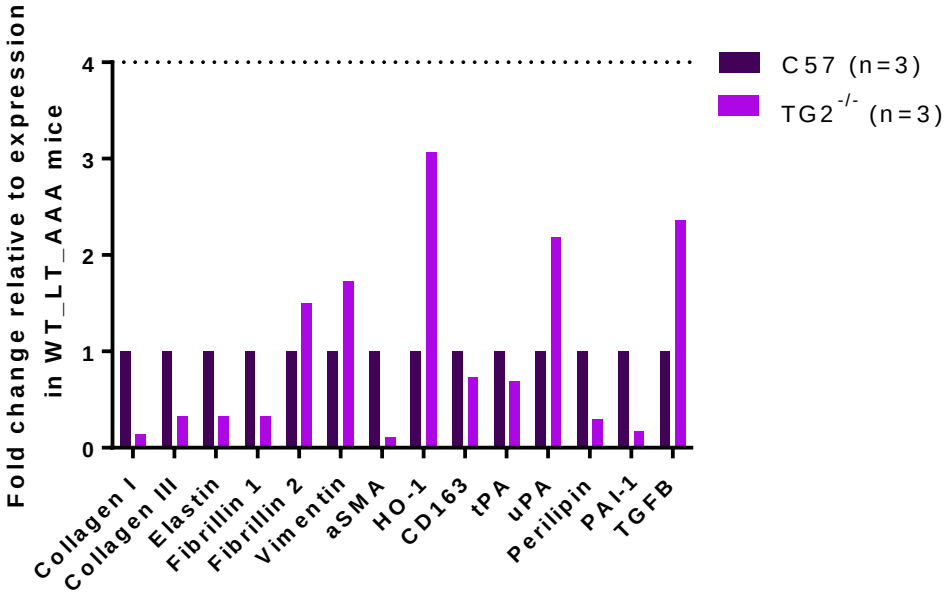

Figure 64. Gene transcript expression levels in the long-term $CaCl_2$ injury model

Panel A shows expression levels in un-operated (n=9), "short-term" operated (n=10) and "long-term" operated vessels from C57Bl/6 mice. Data is presented as $2^{-\Delta Ct}$ values (mean ± 95% CI) and highlights those transcripts that are significantly altered in the long-term model (see text for details). **Panel B** shows expression levels of the same transcripts in long-term operated samples (n=3 per genotype) with data presented as fold change relative to the expression level of that particular gene transcript in long-term operated vessels from WT mice. No significant difference was seen between WT and $TG2^{-/-}$ mice in any of the transcripts studied. Statistical analysis was performed using Mann-Whitney testing (for 2 groups) or Kruksal-Wallis testing with Dunn's correction (for multiple groups). Dotted line reflects a 4-fold increase in expression relative to WT. * = $p<0.05$. ** = $p<0.01$, *** = $p<0.001$

7.6.4 MMPs

As with the short-term model, qPCR was performed in samples harvested from the long-term model (n=3 per genotype) to investigate the expression of MMP-2,-9 and-12, as well as MT-MMP and TIMPs 1 and 2. These data are summarised in Figure 65. Panel A reflects expression levels (as $2^{-\Delta Ct}$ values) of MMPs in un-operated, "short-term" (6 week) and "long-term" (6 month) operated tissue from C57Bl/6 mice. Expression levels of MMP-9 were unchanged relative to baseline or the 6 week model whilst MMP-2 (11-fold decrease, p=0.0074) and TIMP-2 (6-fold decrease, p-0.0112) levels were decreased relative to basal expression. Similar to the 6 week model, expression levels of both MMP-12 and TIMP-1 were dramatically increased in aortic tissue harvested at 6 months. MMP-12 expression showed a >400-fold increase (p=0.0013) relative to baseline (c.f. 17-fold at 6 weeks) and TIMP-1 levels had increased by 30-fold (p=0.0019) relative to baseline as compared to the doubling in expression levels seen at 6 weeks. Clearly MMP-12 and TIMP-1 play an important role in progression of vessel dilatation in this model and warrant further study as to their potential interactions with the transglutaminases under investigation.

Gene Transcript	C57Bl/6 (n=3) Mean $2^{-\Delta Ct}$ (95% CI)	$TG2^{-/-}$(n=3) Mean $2^{-\Delta Ct}$ (95% CI)
MMP-2	0.02 (0.004 – 0.07)	0.01 (0.005 – 0.02)
MMP-9	0.03 (0.01 – 0.07)	0.01 (0.005 – 0.02)
MMP-12	2.37 (0.61 – 9.27)	7.04 (3.28 – 15.11)
MT-MMP	0.60 (0.23 – 1.56)	1.68 (1.35 – 2.10)
TIMP-1	2.03 (0.43 – 9.50)	3.33 (1.13 – 9.83)
TIMP-2	0.11 (0.07 – 0.17)	0.06 (0.02 – 0.15)

Table 5. Expression levels of the MMPs in the long-term $CaCl_2$ injury model

Panel B of Figure 65 shows relative expression levels of MMPs in vessels from $TG2^{-/-}$ mice (compared to WT) subject to the long-term $CaCl_2$ model. Although both MMP-12 and TIMP-1 showed increased levels in $TG2^{-/-}$ samples relative to those

from C57Bl/6 mice (see Table 6) no statistically significant difference was found between WT and $TG2^{-/-}$ mice in any of the MMPs/TIMPs investigated with the 6 month model.

A.

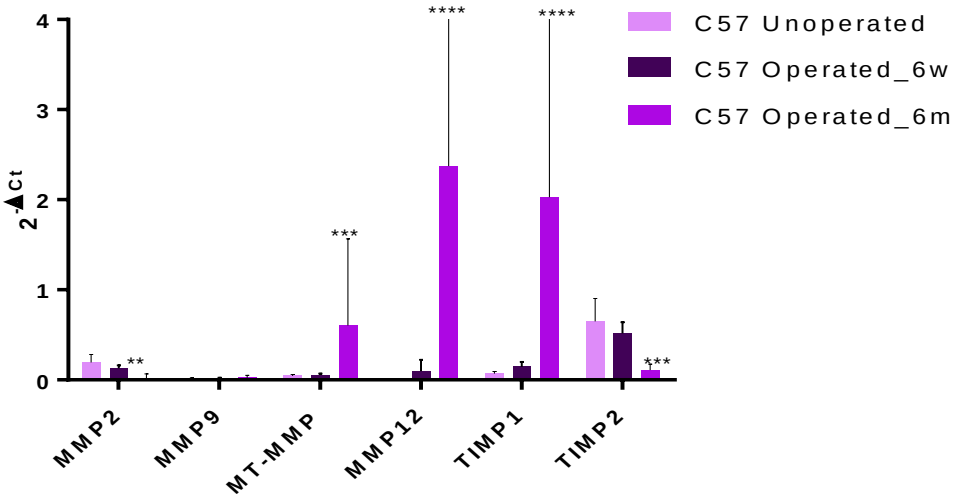

B.

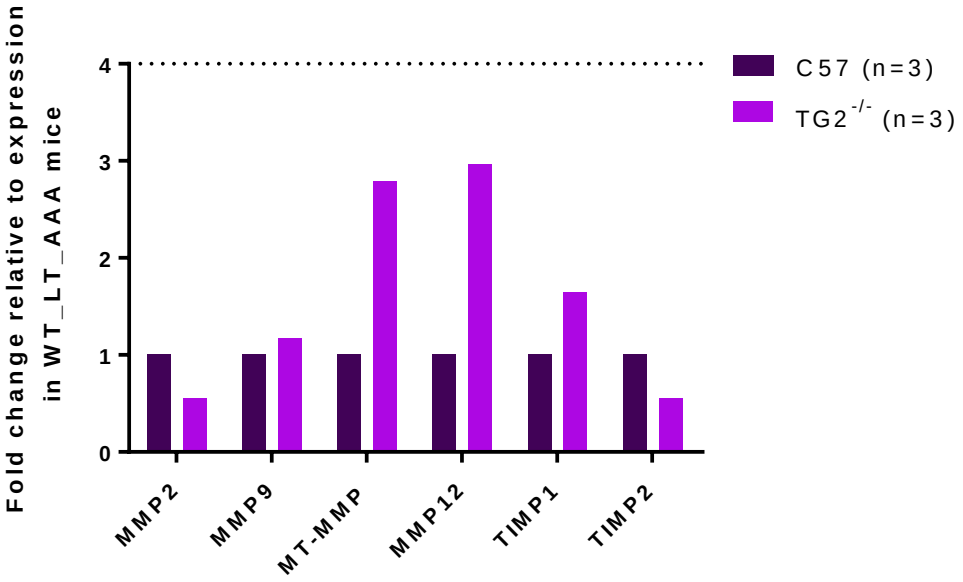

Figure 65. Expression of the MMPs in the long-term $CaCl_2$ injury model

Panel A. shows expression levels in un-operated (n=9), "short-term" (6 week) operated (n=10) and "long-term" (6 month) operated (n=3) vessels from WT mice. Data is presented as $2^{-\Delta Ct}$ values (mean with 95% CI) and highlights that transcripts that were significantly changed in the long-term model (see text for detail). **Panel B** shows expression levels of the same transcripts in long-term operated samples (n=3 per genotype) with data presented as fold change relative to the expression level of that particular MMP in long-term operated vessels from WT mice. Statistical analysis was performed using Mann-Whitney testing (for 2 groups) or Kruksal-Wallis testing with Dunn's correction (for multiple groups). Dotted line reflects a 4-fold increase in expression relative to WT. * = $p<0.05$. ** = $p<0.01$, *** = $p<0.001$

7.7 Carotid aneurysm model

7.7.1 Survival

Due to the high mortality observed with the $CaCl_2$ model of AAA in those mice deficient in the FXIII-A gene, we wanted to investigate whether a modified model could be established. This would need to allow vascular injury and repair to be investigated, without the high associated animal mortality. As carotid ligation experiments on DKO mice were well tolerated, and the original description of the $CaCl_2$ model was in the (rabbit) carotid artery,(Gertz et al., 1988) we decided to trial the $CaCl_2$ model in murine carotid arteries. This methodology is identical to that described in section 4.12 except that the right carotid artery is exposed to 0.5M $CaCl_2$ after access through a midline anterior neck incision. This model has been utilised by Gallo *et al* (Gallo et al., 2012) to investigate the role of chemokine receptor 3 in aneurysm formation and likewise, Pimiento *et al* (Pimiento et al., 2008) have reported success with this model in aged mice subject to 0.5M $CaCl_2$ exposure and harvest at 5 weeks.

Mice from C57Bl/6 (n=20) and DKO (n=9) genotype groups had 0.5M $CaCl_2$ applied to the common carotid artery and vessels were harvested at 6 weeks in line with our previous work. Only one death was observed over the post-op period. This occurred in the DKO group but was due to fighting behaviours between male mice. Although substantial weight loss was observed in the mice in the immediate post-op period, there was no difference between genotypes in terms of % weight loss and no mouse lost >15% of their body weight. Intra-operative analgesia could not be administered with this model, because of the risk of local anaesthetic toxicity to the vagus nerve, however, no animal showed signs of post-op distress and there were no wound complications observed in this cohort.

7.7.2 Diameter change and aneurysm proportions

Vessels subject to 0.5M $CaCl_2$ injury to the ventral surface of the right common carotid artery and vessels harvested under terminal anaesthesia at 6 weeks. The % change in vessel diameter was calculated from images captured *in vivo* pre-and post-injury. Each experimental group showed a mean % increase in carotid diameter (C57 43.1 ± 34.8, DKO 20.7 ± 15.9) with the DKO mice showing a statistically significant smaller increase in diameter over the 6 week period ($p=0.028$).

Under the conditions as described, 8/20 (40.0%) of C57Bl/6 mice studied developed an aneurysm (>50% dilatation) as compared with 0/8 of the surviving DKO mice. This showed a trend towards significance on analysis with Fisher's Exact Test (p=0.063) but shows a similar pattern to the results obtained in the aorta, without the significant mortality. These data suggest that calcium chloride injury to the carotid artery may represent a feasible model for assessing vessel damage and repair in future studies.

7.7.3 Histology

Although formal qualitative and quantitative analysis of histology from the carotid artery model was not undertaken, representative images are shown in Figure 67. In general the injured vessels showed the characteristic elastic fibre flattening and loss of waviness, but without the elastic breaks that were seen in the aortic injury. Calcium deposition was not a prominent feature, in line with our observation that vessel calcification is closely correlated with elastic fibre damage. Further work is required to ensure that the carotid and aortic models are comparable in terms of histological features but initial findings suggest that this would be a viable alternative to aortic injury as a way to reduce operative mortality.

A.

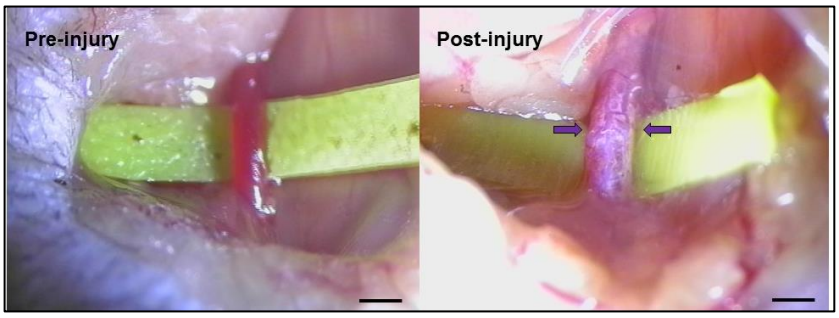

B.

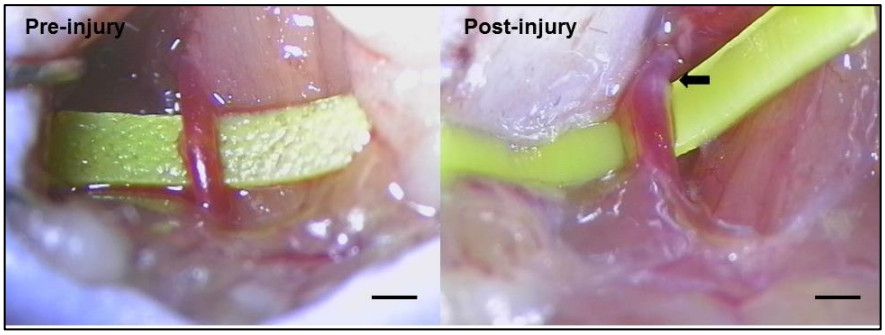

C.

	C57Bl/6	DKO
Mortality	0/20	1/9
Proportion developing an AAA	40%	0%

D.

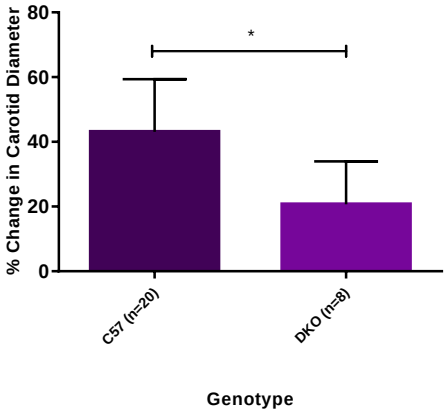

Figure 66. Summary results – carotid $CaCl_2$ injury model

Panels A and B. Representative images from the carotid injury model from a C57Bl/6 **(A)** and DKO **(B)** mouse showing pre- and post-injury appearances. Scale bars represent 500µm. **Panel C.** summarises mortality rates and the proportion of mice of each genotype that develop an "aneurysm" (% diameter change >50%). Data were analysed using Fishers Exact Test (of proportions), p=0.063. **Panel D.** Summary results from the carotid injury aneurysm model in C57Bl/6 and DKO mice. Data is shown as mean % change in aortic diameter (from baseline) with 95% confidence intervals. Student's t-test (with Welch's correction) revealed a statistically significant difference between the two groups (*, p=0.028)

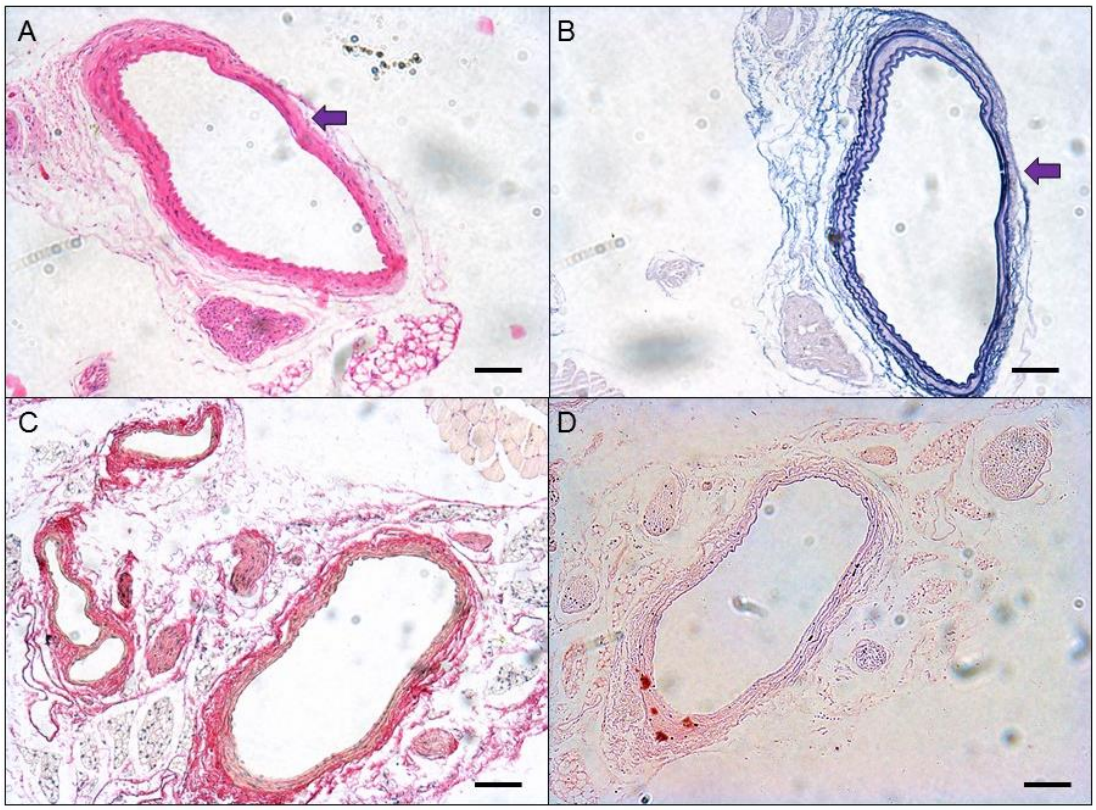

Figure 67. Representative histology – carotid $CaCl_2$ injury model

Figure shows representative images from a C57Bl/6 carotid artery with sections from the area of injury following exposure to 0.5M $CaCl_2$. Images are from 5µm sections, captured at 2.5X magnification and imaged at 10X magnification. Scale bars represent 100µm. **Panel A** shows a section stained for haematoxylin and eosin and highlights (arrow) a relative loss of cellularity at the site of injury. **Panel B** is stained with Miller van Gieson stain (for elastin) and highlights elastin flattening and loss of normal fibre waviness. **Panel C** is a Sirius Red stained section (for collagen) and **panel D** is stained with Alizrin Red (for calcium) and shows a lack of calcium staining (consistent with the absence of elastin breaks in panel B). Similar images were obtained from the DKO carotid vessels.

AORTIC MODEL
- $CaCl_2$ model established
- Elastin loss, damage & fibre breakage observed
- Collagen density ↓ with ↑ elastin damage
- True luminal dilatation

SHORT-TERM
- FXIII-A-/- and DKO have ↑ mortality ? Due to incipient fibrosis?
- DKO have ↓ propensity to AAA ? Elastin fibres resistant to breakage
- Medial calcification occurs despite dual TG deficiency

LONG-TERM
- AAA induction and progression occur by different mechanisms
- WT mice show static progression ? Due to repair
- TG2-/- mice show continued progression ? Due to failure of repair

mRNA EXPRESSION
- No evidence of reciprocal upregulation
- TG7 ↑ in short and long term model
- Pattern of transcript expression change (e.g. ↓ αSMA, ↑ HO-1, ↑ fibrillin-2) similar between FXIII-A-/- and DKO mice in short-term and TG2-/- and WT in long term

CAROTID MODEL
- Carotid aneurysm model feasible and safe – further characterisation required
- DKO have ↓ propensity to AAA
- No ↑ mortality observed

Figure 68. Summary diagram - the injured aorta

This figure summarises the main findings from Chapter 7 pertaining to the establishment of the $CaCl_2$ model, the findings from the short (6-week) and long (6-month) -term protocols and the main results from our mRNA expression studies. It also highlights that we have begun to investigate the carotid site as an alternative injury model and that our initial work has shown this to be feasible with similar results to those seen at the aorta. These results are discussed in full in section 7.8.

7.8 Discussion

This chapter summarises the process involved in establishing and optimising the $CaCl_2$ model of AAA and presents the key findings (summarised in Figure 68) related to our hypothesis that TG2 is involved in the response to aneurysm induction, possibly through a vascular repair role.

The $CaCl_2$ model is technically challenging and requires a considerable time investment to ensure that a reproducible, targeted injury is being applied to the ventral aorta each time the model is undertaken. We have established this model and have determined that a $CaCl_2$ concentration of 0.5M consistently results in gross inflammatory change +/- vessel dilatation. Through this work we have shown characteristic histopathological changes of elastin loss, damage and fibre breaks and have confirmed that our model results in true luminal dilatation and not simply external inflammatory tissue deposition as has previously been hypothesised.(Freestone et al., 1997)

Unexpectedly, the CaCl2 model resulted in a high mortality rate in both the FXIII-A-/- and DKO mice. We have not seen high mortality rates in our non-operated transgenic mice and deaths occur 1-5 days after surgery, hence deaths are occurring either secondary to CaCl2 application itself or because of the insult of the surgical procedure. Whilst it would be easy to assume that these deaths were simply due to impaired coagulation and bleeding, this was not the case and at least 33% of deaths in these mice were associated with post-mortem findings suggestive of cardiac pathology +/- embolization. These mice showed no evidence of aortic dilatation, vessel rupture or bleeding nor any evidence of widespread intra-abdominal inflammation or calcification from diffuse CaCl2 exposure. Although less dramatic, similar high mortality levels were also observed in ApoE-/-.FXIII-A-/- (~13%) and TKO (ApoE-/-.TG2-/-.FXIII-A-/-) (~20%) mice subject to a high fat feeding protocol. These mice had unclear causes of death but at least one showed evidence of intrathoracic haemorrhage and the surviving mice from the ApoE-/-.FXIII-A-/- and TKO group showed evidence of cardiac fibrosis, as we have demonstrated in our FXIII-A-/- and DKO mice in this work.

When considered together, this mortality data suggests that FXIII-A has a role in vessel integrity/stability and that deficiency results in “leaky” capillaries within the heart (resulting in fibrotic change) and increases likelihood of death (from a presumed cardiac cause) when the mouse is subject to physiological stress – either operative or dietary in the form of high fat feeding. TG2 deficiency worsens the observed FXIII-$A^{-/-}$ phenotype and DKO animals exhibit greater levels of cardiac

fibrosis and higher mortality rates. One possible mechanism is that the incipient cardiac fibrosis could predispose to cardiac arrhythmias leading to sudden death, heart failure and/or the formation of atrial thrombus which could subsequently embolise to distal sites as was observed in our post-op mice.

Given that the TKO mice show worse outcomes after carotid ligation than our DKO animals, we hypothesise that additional ApoE deficiency again worsens the observed vascular phenotype. ApoE deficient mice have been shown to have increased large vessel permeability with greater Evans Blue leakage in areas of the aorta normally prone to atherosclerosis.(Methia et al., 2001, Hafezi-Moghadam et al., 2007) Studies to investigate the combined effects of ApoE and FXIII-A on endothelial barrier function, and how this is affected by physiological stress have not yet been reported

It should, of course, be considered that the high mortality rate seen in our FXIII-A-deficient and DKO mice could be biasing the results obtained using the $CaCl_2$ model and we are in some way "selecting out" a DKO population with less propensity to vessel injury. We believe this is unlikely as the FXIII-$A^{-/-}$ mice, which also exhibited a high post-op mortality rate, showed similar changes in aortic diameter to WT mice, both in terms of mean % change in diameter and with regards the proportion of mice showing aneurysm development. Likewise, the application of $CaCl_2$ to the carotid artery, which did not result in high mortality rates in the DKO group, generated similar results in terms of diameter change as those achieved with the aortic model. Finally, the embolic pathology observed at post-mortem occurred at anatomical sites with blood supply *proximal* to the infra-renal abdominal aorta, thus suggesting that the cause of death in these mice is distinct from the site of vascular injury.

The "short-term" (6 week) aneurysm protocol has revealed that $CaCl_2$ application results in an increase in aortic diameter of 60-70% in WT mice, which is similar to that seen in TG2- and FXIII-A deficient animals. In contrast to our expectations, the DKO animals surviving to harvest showed a smaller average increase in aortic diameter of just 40%, below the 50% threshold of "aneurysm" development. Sub-group analysis has determined that this lower % diameter change may reflect a lesser propensity to develop aneurysms in the DKO group, i.e. more mice are in the "non-AAA group" than in the "AAA" group. The average size of vessel in each sub-group does not differ significantly across genotypes although the TG$2^{-/-}$ mice did show a trend towards developing bigger "non-aneurysms" at 6 weeks. If propensity to aneurysm development really is different in the DKO mice this could reflect an intrinsic difference in baseline structure, for example a greater elastin content or a

resistance of elastin to injury. Given that elastin is a known substrate of TG2, one might hypothesize that TG2-deficiency would result in elastin that is less well cross-linked and hence more vulnerable to degradation and loss. Our baseline studies suggest that aortas from the DKO mice have “normal” amounts of elastin but instead have decreased cellularity and show low-level fibrotic change. Histological analysis has shown that the DKO injured vessels have a higher proportion of “damaged but intact” elastin fibres than vessels from the other genotypes and hence we believe that the DKO mice are relatively resistant to aneurysm development secondary to a relative resistance of elastin fibres to breakage. This may be due to aortic fibrosis or because of an as yet undetermined change in elastin fibre structure.

We had anticipated that collagen deposition would be increased in our post-injury vessels as a compensatory response to elastin damage. Although we have not quantified collagen content post-operatively, our initial analysis shows that collagen density actually *decreases* as the degree of elastin damage increases. Mechanistically this loss of collagen could facilitate inflammatory cell infiltration leading to elastin fibre damage. Alternatively, collagen loss could occur secondary to the recruitment of invading macrophages attracted by the presence of elastin degradation products.

In our work we have shown a clear correlation between elastin damage and medial calcification in the $CaCl_2$ model. This relationship has been investigated previously by Basalyga *et al* (Basalyga et al., 2004) in rats. They showed that mural calcification occurred within one week of injury and that Ca^{2+} deposits associated with elastic fibres grew over time and resulted in connection of adjacent structures, elastic flattening and damage. They hypothesised that the increase in permeability seen in this model (measured using Evan’s Blue leakage) could be responsible for Ca^{2+} influx into the vessel wall. If this was the case then we might expect to see a greater degree of calcification (and elastin damage) in our FXIII-$A^{-/-}$ and DKO mice, which have higher basal endothelial permeability, but this was not observed, suggesting that calcification occurs prior to an increase in permeability.

Of significance is the fact that we have seen evidence of medial calcification in all of our transgenic lines at 6 weeks and in WT and $TG2^{-/-}$ groups at 6 months. Vascular calcification is seen in aging, in Diabetes Mellitus and in renal failure, yet remains poorly understood. $TG2^{-/-}$ has been reported to be a key regulator of vascular calcification, acting via β-catenin signalling to mediate osteoblastic transformation of VSMCs.(Faverman et al., 2008) TG2 inhibitors have been shown to prevent vascular calcification (Beazley et al., 2013, Beazley et al., 2012) and NIH-funded

projects are in progress to investigate the role of TG2 in vascular calcification in chronic kidney disease (CKD). Likewise, TG2 and/or FXIII-A activity has been implicated in the ectopic calcification seen in atherosclerotic lesions,(Johnson et al., 2008a, Matlung et al., 2009) with parallels drawn with their postulated roles in bone development and mineralisation. Work from our group (and supported by this thesis) has shown that bone development is normal in mice lacking both TG2 and FXIII-A (Cordell et al., 2015) and that chondrocytic metaplasia (the precursor of plaque calcification) of atherosclerotic lesions can occur in TKO animals (although they develop smaller brachiocephalic lesions than either WT or single-TG deficient mice – paper in preparation). The results presented here clearly demonstrate that in-vivo vascular calcification in response to arterial injury can also occur “normally” in the face of dual TG-deficiency.

We have not found any evidence that the short-term $CaCl_2$ model significantly changes transglutaminase expression in the WT aorta and specifically we have not seen evidence of TG2 upregulation as previously reported by Munezane *et al* in a combined elastase/$CaCl_2$ model.(Munezane et al., 2010) Likewise the absence of TG2 or FXIII-A did not induce upregulation of the alternate enzyme in the context of vessel injury. Quantitative real-time PCR did reveal that expression of TG7 was increased in injured vessels from FXIII-$A^{-/-}$ and DKO vessels (by ~18-fold) which may reflect attempts at compensation. Increases in TG7 were also seen in both WT and $TG2^{-/-}$ mice subject to the 6 month $CaCl_2$ protocol and although expression was not at the level of TG2 expression, may provide evidence for cooperative action of these enzymes which has not been previously reported. Further assays, including Western blotting, are needed to confirm the presence of increased TG7 protein (rather than just mRNA) in the aorta, as well as the presence of transglutaminase activity, which would be required for functional compensation.

Other expression data has shown that fibrillin-2, HO-1 and uPA expression are increased in all of the transgenic groups following injury, although not in the WT injured vessels when compared to baseline. Increased fibrillin-2 may reflect attempts at stabilising or repairing the damaged elastin media, whilst upregulation of (macrophage) HO-1 expression has been reported to have a protective anti-inflammatory action against AAA in both humans (Schillinger et al., 2002) and in a rat elastase model. (Nakahashi et al., 2002) Alternatively, the higher levels of expression of HO-1 (particularly in DKO mice) could reflect upregulation due to the presence of haem from “leaky” vessels. This process is known to occur in heart failure, when increased pulmonary vascular permeability leads to haemosiderin accumulation in siderophages or “heart-failure cells”. HO-1 expression and activity

has been shown to be increased in the lungs of rats exposed to a volume overload model of heart failure.(Lam et al., 2005) Although we did not see differential HO-1 expression in baseline vessels, the $CaCl_2$ model is known to increase aortic endothelial permeabiity (Basalyga et al., 2004) and hence DKO mice might be seen to have a "double hit" in terms of vessel permeability which could increase haem leakage and promote HO-1 expression.

Interestingly, the gene transcripts that were changed in the DKO mice in the short-term model were also those that were altered in the WT (and $TG2^{-/-}$) mice in the 6 month protocol. Hence, for example, α-SMA was decreased (along with structural proteins such as collagen (I and II) and vimentin, whilst fibrillin-2, HO-1 and uPA were again all increased. It appears, therefore, that the gene expression profile of the DKO mice at 6 weeks seems to be reflecting an insult similar to that experienced by the WT mice at 6 months; as if they are having an accelerated response to injury, or are more "injured" basally. Despite this, the DKO mice do not show greater aneurysmal dilatation; we hypothesise that the fibrotic change of the vessels in these animals is masking the normal inflammation and dilatation that might be expected.

We found no change in expression of MMP-2 and -9, either between un-operated and operated samples in WT mice or between genotypes in the short-term model. MMP-2 levels were decreased in the long-term model, although again there was no difference between WT and $TG2^{-/-}$ mice. MMP-9 levels did not differ across any of the experimental conditions or genotypes investigated. Whilst this appears to conflict previous work which has shown that MMP-2 or -9 deficient mice have attenuated or absent aneurysm formation (Longo et al., 2002, Pyo et al., 2000a) it might be that these enzymes are required for *initiation* of aneurysm formation and/or early growth, but that once established do not play a role in this model. Alternatively, given that the source of MMP-9 is probably due to both increased production by VSMCs and release from infiltrating macrophages, this model, which appears to cause VSMC apoptosis/de-differentiation) may not result in the increased MMP-9 expression that has been reported in human samples.(McMillan and Pearce, 1999)

Interestingly, MMP-12 expression was detectable in the aortas of the transgenic mice (but not WT), was increased in WT mice in the short-term model, and was greatly increased in the injured aortas of $TG2^{-/-}$(4.5-fold), $FXIII\text{-}A^{-/-}$(13-fold) and DKO (8-fold) mice at 6 weeks. Likewise, the 6 month model resulted in dramatic increases (400-fold) in MMP-12 expression compared to baseline in both WT and TG2-deficient animals. Infiltrating macrophages, the source of MMP-12, are known

to respond to the presence of elastin fragments and/or degradation products which act as a chemoattractant to these inflammatory cells. The cross-linking role of TG2 could hypothetically stabilise elastin and inhibit this chemokinesis and therefore could reduce MMP-12 production (and further ECM breakdown) as shown in Figure 69. However, we have not seen large differences in MMP-12 expression between the WT and $TG2^{-/-}$ mice at 6 months and have seen equally large increases in MMP-12 expression in the single deficient FXIII-$A^{-/-}$ mice. This implies that there are multiple mechanisms resulting in macrophage infiltration (and MMP-12 release). Equally, this model may represent too severe an insult and thus the normal protective role of TG2 is overwhelmed. We have immunohistochemical data which has not yet been fully quantified but which appears to show increased staining for MMP-12 in the DKO injured vessels in the adventitia and surrounding inflammatory tissue. Clearly more work is needed to tease out the role of MMP-12 in this animal model, its relevance to the human situation and the relationship between MMP-12 and the transglutaminases.

The $CaCl_2$ model is poorly characterised in terms of its longer-term effects. This, combined with an increasingly widespread view that aneurysm initiation and progression occur by different mechanisms, has prompted us to investigate the histological and mRNA changes that occur in the $CaCl_2$ model after a 6 month period. Ideally we would have liked to study this protocol in all four experimental groups however when this was established we had not determined that the DKO mice show a decreased propensity to aneurysm development (which may or may not persist with increased exposure). Also, the high mortality of the FXIII-$A^{-/-}$ and DKO mice would have meant that prohibitively large numbers of mice would have been required to generate meaningful data. The results from this extended protocol show that the C57Bl/6 mice appeared to remain static between 6 weeks and 6 months, both in terms of % diameter change and aneurysm proportion. In contrast, the $TG2^{-/-}$ mice developed larger aneurysms and almost all animals developed an “aneurysm” as defined previously. This is unusual as the $CaCl_2$ model usually only generates an aneurysm in 50-60% of control mice (using 0.25M or 0.5M $CaCl_2$ (personal communication, Baxter group, Nebraska)) and suggests that the TG2-deficient mice are different in terms of their propensity to develop aneurysms. The larger average diameter of the $TG2^{-/-}$ “aneurysm” group, may also reflect a difference in terms of progression of disease, or a failure of the ability to repair damage in these mice.

As yet we have not been able to fully identify the mechanism behind why the TG2-deficient mice show increased aneurysm development – expression data is not

statistically different between the genotypes, and histology – as assessed by elastin breakage scoring – is also not different between the groups. This suggests that the results observed in the long term model in the $TG2^{-/-}$ and C57Bl/6 mice are occurring via a different mechanism to that observed in the DKO mice in the short-term model. This is predictable, as if the $CaCl_2$ injury is sufficient to cause elastin breakage (which it does in all genotypes) then it would seem unlikely that TG2 could cause complete repair of these fibres. If TG2 is facilitating repair, or vascular remodelling, then it would seem likely that this would occur through mechanisms outside of the vessel media, similar to those seen in the inward remodelling response to reduced blood flow.(Bakker et al., 2005, Bakker et al., 2006) Interestingly, the $TG2^{-/-}$ vessels exposed to $CaCl_2$ and harvested at 6 months do appear to show lower collagen density, this requires formal quantification but may contribute to the continued expansion and larger aortic diameters seen in this group.

Of primary importance for future work is the finding that the carotid aneurysm model generates similar differences in vessel diameter between the WT and DKO groups as are seen in the aortic model, but without the associated high mortality. We plan to validate our histological and mRNA expression findings at this alternative anatomical site so that planned future work can be carried out in the carotid artery and can be easily compared with the findings presented here.

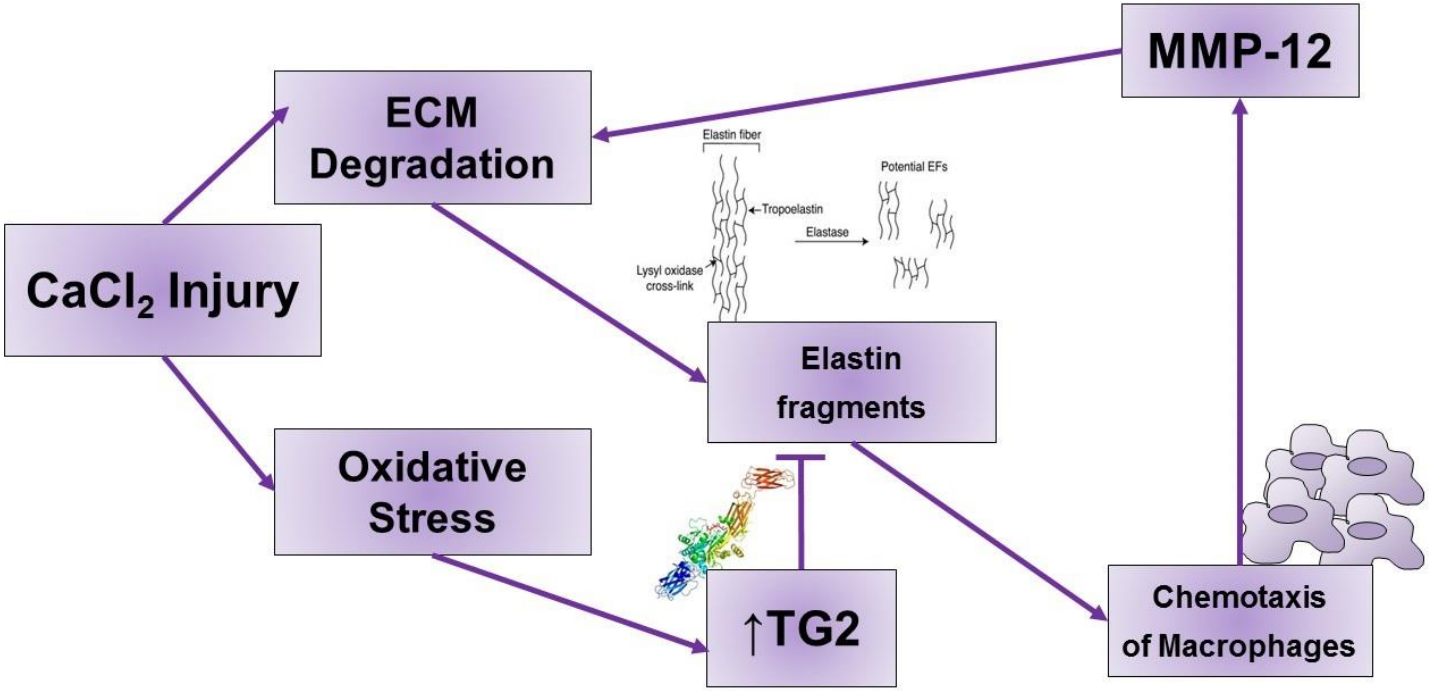

Figure 69. Proposed relationship between TG2 and MMP-12 in AAA formation

Schematic highlighting the potential relationship between TG2 and MMP-12 in AAA formation. The $CaCl_2$ injury model promotes elastin damage and ECM degradation which results in the generation of elastin fibres and EDPs which are known to be chemotactic to inflammatory macrophages. Through up-regulation of TG2, the production of elastin fragments could be reduced and hence macrophage infiltration could be limited with a subsequent reduction in MMP-12 release. This mechanism could potentially reduce further ECM degradation and could stabilise the vascular injury induced by this experimental model.

Chapter 8: Discussion and Future Work

Chapter 8: Discussion and Future Work

8.1 Original research question

The aim of this project was to elucidate the roles of TG2 and FXIII-A in basal vessel structure and function, and secondly, to study the contribution of these enzymes to aneurysm progression and development.

There is a wealth of literature proposing the involvement of TG2 in cardiovascular pathology with suggested roles in arterial remodelling,(Bakker et al., 2005) atherosclerosis (Haroon et al., 2001) and arterial calcification,(Faverman et al., 2008) amongst others. Equally, FXIII-A has been purported to have roles in vessel remodelling,(Bakker et al., 2006) repair after myocardial infarction (Nahrendorf et al., 2006) and in the maintenance of vascular permeability,(Noll et al., 1999b, Wozniak et al., 2001) in addition to its well established clotting function. Many authors suggest that these two enzymes are complementary and that one enzyme can compensate for the other in the face of deficiency. Essential functions for this transglutaminase pair have been proposed in the skeletal system (in bone development and calcification (Tarantino et al., 2009)) and in the cardiovascular system (in atherosclerotic plaque calcification (Van Herck et al., 2010) and inward arterial remodelling (Bakker et al., 2006)). Despite these assertions, we found that mice deficient in TG2 show no difference in atherosclerotic plaque formation or composition (Williams et al., 2010) and that those lacking both enzymes demonstrate no gross phenotypic change and normal bone development.(Cordell et al., 2015) Work currently in preparation has also revealed that although double-deficient mice (on an $ApoE^{-/-}$ background) develop smaller atherosclerotic lesions in the brachiocephalic artery, these plaques show cartilaginous metaplasia (the precursor stage to plaque calcification) at a rate similar to WT lesions of a comparable size.

As an alternative to fat-feeding, these TKO ($TG2^{-/-}$.FXIII-$A^{-/-}$.$ApoE^{-/-}$) mice were, in previous studies, subject to carotid ligation as a model for atherosclerosis, local vessel remodelling and neointimal formation. This unexpectedly gave rise to fatal carotid artery rupture, suggesting an intrinsic vessel weakness in TKO animals. Histological analysis of ligated vessels from mice lacking either ApoE and TG2 or Apo E and FXIII-A and from sham-operated vessels in the TKO mice suggests that under basal conditions both TG2 and FXIII-A contribute to arterial integrity but that TG2 is more important under conditions of vascular stress or injury. Given that the vessels from TG2-deficient mice in this study showed medial elastin breaks and

luminal area expansion – both features of aneurysm development – we sought to investigate the role of these enzymes in the $CaCl_2$ model of aneurysm development.

Various animal models have been developed to allow study of the early stages of aneurysm development and evaluation of potential therapeutic targets. The relative advantages and disadvantages of the three main murine models have been discussed in the Introduction but briefly, we chose the $CaCl_2$ model because it can be undertaken in both male and female mice, does not require a hyperlipidaemic background (which had concerned reviewers of our original funding application) and more accurately represents the human situation in terms of anatomical site, elastin breakdown, and vascular inflammation.(Wang et al., 2013a) Over the course of this project we have established and optimised this model and it has already been used by other groups in our Institute in work investigating the role of the Orai1 calcium channel in AAA development.(Bailey et al.)

This thesis has shown that, despite reservations in the literature,(Freestone et al., 1997) the calcium chloride model results in true luminal expansion (and not just peri-adventitial inflammation and thickening) and, surprisingly, demonstrated that collagen density is reduced at sites of elastin damage. We were expecting to find that the model induced collagen deposition at areas of elastin loss/damage, to reinforce the arterial wall, however this was not the case on histological analysis. Collagen loss could precede inflammatory cell infiltration, facilitating cell migration, or could occur subsequent to macrophage recruitment triggered by the presence of elastin degradation products.

Given the essential role that has been proposed for TG2 in ectopic calcification, an important finding from this work is that $TG2^{-/-}$, $FXIII\text{-}A^{-/-}$ and DKO mice all show calcification of the aortic media in association with elastin fibre damage. This calcification is not present at 24 hours post injury, and hence is not due to $CaCl_2$ exposure directly, but occurs as a consequence of the inflammatory response generated by the injury model. Whether this process reflects the human situation is unclear, however this model represents a reproducible injury which should, if the literature is correct, induce transglutaminase activity. The results presented here demonstrate that in-vivo vascular calcification in response to arterial injury occurs “normally” in the face of dual TG-deficiency and thus challenges a view held by several influential papers within the field of transglutaminase research.

Despite the distinct mechanisms of activation of FXIII-A and TG2 – plasma FXIII-A is activated by thrombin cleavage whereas extracellular TG2 becomes catalytically active on reduction of key residues – many have suggested that these enzymes

can act interchangeably or can compensate for each other. Whilst our previous work has not shown any evidence of reciprocal mRNA upregulation between TG2 and FXIII-A (Cordell et al., 2015) this, and other findings, were complicated by the presence of additional ApoE deficiency. An important outcome from this thesis is the generation of a $TG2^{-/-}$.$FXIII\text{-}A^{-/-}$ KO mouse on a defined C57Bl/6 background which will enable further study of the relative contributions of these two enzymes to normal physiology as well as to the development of disease.

As expected, this DKO mouse had a grossly normal cardiovascular phenotype and this work has demonstrated no evidence for TG2/FXIII-A upregulation in the aorta, either at baseline, or after short- or long-term injury. Interestingly we *have* observed upregulated transcription of TG7 (which is relatively unstudied) in the injured vessels of $FXIII\text{-}A^{-/-}$ and DKO mice at 6 weeks, and in $TG2^{-/-}$ and WT mice at 6 months. These findings require additional confirmatory work but may provide evidence of a previously unreported role for TG7 in vascular injury.

Our previous work has suggested that FXIII-A is important in the maintenance of arterial integrity. Lack of FXIII-A leads to impaired vessel integrity or increased “leakiness” that results in insipient haemorrhage and haemosiderin deposition. This in turn triggers an inflammatory response that ultimately results in cardiovascular fibrosis. We hypothesised that TG2 can compensate for FXIII-A deficiency under basal conditions, either through a vascular stabilising function or through a subsequent repair function. The findings from this thesis supoort this and DKO mice show more cardiac fibrosis (and higher surgical mortality) than single-FXIII-A-deficient animals, although deficiency of FXIII-A alone is sufficient to result in increased endothelial permeability in the aorta.

This finding has three important consequences; firstly the observation that $FXIII\text{-}A^{-/-}$ and DKO mice spontaneously develop mild cardiac fibrosis without the need for a hypercholesterolamic background or high-fat feeding means that we have identified a potential pre-clinical model of fibrosis which can be used in future studies. Secondly, FXIII-A is currently considered to be a viable anti-thrombotic target because of its role in fibrin-cross-linking and clot stabilisation. Whilst the literature emphasises the need for any FXIII-A inhibitor therapy to be “specific and targeted” to prevent bleeding complications,(Richardson et al., 2013) our work highlights a potential side-effect of FXIII-A inhibition that has not previously been considered. Thirdly, TG2 has been proposed to be involved in the development of fibrosis in response to injury in various organs.(Johnson et al., 2003b, Olsen et al., 2011a, Grenard et al., 2001) Despite this, we have found that mice lacking TG2 in addition

to FXIII-A show *increased* fibrotic change rather than the relative improvement in pathology that might be expected from reading of the literature.

Under conditions of carotid artery ligation, the $TG2^{-/-}$.$ApoE^{-/-}$ mice showed increased elastic lamellar number, increased elastin breaks and increased medial area. Likewise, our DKO mice showed increased elastic lamellar number and a lack of the expected inward vessel remodelling. These findings could be due to a baseline deficiency in medial elastin (and an attempt to increase tropoelastin formation as compensation), or could be secondary to a failure of the normal vascular repair or remodelling functions which have been attributed to TG2.(Bakker et al., 2005, Bakker et al., 2008) We have not found evidence of basal deficiencies in elastin content, structure or function in the aortas of our TG2-deficient mice, but our long-term aneurysm model results suggests that TG2 knock-out results in a failure to stabilise the injured aorta and progression of arterial dilatation.

Surprisingly, we have found that our DKO mice were less susceptible to aneurysm formation. From the carotid artery rupture and mortality seen in the TKO mice, we had assumed that these mice would have weaker vessels that were *more* liable to show aneurysmal change. Whilst there are certainly intrinsic differences in the aortas from these mice (as shown by their decreased tension on myographic testing) they appear to be relatively resistant to elastin breakage and subsequent dilatation. We hypothesise that this is due to basal fibrotic change in these vessels which occurs as shown in Figure 70. This relative “protection” is outweighed by the increased mortality in these animals which seems to occur with the addition of *any* additional cardiovascular stress (e.g. fat feeding, ApoE deficiency, ligation or prolonged surgery) and may be due to unmasking of an as yet unqualified cardiac phenotype secondary to vascular or myocardial fibrosis.

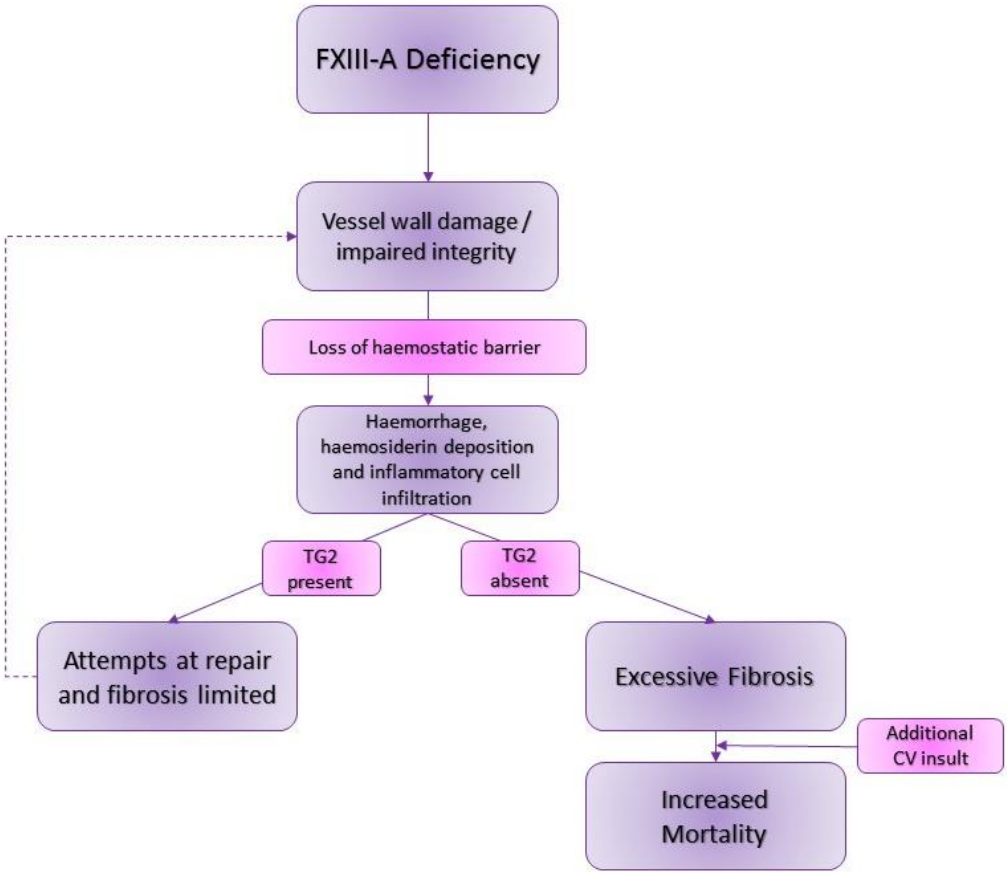

Figure 70. Cardiac fibrosis and increased mortality

Schematic of possible pathway linking FXIII-A deficiency, observed cardiovascular fibrosis and increased mortality rate.

8.2 Limitations

Although this work has generated several key findings related to the role of transglutaminases in vascular integrity and repair and aneurysm formation; there are a number of limitations which need to be considered.

As with any transgenic mouse model these results need to be interpreted with caution. The literature is littered with examples of gene knockouts which have widely varying effects in humans when compare to their murine counterparts. For example, PAI-1 deficiency in humans is rare and causes severe bleeding whereas serpine-1 (the mouse ortholog) knock-out mice are viable and able to reproduce with no increased tendency to bleed.(Iwaki et al., 2012, Iwaki et al., 2011) Likewise, Shapiro has discussed some of the pitfalls of the use of transgenic mice in research into emphysema and COPD,(Shapiro, 2007) where complexities in the genetic locus for mouse α-1-AT are such that mice have either 4 or 5 genes depending on their strain. These examples highlight that murine models can only ever represent the human situation and not reflect it entirely.

An important example here, which may be very relevant to our work, is that of *elafin*, an inhibitor of neutrophil elastase (NE), that is present in humans but lacking in mice. NE can promote ECM degradation, has potential roles in aneurysm formation as well as atherosclerotic plaque disruption and has recently been proposed to be the link between inflammation and insulin resistance.(Mansuy-Aubert et al., 2013, Talukdar et al., 2012) Clearly the ability to inhibit NE has huge therapeutic potential and in retrospect it seems surprising that so many murine atherosclerosis studies have been undertaken without acknowledgement of the lack of elafin and attempts to extrapolate to the human situation. Our plan to study this further is outlined below.

The unexpectedly high mortality of the $CaCl_2$ aneurysm model in mice lacking the FXIII-A gene has obvious implications in terms of mouse numbers, time, and associated breeding, husbandry and operating costs. However, operating on these mice still provided important data, both in terms of their propensity to aneurysm development and their causes of death. Although we were able to examine the majority of mice post-mortem there were a small number found dead by animal house staff, and in some cases mice were examined but no obvious pathology could be found. This highlights some of the difficulties of murine work, but >1/3 of deaths were able to be attributed to cardiac causes and/or distal thromboembolic events. It would be valuable to be able to establish whether these events are the result of primary atrial thrombus and one could imagine that continuous cardiac monitoring could identify problems with cardiac physiology that are as yet unknown.

We have previously attempted to insert intra-vascular telemetry devices into our DKO animals but they are prone to acute, fatal, cardiac dysfunction and alternative methods would need to be sought for this to be a viable avenue of future study.

The application of $CaCl_2$ to the ventral surface of the abdominal aorta promotes significant inflammation and scarring. Whilst this is to be expected, and can be dissected to allow vessel diameter measurements and vessel harvesting for mRNA analysis etc., it is difficult to ensure that only the vessel itself is harvested and that variable amounts of fibrotic/inflammatory tissue are not processed at the same time. This has implications for the analysis of post-operative aortic collagen and elastin content and means that we will need to adopt a morphological approach to obtain meaningful data because of the potential heterogeneity of samples.

8.3 Future directions

We have identified that the application of $CaCl_2$ to the common *carotid* artery is a viable alternative injury model which appears to be well tolerated in our DKO mouse line. Although we have characterised this model in terms of morphological and histological outcomes we also made attempts to extract mRNA from un-operated and post-injury carotid vessels using the methodology as previously outlined. Insufficient mRNA was obtained from single vessels using the Trizol extraction process to allow reverse transcription to cDNA and hence in the future, multiple samples will need to be pooled to allow changes in gene expression to be quantified.

Such mRNA data is difficult to interpret without supporting evidence of changes in protein levels, however, we have identified some important trends in *aortic* mRNA expression across the genotype groups. Alpha-smooth muscle actin expression was decreased in all groups following calcium chloride injury, presumably as a result of VSMC loss or de-differentiation, but was more decreased in FXIII-$A^{-/-}$ mice and further still in DKO animals. This could suggest that the calcium chloride model causes a greater degree of VSMC apoptosis in these lines or that they have decreased cellularity prior to injury (as is suggested from our basal biochemistry data). Work to confirm these findings and investigate them further is currently in progress and we are attempting to optimise a TUNEL assay of apoptosis to allow quantification of cell death in our aneurysm histological samples.

The finding that $TG2^{-/-}$ mice develop larger aneurysms than control animals in a 6 month model of injury could be explained by 1) an intrinsic vessel weakness only manifest after prolonged injury, i.e. a protective role for TG2, 2) a lack of vascular repair normally present, i.e. a reparative role for TG2 or 3) both of these

mechanisms. Further work is necessary to elucidate the mechanisms by which TG2 appears able to effect stabilisation in this model but could include the cross-linking of collagen and other structural proteins, or interaction with fibronectin and other integrins. The ability to assay collagen density in our samples would be useful in this work – at present we are able to qualitatively assess collagen distribution but hard calibration of our multiphoton microscopy would be required for quantification. Alternatively, use of the periadventitial elastase model may provide complementary results if it results in less scar tissue and allows for direct post-injury measurement of collagen (and elastin) content in harvested vessels.

There is an increasingly prevalent view that TG2 functions predominantly as a structural protein and is usually inactive in terms of its transamidating activity. The work presented here assumes that murine extracellular TG2 can be (and is) activated in response to vessel injury, which may not be the case in mice. Constitutive activation of TG2 would allow assessment of the intrinsic vascular repair activity of TG2, if present. The transgenic $TG2^{R579A/R579A}$ mouse does not require GDP binding for activation and hence shows constitutive transamidating activity intracellularly (and presumably extracellularly if it can be secreted/released). This line has been utilised in the study of the role of TG2 in glucose homeostasis (Iismaa et al., 2013) but full characterisation has not been reported. Its use in studies similar to ours may prove crucial to attempts to delineate the transglutaminase function of TG2 from its other pleiotropic roles in the setting of vascular repair.

Our FXIII-$A^{-/-}$ mice (both male and female) develop spontaneous myocardial fibrosis without the need for high fat-feeding or background hyperlipidaemia. If, as suspected from their normal unstressed phenotype, these mice lack any limiting cardiac pathology, this would represent a useful model to assess potential novel therapies. Although the morphology of fibrotic change in our mice is similar to that seen in virally-induced fibrosis, cardiac fibrosis is seen in hypertensive heart disease, secondary to diabetes and in the response to myocardial ischaemia. If FXIII-A deficiency results in spontaneous fibrosis, exogenous FXIII-A administration may be a viable option for treating fibrosis in a number of disease states. Further work is planned to assess the relative contributions of plasma vs. cellular FXIII-A to this process, whilst also extending our work investigating the cellular source of plasma FXIII-A, which we hypothesise to be a resident macrophage located with the cardiovascular system.

Although many of these research streams will be devloped in parallel, we initially plan to investigate the role of elafin in vascular repair and a full discussion of this work is outlined below.

8.3.1 Elafin/trappin-2

MMP-12, or *macrophage* elastase, produced by infiltrating macrophages is key to the later stages of aneurysm development and progression and our immunohistochemical data provides evidence of MMP-12 in inflammatory tissue surrounding injured vessels. However, some authors suggest that neutrophils may play a prominent role in the early phase of aneurysmal development (Tilson, 2005, Eliason et al., 2005a, Hannawa et al., 2005) and hence it would seem likely that *neutrophil* elastase is a viable target for study and therapeutic inhibition.

Neutrophil elastase is covalently inactivated by serpins and, in addition, is non-covalently inhibited by trappin-2 (pro-elafin). Trappin-2 has a repeated cementoin domain that enables it to be covalently cross-linked by transglutaminases to ECM proteins including collagen IV, fibronectin and elastin.(Guyot et al., 2005) Cross-linking confers localised protection against proteolysis, most obviously at the site of synthesis and secretion but possibly also following circulation in the bloodstream and capture at distal sites. Cleavage of the cementoin domain from trappin-2 yields elafin, an anti-protease that has a single potential cross-linking site.(Tsunemi et al., 1996) This may allow it to be covalently retained in the ECM but presumably with a reduced efficiency relative to trappin-2.

Elafin expression has been reported in T-lymphocytes, and in inflammatory cells in atherosclerotic plaques. Elafin/trappin-2 has considerable therapeutic potential, (Shaw and Wiedow, 2011) has narrow anti-protease specificity and diffuses well into affected tissues.(Doucet et al., 2007, Sallenave, 2010) A single clinical trial has been undertaken to assess the capacity of elafin to reduce inflammation following coronary artery bypass grafting (Alam et al., 2015) and further Phase II trials are investigating its use in kidney transplantation and following oesophagectomy.

Mice lack an ortholog of trappin-2, i.e. they do not have an elastase inhibitor that is retained in tissues.(Williams et al., 2006) In some studies, mice (and larger species) have been locally infected with trappin-2 expressing adenoviruses and these have been shown to protect against lung (Simpson et al., 2001) and genital infections,(Drannik et al., 2013) or with trappin-2 expressing lactobacilli that protect against inflammatory bowel diseases.(Motta et al., 2012) In addition, transgenic mice have been constructed where trappin-2 expression is driven by the CMV promoter and these animals express strongly in epithelial tissues similar to the

expression of the endogenous human gene.(Sallenave et al., 2003) Collaborations are already in place to utilise these mice in our planned work.

Mice have also been constructed that express trappin-2 in vascular tissues under the control of the pre-proendothelin promoter, and these mice are protected against myocardial fibrosis following viral myocarditis (Zaidi et al., 1999) or coronary ligation.(Ohta et al., 2004) However, while localized over-production of elafin can provide cardiovascular protection, it is not clear whether (i) endogenously synthesized elafin, from epithelial tissues or exogenously administered trappin-2 can be captured and retained in cardiovascular lesions, or (ii) production by macrophages in cardiovascular lesions affords local protection.

Whilst this work, and that published by our group relating to atherosclerosis in the TKO mice (Williams et al., 2010) suggest that TG2 cross-linking of the ECM *per se* has little effect on mouse models of early aneurysm and atherosclerosis, it may be that the protective effect of TGs will only be adequately reproduced where trappin-2 is present, i.e. that a major role of induced and activated TGs in response to injury is to capture and retain circulating trappin-2. We are planning a programme of work in which trappin-2 will be administered to TG2 expressing and TG2 knockout mice and aneurysm development will be assessed. Atherosclerosis and the possible role of FXIII-A in trappin-2 retention will be assessed in subsequent projects if trappin-2 proves protective against aneurysm development.

8.4 Clinical and translational implications

This work adds to the understanding of the pathobiology of aneurysm development and crucially provides additional knowledge about one of the key animal models in use in aneurysm research. We have not found clear evidence of a vascular protective effect of TG2, however important evidence supporting its role in vascular repair is presented. The clinical implications of this work more likely pertain to the use of TG2 and FXIII-A inhibitors which are currently under investigation for a variety of conditions. A better understanding of the potential side-effects of these inhibitors (for example in terms of cardiac fibrosis or vessel integrity) is important if future treatments are to be safe and effective.

8.8 Conclusions

In summary, there are several main conclusions to be drawn from this thesis. Both FXIII-$A^{-/-}$ and TG2 have roles in the maintenance of basal vessel integrity. Whilst endothelial permeability is increased in both FXIII-$A^{-/-}$ and DKO mice, and both

groups show evidence of decreased aortic cellularity, the DKO group shows more cardiac (and likely aortic) fibrosis and the DKO mice show a functional deficit which is not seen with single gene deficiency. We have not seen evidence of a clear protective effect of TG2 in the response to aneurysm development however our DKO animals showed an unexpected decreased propensity to aneurysm development at 6 weeks. These data may be explained by increased basal fibrosis, however both FXIII-A and DKO mice are at risk of increased mortality through a presumed cardiac mechanism. This finding has important implications given that inhibition of one or both enzymes has been proposed as a potential target for conditions as diverse as thrombosis, neurodegeneration and cancer.

In an extended aneurysm model there is evidence that aneurysm initiation and progression occur by different mechanisms and that TG2 is involved in vessel repair or stabilisation of injury. This project has provided evidence that vascular calcification can progress normally in the presence of dual TG2 and FXIII-A deficiency and we have seen no evidence for reciprocal enzyme compensation although TG7 may be upregulated under conditions of vascular injury.

Finally, we have established the $CaCl_2$ model of aneurysm formation, a novel $TG2^{-/-}$.$FXIII\text{-}A^{-/-}$ mouse line has been generated and initial characterisation of this line has been undertaken. The ability to study the distinct and overlapping roles of TG2 and FXIII-A in the cardiovascular system, without associated ApoE deficiency, is now possible, and these mice represent an important, previously unpublished, research tool in the field of transglutaminase study.

List of Abbreviations

5-LO	Lipoxygenase-5
α-1-AT	α-1-antitrypsin
α-2-PI	α-2-plasmin inhibitor
AAA	Abdominal aortic aneurysm
AAAP	Aortic aneurysm associated protein
ACEi	Angiotensin converting enzyme inhibitor
ADAM	A disintegrin and metalloproteinase
ADAMTS	A disintegrin and metalloproteinase with thrombospondin motifs
AGEs	Advance glycated end-products
AGM	Aorto-gonadal mesonephros
AIE	Anion exchanger
AIF	Apoptosis inducing factor
ALS	Amyotrophic lateral sclerosis
Ang II	Angiotensin II
ApoE	Apolipoprotein E
APSS	Acral peeling skin syndrome
ARB	Angiotensin-II receptor blocker
AT	Angiotensin (receptor)
AU	Arbitrary units
AUC	Area-under-the-curve
BAX	Apoptosis regulator BAX, also known as Bcl-2-like protein 4
BBB	Blood-brain barrier
BMP	Bone morphogenic protein
BP	Blood pressure
BSA	Bovine serum albumin
$CaCl_2$	Calcium chloride
CCR2	C-C chemokine receptor type-2

CD	Coeliac disease
cDNA	Complementary DNA
CE	Cell envelope
CI	Confidence intervals
CKD	Chronic Kidney Disease
CMP	Common myeloid precursor
CMV	Cytomegalovirus
COPD	Chronic obstructive pulmonary disease
Co-Smad	Common mediator Smad
CREB	Cyclic AMP (cAMP) response element binding protein
CTAD	Citrate theophylline adenine dipyridamol buffer
CV	Cardiovascular
DKO	Double knock-out (in relation to transgenic mice)
DM	Diabetes Mellitus
DNA	Deoxyribonucleic acid
EBP	Elastin binding protein
ECM	Extracellular matrix
EDP	Elastin degradation product / Elastin derived peptides
EDS	Ehlers Danlos Syndrome
EDTA	Ethylenediaminetetraacetic acid
EEL	External elastic lamina
EF	Elastin fragment
EGF	Epidermal growth factor
ELISA	Enzyme-linked immunosorbent assay
EMILIN	Elastin microfibril interface located protein
ESVS	European Society for Vascular Surgery
Flt-3	FMS-like tyrosine kinase 3
FXIII-A	Factor XIII-A

GAPDH	Glyceraldehyde 3-phosphate dehydrogenase
GMP	Granulocyte / macrophage precursor
GTT	Glucose tolerance test
GWAS	Genome-wide association study
H&E	Haematoxylin and eosin
HCl	Hydrochloric acid
HIF	Hypoxia inducible factor
HSC	Haematopoietic stem cell
IEL	Internal elastic lamina
IFN-γ	Interferon-gamma
Ig	Immunoglobulin
IGF-1	Insulin-like grwoth factor 1
IL	Interleukin
ILT	Intraluminal thrombus
ITT	Insulin tolerance test
IVC	Inferior *vena cava*
JNK	cJun N-terminal kinase
KO	Knock out
LAP	Latency associated peptide
LDL(R)	Low-density lipoprotein (receptor)
MAGP	Microfibril associated glycoprotein
MANDP	Metaphyseal anadysplasia
MAPK	Mitogen activated protein kinase
MDC	Monodansylcadaverine
MEF	Mouse embryonic fibroblast
MEP	Megakaryocyte / erythrocyte progenitor
MI	Myocardial infarction
miRNA/miR	MicroRNA

MMP	Matrix metalloproteinase
MODY	Maturity-onset diabetes of the young
MP	Megakaryocyte precursor
mRNA	Messenger RNA
MyD88	Myeloid differentiation factor-88
NAAASP	National AAA screening programme
NaCl	Sodium chloride (“normal saline solution”)
NaOH	Sodium hydroxide
NE	Neutrophil elastase
NFκB	Nuclear factor kappa B
NICE	The National Institute for Health and Care Excellence
NOS	Nitric oxide synthase
OR	Odds ratio
PAI	Plasminogen activator inhibitor
PAR-1	Protease/Proteinase activated receptor-1
PBS	Phosphate buffered saline
PCR	Polymerase chain reaction
PDGF	Platelet derived growth factor
Pf4	Platelet-factor 4
PFA	Paraformaldehyde
PGK	Phosphoglycerate kinase
PI3K	Phosphatidyl-inositol 3 kinase
PPE	Porcine pancreatic elastase
pRb	Retinoblastoma protein
PWV	Pulse wave velocity
q-PCR	(quantitative) Real-time polymerase chain reaction
RBC	Red blood cell
RECK	Reversion-inducing cysteine rich protein with Kazal motifs

ROS	Reactive oxygen species
Rpl-32	Ribosomal protein L-32
R-Smad	Receptor associated Smad
SAS	Supravalvular aortic stenosis
SDS	Sodium dodecyl sulphate
SFA	Superficial femoral artery
SLPI	Secretory leucocyte protease inhibitor
SMA	Smooth muscle actin
SMC	Smooth muscle cell
SNP	Single nucleotide polymorphism
SP1	Transcription factor SP1, also known as Specificity Protein 1
TAA(D)	Thoracic aortic aneurysm (+/- dissection)
TAFI	Thrombin activatable fibrinolysis inhibitor
TAK-1	TGF-β activated kinase 1
TBS	Tris-buffered saline
TF	Tissue factor
TG	Transglutaminase
TGF-β	Transforming growth factor-beta
TGFβR	TGF-β Receptor (types I and II)
TIMP	Tissue inhibitor of metalloproteinases
TKO	Triple knock-out (in relation to transgenic mice)
TNF-α	Tumour necrosis factor-alpha
TSP	Thrombospondin
tPA	Tissue plasminogen activator
tTG	Tissue transglutaminase (TG2)
uPA	Urokinase plasminogen activator
VEGF	Vascular endothelial growth factor
VEGFR	VEGF Receptor (types 1, 2 and 3)

VSMC	Vascular smooth muscle cell
WT	Wild-type

Appendix A: Murine ear code identification system

Mice within the CEU at the University of Leeds undergo ear notching to enable identification of individual animals housed within the same cage

● = site of ear notching

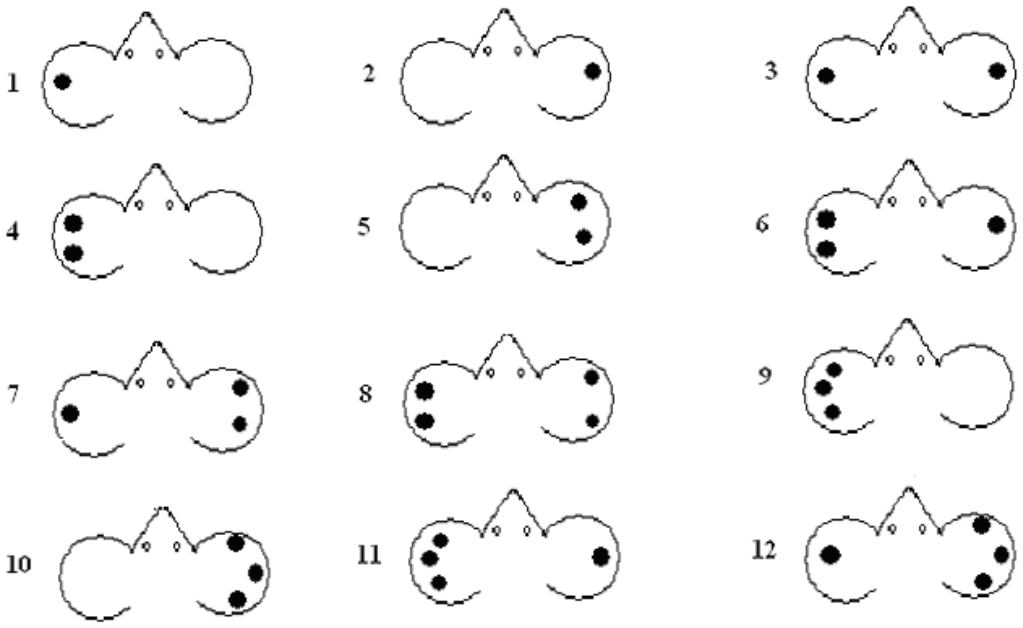

Appendix B: Standard Solutions

FXIII-A Activity Assay Reaction Mix	
Pre-diluted DTT (1mM stock) (Sigma, UK)	2.2mls
Pre-diluted Biotin (3mM stock) (Pierce, Thermofisher, UK)	2.2mls
100mM $CaCl_2$	2.2mls
Thrombin (250U/ml) (Calbiochem, UK)	87µl
TBS (pH 8.3)	13.113mls
Total Volume	19.8mls

10X Tris-buffered saline (TBS), pH 8.3	
Tris	96g
NaCl	163.6g

Make up to 2 litres with dH2O and adjust pH to 8.3. Dilute 1 in 10 to give 1X stock solution with 40mM Tris and 140mM NaCl

Appendix C: Wire myography solutions

Hanks pH7.4 (filter sterilise)

Component	Mw (g/mol)	Conc. (mM)	g/L	g/500ml	g/200ml
NaCl	58.44	137	8.0063	4.0031	1.6012
$NaH_2PO_4{}^{-}2H_2O$	156.01	0.34	0.05304	0.02652	0.01061
KCl	74.56	5.4	0.4026	0.2013	0.08052
KH_2PO_4	136.09	0.44	0.05988	0.02994	0.01198
Glucose	180.16	8	1.4413	0.7206	0.28824
HEPES	238.3	5	1.1915	0.5957	0.2383
$CaCl_2$	110.98	0.01	0.00111	0.00055	0.00022

Krebs pH7.4 (filter sterilise)

Component	Mw (g/mol)	Conc. (mM)	g/L	g/500ml	g/200ml
NaCl	58.44	125	7.3050	3.6525	1.461
KCl	74.56	3.8	0.2833	0.1416	0.05664
$NaHCO_3$	84.01	25	2.1002	1.0501	0.42004
$MgSO_4{}^{-}7H_2O$	246.47	1.5	0.3697	0.1849	0.07394
KH_2PO4	136.09	1.2	0.1633	0.08165	0.03266
Glucose	180.16	8	1.4412	0.7206	0.28824
$CaCl_2$	110.98	1.2	0.1332	0.0666	0.02664
EDTA	292.24	0.02	0.0058	0.0029	0.00117

60K Krebs pH7.4 (filter sterilise)

Component	Mw (g/mol)	Conc. (mM)	g/L	g/500ml	g/200ml
NaCl	58.44	68.8	4.02	2.01	0.804
KCl	74.56	60	4.47	2.23	0.892
$NaHCO_3$	84.01	25	2.1002	1.0501	0.42004
$MgSO_4{}^{-}7H_2O$	246.47	1.5	0.3697	0.1849	0.07394
KH_2PO4	136.09	1.2	0.1633	0.0817	0.03266
Glucose	180.16	8	1.4412	0.7206	0.28824
$CaCl_2$	110.98	1.2	0.1332	0.0666	0.02664
EDTA	292.24	0.02	0.00584	0.00292	0.00117

Appendix D: Histology – additional methodological detail

4% Paraformaldehyde (for tissue fixation)

Heat 800mls of distilled water to 40-45ºC, add 5 tablets of PBS and dissolve, keeping the solution at temperature. Add 40g of PFA and 6ml of NaOH and observe the solution clearing. Once clear, remove the solution from the hot plate and filter through filter paper. Allow the temperature to fall to approximately 22ºC and then top-up to 1litre final volume with water and adjust pH to 7.02-7.05 with HCl.

Histology processing

PFA-fixed samples were stored in 4% PFA for a minimum of 24 hours and then dehydrated using the Leica TP1020 tissue processing carousel (Leica Microsystems, UK) before paraffin embedding. All samples were subject to a 17 hour processing programme as detailed below.

1	70% Ethanol	30 minutes
2	70% Ethanol	30 minutes
3	70% Ethanol	30 minutes
4	90% Ethanol	1 hour
5	100% Ethanol	2 hours
6	100% Ethanol	2 hours
7	100% Ethanol	2 hours 30 minutes
8	Histoclear	30 minutes
9	Histoclear	1 hour 30 minutes
10	Histoclear	1 hour 30 minutes
11	Paraffin	1 hour 30 minutes
12	Paraffin	2 hours

Slide coating

All microscopy slides were pre-coated prior to use. Briefly, slides were immersed in 10% HCl in 100% ethanol for 1 minute, followed by 2 washes in distilled water, followed by immersion in 100% ethanol for 1 minute. The slides were then dried at

80ºC for 5 minutes before immersion in 2% TEPSA-acetone (for 20 seconds), 100% acetone (for 1 minute) and then 2 washes in distilled water. Slides were then dried overnight at 60ºC and then left to cool prior to storage.

Sirius Red solution

Add 0.5g Sirius Red (Sigma Aldrich, UK) to 500ml of saturated aqueous solution of picric acid (Sigma Aldrich, UK).

Aldehyde Fuchsin solution

Add 1.35g of pararosanilin (Sigma Aldrich, UK) to 250ml of 60% EtOH and mix well. Add 2.4ml of paraldehyde and 3.75ml of HCl, mix well and set aside for 3 days. Filter solution and use only if metallic sheen present. Solution should be used within 10 days.

Alizarin Red solution

Add 2g of Alizarin Red S (Sigma Aldrich, UK) to 100ml of distilled water and adjust pH to 4.1-4.3 with 10% ammonium hydroxide

Potassium Ferrocyanide solution

Add 12.5g of potassium hexacyanoferrate (II) 3-hydrate (PHF) (Sigma Aldrich, UK) to 250ml distilled water and stir. Add 237.5ml of distilled water to 12.5ml (40%) HCl and mix slowly; combine with PHF solution and leave overnight until solution has turned green.

Appendix E: Quantitative real time PCR primer sequences

Gene Transcript	Forward Primer Sequence	Reverse Primer Sequence
Elastin	AAAGCCTGGGAAAGTTCCTG	TACACCTGGAAGACCAACAC
Collagen I	ATGGATTCCCGTTCGAGTACG	TCAGCTGGATAGCGACATCG
Collagen III	CACCCTTCTTCATCCCACTCTTA	ACCAAGGTGGCTGCATCC
Vimentin	CGGAAAGTGGAATCCTTGCA	CACATCGATCTGGACATGCTGT
aSMA	ACTGGGACGACATGGAAAAG	GTTCAGTGGTGCCTCTGTCA
MMP2	CTGATAACCTGGATGCCGTCGT	TGCTTCCAAACTTCACGCTCTT
MMP9	GTCTCGGGAAGGCTCTGCTGTT	CTCTGGGGATCCACCTTCTGAG
FXIII-A	TGCTGGTGTCTTTAACACATTTTTAA	TGGGCCGAGAATGAATTGGT
TG1	TTCGCTACCCGTACCGTCA	CTTCATCCAGCAGTCGTT
TG2	ATTGGCAGTGTGGACATTC	TCGTGGGCGGAGTTGTA
TG3	AAGAAGCTGACCATGAGTGCTTT	TGCGCCCTTCGATTCATAG
TG4	CCCATCTATTTGACCATAACTTTGAA	GCGAGAAACACCCTTGATT
TG5	AGGCAGGATTCTGGAGAATATG	GGGCCACAGCCACAGCAGTAGAG
TG6	TCCGAGTCAATGTGAGCG	GTCTTCTGTCAGGTCTCCTTTGTA
TG7	ATGTGCACGGTAATGAGATGCT	TGTGTGCAGAATGGAAATTGG
CD163	ATGGGTGGACACAGAATGGTT	CAGGAGCGTTAGTGACAGCAG
tPA	CAACAGCGGCCTGGTACAA	CCCCATTGAAGCATCTTGGTT
uPA	GAAACCCTACAATGCCCACAGA	GACAAACTGCCTTAGGCCAATC
Perilipin	CTGTGTGCAATGCCTATGAGA	CTGGAGGGTATTGAAGAGCCG
PAI-1	ACGGTGATGCGATATAATGTAAACG	CATTCCTGAGAAACACAGCATTG
Fibrillin 1	CCTGTGCTATGATGGGTTCA	AGGTCCCACTAAGGCAGATG
Fibrillin 2	CCACTCCTATTGCTGCCCAG	TTGGGGCGGGAACAGAATC
MT-MMP	CCCAAGGCAGCAACTTCA	CAATGGCAGCTGAGAGTGAC
B-Actin	CGTGAAAAGATGACCCAGATCA	TCGTACGACCAGAGGCATACAG
HO-1	AACAAGCAGAACCCAGTCTATG	TGAGCAGGAAGGCGGTCTTA
MMP12	GCTAGAAGCAACTGGGCAAC	ACCGCTTCATCCATCTTGAC
TIMP1	GTGGGAAATGCCGCAGAT	GGGCATATCCACAGAGGCTTT
TIMP2	CCAGAAGAAGAGCCTGAACCA	GTCCATCCAGAGGCACTCATC
TGFB	CACCGGAGAGCCCTGGATA	TGTACAGCTGCCGCACACA
rpl32	AAAATTAAGCGAAACTGGCGG	TGTTGCTCCCATAACCGATG

References

ABDUL-HUSSIEN, H., HANEMAAIJER, R., KLEEMANN, R., VERHAAREN, B. F., VAN BOCKEL, J. H. & LINDEMAN, J. H. 2010. The pathophysiology of abdominal aortic aneurysm growth: corresponding and discordant inflammatory and proteolytic processes in abdominal aortic and popliteal artery aneurysms. *J Vasc Surg,* 51**,** 1479-87.

ADANY, R. & MUSZBEK, L. 1989. Immunohistochemical detection of factor XIII subunit a in histiocytes of human uterus. *Histochemistry,* 91**,** 169-74.

AESCHLIMANN, D., WETTERWALD, A., FLEISCH, H. & PAULSSON, M. 1993. Expression of tissue transglutaminase in skeletal tissues correlates with events of terminal differentiation of chondrocytes. *J Cell Biol,* 120**,** 1461-70.

AHN, J. S., KIM, M. K., HAHN, J. H., PARK, J. H., PARK, K. H., CHO, B. R., PARK, S. B. & KIM, D. J. 2008. Tissue transglutaminase-induced down-regulation of matrix metalloproteinase-9. *Biochem Biophys Res Commun,* 376**,** 743-7.

AILAWADI, G., ELIASON, J. L. & UPCHURCH, G. R., JR. 2003. Current concepts in the pathogenesis of abdominal aortic aneurysm. *J Vasc Surg,* 38**,** 584-8.

AIRHART, N., BROWNSTEIN, B. H., COBB, J. P., SCHIERDING, W., ARIF, B., ENNIS, T. L., THOMPSON, R. W. & CURCI, J. A. 2014. Smooth muscle cells from abdominal aortic aneurysms are unique and can independently and synergistically degrade insoluble elastin. *J Vasc Surg,* 60**,** 1033-41; discussion 1041-2.

AL JALLAD, H. F., NAKANO, Y., CHEN, J. L., MCMILLAN, E., LEFEBVRE, C. & KAARTINEN, M. T. 2006. Transglutaminase activity regulates osteoblast differentiation and matrix mineralization in MC3T3-E1 osteoblast cultures. *Matrix Biol.,* 25**,** 135-148.

ALAM, S. R., LEWIS, S. C., ZAMVAR, V., PESSOTTO, R., DWECK, M. R., KRISHAN, A., GOODMAN, K., OATEY, K., HARKESS, R., MILNE, L., THOMAS, S., MILLS, N. M., MOORE, C., SEMPLE, S., WIEDOW, O., STIRRAT, C., MIRSADRAEE, S., NEWBY, D. E. & HENRIKSEN, P. A. 2015. Perioperative elafin for ischaemia-reperfusion injury during coronary artery bypass graft surgery: a randomised-controlled trial. *Heart,* 101**,** 1639-45.

ALBIG, A. R., BECENTI, D. J., ROY, T. G. & SCHIEMANN, W. P. 2008. Microfibril-associate glycoprotein-2 (MAGP-2) promotes angiogenic cell sprouting by blocking notch signaling in endothelial cells. *Microvasc Res,* 76**,** 7-14.

ALEXANDER, J. J. 2004. The pathobiology of aortic aneurysms. *Journal of Surgical Research,* 117**,** 163-175.

ALI, M. A., CHOW, A. K., KANDASAMY, A. D., FAN, X., WEST, L. J., CRAWFORD, B. D., SIMMEN, T. & SCHULZ, R. 2012. Mechanisms of cytosolic targeting of matrix metalloproteinase-2. *J Cell Physiol,* 227**,** 3397-404.

ANIDJAR, S., SALZMANN, J. L., GENTRIC, D., LAGNEAU, P., CAMILLERI, J. P. & MICHEL, J. B. 1990. Elastase-induced experimental aneurysms in rats. *Circulation,* 82**,** 973-981.

ARONSON, D. 2003. Cross-linking of glycated collagen in the pathogenesis of arterial and myocardial stiffening of aging and diabetes. *J Hypertens,* 21**,** 3-12.

ASAHINA, T., KOBAYASHI, T., OKADA, Y., GOTO, J. & TERAO, T. 2000. Maternal blood coagulation factor XIII is associated with the development of cytotrophoblastic shell. *Placenta,* 21**,** 388-93.

AVERY, C. A., PEASE, R. J., SMITH, K., BOOTHBY, M., BUCKLEY, H. M., GRANT, P. J. & FISHWICK, C. W. 2015. (+/-) cis-Bisamido epoxides: A novel series of potent FXIII-A inhibitors. *Eur J Med Chem,* 98**,** 49-53.

AZEVEDO, A., PRADO, A. F., ANTONIO, R. C., ISSA, J. P. & GERLACH, R. F. 2014. Matrix metalloproteinases are involved in cardiovascular diseases. *Basic Clin Pharmacol Toxicol,* 115**,** 301-14.

BADARAU, E., COLLIGHAN, R. J. & GRIFFIN, M. 2013. Recent advances in the development of tissue transglutaminase (TG2) inhibitors. *Amino Acids,* 44**,** 119-27.

BAILEY, C. J. & FLATT, P. R. 1982. Hormonal control of glucose homeostasis during development and ageing in mice. *Metabolism,* 31**,** 238-46.

BAILEY, M. A., RODE, B., APPLEBY, H. L., GREEN, B. L., SALTOS, A. A., SIMPSON, C., BRUNS, A. R., GOSSAIN, R., PLANTE, J., BRIDGE, K. I., GRIFFIN, K. J., SHIRES, M., SIMMONS, K., PORTER, K. E., WHEATCROFT, S. B., YULDASHEVA, N. Y., PLEIN, S., FOSTER, R., SCOTT, D. J. A. & BEECH, D. J. Small molecule inhibitors of the Orai1 calcium channel to attenuate abdominal aortic aneurysm growth. *Nature Medicine - in preparation*

BAKKER, E. N., BUUS, C. L., SPAAN, J. A., PERREE, J., GANGA, A., ROLF, T. M., SOROP, O., BRAMSEN, L. H., MULVANY, M. J. & VANBAVEL, E. 2005. Small artery remodeling depends on tissue-type transglutaminase. *Circ.Res.,* 96**,** 119-126.

BAKKER, E. N., PISTEA, A., SPAAN, J. A., ROLF, T., DE VRIES, C. J., VAN ROOIJEN, N., CANDI, E. & VANBAVEL, E. 2006. Flow-dependent remodeling of small arteries in mice deficient for tissue-type transglutaminase: possible compensation by macrophage-derived factor XIII. *Circ Res,* 99**,** 86-92.

BAKKER, E. N., PISTEA, A. & VANBAVEL, E. 2008. Transglutaminases in vascular biology: relevance for vascular remodeling and atherosclerosis. *J.Vasc.Res.,* 45**,** 271-278.

BALKLAVA, Z., VERDERIO, E., COLLIGHAN, R., GROSS, S., ADAMS, J. & GRIFFIN, M. 2002. Analysis of tissue transglutaminase function in the migration of Swiss 3T3 fibroblasts: the active-state conformation of the enzyme does not affect cell motility but is important for its secretion. *J Biol Chem,* 277**,** 16567-75.

BARBER, R. D., HARMER, D. W., COLEMAN, R. A. & CLARK, B. J. 2005. GAPDH as a housekeeping gene: analysis of GAPDH mRNA expression in a panel of 72 human tissues. *Physiol Genomics,* 21**,** 389-95.

BARBIER, M., GROSS, M. S., AUBART, M., HANNA, N., KESSLER, K., GUO, D. C., TOSOLINI, L., HO-TIN-NOE, B., REGALADO, E., VARRET, M., ABIFADEL, M., MILLERON, O., ODENT, S., DUPUIS-GIROD, S., FAIVRE, L., EDOUARD, T., DULAC, Y., BUSA, T.,

GOUYA, L., MILEWICZ, D. M., JONDEAU, G. & BOILEAU, C. 2014. MFAP5 loss-of-function mutations underscore the involvement of matrix alteration in the pathogenesis of familial thoracic aortic aneurysms and dissections. *Am J Hum Genet,* 95**,** 736-43.

BARTEL, D. P. 2004. MicroRNAs: genomics, biogenesis, mechanism, and function. *Cell,* 116**,** 281-97.

BARTOLI, M. A., PARODI, F. E., CHU, J., PAGANO, M. B., MAO, D., BAXTER, B. T., BUCKLEY, C., ENNIS, T. L. & THOMPSON, R. W. 2006. Localized administration of doxycycline suppresses aortic dilatation in an experimental mouse model of abdominal aortic aneurysm. *Ann Vasc Surg,* 20**,** 228-36.

BASALYGA, D. M., SIMIONESCU, D. T., XIONG, W., BAXTER, B. T., STARCHER, B. C. & VYAVAHARE, N. R. 2004. Elastin degradation and calcification in an abdominal aorta injury model: role of matrix metalloproteinases. *Circulation,* 110**,** 3480-7.

BAUMGARTNER, W., GOLENHOFEN, N., WETH, A., HIIRAGI, T., SAINT, R., GRIFFIN, M. & DRENCKHAHN, D. 2004. Role of transglutaminase 1 in stabilisation of intercellular junctions of the vascular endothelium. *Histochem.Cell Biol.,* 122**,** 17-25.

BEAZLEY, K. E., BANYARD, D., LIMA, F., DEASEY, S. C., NURMINSKY, D. I., KONOPLYANNIKOV, M. & NURMINSKAYA, M. V. 2013. Transglutaminase inhibitors attenuate vascular calcification in a preclinical model. *Arterioscler Thromb Vasc Biol,* 33**,** 43-51.

BEAZLEY, K. E., DEASEY, S., LIMA, F. & NURMINSKAYA, M. V. 2012. Transglutaminase 2-mediated activation of beta-catenin signaling has a critical role in warfarin-induced vascular calcification. *Arterioscler Thromb Vasc Biol,* 32**,** 123-30.

BECK, E., DUCKERT, F. & ERNST, M. 1961. The influence of fibrin stabilizing factor on the growth of fibroblasts in vitro and wound healing. *Thromb Diath Haemorrh,* 6**,** 485-91.

BELKIN, A. M., ZEMSKOV, E. A., HANG, J., AKIMOV, S. S., SIKORA, S. & STRONGIN, A. Y. 2004. Cell-surface-associated tissue transglutaminase is a target of MMP-2 proteolysis. *Biochemistry,* 43**,** 11760-9.

BERGERS, G. & BENJAMIN, L. E. 2003. Tumorigenesis and the angiogenic switch. *Nat Rev Cancer,* 3**,** 401-10.

BERILLIS, P. 2013. The Role of Collagen in the Aorta's Structure. *The Open Circulation and Vascular Journal,* 6**,** 1-8.

BERNASSOLA, F., FEDERICI, M., CORAZZARI, M., TERRINONI, A., HRIBAL, M. L., DE, L., V, RANALLI, M., MASSA, O., SESTI, G., MCLEAN, W. H., CITRO, G., BARBETTI, F. & MELINO, G. 2002. Role of transglutaminase 2 in glucose tolerance: knockout mice studies and a putative mutation in a MODY patient. *FASEB J.,* 16**,** 1371-1378.

BHAMIDIPATI, C. M., MEHTA, G. S., LU, G., MOEHLE, C. W., BARBERY, C., DIMUSTO, P. D., LASER, A., KRON, I. L., UPCHURCH, G. R., JR. & AILAWADI, G. 2012. Development of a novel murine model of aortic aneurysms using peri-adventitial elastase. *Surgery,* 152**,** 238-46.

BIJLI, K. M., KANTER, B. G., MINHAJUDDIN, M., LEONARD, A., XU, L., FAZAL, F. & RAHMAN, A. 2014. Regulation of endothelial cell

inflammation and lung polymorphonuclear lymphocyte infiltration by transglutaminase 2. *Shock,* 42**,** 562-9.

BIROS, E., WALKER, P. J., NATAATMADJA, M., WEST, M. & GOLLEDGE, J. 2012. Downregulation of transforming growth factor, beta receptor 2 and Notch signaling pathway in human abdominal aortic aneurysm. *Atherosclerosis,* 221**,** 383-6.

BLACHER, J., ASMAR, R., DJANE, S., LONDON, G. M. & SAFAR, M. E. 1999. Aortic pulse wave velocity as a marker of cardiovascular risk in hypertensive patients. *Hypertension,* 33**,** 1111-7.

BOWN, M. J., JONES, G. T., HARRISON, S. C., WRIGHT, B. J., BUMPSTEAD, S., BAAS, A. F., GRETARSDOTTIR, S., BADGER, S. A., BRADLEY, D. T., BURNAND, K., CHILD, A. H., CLOUGH, R. E., COCKERILL, G., HAFEZ, H., SCOTT, D. J., FUTERS, S., JOHNSON, A., SOHRABI, S., SMITH, A., THOMPSON, M. M., VAN BOCKXMEER, F. M., WALTHAM, M., MATTHIASSON, S. E., THORLEIFSSON, G., THORSTEINSDOTTIR, U., BLANKENSTEIJN, J. D., TEIJINK, J. A., WIJMENGA, C., DE GRAAF, J., KIEMENEY, L. A., ASSIMES, T. L., MCPHERSON, R., CONSORTIUM, C. A., GLOBAL, B. C., CONSORTIUM, D., CONSORTIUM, V., FOLKERSEN, L., FRANCO-CERECEDA, A., PALMEN, J., SMITH, A. J., SYLVIUS, N., WILD, J. B., REFSTRUP, M., EDKINS, S., GWILLIAM, R., HUNT, S. E., POTTER, S., LINDHOLT, J. S., FRIKKE-SCHMIDT, R., TYBJAERG-HANSEN, A., HUGHES, A. E., GOLLEDGE, J., NORMAN, P. E., VAN RIJ, A., POWELL, J. T., ERIKSSON, P., STEFANSSON, K., THOMPSON, J. R., HUMPHRIES, S. E., SAYERS, R. D., DELOUKAS, P. & SAMANI, N. J. 2011. Abdominal aortic aneurysm is associated with a variant in low-density lipoprotein receptor-related protein 1. *Am J Hum Genet,* 89**,** 619-27.

BOWN, M. J., SUTTON, A. J., BELL, P. R. & SAYERS, R. D. 2002. A meta-analysis of 50 years of ruptured abdominal aortic aneurysm repair. *Br J Surg,* 89**,** 714-30.

BRADY, A. R., THOMPSON, S. G., FOWKES, F. G., GREENHALGH, R. M., POWELL, J. T. & PARTICIPANTS, U. K. S. A. T. 2004. Abdominal aortic aneurysm expansion: risk factors and time intervals for surveillance. *Circulation,* 110**,** 16-21.

BRESSAN, G. M., DAGA-GORDINI, D., COLOMBATTI, A., CASTELLANI, I., MARIGO, V. & VOLPIN, D. 1993. Emilin, a component of elastic fibers preferentially located at the elastin-microfibrils interface. *J Cell Biol,* 121**,** 201-12.

BREW, K. & NAGASE, H. 2010. The tissue inhibitors of metalloproteinases (TIMPs): an ancient family with structural and functional diversity. *Biochim Biophys Acta,* 1803**,** 55-71.

BROPHY, C. M., TILSON, J. E., BRAVERMAN, I. M. & TILSON, M. D. 1988. Age of onset, pattern of distribution, and histology of aneurysm development in a genetically predisposed mouse model. *J.Vasc.Surg.,* 8**,** 45-48.

BUNGAY, P. J., OWEN, R. A., COUTTS, I. C. & GRIFFIN, M. 1986. A role for transglutaminase in glucose-stimulated insulin release from the pancreatic beta-cell. *Biochem J,* 235**,** 269-78.

BUUS, N. H., VANBAVEL, E. & MULVANY, M. J. 1994. Differences in sensitivity of rat mesenteric small arteries to agonists when studied as ring preparations or as cannulated preparations. *Br J Pharmacol,* 112**,** 579-87.

CAMPA, J. S., GREENHALGH, R. M. & POWELL, J. T. 1987. Elastin degradation in abdominal aortic aneurysms. *Atherosclerosis,* 65**,** 13-21.

CAO, R. Y., AMAND, T., FORD, M. D., PIOMELLI, U. & FUNK, C. D. 2010. The Murine Angiotensin II-Induced Abdominal Aortic Aneurysm Model: Rupture Risk and Inflammatory Progression Patterns. *Front Pharmacol.,* 1**,** 9.

CARSTEN, C. G., III, CALTON, W. C., JOHANNING, J. M., ARMSTRONG, P. J., FRANKLIN, D. P., CAREY, D. J. & ELMORE, J. R. 2001. Elastase is not sufficient to induce experimental abdominal aortic aneurysms. *J.Vasc.Surg.,* 33**,** 1255-1262.

CASSIDY, A. J., VAN STEENSEL, M. A., STEIJLEN, P. M., VAN GEEL, M., VAN DER VELDEN, J., MORLEY, S. M., TERRINONI, A., MELINO, G., CANDI, E. & MCLEAN, W. H. 2005. A homozygous missense mutation in TGM5 abolishes epidermal transglutaminase 5 activity and causes acral peeling skin syndrome. *Am J Hum Genet,* 77**,** 909-17.

CHAMBERLAIN, C. M., ANG, L. S., BOIVIN, W. A., COOPER, D. M., WILLIAMS, S. J., ZHAO, H., HENDEL, A., FOLKESSON, M., SWEDENBORG, J., ALLARD, M. F., MCMANUS, B. M. & GRANVILLE, D. J. 2010. Perforin-independent extracellular granzyme B activity contributes to abdominal aortic aneurysm. *Am.J.Pathol.,* 176**,** 1038-1049.

CHAU, D. Y., COLLIGHAN, R. J., VERDERIO, E. A., ADDY, V. L. & GRIFFIN, M. 2005. The cellular response to transglutaminase-cross-linked collagen. *Biomaterials,* 26**,** 6518-29.

CHIOU, A. C., CHIU, B. & PEARCE, W. H. 2001. Murine aortic aneurysm produced by periarterial application of calcium chloride. *J.Surg.Res.,* 99**,** 371-376.

CHO, S. Y., CHOI, K., JEON, J. H., KIM, C. W., SHIN, D. M., LEE, J. B., LEE, S. E., KIM, C. S., PARK, J. S., JEONG, E. M., JANG, G. Y., SONG, K. Y. & KIM, I. G. 2010. Differential alternative splicing of human transglutaminase 4 in benign prostate hyperplasia and prostate cancer. *Exp Mol Med,* 42**,** 310-8.

CLARK, I. M., SWINGLER, T. E., SAMPIERI, C. L. & EDWARDS, D. R. 2008. The regulation of matrix metalloproteinases and their inhibitors. *Int J Biochem Cell Biol,* 40**,** 1362-78.

CLARK, J. M. & GLAGOV, S. 1985. Transmural organization of the arterial media. The lamellar unit revisited. *Arteriosclerosis,* 5**,** 19-34.

CLARKE, D. D., MYCEK, M. J., NEIDLE, A. & WAELSCH, H. 1959. The incorporation of amines into protein. *Archives of Biochemistry and Biophysics,* 79**,** 338-354.

COMBS, M. D., KNUTSEN, R. H., BROEKELMANN, T. J., TOENNIES, H. M., BRETT, T. J., MILLER, C. A., KOBER, D. L., CRAFT, C. S., ATKINSON, J. J., SHIPLEY, J. M., TRASK, B. C. & MECHAM, R. P. 2013. Microfibril-associated glycoprotein 2 (MAGP2) loss of function has pleiotropic effects in vivo. *J Biol Chem,* 288**,** 28869-80.

CORDELL, P. A., KILE, B. T., STANDEVEN, K. F., JOSEFSSON, E. C., PEASE, R. J. & GRANT, P. J. 2010. Association of coagulation factor XIII-A with Golgi proteins within monocyte-macrophages: implications for subcellular trafficking and secretion. *Blood,* 115**,** 2674-2681.

CORDELL, P. A., NEWELL, L. M., STANDEVEN, K. F., ADAMSON, P. J., SIMPSON, K. R., SMITH, K. A., JACKSON, C. L., GRANT, P. J. & PEASE, R. J. 2015. Normal Bone Deposition Occurs in Mice Deficient in Factor XIII-A and Transglutaminase 2. *Matrix Biol,* 43**,** 85-96.

CURCI, J. A. 2009. Digging in the "soil" of the aorta to understand the growth of abdominal aortic aneurysms. *Vascular,* 17 Suppl 1**,** S21-9.

CURCI, J. A., LIAO, S., HUFFMAN, M. D., SHAPIRO, S. D. & THOMPSON, R. W. 1998. Expression and localization of macrophage elastase (matrix metalloproteinase-12) in abdominal aortic aneurysms. *J Clin Invest,* 102**,** 1900-10.

CURCI, J. A. & THOMPSON, R. W. 1999. Variable induction of experimental abdominal aortic aneurysms with different preparations of porcine pancreatic elastase. *J.Vasc.Surg.,* 29**,** 385.

DAI, J., LOSY, F., GUINAULT, A. M., PAGES, C., ANEGON, I., DESGRANGES, P., BECQUEMIN, J. P. & ALLAIRE, E. 2005. Overexpression of transforming growth factor-beta1 stabilizes already-formed aortic aneurysms: a first approach to induction of functional healing by endovascular gene therapy. *Circulation,* 112**,** 1008-15.

DALE, M. A., RUHLMAN, M. K. & BAXTER, B. T. 2015. Inflammatory cell phenotypes in AAAs: their role and potential as targets for therapy. *Arterioscler Thromb Vasc Biol,* 35**,** 1746-55.

DANDACHI, N. G. & SHAPIRO, S. D. 2014. A protean protease: MMP-12 fights viruses as a protease and a transcription factor. *Nat Med,* 20**,** 470-2.

DANESHPOUR, N., COLLIGHAN, R., PERRIE, Y., LAMBERT, P., RATHBONE, D., LOWRY, D. & GRIFFIN, M. 2013. Indwelling catheters and medical implants with FXIIIa inhibitors: A novel approach to the treatment of catheter and medical device-related infections. *Eur J Pharm Biopharm,* 83**,** 106-13.

DANESHPOUR, N., GRIFFIN, M., COLLIGHAN, R. & PERRIE, Y. 2011. Targeted delivery of a novel group of site-directed transglutaminase inhibitors to the liver using liposomes: a new approach for the potential treatment of liver fibrosis. *J Drug Target,* 19**,** 624-31.

DARDIK, R., LOSCALZO, J. & INBAL, A. 2006. Factor XIII (FXIII) and angiogenesis. *J.Thromb.Haemost.,* 4**,** 19-25.

DAUGHERTY, A. & CASSIS, L. A. 2004. Mouse models of abdominal aortic aneurysms. *Arterioscler.Thromb.Vasc.Biol.,* 24**,** 429-434.

DAUGHERTY, A., CASSIS, L. A. & LU, H. 2011. Complex pathologies of angiotensin II-induced abdominal aortic aneurysms. *J.Zhejiang.Univ Sci.B,* 12**,** 624-628.

DAUGHERTY, A., MANNING, M. W. & CASSIS, L. A. 2000. Angiotensin II promotes atherosclerotic lesions and aneurysms in apolipoprotein E-deficient mice. *J.Clin.Invest,* 105**,** 1605-1612.

DAUGHERTY, A., RATERI, D. L., CHARO, I. F., OWENS, A. P., HOWATT, D. A. & CASSIS, L. A. 2010. Angiotensin II infusion promotes

ascending aortic aneurysms: attenuation by CCR2 deficiency in apoE-/- mice. *Clin Sci (Lond),* 118**,** 681-9.

DAVIES, G., ABLIN, R. J., MASON, M. D. & JIANG, W. G. 2007. Expression of the prostate transglutaminase (TGase-4) in prostate cancer cells and its impact on the invasiveness of prostate cancer. *J Exp Ther Oncol,* 6**,** 257-64.

DAVIS, F. M., RATERI, D. L. & DAUGHERTY, A. 2014. Mechanisms of aortic aneurysm formation: translating preclinical studies into clinical therapies. *Heart,* 100**,** 1498-505.

DE CRISTOFARO, T., AFFAITATI, A., CARIELLO, L., AVVEDIMENTO, E. V. & VARRONE, S. 1999. The length of polyglutamine tract, its level of expression, the rate of degradation, and the transglutaminase activity influence the formation of intracellular aggregates. *Biochem Biophys Res Commun,* 260**,** 150-8.

DE LAURENZI, V. & MELINO, G. 2001. Gene disruption of tissue transglutaminase. *Mol.Cell Biol.,* 21**,** 148-155.

DECOUX, A., LINDSEY, M. L., VILLARREAL, F., GARCIA, R. A. & SCHULZ, R. 2014. Myocardial matrix metalloproteinase-2: inside out and upside down. *J Mol Cell Cardiol,* 77**,** 64-72.

DOBRIN, P. B. 1989. Pathophysiology and pathogenesis of aortic aneurysms. Current concepts. *Surg.Clin.North Am.,* 69**,** 687-703.

DOBRIN, P. B. 2000. Elastin, Collagen and the Pathophysiology of Arterial Aneurysms. *Development of Aneurysms.* Georgetown, TX: Landes Bioscience.

DODD, B. R. & SPENCE, R. A. 2011. Doxycycline inhibition of abdominal aortic aneurysm growth: a systematic review of the literature. *Curr Vasc Pharmacol,* 9**,** 471-8.

DONG, Z., KUMAR, R., YANG, X. & FIDLER, I. J. 1997. Macrophage-derived metalloelastase is responsible for the generation of angiostatin in Lewis lung carcinoma. *Cell,* 88**,** 801-10.

DOUCET, A., BOUCHARD, D., JANELLE, M. F., BELLEMARE, A., GAGNE, S., TREMBLAY, G. M. & BOURBONNAIS, Y. 2007. Characterization of human pre-elafin mutants: full antipeptidase activity is essential to preserve lung tissue integrity in experimental emphysema. *Biochem J,* 405**,** 455-63.

DRANNIK, A. G., NAG, K., SALLENAVE, J. M. & ROSENTHAL, K. L. 2013. Antiviral activity of trappin-2 and elafin in vitro and in vivo against genital herpes. *J Virol,* 87**,** 7526-38.

DUA, M. M. & DALMAN, R. L. 2010. Hemodynamic influences on abdominal aortic aneurysm disease: Application of biomechanics to aneurysm pathophysiology. *Vascul Pharmacol,* 53**,** 11-21.

DUBBINK, H. J., DE WAAL, L., VAN HAPEREN, R., VERKAIK, N. S., TRAPMAN, J. & ROMIJN, J. C. 1998. The human prostate-specific transglutaminase gene (TGM4): genomic organization, tissue-specific expression, and promoter characterization. *Genomics,* 51**,** 434-44.

DUCHARME, A., FRANTZ, S., AIKAWA, M., RABKIN, E., LINDSEY, M., ROHDE, L. E., SCHOEN, F. J., KELLY, R. A., WERB, Z., LIBBY, P. & LEE, R. T. 2000. Targeted deletion of matrix metalloproteinase-9 attenuates left ventricular enlargement and collagen accumulation after experimental myocardial infarction. *J Clin Invest,* 106**,** 55-62.

DUFTNER, C., SEILER, R., DEJACO, C., FRAEDRICH, G. & SCHIRMER, M. 2006. Increasing evidence for immune-mediated processes and new therapeutic approaches in abdominal aortic aneurysms--a review. *Ann.N.Y.Acad.Sci.,* 1085**,** 331-338.

EARNSHAW, J. J., SHAW, E., WHYMAN, M. R., POSKITT, K. R. & HEATHER, B. P. 2004. Screening for abdominal aortic aneurysms in men. *BMJ,* 328**,** 1122-1124.

ECKERT, R. L., KAARTINEN, M. T., NURMINSKAYA, M., BELKIN, A. M., COLAK, G., JOHNSON, G. V. & MEHTA, K. 2014. Transglutaminase regulation of cell function. *Physiol Rev,* 94**,** 383-417.

ELIASON, J. L., HANNAWA, K. K., AILAWADI, G., SINHA, I., FORD, J. W., DEOGRACIAS, M. P., ROELOFS, K. J., WOODRUM, D. T., ENNIS, T. L., HENKE, P. K., STANLEY, J. C., THOMPSON, R. W. & UPCHURCH, G. R., JR. 2005a. Neutrophil depletion inhibits experimental abdominal aortic aneurysm formation. *Circulation,* 112**,** 232-40.

ELIASON, J. L., HANNAWA, K. K., AILAWADI, G., SINHA, I., FORD, J. W., DEOGRACIAS, M. P., ROELOFS, K. J., WOODRUM, D. T., ENNIS, T. L., HENKE, P. K., STANLEY, J. C., THOMPSON, R. W. & UPCHURCH, G. R., JR. 2005b. Neutrophil depletion inhibits experimental abdominal aortic aneurysm formation. *Circulation,* 112**,** 232-240.

ELMORE, J. R., OBMANN, M. A., KUIVANIEMI, H., TROMP, G., GERHARD, G. S., FRANKLIN, D. P., BODDY, A. M. & CAREY, D. J. 2009. Identification of a genetic variant associated with abdominal aortic aneurysms on chromosome 3p12.3 by genome wide association. *J Vasc Surg,* 49**,** 1525-31.

ENGLAND, P. H. 2013. *NHS Abdominal Aortic Aneurysm Screening Programme* [Online]. Available: http://aaa.screening.nhs.uk/aaastatistics.

ESKANDARI, M. K., VIJUNGCO, J. D., FLORES, A., BORENSZTAJN, J., SHIVELY, V. & PEARCE, W. H. 2005. Enhanced abdominal aortic aneurysm in TIMP-1-deficient mice. *J Surg Res,* 123**,** 289-93.

EXECUTIVE, H. H. A. S. 2015. *Statistics - Chronic Obstructive Pulmonary Disease* [Online]. Available: http://www.hse.gov.uk/Statistics/causdis/copd/index.htm [Accessed 17th February 2016].

FALASCA, L., IADEVAIA, V., CICCOSANTI, F., MELINO, G., SERAFINO, A. & PIACENTINI, M. 2005. Transglutaminase type II is a key element in the regulation of the anti-inflammatory response elicited by apoptotic cell engulfment. *J.Immunol.,* 174**,** 7330-7340.

FANJUL-FERNANDEZ, M., FOLGUERAS, A. R., CABRERA, S. & LOPEZ-OTIN, C. 2010. Matrix metalloproteinases: evolution, gene regulation and functional analysis in mouse models. *Biochim Biophys Acta,* 1803**,** 3-19.

FAURY, G., PEZET, M., KNUTSEN, R. H., BOYLE, W. A., HEXIMER, S. P., MCLEAN, S. E., MINKES, R. K., BLUMER, K. J., KOVACS, A., KELLY, D. P., LI, D. Y., STARCHER, B. & MECHAM, R. P. 2003. Developmental adaptation of the mouse cardiovascular system to elastin haploinsufficiency. *J Clin Invest,* 112**,** 1419-28.

FAVERMAN, L., MIKHAYLOVA, L., MALMQUIST, J. & NURMINSKAYA, M. 2008. Extracellular transglutaminase 2 activates beta-catenin signaling in calcifying vascular smooth muscle cells. *FEBS Lett,* 582**,** 1552-7.

FELDMAN, A. L., STETLER-STEVENSON, W. G., COSTOUROS, N. G., KNEZEVIC, V., BAIBAKOV, G., ALEXANDER, H. R., JR., LORANG, D., HEWITT, S. M., SEO, D. W., MILLER, M. S., O'CONNOR, S. & LIBUTTI, S. K. 2004. Modulation of tumor-host interactions, angiogenesis, and tumor growth by tissue inhibitor of metalloproteinase 2 via a novel mechanism. *Cancer Res,* 64**,** 4481-6.

FELLER, I. & WOODBURNE, R. T. 1961. Surgical anatomy of the abdominal aorta. *Ann Surg,* 154(6)Suppl**,** 239-52.

FESUS, L. 1999. Inducible gene expression in apoptosis. *Cell Death.Differ.,* 6**,** 1144-1145.

FESUS, L. & SZONDY, Z. 2005. Transglutaminase 2 in the balance of cell death and survival. *FEBS Lett.,* 579**,** 3297-3302.

FESUS, L., THOMAZY, V. & FALUS, A. 1987. Induction and activation of tissue transglutaminase during programmed cell death. *FEBS Lett.,* 224**,** 104-108.

FOK, J. Y. & MEHTA, K. 2007. Tissue transglutaminase induces the release of apoptosis inducing factor and results in apoptotic death of pancreatic cancer cells. *Apoptosis,* 12**,** 1455-63.

FONTAINE, V., JACOB, M. P., HOUARD, X., ROSSIGNOL, P., PLISSONNIER, D., ANGLES-CANO, E. & MICHEL, J. B. 2002. Involvement of the mural thrombus as a site of protease release and activation in human aortic aneurysms. *Am.J.Pathol.,* 161**,** 1701-1710.

FREESTONE, T., TURNER, R. J., COADY, A., HIGMAN, D. J., GREENHALGH, R. M. & POWELL, J. T. 1995. Inflammation and matrix metalloproteinases in the enlarging abdominal aortic aneurysm. *Arterioscler.Thromb.Vasc.Biol.,* 15**,** 1145-1151.

FREESTONE, T., TURNER, R. J., HIGMAN, D. J., LEVER, M. J. & POWELL, J. T. 1997. Influence of hypercholesterolemia and adventitial inflammation on the development of aortic aneurysm in rabbits. *Arterioscler.Thromb.Vasc.Biol.,* 17**,** 10-17.

GADOTH, A., NEFUSSY, B., BLEIBERG, M., KLEIN, T., ARTMAN, I. & DRORY, V. E. 2015. Transglutaminase 6 Antibodies in the Serum of Patients With Amyotrophic Lateral Sclerosis. *JAMA Neurol,* 72**,** 676-81.

GALIS, Z. S. & KHATRI, J. J. 2002. Matrix metalloproteinases in vascular remodeling and atherogenesis: the good, the bad, and the ugly. *Circ Res,* 90**,** 251-62.

GALLO, A., SAAD, A., ALI, R., DARDIK, A., TELLIDES, G. & GEIRSSON, A. 2012. Circulating interferon-gamma-inducible Cys-X-Cys chemokine receptor 3 ligands are elevated in humans with aortic aneurysms and Cys-X-Cys chemokine receptor 3 is necessary for aneurysm formation in mice. *J Thorac Cardiovasc Surg,* 143**,** 704-10.

GAUDRY, C. A., VERDERIO, E., AESCHLIMANN, D., COX, A., SMITH, C. & GRIFFIN, M. 1999. Cell surface localization of tissue transglutaminase is dependent on a fibronectin-binding site in its N-terminal beta-sandwich domain. *J.Biol.Chem.,* 274**,** 30707-30714.

GERTZ, S. D., KURGAN, A. & EISENBERG, D. 1988. Aneurysm of the rabbit common carotid artery induced by periarterial application of calcium chloride in vivo. *J.Clin.Invest,* 81**,** 649-656.

GLOVER, M. J., KIM, L. G., SWEETING, M. J., THOMPSON, S. G. & BUXTON, M. J. 2014. Cost-effectiveness of the National Health Service Abdominal Aortic Aneurysm Screening Programme in England. *Br J Surg,* 101**,** 976-82.

GO, A. S., MOZAFFARIAN, D., ROGER, V. L., BENJAMIN, E. J., BERRY, J. D., BORDEN, W. B., BRAVATA, D. M., DAI, S., FORD, E. S., FOX, C. S., FRANCO, S., FULLERTON, H. J., GILLESPIE, C., HAILPERN, S. M., HEIT, J. A., HOWARD, V. J., HUFFMAN, M. D., KISSELA, B. M., KITTNER, S. J., LACKLAND, D. T., LICHTMAN, J. H., LISABETH, L. D., MAGID, D., MARCUS, G. M., MARELLI, A., MATCHAR, D. B., MCGUIRE, D. K., MOHLER, E. R., MOY, C. S., MUSSOLINO, M. E., NICHOL, G., PAYNTER, N. P., SCHREINER, P. J., SORLIE, P. D., STEIN, J., TURAN, T. N., VIRANI, S. S., WONG, N. D., WOO, D., TURNER, M. B., AMERICAN HEART ASSOCIATION STATISTICS, C. & STROKE STATISTICS, S. 2013. Heart disease and stroke statistics--2013 update: a report from the American Heart Association. *Circulation,* 127**,** e6-e245.

GOLLEDGE, J., CULLEN, B., MORAN, C. & RUSH, C. 2010. Efficacy of simvastatin in reducing aortic dilatation in mouse models of abdominal aortic aneurysm. *Cardiovasc Drugs Ther,* 24**,** 373-8.

GOLLEDGE, J. & KUIVANIEMI, H. 2013. Genetics of abdominal aortic aneurysm. *Curr Opin Cardiol,* 28**,** 290-6.

GOODALL, S., CROWTHER, M., BELL, P. R. & THOMPSON, M. M. 2002. The association between venous structural alterations and biomechanical weakness in patients with abdominal aortic aneurysms. *J Vasc Surg,* 35**,** 937-42.

GOODALL, S., CROWTHER, M., HEMINGWAY, D. M., BELL, P. R. & THOMPSON, M. M. 2001. Ubiquitous elevation of matrix metalloproteinase-2 expression in the vasculature of patients with abdominal aneurysms. *Circulation,* 104**,** 304-9.

GRENARD, P., BRESSON-HADNI, S., EL ALAOUI, S., CHEVALLIER, M., VUITTON, D. A. & RICARD-BLUM, S. 2001. Transglutaminase-mediated cross-linking is involved in the stabilization of extracellular matrix in human liver fibrosis. *J Hepatol,* 35**,** 367-75.

GRETARSDOTTIR, S., BAAS, A. F., THORLEIFSSON, G., HOLM, H., DEN HEIJER, M., DE VRIES, J. P., KRANENDONK, S. E., ZEEBREGTS, C. J., VAN STERKENBURG, S. M., GEELKERKEN, R. H., VAN RIJ, A. M., WILLIAMS, M. J., BOLL, A. P., KOSTIC, J. P., JONASDOTTIR, A., JONASDOTTIR, A., WALTERS, G. B., MASSON, G., SULEM, P., SAEMUNDSDOTTIR, J., MOUY, M., MAGNUSSON, K. P., TROMP, G., ELMORE, J. R., SAKALIHASAN, N., LIMET, R., DEFRAIGNE, J. O., FERRELL, R. E., RONKAINEN, A., RUIGROK, Y. M., WIJMENGA, C., GROBBEE, D. E., SHAH, S. H., GRANGER, C. B., QUYYUMI, A. A., VACCARINO, V., PATEL, R. S., ZAFARI, A. M., LEVEY, A. I., AUSTIN, H., GIRELLI, D., PIGNATTI, P. F., OLIVIERI, O., MARTINELLI, N., MALERBA, G., TRABETTI, E., BECKER, L. C., BECKER, D. M., REILLY, M. P., RADER, D. J., MUELLER, T., DIEPLINGER, B., HALTMAYER, M., URBONAVICIUS, S.,

LINDBLAD, B., GOTTSATER, A., GAETANI, E., POLA, R., WELLS, P., RODGER, M., FORGIE, M., LANGLOIS, N., CORRAL, J., VICENTE, V., FONTCUBERTA, J., ESPANA, F., GRARUP, N., JORGENSEN, T., WITTE, D. R., HANSEN, T., PEDERSEN, O., ABEN, K. K., DE GRAAF, J., HOLEWIJN, S., FOLKERSEN, L., FRANCO-CERECEDA, A., ERIKSSON, P., COLLIER, D. A., STEFANSSON, H., STEINTHORSDOTTIR, V., RAFNAR, T., VALDIMARSSON, E. M., MAGNADOTTIR, H. B., SVEINBJORNSDOTTIR, S., OLAFSSON, I., MAGNUSSON, M. K., PALMASON, R., HARALDSDOTTIR, V., ANDERSEN, K., ONUNDARSON, P. T., THORGEIRSSON, G., KIEMENEY, L. A., POWELL, J. T., CAREY, D. J., KUIVANIEMI, H., LINDHOLT, J. S., JONES, G. T., KONG, A., BLANKENSTEIJN, J. D., MATTHIASSON, S. E., et al. 2010. Genome-wide association study identifies a sequence variant within the DAB2IP gene conferring susceptibility to abdominal aortic aneurysm. *Nat Genet,* 42**,** 692-7.

GRIFFIN, K., SIMPSON, K., BECKERS, C., BROWN, J., VACHER, J., OUWEHAND, W., ALEXANDER, W., PEASE, R. & GRANT, P. 2015. Use of a novel floxed mouse to characterise the cellular source of plasma coagulation FXIII-A. *Lancet,* 385 Suppl 1**,** S39.

GRIFFIN, M., CASADIO, R. & BERGAMINI, C. M. 2002. Transglutaminases: nature's biological glues. *Biochem.J.,* 368**,** 377-396.

GROSS, J. & LAPIERE, C. M. 1962. Collagenolytic activity in amphibian tissues: a tissue culture assay. *Proc Natl Acad Sci U S A,* 48**,** 1014-22.

GUNDEMIR, S., COLAK, G., TUCHOLSKI, J. & JOHNSON, G. V. 2012. Transglutaminase 2: a molecular Swiss army knife. *Biochim Biophys Acta,* 1823**,** 406-19.

GUO, Y. C., LIN, J. J., LIAO, Y. C., TSAI, P. C., LEE, Y. C. & SOONG, B. W. 2014. Spinocerebellar ataxia 35: novel mutations in TGM6 with clinical and genetic characterization. *Neurology,* 83**,** 1554-61.

GURJAR, M. V., SHARMA, R. V. & BHALLA, R. C. 1999. eNOS gene transfer inhibits smooth muscle cell migration and MMP-2 and MMP-9 activity. *Arterioscler Thromb Vasc Biol,* 19**,** 2871-7.

GUYOT, N., ZANI, M. L., MAUREL, M. C., DALLET-CHOISY, S. & MOREAU, T. 2005. Elafin and its precursor trappin-2 still inhibit neutrophil serine proteinases when they are covalently bound to extracellular matrix proteins by tissue transglutaminase. *Biochemistry,* 44**,** 15610-15618.

HADJIVASSILIOU, M., AESCHLIMANN, P., STRIGUN, A., SANDERS, D. S., WOODROOFE, N. & AESCHLIMANN, D. 2008a. Autoantibodies in gluten ataxia recognize a novel neuronal transglutaminase. *Ann Neurol,* 64**,** 332-43.

HADJIVASSILIOU, M., SANDERS, D. S., WOODROOFE, N., WILLIAMSON, C. & GRUNEWALD, R. A. 2008b. Gluten ataxia. *Cerebellum,* 7**,** 494-8.

HAFEZI-MOGHADAM, A., THOMAS, K. L. & WAGNER, D. D. 2007. ApoE deficiency leads to a progressive age-dependent blood-brain barrier leakage. *Am.J.Physiol Cell Physiol,* 292**,** C1256-C1262.

HALLORAN, B. G., DAVIS, V. A., MCMANUS, B. M., LYNCH, T. G. & BAXTER, B. T. 1995. Localization of aortic disease is associated with intrinsic differences in aortic structure. *J Surg Res,* 59**,** 17-22.

HANCE, K. A., TATARIA, M., ZIPORIN, S. J., LEE, J. K. & THOMPSON, R. W. 2002. Monocyte chemotactic activity in human abdominal aortic aneurysms: role of elastin degradation peptides and the 67-kD cell surface elastin receptor. *J Vasc Surg,* 35**,** 254-61.

HANNAWA, K. K., ELIASON, J. L., WOODRUM, D. T., PEARCE, C. G., ROELOFS, K. J., GRIGORYANTS, V., EAGLETON, M. J., HENKE, P. K., WAKEFIELD, T. W., MYERS, D. D., STANLEY, J. C. & UPCHURCH, G. R., JR. 2005. L-selectin-mediated neutrophil recruitment in experimental rodent aneurysm formation. *Circulation,* 112**,** 241-7.

HAROON, Z. A., WANNENBURG, T., GUPTA, M., GREENBERG, C. S., WALLIN, R. & SANE, D. C. 2001. Localization of tissue transglutaminase in human carotid and coronary artery atherosclerosis: implications for plaque stability and progression. *Lab Invest,* 81**,** 83-93.

HARRIS, L. K., SMITH, S. D., KEOGH, R. J., JONES, R. L., BAKER, P. N., KNOFLER, M., CARTWRIGHT, J. E., WHITLEY, G. S. & APLIN, J. D. 2010. Trophoblast- and vascular smooth muscle cell-derived MMP-12 mediates elastolysis during uterine spiral artery remodeling. *Am J Pathol,* 177**,** 2103-15.

HARRISON, S. C., SMITH, A. J., JONES, G. T., SWERDLOW, D. I., RAMPURI, R., BOWN, M. J., ANEURYSM, C., FOLKERSEN, L., BAAS, A. F., DE BORST, G. J., BLANKENSTEIJN, J. D., PRICE, J. F., VAN DER GRAAF, Y., MCLACHLAN, S., AGU, O., HOFMAN, A., UITTERLINDEN, A. G., FRANCO-CERECEDA, A., RUIGROK, Y. M., VAN'T HOF, F. N., POWELL, J. T., VAN RIJ, A. M., CASAS, J. P., ERIKSSON, P., HOLMES, M. V., ASSELBERGS, F. W., HINGORANI, A. D. & HUMPHRIES, S. E. 2013. Interleukin-6 receptor pathways in abdominal aortic aneurysm. *Eur Heart J,* 34**,** 3707-16.

HASEGAWA, G., SUWA, M., ICHIKAWA, Y., OHTSUKA, T., KUMAGAI, S., KIKUCHI, M., SATO, Y. & SAITO, Y. 2003. A novel function of tissue-type transglutaminase: protein disulphide isomerase. *Biochem.J.,* 373**,** 793-803.

HAUTAMAKI, R. D., KOBAYASHI, D. K., SENIOR, R. M. & SHAPIRO, S. D. 1997. Requirement for macrophage elastase for cigarette smoke-induced emphysema in mice. *Science,* 277**,** 2002-4.

HEIDT, T., COURTIES, G., DUTTA, P., SAGER, H. B., SEBAS, M., IWAMOTO, Y., SUN, Y., DA SILVA, N., PANIZZI, P., VAN DER LAAN, A. M., SWIRSKI, F. K., WEISSLEDER, R. & NAHRENDORF, M. 2014. Differential contribution of monocytes to heart macrophages in steady-state and after myocardial infarction. *Circ Res,* 115**,** 284-95.

HELGADOTTIR, A., THORLEIFSSON, G., MAGNUSSON, K. P., GRETARSDOTTIR, S., STEINTHORSDOTTIR, V., MANOLESCU, A., JONES, G. T., RINKEL, G. J., BLANKENSTEIJN, J. D., RONKAINEN, A., JAASKELAINEN, J. E., KYO, Y., LENK, G. M., SAKALIHASAN, N., KOSTULAS, K., GOTTSATER, A., FLEX, A., STEFANSSON, H., HANSEN, T., ANDERSEN, G., WEINSHEIMER, S., BORCH-JOHNSEN, K., JORGENSEN, T., SHAH, S. H.,

QUYYUMI, A. A., GRANGER, C. B., REILLY, M. P., AUSTIN, H., LEVEY, A. I., VACCARINO, V., PALSDOTTIR, E., WALTERS, G. B., JONSDOTTIR, T., SNORRADOTTIR, S., MAGNUSDOTTIR, D., GUDMUNDSSON, G., FERRELL, R. E., SVEINBJORNSDOTTIR, S., HERNESNIEMI, J., NIEMELA, M., LIMET, R., ANDERSEN, K., SIGURDSSON, G., BENEDIKTSSON, R., VERHOEVEN, E. L., TEIJINK, J. A., GROBBEE, D. E., RADER, D. J., COLLIER, D. A., PEDERSEN, O., POLA, R., HILLERT, J., LINDBLAD, B., VALDIMARSSON, E. M., MAGNADOTTIR, H. B., WIJMENGA, C., TROMP, G., BAAS, A. F., RUIGROK, Y. M., VAN RIJ, A. M., KUIVANIEMI, H., POWELL, J. T., MATTHIASSON, S. E., GULCHER, J. R., THORGEIRSSON, G., KONG, A., THORSTEINSDOTTIR, U. & STEFANSSON, K. 2008. The same sequence variant on 9p21 associates with myocardial infarction, abdominal aortic aneurysm and intracranial aneurysm. *Nat Genet,* 40**,** 217-24.

HOUGHTON, A. M. 2015. Matrix metalloproteinases in destructive lung disease. *Matrix Biol,* 44-46**,** 167-74.

HOUGHTON, A. M., HARTZELL, W. O., ROBBINS, C. S., GOMIS-RUTH, F. X. & SHAPIRO, S. D. 2009. Macrophage elastase kills bacteria within murine macrophages. *Nature,* 460**,** 637-41.

HRUZ, T., WYSS, M., DOCQUIER, M., PFAFFL, M. W., MASANETZ, S., BORGHI, L., VERBRUGGHE, P., KALAYDJIEVA, L., BLEULER, S., LAULE, O., DESCOMBES, P., GRUISSEM, W. & ZIMMERMANN, P. 2011. RefGenes: identification of reliable and condition specific reference genes for RT-qPCR data normalization. *BMC.Genomics,* 12**,** 156.

HUANG, L., HAYLOR, J. L., HAU, Z., JONES, R. A., VICKERS, M. E., WAGNER, B., GRIFFIN, M., SAINT, R. E., COUTTS, I. G., EL NAHAS, A. M. & JOHNSON, T. S. 2009. Transglutaminase inhibition ameliorates experimental diabetic nephropathy. *Kidney Int,* 76**,** 383-94.

HUANG, S. & PANG, L. 2012. Comparing statistical methods for quantifying drug sensitivity based on in vitro dose-response assays. *Assay Drug Dev Technol,* 10**,** 88-96.

IISMAA, S. E., APLIN, M., HOLMAN, S., YIU, T. W., JACKSON, K., BURCHFIELD, J. G., MITCHELL, C. J., O'REILLY, L., DAVENPORT, A., CANTLEY, J., SCHMITZ-PEIFFER, C., BIDEN, T. J., COONEY, G. J. & GRAHAM, R. M. 2013. Glucose homeostasis in mice is transglutaminase 2 independent. *PLoS.ONE.,* 8**,** e63346.

IISMAA, S. E., MEARNS, B. M., LORAND, L. & GRAHAM, R. M. 2009. Transglutaminases and disease: lessons from genetically engineered mouse models and inherited disorders. *Physiol Rev.,* 89**,** 991-1023.

INBAL, A., LUBETSKY, A., KRAPP, T., CASTEL, D., SHAISH, A., DICKNEITTE, G., MODIS, L., MUSZBEK, L. & INBAL, A. 2005. Impaired wound healing in factor XIII deficient mice. *Thromb.Haemost.,* 94**,** 432-437.

ITOH, M., KAWAMOTO, T., TATSUKAWA, H., KOJIMA, S., YAMANISHI, K. & HITOMI, K. 2011. In situ detection of active transglutaminases for keratinocyte type (TGase 1) and tissue type (TGase 2) using fluorescence-labeled highly reactive substrate peptides. *J Histochem Cytochem,* 59**,** 180-7.

ITOH, T., IKEDA, T., GOMI, H., NAKAO, S., SUZUKI, T. & ITOHARA, S. 1997. Unaltered secretion of beta-amyloid precursor protein in gelatinase A (matrix metalloproteinase 2)-deficient mice. *J Biol Chem,* 272**,** 22389-92.

IWAKI, T., NAGAHASHI, K., KOBAYASHI, T., UMEMURA, K., TERAO, T. & KANAYAMA, N. 2012. The first report of uncontrollable subchorionic and retroplacental haemorrhage inducing preterm labour in complete PAI-1 deficiency in a human. *Thromb Res,* 129**,** e161-3.

IWAKI, T., TANAKA, A., MIYAWAKI, Y., SUZUKI, A., KOBAYASHI, T., TAKAMATSU, J., MATSUSHITA, T., UMEMURA, K., URANO, T., KOJIMA, T., TERAO, T. & KANAYAMA, N. 2011. Life-threatening hemorrhage and prolonged wound healing are remarkable phenotypes manifested by complete plasminogen activator inhibitor-1 deficiency in humans. *J Thromb Haemost,* 9**,** 1200-6.

JANG, T. H., LEE, D. S., CHOI, K., JEONG, E. M., KIM, I. G., KIM, Y. W., CHUN, J. N., JEON, J. H. & PARK, H. H. 2014. Crystal structure of transglutaminase 2 with GTP complex and amino acid sequence evidence of evolution of GTP binding site. *PLoS One,* 9**,** e107005.

JIANG, W. G., ABLIN, R., DOUGLAS-JONES, A. & MANSEL, R. E. 2003. Expression of transglutaminases in human breast cancer and their possible clinical significance. *Oncol Rep,* 10**,** 2039-44.

JIANG, W. G. & ABLIN, R. J. 2011. Prostate transglutaminase: a unique transglutaminase and its role in prostate cancer. *Biomark Med,* 5**,** 285-91.

JIN, X., STAMNAES, J., KLOCK, C., DIRAIMONDO, T. R., SOLLID, L. M. & KHOSLA, C. 2011. Activation of extracellular transglutaminase 2 by thioredoxin. *J Biol Chem,* 286**,** 37866-73.

JOBE, S. M., LEO, L., EASTVOLD, J. S., DICKNEITE, G., RATLIFF, T. L., LENTZ, S. R. & DI, P. J. 2005. Role of FcRgamma and factor XIIIA in coated platelet formation. *Blood,* 106**,** 4146-4151.

JOHNSON, C. & GALIS, Z. S. 2004. Matrix metalloproteinase-2 and -9 differentially regulate smooth muscle cell migration and cell-mediated collagen organization. *Arterioscler Thromb Vasc Biol,* 24**,** 54-60.

JOHNSON, C., SUNG, H. J., LESSNER, S. M., FINI, M. E. & GALIS, Z. S. 2004. Matrix metalloproteinase-9 is required for adequate angiogenic revascularization of ischemic tissues: potential role in capillary branching. *Circ Res,* 94**,** 262-8.

JOHNSON, G. V., COX, T. M., LOCKHART, J. P., ZINNERMAN, M. D., MILLER, M. L. & POWERS, R. E. 1997. Transglutaminase activity is increased in Alzheimer's disease brain. *Brain Res,* 751**,** 323-9.

JOHNSON, K., HASHIMOTO, S., LOTZ, M., PRITZKER, K. & TERKELTAUB, R. 2001. Interleukin-1 induces pro-mineralizing activity of cartilage tissue transglutaminase and factor XIIIa. *Am J Pathol,* 159**,** 149-63.

JOHNSON, K. A., POLEWSKI, M. & TERKELTAUB, R. A. 2008a. Transglutaminase 2 is central to induction of the arterial calcification program by smooth muscle cells. *Circ.Res.,* 102**,** 529-537.

JOHNSON, K. A., ROSE, D. M. & TERKELTAUB, R. A. 2008b. Factor XIIIA mobilizes transglutaminase 2 to induce chondrocyte hypertrophic differentiation. *J Cell Sci,* 121**,** 2256-64.

JOHNSON, K. A., VAN ETTEN, D., NANDA, N., GRAHAM, R. M. & TERKELTAUB, R. A. 2003a. Distinct transglutaminase 2-independent and transglutaminase 2-dependent pathways mediate articular chondrocyte hypertrophy. *J Biol Chem,* 278**,** 18824-32.

JOHNSON, T. S., EL-KORAIE, A. F., SKILL, N. J., BADDOUR, N. M., EL NAHAS, A. M., NJLOMA, M., ADAM, A. G. & GRIFFIN, M. 2003b. Tissue transglutaminase and the progression of human renal scarring. *J Am Soc Nephrol,* 14**,** 2052-62.

JOHNSTON, W. F., SALMON, M., SU, G., LU, G., STONE, M. L., ZHAO, Y., OWENS, G. K., UPCHURCH, G. R., JR. & AILAWADI, G. 2013. Genetic and pharmacologic disruption of interleukin-1beta signaling inhibits experimental aortic aneurysm formation. *Arterioscler Thromb Vasc Biol,* 33**,** 294-304.

JOURQUIN, J., TREMBLAY, E., BERNARD, A., CHARTON, G., CHAILLAN, F. A., MARCHETTI, E., ROMAN, F. S., SOLOWAY, P. D., DIVE, V., YIOTAKIS, A., KHRESTCHATISKY, M. & RIVERA, S. 2005. Tissue inhibitor of metalloproteinases-1 (TIMP-1) modulates neuronal death, axonal plasticity, and learning and memory. *Eur J Neurosci,* 22**,** 2569-78.

JUNN, E., RONCHETTI, R. D., QUEZADO, M. M., KIM, S. Y. & MOURADIAN, M. M. 2003. Tissue transglutaminase-induced aggregation of alpha-synuclein: Implications for Lewy body formation in Parkinson's disease and dementia with Lewy bodies. *Proc Natl Acad Sci U S A,* 100**,** 2047-52.

JUVONEN, J., SURCEL, H. M., SATTA, J., TEPPO, A. M., BLOIGU, A., SYRJALA, H., AIRAKSINEN, J., LEINONEN, M., SAIKKU, P. & JUVONEN, T. 1997. Elevated circulating levels of inflammatory cytokines in patients with abdominal aortic aneurysm. *Arterioscler Thromb Vasc Biol,* 17**,** 2843-7.

KAARTINEN, V. & WARBURTON, D. 2003. Fibrillin controls TGF-beta activation. *Nat Genet,* 33**,** 331-2.

KARNIK, S. K., BROOKE, B. S., BAYES-GENIS, A., SORENSEN, L., WYTHE, J. D., SCHWARTZ, R. S., KEATING, M. T. & LI, D. Y. 2003. A critical role for elastin signaling in vascular morphogenesis and disease. *Development,* 130**,** 411-23.

KARPUJ, M. V., BECHER, M. W., SPRINGER, J. E., CHABAS, D., YOUSSEF, S., PEDOTTI, R., MITCHELL, D. & STEINMAN, L. 2002. Prolonged survival and decreased abnormal movements in transgenic model of Huntington disease, with administration of the transglutaminase inhibitor cystamine. *Nat Med,* 8**,** 143-9.

KEELING, W. B., ARMSTRONG, P. A., STONE, P. A., BANDYK, D. F. & SHAMES, M. L. 2005. An overview of matrix metalloproteinases in the pathogenesis and treatment of abdominal aortic aneurysms. *Vasc Endovascular Surg,* 39**,** 457-64.

KEILLOR, J. W., APPERLEY, K. Y. & AKBAR, A. 2015. Inhibitors of tissue transglutaminase. *Trends Pharmacol Sci,* 36**,** 32-40.

KENT, K. C., ZWOLAK, R. M., EGOROVA, N. N., RILES, T. S., MANGANARO, A., MOSKOWITZ, A. J., GELIJNS, A. C. & GRECO, G. 2010. Analysis of risk factors for abdominal aortic aneurysm in a cohort of more than 3 million individuals. *J Vasc Surg,* 52**,** 539-48.

KIM, C. W., KUMAR, S., SON, D. J., JANG, I. H., GRIENDLING, K. K. & JO, H. 2014. Prevention of abdominal aortic aneurysm by anti-microRNA-712 or anti-microRNA-205 in angiotensin II-infused mice. *Arterioscler Thromb Vasc Biol,* 34**,** 1412-21.

KIM, D. S., PARK, S. S., NAM, B. H., KIM, I. H. & KIM, S. Y. 2006. Reversal of drug resistance in breast cancer cells by transglutaminase 2 inhibition and nuclear factor-kappaB inactivation. *Cancer Res,* 66**,** 10936-43.

KIM, S. Y., GRANT, P., LEE, J. H., PANT, H. C. & STEINERT, P. M. 1999. Differential expression of multiple transglutaminases in human brain. Increased expression and cross-linking by transglutaminases 1 and 2 in Alzheimer's disease. *J Biol Chem,* 274**,** 30715-21.

KNOX, J. B., SUKHOVA, G. K., WHITTEMORE, A. D. & LIBBY, P. 1997. Evidence for altered balance between matrix metalloproteinases and their inhibitors in human aortic diseases. *Circulation,* 95**,** 205-212.

KOMAROMI, I., BAGOLY, Z. & MUSZBEK, L. 2011. Factor XIII: novel structural and functional aspects. *J Thromb Haemost,* 9**,** 9-20.

KORSGREN, C., LAWLER, J., LAMBERT, S., SPEICHER, D. & COHEN, C. M. 1990. Complete amino acid sequence and homologies of human erythrocyte membrane protein band 4.2. *Proc Natl Acad Sci U S A,* 87**,** 613-7.

KOSEKI-KUNO, S., YAMAKAWA, M., DICKNEITE, G. & ICHINOSE, A. 2003. Factor XIII A subunit-deficient mice developed severe uterine bleeding events and subsequent spontaneous miscarriages. *Blood,* 102**,** 4410-4412.

KOSTKA, G., GILTAY, R., BLOCH, W., ADDICKS, K., TIMPL, R., FASSLER, R. & CHU, M. L. 2001. Perinatal lethality and endothelial cell abnormalities in several vessel compartments of fibulin-1-deficient mice. *Mol Cell Biol,* 21**,** 7025-34.

KOTSAKIS, P. & GRIFFIN, M. 2007. Tissue transglutaminase in tumour progression: friend or foe? *Amino.Acids,* 33**,** 373-384.

KRISHNA, S. M., DEAR, A. E., NORMAN, P. E. & GOLLEDGE, J. 2010. Genetic and epigenetic mechanisms and their possible role in abdominal aortic aneurysm. *Atherosclerosis,* 212**,** 16-29.

KUZUYA, M., NAKAMURA, K., SASAKI, T., CHENG, X. W., ITOHARA, S. & IGUCHI, A. 2006. Effect of MMP-2 deficiency on atherosclerotic lesion formation in apoE-deficient mice. *Arterioscler Thromb Vasc Biol,* 26**,** 1120-5.

LACOLLEY, P., REGNAULT, V., NICOLETTI, A., LI, Z. & MICHEL, J. B. 2012. The vascular smooth muscle cell in arterial pathology: a cell that can take on multiple roles. *Cardiovasc Res,* 95**,** 194-204.

LAFLEUR, M. A., TESTER, A. M. & THOMPSON, E. W. 2003. Selective involvement of TIMP-2 in the second activational cleavage of pro-MMP-2: refinement of the pro-MMP-2 activation mechanism. *FEBS Lett,* 553**,** 457-63.

LAHAV, J., KARNIEL, E., BAGOLY, Z., SHEPTOVITSKY, V., DARDIK, R. & INBAL, A. 2009. Coagulation factor XIII serves as protein disulfide isomerase. *Thromb Haemost,* 101**,** 840-4.

LAI, T. S., HAUSLADEN, A., SLAUGHTER, T. F., EU, J. P., STAMLER, J. S. & GREENBERG, C. S. 2001. Calcium regulates S-nitrosylation,

denitrosylation, and activity of tissue transglutaminase. *Biochemistry,* 40**,** 4904-10.

LAI, T. S., LIU, Y., LI, W. & GREENBERG, C. S. 2007. Identification of two GTP-independent alternatively spliced forms of tissue transglutaminase in human leukocytes, vascular smooth muscle, and endothelial cells. *FASEB J,* 21**,** 4131-43.

LAM, C. F., CROATT, A. J., RICHARDSON, D. M., NATH, K. A. & KATUSIC, Z. S. 2005. Heart failure increases protein expression and enzymatic activity of heme oxygenase-1 in the lung. *Cardiovasc Res,* 65**,** 203-10.

LAMBERT, R. 2007. Breeding Strategies for Maintaining Colonies of Laboratory Mice. Jackson Laboratories.

LARSSON, E., GRANATH, F., SWEDENBORG, J. & HULTGREN, R. 2009. A population-based case-control study of the familial risk of abdominal aortic aneurysm. *J Vasc Surg,* 49**,** 47-50; discussion 51.

LASKOWITZ, D. T., LEE, D. M., SCHMECHEL, D. & STAATS, H. F. 2000. Altered immune responses in apolipoprotein E-deficient mice. *J.Lipid Res.,* 41**,** 613-620.

LAUER, P., METZNER, H. J., ZETTLMEISSL, G., LI, M., SMITH, A. G., LATHE, R. & DICKNEITE, G. 2002. Targeted Inactivation of the Mouse Locus Encoding Coagulation Factor XIII-A: Hemostatic Abnormalities in Mutant Mice and Characterization of the Coagulation Deficit. *Thromb.Haemost.,* 88**,** 967-974.

LAVINE, R. L., CHICK, W. L., LIKE, A. A. & MAKDISI, T. W. 1971. Glucose tolerance and insulin secretion in neonatal and adult mice. *Diabetes,* 20**,** 134-9.

LEDERLE, F. A. 2012. The strange relationship between diabetes and abdominal aortic aneurysm. *Eur J Vasc Endovasc Surg,* 43**,** 254-6.

LEDERLE, F. A., NELSON, D. B. & JOSEPH, A. M. 2003. Smokers' relative risk for aortic aneurysm compared with other smoking-related diseases: a systematic review. *J Vasc Surg,* 38**,** 329-34.

LEE, J., KIM, Y. S., CHOI, D. H., BANG, M. S., HAN, T. R., JOH, T. H. & KIM, S. Y. 2004. Transglutaminase 2 induces nuclear factor-kappaB activation via a novel pathway in BV-2 microglia. *J Biol Chem,* 279**,** 53725-35.

LEGGATE, J., ALLAIN, R., ISAAC, L. & BLAIS, B. W. 2006. Microplate fluorescence assay for the quantification of double stranded DNA using SYBR Green I dye. *Biotechnol Lett,* 28**,** 1587-94.

LEIDY, E. M., STERN, A. M., FRIEDMAN, P. A. & BUSH, L. R. 1990. Enhanced thrombolysis by a factor XIIIa inhibitor in a rabbit model of femoral artery thrombosis. *Thromb Res,* 59**,** 15-26.

LEITER, E. H. 2002. Mice with targeted gene disruptions or gene insertions for diabetes research: problems, pitfalls, and potential solutions. *Diabetologia,* 45**,** 296-308.

LI, D. Y., BROOKE, B., DAVIS, E. C., MECHAM, R. P., SORENSEN, L. K., BOAK, B. B., EICHWALD, E. & KEATING, M. T. 1998a. Elastin is an essential determinant of arterial morphogenesis. *Nature,* 393**,** 276-80.

LI, D. Y., FAURY, G., TAYLOR, D. G., DAVIS, E. C., BOYLE, W. A., MECHAM, R. P., STENZEL, P., BOAK, B. & KEATING, M. T. 1998b. Novel arterial pathology in mice and humans hemizygous for elastin. *J.Clin.Invest,* 102**,** 1783-1787.

LI, Z. & RANA, T. M. 2014. Therapeutic targeting of microRNAs: current status and future challenges. *Nat Rev Drug Discov,* 13**,** 622-38.

LIANG, J., LIU, E., YU, Y., KITAJIMA, S., KOIKE, T., JIN, Y., MORIMOTO, M., HATAKEYAMA, K., ASADA, Y., WATANABE, T., SASAGURI, Y., WATANABE, S. & FAN, J. 2006. Macrophage metalloelastase accelerates the progression of atherosclerosis in transgenic rabbits. *Circulation,* 113**,** 1993-2001.

LIN, C. Y., TSAI, P. H., KANDASWAMI, C. C., CHANG, G. D., CHENG, C. H., HUANG, C. J., LEE, P. P., HWANG, J. J. & LEE, M. T. 2011. Role of tissue transglutaminase 2 in the acquisition of a mesenchymal-like phenotype in highly invasive A431 tumor cells. *Mol Cancer,* 10**,** 87.

LINDEMAN, J. H., RABELINK, T. J. & VAN BOCKEL, J. H. 2011. Immunosuppression and the abdominal aortic aneurysm: Doctor Jekyll or Mister Hyde? *Circulation,* 124**,** e463-5.

LIU, S. L., BAE, Y. H., YU, C., MONSLOW, J., HAWTHORNE, E. A., CASTAGNINO, P., BRANCHETTI, E., FERRARI, G., DAMRAUER, S. M., PURE, E. & ASSOIAN, R. K. 2015. Matrix metalloproteinase-12 is an essential mediator of acute and chronic arterial stiffening. *Sci Rep,* 5**,** 17189.

LONGO, G. M., BUDA, S. J., FIOTTA, N., XIONG, W., GRIENER, T., SHAPIRO, S. & BAXTER, B. T. 2005. MMP-12 has a role in abdominal aortic aneurysms in mice. *Surgery,* 137**,** 457-62.

LONGO, G. M., XIONG, W., GREINER, T. C., ZHAO, Y., FIOTTI, N. & BAXTER, B. T. 2002. Matrix metalloproteinases 2 and 9 work in concert to produce aortic aneurysms. *J.Clin.Invest,* 110**,** 625-632.

LOPEZ-CANDALES, A., HOLMES, D. R., LIAO, S., SCOTT, M. J., WICKLINE, S. A. & THOMPSON, R. W. 1997. Decreased vascular smooth muscle cell density in medial degeneration of human abdominal aortic aneurysms. *Am J Pathol,* 150**,** 993-1007.

LORAND, L. 2000a. Sol Sherry Lecture in Thrombosis : research on clot stabilization provides clues for improving thrombolytic therapies. *Arterioscler Thromb Vasc Biol,* 20**,** 2-9.

LORAND, L. 2000b. Sol Sherry Lecture in Thrombosis : Research on Clot Stabilization Provides Clues for Improving Thrombolytic Therapies. *Arteriosclerosis, Thrombosis, and Vascular Biology,* 20**,** 2-9.

LORAND, L. & GRAHAM, R. M. 2003. Transglutaminases: crosslinking enzymes with pleiotropic functions. *Nat.Rev.Mol.Cell Biol.,* 4**,** 140-156.

LUNDEBERG, E., VAN DER DOES, A. M., KENNE, E., SOEHNLEIN, O. & LINDBOM, L. 2015. Assessing large-vessel endothelial permeability using near-infrared fluorescence imaging--brief report. *Arterioscler Thromb Vasc Biol,* 35**,** 783-6.

LUTTUN, A., LUTGENS, E., MANDERVELD, A., MARIS, K., COLLEN, D., CARMELIET, P. & MOONS, L. 2004. Loss of matrix metalloproteinase-9 or matrix metalloproteinase-12 protects apolipoprotein E-deficient mice against atherosclerotic media destruction but differentially affects plaque growth. *Circulation,* 109**,** 1408-14.

MAEGDEFESSEL, L., AZUMA, J., TOH, R., DENG, A., MERK, D. R., RAIESDANA, A., LEEPER, N. J., RAAZ, U., SCHOELMERICH, A. M., MCCONNELL, M. V., DALMAN, R. L., SPIN, J. M. & TSAO, P. S.

2012a. MicroRNA-21 blocks abdominal aortic aneurysm development and nicotine-augmented expansion. *Sci Transl Med,* 4**,** 122ra22.

MAEGDEFESSEL, L., AZUMA, J., TOH, R., MERK, D. R., DENG, A., CHIN, J. T., RAAZ, U., SCHOELMERICH, A. M., RAIESDANA, A., LEEPER, N. J., MCCONNELL, M. V., DALMAN, R. L., SPIN, J. M. & TSAO, P. S. 2012b. Inhibition of microRNA-29b reduces murine abdominal aortic aneurysm development. *J Clin Invest,* 122**,** 497-506.

MAEGDEFESSEL, L., SPIN, J. M., ADAM, M., RAAZ, U., TOH, R., NAKAGAMI, F. & TSAO, P. S. 2013. Micromanaging abdominal aortic aneurysms. *Int J Mol Sci,* 14**,** 14374-94.

MAIER, A., GEE, M. W., REEPS, C., ECKSTEIN, H. H. & WALL, W. A. 2010. Impact of calcifications on patient-specific wall stress analysis of abdominal aortic aneurysms. *Biomech.Model.Mechanobiol.,* 9**,** 511-521.

MAKI, J. M., RASANEN, J., TIKKANEN, H., SORMUNEN, R., MAKIKALLIO, K., KIVIRIKKO, K. I. & SOININEN, R. 2002. Inactivation of the lysyl oxidase gene Lox leads to aortic aneurysms, cardiovascular dysfunction, and perinatal death in mice. *Circulation,* 106**,** 2503-2509.

MANSFIELD, M. W., KOHLER, H. P., ARIENS, R. A., MCCORMACK, L. J. & GRANT, P. J. 2000. Circulating levels of coagulation factor XIII in subjects with type 2 diabetes and in their first-degree relatives. *Diabetes Care,* 23**,** 703-5.

MANSUY-AUBERT, V., ZHOU, Q. L., XIE, X., GONG, Z., HUANG, J. Y., KHAN, A. R., AUBERT, G., CANDELARIA, K., THOMAS, S., SHIN, D. J., BOOTH, S., BAIG, S. M., BILAL, A., HWANG, D., ZHANG, H., LOVELL-BADGE, R., SMITH, S. R., AWAN, F. R. & JIANG, Z. Y. 2013. Imbalance between neutrophil elastase and its inhibitor alpha1-antitrypsin in obesity alters insulin sensitivity, inflammation, and energy expenditure. *Cell Metab,* 17**,** 534-48.

MARTIGNETTI, J. A., AQEEL, A. A., SEWAIRI, W. A., BOUMAH, C. E., KAMBOURIS, M., MAYOUF, S. A., SHETH, K. V., EID, W. A., DOWLING, O., HARRIS, J., GLUCKSMAN, M. J., BAHABRI, S., MEYER, B. F. & DESNICK, R. J. 2001. Mutation of the matrix metalloproteinase 2 gene (MMP2) causes a multicentric osteolysis and arthritis syndrome. *Nat Genet,* 28**,** 261-5.

MATLUNG, H. L., GROEN, H. C., DE VOS, J., VAN WALSUM, T., VAN DER LUGT, A., NIESSEN, W. J., WENTZEL, J. J., VANBAVEL, E. & BAKKER, E. N. 2009. Calcification locates to transglutaminases in advanced human atherosclerotic lesions. *Am J Pathol,* 175**,** 1374-9.

MCLAUGHLIN, P. J., CHEN, Q., HORIGUCHI, M., STARCHER, B. C., STANTON, J. B., BROEKELMANN, T. J., MARMORSTEIN, A. D., MCKAY, B., MECHAM, R., NAKAMURA, T. & MARMORSTEIN, L. Y. 2006. Targeted disruption of fibulin-4 abolishes elastogenesis and causes perinatal lethality in mice. *Mol Cell Biol,* 26**,** 1700-9.

MCMILLAN, W. D. & PEARCE, W. H. 1999. Increased plasma levels of metalloproteinase-9 are associated with abdominal aortic aneurysms. *J Vasc Surg,* 29**,** 122-7; discussion 127-9.

MCMILLAN, W. D., TAMARINA, N. A., CIPOLLONE, M., JOHNSON, D. A., PARKER, M. A. & PEARCE, W. H. 1997. Size matters: the relationship between MMP-9 expression and aortic diameter. *Circulation,* 96**,** 2228-32.

MEARNS, B., NANDA, N., IISMAA, S. & GRAHAM, R. 2002. Impaired wound healing and altered fibroblast cytoskeletal dynamics in Gh knockout mice. *Minerva Biotecnologica,* 14**,** 218.

MECHAM, R. P. & GIBSON, M. A. 2015. The microfibril-associated glycoproteins (MAGPs) and the microfibrillar niche. *Matrix Biol,* 47**,** 13-33.

MELINO, G., ANNICCHIARICO-PETRUZZELLI, M., PIREDDA, L., CANDI, E., GENTILE, V., DAVIES, P. J. & PIACENTINI, M. 1994. Tissue transglutaminase and apoptosis: sense and antisense transfection studies with human neuroblastoma cells. *Mol Cell Biol,* 14**,** 6584-96.

MESH, C. L., BAXTER, B. T., PEARCE, W. H., CHISHOLM, R. L., MCGEE, G. S. & YAO, J. S. 1992. Collagen and elastin gene expression in aortic aneurysms. *Surgery,* 112**,** 256-261.

METHIA, N., ANDRE, P., HAFEZI-MOGHADAM, A., ECONOMOPOULOS, M., THOMAS, K. L. & WAGNER, D. D. 2001. ApoE deficiency compromises the blood brain barrier especially after injury. *Mol.Med.,* 7**,** 810-815.

MIKKOLA, H., SYRJALA, M., RASI, V., VAHTERA, E., HAMALAINEN, E., PELTONEN, L. & PALOTIE, A. 1994. Deficiency in the A-subunit of coagulation factor XIII: two novel point mutations demonstrate different effects on transcript levels. *Blood,* 84**,** 517-25.

MILLER, F. J., JR., SHARP, W. J., FANG, X., OBERLEY, L. W., OBERLEY, T. D. & WEINTRAUB, N. L. 2002. Oxidative stress in human abdominal aortic aneurysms: a potential mediator of aneurysmal remodeling. *Arterioscler Thromb Vasc Biol,* 22**,** 560-5.

MIN, S. K., MIN, S. I., JEONG, E. M., CHO, S. Y., HA, J., KIM, S. J. & KIM, I. G. 2014. Intimal hyperplasia in loop-injured carotid arteries is attenuated in transglutaminase 2-null mice. *J Korean Med Sci,* 29**,** 363-9.

MINION, D. J., DAVIS, V. A., NEJEZCHLEB, P. A., WANG, Y., MCMANUS, B. M. & BAXTER, B. T. 1994. Elastin is increased in abdominal aortic aneurysms. *J.Surg.Res.,* 57**,** 443-446.

MISHRA, S. & MURPHY, L. J. 2004. Tissue transglutaminase has intrinsic kinase activity: identification of transglutaminase 2 as an insulin-like growth factor-binding protein-3 kinase. *J Biol Chem,* 279**,** 23863-8.

MITHIEUX, S. M. & WEISS, A. S. 2005. Elastin. *Adv.Protein Chem.,* 70**,** 437-461.

MIYAMA, N., DUA, M. M., YEUNG, J. J., SCHULTZ, G. M., ASAGAMI, T., SHO, E., SHO, M. & DALMAN, R. L. 2010. Hyperglycemia limits experimental aortic aneurysm progression. *J Vasc Surg,* 52**,** 975-83.

MOCHIZUKI, S., BRASSART, B. & HINEK, A. 2002. Signaling pathways transduced through the elastin receptor facilitate proliferation of arterial smooth muscle cells. *J Biol Chem,* 277**,** 44854-63.

MOLL, F. L., POWELL, J. T., FRAEDRICH, G., VERZINI, F., HAULON, S., WALTHAM, M., VAN HERWAARDEN, J. A., HOLT, P. J., VAN KEULEN, J. W., RANTNER, B., SCHLOSSER, F. J., SETACCI, F. & RICCO, J. B. 2011. Management of abdominal aortic aneurysms clinical practice guidelines of the European society for vascular surgery. *Eur.J.Vasc.Endovasc.Surg.,* 41 Suppl 1**,** S1-S58.

MORAN, C. S., JOSE, R. J., MOXON, J. V., ROOMBERG, A., NORMAN, P. E., RUSH, C., KORNER, H. & GOLLEDGE, J. 2013. Everolimus limits

aortic aneurysm in the apolipoprotein E-deficient mouse by downregulating C-C chemokine receptor 2 positive monocytes. *Arterioscler Thromb Vasc Biol,* 33**,** 814-21.

MORGUNOVA, E., TUUTTILA, A., BERGMANN, U. & TRYGGVASON, K. 2002. Structural insight into the complex formation of latent matrix metalloproteinase 2 with tissue inhibitor of metalloproteinase 2. *Proc Natl Acad Sci U S A,* 99**,** 7414-9.

MORRIS, D. R., BIROS, E., CRONIN, O., KUIVANIEMI, H. & GOLLEDGE, J. 2014. The association of genetic variants of matrix metalloproteinases with abdominal aortic aneurysm: a systematic review and meta-analysis. *Heart,* 100**,** 295-302.

MOSHER, D. F. 2014. Factor XIII and adipocyte biology. *Blood,* 124**,** 1213-4.

MOTTA, J. P., BERMUDEZ-HUMARAN, L. G., DERAISON, C., MARTIN, L., ROLLAND, C., ROUSSET, P., BOUE, J., DIETRICH, G., CHAPMAN, K., KHARRAT, P., VINEL, J. P., ALRIC, L., MAS, E., SALLENAVE, J. M., LANGELLA, P. & VERGNOLLE, N. 2012. Food-grade bacteria expressing elafin protect against inflammation and restore colon homeostasis. *Sci Transl Med,* 4**,** 158ra144.

MUNEZANE, T., HASEGAWA, T., SURITALA, TANAKA, A., OKADA, K. & OKITA, Y. 2010. Activation of transglutaminase type 2 for aortic wall protection in a rat abdominal aortic aneurysm formation. *J.Vasc.Surg.,* 52**,** 967-974.

MUSZBEK, L., BAGOLY, Z., CAIRO, A. & PEYVANDI, F. 2011a. Novel aspects of factor XIII deficiency. *Curr.Opin.Hematol.,* 18**,** 366-372.

MUSZBEK, L., BERECZKY, Z., BAGOLY, Z., KOMAROMI, I. & KATONA, E. 2011b. Factor XIII: a coagulation factor with multiple plasmatic and cellular functions. *Physiol Rev.,* 91**,** 931-972.

MUSZBEK, L., YEE, V. C. & HEVESSY, Z. 1999. Blood coagulation factor XIII: structure and function. *Thromb.Res.,* 94**,** 271-305.

MYNENI, V. D., HITOMI, K. & KAARTINEN, M. T. 2014. Factor XIII-A transglutaminase acts as a switch between preadipocyte proliferation and differentiation. *Blood,* 124**,** 1344-53.

NAAASP 2014. National AAA Screening Programme: 2013/4 Screening Data report.

NAGASAWA, H., MIYAMOTO, M. & FUJIMOTO, M. 1973. [Reproductivity in inbred strains of mice and project for their efficient production (author's transl)]. *Jikken Dobutsu,* 22**,** 119-26.

NAGASE, H., VISSE, R. & MURPHY, G. 2006. Structure and function of matrix metalloproteinases and TIMPs. *Cardiovasc Res,* 69**,** 562-73.

NAHRENDORF, M., HU, K., FRANTZ, S., JAFFER, F. A., TUNG, C. H., HILLER, K. H., VOLL, S., NORDBECK, P., SOSNOVIK, D., GATTENLOHNER, S., NOVIKOV, M., DICKNEITE, G., REED, G. L., JAKOB, P., ROSENZWEIG, A., BAUER, W. R., WEISSLEDER, R. & ERTL, G. 2006. Factor XIII deficiency causes cardiac rupture, impairs wound healing, and aggravates cardiac remodeling in mice with myocardial infarction. *Circulation,* 113**,** 1196-202.

NAKAHASHI, T. K., HOSHINA, K., TSAO, P. S., SHO, E., SHO, M., KARWOWSKI, J. K., YEH, C., YANG, R. B., TOPPER, J. N. & DALMAN, R. L. 2002. Flow loading induces macrophage antioxidative

gene expression in experimental aneurysms. *Arterioscler Thromb Vasc Biol,* 22**,** 2017-22.

NAKAMURA, T., LOZANO, P. R., IKEDA, Y., IWANAGA, Y., HINEK, A., MINAMISAWA, S., CHENG, C. F., KOBUKE, K., DALTON, N., TAKADA, Y., TASHIRO, K., ROSS JR, J., HONJO, T. & CHIEN, K. R. 2002. Fibulin-5/DANCE is essential for elastogenesis in vivo. *Nature,* 415**,** 171-5.

NAKANO, Y., ADDISON, W. N. & KAARTINEN, M. T. 2007. ATP-mediated mineralization of MC3T3-E1 osteoblast cultures. *Bone,* 41**,** 549-61.

NAKAOKA, H., PEREZ, D. M., BAEK, K. J., DAS, T., HUSAIN, A., MISONO, K., IM, M. J. & GRAHAM, R. M. 1994. Gh: a GTP-binding protein with transglutaminase activity and receptor signaling function. *Science,* 264**,** 1593-1596.

NANDA, N., IISMAA, S. E., OWENS, W. A., HUSAIN, A., MACKAY, F. & GRAHAM, R. M. 2001. Targeted inactivation of Gh/tissue transglutaminase II. *J.Biol.Chem.,* 276**,** 20673-20678.

NAR, H., WERLE, K., BAUER, M. M., DOLLINGER, H. & JUNG, B. 2001. Crystal structure of human macrophage elastase (MMP-12) in complex with a hydroxamic acid inhibitor. *J Mol Biol,* 312**,** 743-51.

NARDACCI, R., LO IACONO, O., CICCOSANTI, F., FALASCA, L., ADDESSO, M., AMENDOLA, A., ANTONUCCI, G., CRAXI, A., FIMIA, G. M., IADEVAIA, V., MELINO, G., RUCO, L., TOCCI, G., IPPOLITO, G. & PIACENTINI, M. 2003. Transglutaminase type II plays a protective role in hepatic injury. *Am J Pathol,* 162**,** 1293-303.

NAUKKARINEN, J., SURAKKA, I., PIETILAINEN, K. H., RISSANEN, A., SALOMAA, V., RIPATTI, S., YKI-JARVINEN, H., VAN DUIJN, C. M., WICHMANN, H. E., KAPRIO, J., TASKINEN, M. R., PELTONEN, L. & CONSORTIUM, E. 2010. Use of genome-wide expression data to mine the "Gray Zone" of GWA studies leads to novel candidate obesity genes. *PLoS Genet,* 6**,** e1000976.

NEWBY, A. C. 2006. Matrix metalloproteinases regulate migration, proliferation, and death of vascular smooth muscle cells by degrading matrix and non-matrix substrates. *Cardiovasc Res,* 69**,** 614-24.

NEWBY, A. C. 2012. Matrix metalloproteinase inhibition therapy for vascular diseases. *Vascul Pharmacol,* 56**,** 232-44.

NEWBY, A. C. 2015. Metalloproteinases promote plaque rupture and myocardial infarction: A persuasive concept waiting for clinical translation. *Matrix Biol,* 44-46**,** 157-66.

NICE, N. I. F. H. A. C. E. 2015. Coeliac Disease: Recognition, Assessment & Management. *In:* EXCELLENCE, N. I. F. H. A. C. (ed.).

NOLL, T., WOZNIAK, G., MCCARSON, K., HAJIMOHAMMAD, A., METZNER, H. J., INSERTE, J., KUMMER, W., HEHRLEIN, F. W. & PIPER, H. M. 1999a. Effect of factor XIII on endothelial barrier function. *J.Exp.Med.,* 189**,** 1373-1382.

NOLL, T., WOZNIAK, G., MCCARSON, K., HAJIMOHAMMAD, A., METZNER, H. J., INSERTE, J., KUMMER, W., HEHRLEIN, F. W. & PIPER, H. M. 1999b. Effect of factor XIII on endothelial barrier function. *J Exp Med,* 189**,** 1373-82.

NORDON, I. M., HINCHLIFFE, R. J., HOLT, P. J., LOFTUS, I. M. & THOMPSON, M. M. 2009. Review of current theories for abdominal aortic aneurysm pathogenesis. *Vascular,* 17**,** 253-263.

NORDON, I. M., HINCHLIFFE, R. J., LOFTUS, I. M. & THOMPSON, M. M. 2011. Pathophysiology and epidemiology of abdominal aortic aneurysms. *Nat Rev Cardiol,* 8**,** 92-102.

NORMAN, P. E. & POWELL, J. T. 2010. Site specificity of aneurysmal disease. *Circulation,* 121**,** 560-8.

NURMINSKAYA, M., BEAZLEY, K. E., SMITH, E. P. & BELKIN, A. M. 2014. Transglutaminase 2 promotes PDGF-mediated activation of PDGFR/Akt1 and beta-catenin signaling in vascular smooth muscle cells and supports neointima formation. *J Vasc Res,* 51**,** 418-28.

NURMINSKAYA, M. & KAARTINEN, M. T. 2006. Transglutaminases in mineralized tissues. *Front Biosci.,* 11**,** 1591-1606.

NURMINSKAYA, M., MAGEE, C., NURMINSKY, D. & LINSENMAYER, T. F. 1998. Plasma transglutaminase in hypertrophic chondrocytes: expression and cell-specific intracellular activation produce cell death and externalization. *J.Cell Biol.,* 142**,** 1135-1144.

ODII, B. O. & COUSSONS, P. 2014. Biological functionalities of transglutaminase 2 and the possibility of its compensation by other members of the transglutaminase family. *ScientificWorldJournal,* 2014**,** 714561.

OHTA, K., NAKAJIMA, T., CHEAH, A. Y., ZAIDI, S. H., KAVIANI, N., DAWOOD, F., YOU, X. M., LIU, P., HUSAIN, M. & RABINOVITCH, M. 2004. Elafin-overexpressing mice have improved cardiac function after myocardial infarction. *Am J Physiol Heart Circ Physiol,* 287**,** H286-92.

OLSEN, K. C., SAPINORO, R. E., KOTTMANN, R. M., KULKARNI, A. A., IISMAA, S. E., JOHNSON, G. V., THATCHER, T. H., PHIPPS, R. P. & SIME, P. J. 2011a. Transglutaminase 2 and its role in pulmonary fibrosis. *Am J Respir Crit Care Med,* 184**,** 699-707.

OLSEN, K. C., SAPINORO, R. E., KOTTMANN, R. M., KULKARNI, A. A., IISMAA, S. E., JOHNSON, G. V., THATCHER, T. H., PHIPPS, R. P. & SIME, P. J. 2011b. Transglutaminase 2 and its Role in Pulmonary Fibrosis. *Am.J.Respir.Crit Care Med.*

ORBE, J., FERNANDEZ, L., RODRIGUEZ, J. A., RABAGO, G., BELZUNCE, M., MONASTERIO, A., RONCAL, C. & PARAMO, J. A. 2003. Different expression of MMPs/TIMP-1 in human atherosclerotic lesions. Relation to plaque features and vascular bed. *Atherosclerosis,* 170**,** 269-76.

ORR, A. W., STOCKTON, R., SIMMERS, M. B., SANDERS, J. M., SAREMBOCK, I. J., BLACKMAN, B. R. & SCHWARTZ, M. A. 2007. Matrix-specific p21-activated kinase activation regulates vascular permeability in atherogenesis. *J Cell Biol,* 176**,** 719-27.

OWENS, A. P., 3RD, RATERI, D. L., HOWATT, D. A., MOORE, K. J., TOBIAS, P. S., CURTISS, L. K., LU, H., CASSIS, L. A. & DAUGHERTY, A. 2011. MyD88 deficiency attenuates angiotensin II-induced abdominal aortic aneurysm formation independent of signaling through Toll-like receptors 2 and 4. *Arterioscler Thromb Vasc Biol,* 31**,** 2813-9.

OWENS, G. K., KUMAR, M. S. & WAMHOFF, B. R. 2004. Molecular regulation of vascular smooth muscle cell differentiation in development and disease. *Physiol Rev,* 84**,** 767-801.

PAGE-MCCAW, A., EWALD, A. J. & WERB, Z. 2007. Matrix metalloproteinases and the regulation of tissue remodelling. *Nat Rev Mol Cell Biol,* 8**,** 221-33.

PAPAHARALAMBUS, C. A. & GRIENDLING, K. K. 2007. Basic mechanisms of oxidative stress and reactive oxygen species in cardiovascular injury. *Trends Cardiovasc Med,* 17**,** 48-54.

PARK, K. S., HAN, B. G., LEE, K. H., KIM, D. S., KIM, J. M., JEON, H., KIM, H. S., SUH, S. W., LEE, E. H., KIM, S. Y. & LEE, B. I. 2009. Depletion of nucleophosmin via transglutaminase 2 cross-linking increases drug resistance in cancer cells. *Cancer Lett.,* 274**,** 201-207.

PAWLINSKI, R., FERNANDES, A., KEHRLE, B., PEDERSEN, B., PARRY, G., ERLICH, J., PYO, R., GUTSTEIN, D., ZHANG, J., CASTELLINO, F., MELIS, E., CARMELIET, P., BARETTON, G., LUTHER, T., TAUBMAN, M., ROSEN, E. & MACKMAN, N. 2002. Tissue factor deficiency causes cardiac fibrosis and left ventricular dysfunction. *Proc.Natl.Acad.Sci.U.S.A,* 99**,** 15333-15338.

PEREIRA, A. M., STRASBERG-RIEBER, M. & RIEBER, M. 2005. Invasion-associated MMP-2 and MMP-9 are up-regulated intracellularly in concert with apoptosis linked to melanoma cell detachment. *Clin Exp Metastasis,* 22**,** 285-95.

PETERS, L. L., JINDEL, H. K., GWYNN, B., KORSGREN, C., JOHN, K. M., LUX, S. E., MOHANDAS, N., COHEN, C. M., CHO, M. R., GOLAN, D. E. & BRUGNARA, C. 1999. Mild spherocytosis and altered red cell ion transport in protein 4. 2-null mice. *J Clin Invest,* 103**,** 1527-37.

PETERSEN, E., WAGBERG, F. & ANGQUIST, K. A. 2002. Proteolysis of the abdominal aortic aneurysm wall and the association with rupture. *Eur J Vasc Endovasc Surg,* 23**,** 153-7.

PETRINEC, D., LIAO, S., HOLMES, D. R., REILLY, J. M., PARKS, W. C. & THOMPSON, R. W. 1996. Doxycycline inhibition of aneurysmal degeneration in an elastase-induced rat model of abdominal aortic aneurysm: preservation of aortic elastin associated with suppressed production of 92 kD gelatinase. *J Vasc Surg,* 23**,** 336-46.

PHATAK, V. M., CROFT, S. M., RAMESHAIAH SETTY, S. G., SCARPELLINI, A., HUGHES, D. C., REES, R., MCARDLE, S. & VERDERIO, E. A. 2013. Expression of transglutaminase-2 isoforms in normal human tissues and cancer cell lines: dysregulation of alternative splicing in cancer. *Amino Acids,* 44**,** 33-44.

PHINIKARIDOU, A., ANDIA, M. E., PROTTI, A., INDERMUEHLE, A., SHAH, A., SMITH, A., WARLEY, A. & BOTNAR, R. M. 2012. Noninvasive magnetic resonance imaging evaluation of endothelial permeability in murine atherosclerosis using an albumin-binding contrast agent. *Circulation,* 126**,** 707-19.

PIMIENTO, J. M., MALONEY, S. P., TANG, P. C., MUTO, A., WESTVIK, T. S., FITZGERALD, T. N., FANCHER, T. T., TELLIDES, G. & DARDIK, A. 2008. Endothelial nitric oxide synthase stimulates aneurysm growth in aged mice. *J Vasc Res,* 45**,** 251-8.

PINKERT, C. A. 2012. *Transgenic Animal technology: A Laboratory Handbook,* San Diego, California, USA, Academic Press Ltd.

POON, M. C., RUSSELL, J. A., LOW, S., SINCLAIR, G. D., JONES, A. R., BLAHEY, W., RUETHER, B. A. & HOAR, D. I. 1989. Hemopoietic origin of factor XIII A subunits in platelets, monocytes, and plasma.

Evidence from bone marrow transplantation studies. *J.Clin.Invest,* 84**,** 787-792.

PRIME, M. 2011. The Development of Potent and Selective Transglutaminase-2 Inhibitors for the Treatment of Huntington's Disease. *5th annual conference on HD therapeutics, 5-8 Feb, Palm Springs, USA* [Online]. Available: http://evotec.sissy.bgcc.at/uploads/media_library/14/FINAL_PRINT_TG2_Poster.pdf.

PROCKOP, D. J., KIVIRIKKO, K. I., TUDERMAN, L. & GUZMAN, N. A. 1979a. The biosynthesis of collagen and its disorders (first of two parts). *N Engl J Med,* 301**,** 13-23.

PROCKOP, D. J., KIVIRIKKO, K. I., TUDERMAN, L. & GUZMAN, N. A. 1979b. The biosynthesis of collagen and its disorders (second of two parts). *N Engl J Med,* 301**,** 77-85.

PYO, R., LEE, J. K., SHIPLEY, J. M., CURCI, J. A., MAO, D., ZIPORIN, S. J., ENNIS, T. L., SHAPIRO, S. D., SENIOR, R. M. & THOMPSON, R. W. 2000a. Targeted gene disruption of matrix metalloproteinase-9 (gelatinase B) suppresses development of experimental abdominal aortic aneurysms. *J Clin Invest,* 105**,** 1641-9.

PYO, R., LEE, J. K., SHIPLEY, J. M., CURCI, J. A., MAO, D., ZIPORIN, S. J., ENNIS, T. L., SHAPIRO, S. D., SENIOR, R. M. & THOMPSON, R. W. 2000b. Targeted gene disruption of matrix metalloproteinase-9 (gelatinase B) suppresses development of experimental abdominal aortic aneurysms. *J.Clin.Invest,* 105**,** 1641-1649.

QI, J. H., EBRAHEM, Q., MOORE, N., MURPHY, G., CLAESSON-WELSH, L., BOND, M., BAKER, A. & ANAND-APTE, B. 2003. A novel function for tissue inhibitor of metalloproteinases-3 (TIMP3): inhibition of angiogenesis by blockage of VEGF binding to VEGF receptor-2. *Nat Med,* 9**,** 407-15.

RAJAGOPALAN, S., MENG, X. P., RAMASAMY, S., HARRISON, D. G. & GALIS, Z. S. 1996. Reactive oxygen species produced by macrophage-derived foam cells regulate the activity of vascular matrix metalloproteinases in vitro. Implications for atherosclerotic plaque stability. *J Clin Invest,* 98**,** 2572-9.

RAMIREZ, F., SAKAI, L. Y., RIFKIN, D. B. & DIETZ, H. C. 2007. Extracellular microfibrils in development and disease. *Cell Mol Life Sci,* 64**,** 2437-46.

RATERI, D. L., MOORLEGHEN, J. J., BALAKRISHNAN, A., OWENS, A. P., 3RD, HOWATT, D. A., SUBRAMANIAN, V., PODURI, A., CHARNIGO, R., CASSIS, L. A. & DAUGHERTY, A. 2011. Endothelial cell-specific deficiency of Ang II type 1a receptors attenuates Ang II-induced ascending aortic aneurysms in LDL receptor-/- mice. *Circ Res,* 108**,** 574-81.

REILLY, C. F. 1990. Rat vascular smooth muscle cells immortalized with SV40 large T antigen possess defined smooth muscle cell characteristics including growth inhibition by heparin. *J Cell Physiol,* 142**,** 342-51.

RICHARDSON, V. R., CORDELL, P., STANDEVEN, K. F. & CARTER, A. M. 2013. Substrates of Factor XIII-A: roles in thrombosis and wound healing. *Clin Sci (Lond),* 124**,** 123-37.

RITTER, S. J. & DAVIES, P. J. 1998. Identification of a transforming growth factor-beta1/bone morphogenetic protein 4 (TGF-beta1/BMP4) response element within the mouse tissue transglutaminase gene promoter. *J Biol Chem,* 273**,** 12798-806.

ROBINSON, B. R., HOUNG, A. K. & REED, G. L. 2000. Catalytic life of activated factor XIII in thrombi. Implications for fibrinolytic resistance and thrombus aging. *Circulation,* 102**,** 1151-7.

RODOLFO, C., MORMONE, E., MATARRESE, P., CICCOSANTI, F., FARRACE, M. G., GAROFANO, E., PIREDDA, L., FIMIA, G. M., MALORNI, W. & PIACENTINI, M. 2004. Tissue transglutaminase is a multifunctional BH3-only protein. *J Biol Chem,* 279**,** 54783-92.

ROSELAAR, S. E. & DAUGHERTY, A. 1998. Apolipoprotein E-deficient mice have impaired innate immune responses to Listeria monocytogenes in vivo. *J.Lipid Res.,* 39**,** 1740-1743.

ROSENBLOOM, J., ABRAMS, W. R. & MECHAM, R. 1993. Extracellular matrix 4: the elastic fiber. *FASEB J,* 7**,** 1208-18.

SALLENAVE, J. M. 2010. Secretory leukocyte protease inhibitor and elafin/trappin-2: versatile mucosal antimicrobials and regulators of immunity. *Am J Respir Cell Mol Biol,* 42**,** 635-43.

SALLENAVE, J. M., CUNNINGHAM, G. A., JAMES, R. M., MCLACHLAN, G. & HASLETT, C. 2003. Regulation of pulmonary and systemic bacterial lipopolysaccharide responses in transgenic mice expressing human elafin. *Infect Immun,* 71**,** 3766-74.

SANE, D. C., KONTOS, J. L. & GREENBERG, C. S. 2007. Roles of transglutaminases in cardiac and vascular diseases. *Front Biosci.,* 12**,** 2530-2545.

SANG, Q. X. 1998. Complex role of matrix metalloproteinases in angiogenesis. *Cell Res,* 8**,** 171-7.

SANTHANAM, L., TUDAY, E. C., WEBB, A. K., DOWZICKY, P., KIM, J. H., OH, Y. J., SIKKA, G., KUO, M., HALUSHKA, M. K., MACGREGOR, A. M., DUNN, J., GUTBROD, S., YIN, D., SHOUKAS, A., NYHAN, D., FLAVAHAN, N. A., BELKIN, A. M. & BERKOWITZ, D. E. 2010. Decreased S-nitrosylation of tissue transglutaminase contributes to age-related increases in vascular stiffness. *Circ Res,* 107**,** 117-25.

SARAFF, K., BABAMUSTA, F., CASSIS, L. A. & DAUGHERTY, A. 2003. Aortic dissection precedes formation of aneurysms and atherosclerosis in angiotensin II-infused, apolipoprotein E-deficient mice. *Arterioscler Thromb Vasc Biol,* 23**,** 1621-6.

SARANG, Z., MOLNAR, P., NEMETH, T., GOMBA, S., KARDON, T., MELINO, G., COTECCHIA, S., FESUS, L. & SZONDY, Z. 2005. Tissue transglutaminase (TG2) acting as G protein protects hepatocytes against Fas-mediated cell death in mice. *Hepatology,* 42**,** 578-87.

SATPATHY, M., SHAO, M., EMERSON, R., DONNER, D. B. & MATEI, D. 2009. Tissue transglutaminase regulates matrix metalloproteinase-2 in ovarian cancer by modulating cAMP-response element-binding protein activity. *J Biol Chem,* 284**,** 15390-9.

SAUER, B. & HENDERSON, N. 1988. Site-specific DNA recombination in mammalian cells by the Cre recombinase of bacteriophage P1. *Proc.Natl.Acad.Sci.U.S.A,* 85**,** 5166-5170.

SCHILLINGER, M., EXNER, M., MLEKUSCH, W., DOMANOVITS, H., HUBER, K., MANNHALTER, C., WAGNER, O. & MINAR, E. 2002. Heme oxygenase-1 gene promoter polymorphism is associated with abdominal aortic aneurysm. *Thromb Res,* 106**,** 131-6.

SCHNEIDER, H. & MOSER, R. W. 2016. Classics revisited. Raissa Nitabuch, on the uteroplacental circulation and the fibrinous membrane. *Placenta,* 40**,** 34-9.

SENER, A., DUNLOP, M. E., GOMIS, R., MATHIAS, P. C., MALAISSE-LAGAE, F. & MALAISSE, W. J. 1985. Role of transglutaminase in insulin release. Study with glycine and sarcosine methylesters. *Endocrinology,* 117**,** 237-42.

SHAPIRO, S. D. 2007. Transgenic and gene-targeted mice as models for chronic obstructive pulmonary disease. *Eur Respir J,* 29**,** 375-8.

SHAW, L. & WIEDOW, O. 2011. Therapeutic potential of human elafin. *Biochem Soc Trans,* 39**,** 1450-4.

SHIPLEY, J. M., WESSELSCHMIDT, R. L., KOBAYASHI, D. K., LEY, T. J. & SHAPIRO, S. D. 1996. Metalloelastase is required for macrophage-mediated proteolysis and matrix invasion in mice. *Proc Natl Acad Sci U S A,* 93**,** 3942-6.

SHO, E., CHU, J., SHO, M., FERNANDES, B., JUDD, D., GANESAN, P., KIMURA, H. & DALMAN, R. L. 2004. Continuous periaortic infusion improves doxycycline efficacy in experimental aortic aneurysms. *J Vasc Surg,* 39**,** 1312-21.

SIEGEL, M. & KHOSLA, C. 2007. Transglutaminase 2 inhibitors and their therapeutic role in disease states. *Pharmacol Ther,* 115**,** 232-45.

SIGMA-ALDRICH. 2016. *Matrix Metalloproteinases* [Online]. Available: http://www.sigmaaldrich.com/life-science/metabolomics/enzyme-explorer/cell-signaling-enzymes/matrix-metalloproteinases.html [Accessed 10th February 2016].

SILENCE, J., COLLEN, D. & LIJNEN, H. R. 2002. Reduced atherosclerotic plaque but enhanced aneurysm formation in mice with inactivation of the tissue inhibitor of metalloproteinase-1 (TIMP- 1) gene. *Circ.Res.,* 90**,** 897-903.

SILENCE, J., LUPU, F., COLLEN, D. & LIJNEN, H. R. 2001. Persistence of atherosclerotic plaque but reduced aneurysm formation in mice with stromelysin-1 (MMP-3) gene inactivation. *Arterioscler Thromb Vasc Biol,* 21**,** 1440-5.

SIMPSON, A. J., WALLACE, W. A., MARSDEN, M. E., GOVAN, J. R., PORTEOUS, D. J., HASLETT, C. & SALLENAVE, J. M. 2001. Adenoviral augmentation of elafin protects the lung against acute injury mediated by activated neutrophils and bacterial infection. *J Immunol,* 167**,** 1778-86.

SIWIK, D. A., PAGANO, P. J. & COLUCCI, W. S. 2001. Oxidative stress regulates collagen synthesis and matrix metalloproteinase activity in cardiac fibroblasts. *Am J Physiol Cell Physiol,* 280**,** C53-60.

SMALL, K., FENG, J. F., LORENZ, J., DONNELLY, E. T., YU, A., IM, M. J., DORN, G. W., 2ND & LIGGETT, S. B. 1999. Cardiac specific overexpression of transglutaminase II (G(h)) results in a unique hypertrophy phenotype independent of phospholipase C activation. *J Biol Chem,* 274**,** 21291-6.

SOENDERGAARD, C., KVIST, P. H., SEIDELIN, J. B. & NIELSEN, O. H. 2013. Tissue-regenerating functions of coagulation factor XIII. *J.Thromb.Haemost.,* 11**,** 806-816.

SONG, Y. C., SHENG, D., TAUBENFELD, S. M. & MATSUEDA, G. R. 1994. A microtiter assay for factor XIII using fibrinogen and biotinylcadaverine as substrates. *Anal.Biochem.,* 223**,** 88-92.

SOURI, M., KOSEKI-KUNO, S., TAKEDA, N., DEGEN, J. L. & ICHINOSE, A. 2008a. Administration of factor XIII B subunit increased plasma factor XIII A subunit levels in factor XIII B subunit knock-out mice. *Int J Hematol,* 87**,** 60-8.

SOURI, M., KOSEKI-KUNO, S., TAKEDA, N., YAMAKAWA, M., TAKEISHI, Y., DEGEN, J. L. & ICHINOSE, A. 2008b. Male-specific cardiac pathologies in mice lacking either the A or B subunit of factor XIII. *Thromb.Haemost.,* 99**,** 401-408.

STRNAD, P., HARADA, M., SIEGEL, M., TERKELTAUB, R. A., GRAHAM, R. M., KHOSLA, C. & OMARY, M. B. 2007. Transglutaminase 2 regulates mallory body inclusion formation and injury-associated liver enlargement. *Gastroenterology,* 132**,** 1515-26.

SUMI, Y., INOUE, N., AZUMI, H., SENO, T., OKUDA, M., HIRATA, K., KAWASHIMA, S., HAYASHI, Y., ITOH, H. & YOKOYAMA, M. 2002. Expression of tissue transglutaminase and elafin in human coronary artery: implication for plaque instability. *Atherosclerosis,* 160**,** 31-39.

SZABO, A., PEROU, C. M., KARACA, M., PERREARD, L., PALAIS, R., QUACKENBUSH, J. F. & BERNARD, P. S. 2004. Statistical modeling for selecting housekeeper genes. *Genome Biol,* 5**,** R59.

SZCZESNY, G., VEIHELMANN, A., MASSBERG, S., NOLTE, D. & MESSMER, K. 2004. Long-term anaesthesia using inhalatory isoflurane in different strains of mice-the haemodynamic effects. *Lab Anim,* 38**,** 64-9.

SZONDY, Z., SARANG, Z., MOLNAR, P., NEMETH, T., PIACENTINI, M., MASTROBERARDINO, P. G., FALASCA, L., AESCHLIMANN, D., KOVACS, J., KISS, I., SZEGEZDI, E., LAKOS, G., RAJNAVOLGYI, E., BIRCKBICHLER, P. J., MELINO, G. & FESUS, L. 2003. Transglutaminase 2-/- mice reveal a phagocytosis-associated crosstalk between macrophages and apoptotic cells. *Proc.Natl.Acad.Sci.U.S.A,* 100**,** 7812-7817.

TAHERZADEH, Z., VANBAVEL, E., DE, V. J., MATLUNG, H. L., VAN, M. G., BREWSTER, L. M., SEGHERS, L., QUAX, P. H. & BAKKER, E. N. 2010. Strain-dependent susceptibility for hypertension in mice resides in the natural killer gene complex. *Am.J.Physiol Heart Circ.Physiol,* 298**,** H1273-H1282.

TALUKDAR, S., OH DA, Y., BANDYOPADHYAY, G., LI, D., XU, J., MCNELIS, J., LU, M., LI, P., YAN, Q., ZHU, Y., OFRECIO, J., LIN, M., BRENNER, M. B. & OLEFSKY, J. M. 2012. Neutrophils mediate insulin resistance in mice fed a high-fat diet through secreted elastase. *Nat Med,* 18**,** 1407-12.

TANGIRALA, R. K., RUBIN, E. M. & PALINSKI, W. 1995. Quantitation of atherosclerosis in murine models: correlation between lesions in the aortic origin and in the entire aorta, and differences in the extent of lesions between sexes in LDL receptor-deficient and apolipoprotein E-deficient mice. *J Lipid Res,* 36**,** 2320-8.

TARANTINO, U., OLIVA, F., TAURISANO, G., ORLANDI, A., PIETRONI, V., CANDI, E., MELINO, G. & MAFFULLI, N. 2009. FXIIIA and TGF-beta over-expression produces normal musculo-skeletal phenotype in TG2-/- mice. *Amino.Acids,* 36**,** 679-684.

TATSUKAWA, H., FUKAYA, Y., FRAMPTON, G., MARTINEZ-FUENTES, A., SUZUKI, K., KUO, T. F., NAGATSUMA, K., SHIMOKADO, K., OKUNO, M., WU, J., IISMAA, S., MATSUURA, T., TSUKAMOTO, H., ZERN, M. A., GRAHAM, R. M. & KOJIMA, S. 2009a. Role of transglutaminase 2 in liver injury via cross-linking and silencing of transcription factor Sp1. *Gastroenterology,* 136**,** 1783-1795.

TATSUKAWA, H., FUKAYA, Y., FRAMPTON, G., MARTINEZ-FUENTES, A., SUZUKI, K., KUO, T. F., NAGATSUMA, K., SHIMOKADO, K., OKUNO, M., WU, J., IISMAA, S., MATSUURA, T., TSUKAMOTO, H., ZERN, M. A., GRAHAM, R. M. & KOJIMA, S. 2009b. Role of transglutaminase 2 in liver injury via cross-linking and silencing of transcription factor Sp1. *Gastroenterology,* 136**,** 1783-95 e10.

TEDESCO, M. M., TERASHIMA, M., BLANKENBERG, F. G., LEVASHOVA, Z., SPIN, J. M., BACKER, M. V., BACKER, J. M., SHO, M., SHO, E., MCCONNELL, M. V. & DALMAN, R. L. 2009. Analysis of in situ and ex vivo vascular endothelial growth factor receptor expression during experimental aortic aneurysm progression. *Arterioscler Thromb Vasc Biol,* 29**,** 1452-7.

TELCI, D., COLLIGHAN, R. J., BASAGA, H. & GRIFFIN, M. 2009. Increased TG2 expression can result in induction of transforming growth factor beta1, causing increased synthesis and deposition of matrix proteins, which can be regulated by nitric oxide. *J Biol Chem,* 284**,** 29547-58.

TENGER, C. & ZHOU, X. 2003. Apolipoprotein E modulates immune activation by acting on the antigen-presenting cell. *Immunology,* 109**,** 392-7.

THOMAS, H., BECK, K., ADAMCZYK, M., AESCHLIMANN, P., LANGLEY, M., OITA, R. C., THIEBACH, L., HILS, M. & AESCHLIMANN, D. 2013. Transglutaminase 6: a protein associated with central nervous system development and motor function. *Amino Acids,* 44**,** 161-77.

THOMPSON, R. W., CURCI, J. A., ENNIS, T. L., MAO, D., PAGANO, M. B. & PHAM, C. T. 2006. Pathophysiology of abdominal aortic aneurysms: insights from the elastase-induced model in mice with different genetic backgrounds. *Ann.N.Y.Acad.Sci.,* 1085**,** 59-73.

THOMPSON, R. W., GERAGHTY, P. J. & LEE, J. K. 2002. Abdominal aortic aneurysms: basic mechanisms and clinical implications. *Curr Probl Surg,* 39**,** 110-230.

THOMPSON, R. W., HOLMES, D. R., MERTENS, R. A., LIAO, S., BOTNEY, M. D., MECHAM, R. P., WELGUS, H. G. & PARKS, W. C. 1995. Production and localization of 92-kilodalton gelatinase in abdominal aortic aneurysms. An elastolytic metalloproteinase expressed by aneurysm-infiltrating macrophages. *J Clin Invest,* 96**,** 318-26.

TILSON, M. D., 3RD 2005. The polymorphonuclear leukocyte and the abdominal aortic aneurysm: a neglected cell type and a neglected disease. *Circulation,* 112**,** 154-6.

TOROCSIK, D., BARDOS, H., NAGY, L. & ADANY, R. 2005. Identification of factor XIII-A as a marker of alternative macrophage activation. *Cell Mol.Life Sci.,* 62**,** 2132-2139.

TOTH, B., GARABUCZI, E., SARANG, Z., VEREB, G., VAMOSI, G., AESCHLIMANN, D., BLASKO, B., BECSI, B., ERDODI, F., LACY-HULBERT, A., ZHANG, A., FALASCA, L., BIRGE, R. B., BALAJTHY, Z., MELINO, G., FESUS, L. & SZONDY, Z. 2009. Transglutaminase 2 is needed for the formation of an efficient phagocyte portal in macrophages engulfing apoptotic cells. *J.Immunol.,* 182**,** 2084-2092.

TSAMIS, A., KRAWIEC, J. T. & VORP, D. A. 2013. Elastin and collagen fibre microstructure of the human aorta in ageing and disease: a review. *J R Soc Interface,* 10**,** 20121004.

TSUI, J. C. 2010. Experimental models of abdominal aortic aneurysms. *Open Cardiovasc Med J,* 4**,** 221-30.

TSUNEMI, M., MATSUURA, Y., SAKAKIBARA, S. & KATSUBE, Y. 1996. Crystal structure of an elastase-specific inhibitor elafin complexed with porcine pancreatic elastase determined at 1.9 A resolution. *Biochemistry,* 35**,** 11570-6.

TUNG, W. S., LEE, J. K. & THOMPSON, R. W. 2001. Simultaneous analysis of 1176 gene products in normal human aorta and abdominal aortic aneurysms using a membrane-based complementary DNA expression array. *J Vasc Surg,* 34**,** 143-50.

VAN DEN AKKER, J., VAN WEERT, A., AFINK, G., BAKKER, E. N., VAN DER POL, E., BOING, A. N., NIEUWLAND, R. & VANBAVEL, E. 2012. Transglutaminase 2 is secreted from smooth muscle cells by transamidation-dependent microparticle formation. *Amino Acids,* 42**,** 961-73.

VAN HERCK, J. L., SCHRIJVERS, D. M., DE MEYER, G. R., MARTINET, W., VAN HOVE, C. E., BULT, H., VRINTS, C. J. & HERMAN, A. G. 2010. Transglutaminase 2 deficiency decreases plaque fibrosis and increases plaque inflammation in apolipoprotein-E-deficient mice. *J Vasc Res,* 47**,** 231-40.

VAN HINSBERGH, V. W. & KOOLWIJK, P. 2008. Endothelial sprouting and angiogenesis: matrix metalloproteinases in the lead. *Cardiovasc Res,* 78**,** 203-12.

VAN WART, H. E. & BIRKEDAL-HANSEN, H. 1990. The cysteine switch: a principle of regulation of metalloproteinase activity with potential applicability to the entire matrix metalloproteinase gene family. *Proc Natl Acad Sci U S A,* 87**,** 5578-82.

VERDERIO, E., NICHOLAS, B., GROSS, S. & GRIFFIN, M. 1998. Regulated expression of tissue transglutaminase in Swiss 3T3 fibroblasts: effects on the processing of fibronectin, cell attachment, and cell death. *Exp Cell Res,* 239**,** 119-38.

VERDERIO, E. A., JOHNSON, T. & GRIFFIN, M. 2004. Tissue transglutaminase in normal and abnormal wound healing: review article

1. *Amino.Acids,* 26**,** 387-404.

VERDERIO, E. A., TELCI, D., OKOYE, A., MELINO, G. & GRIFFIN, M. 2003. A novel RGD-independent cel adhesion pathway mediated by fibronectin-bound tissue transglutaminase rescues cells from anoikis. *J Biol Chem,* 278**,** 42604-14.

VERMA, A. & MEHTA, K. 2007. Tissue transglutaminase-mediated chemoresistance in cancer cells. *Drug Resist.Updat.,* 10**,** 144-151.

VISSE, R. & NAGASE, H. 2003. Matrix metalloproteinases and tissue inhibitors of metalloproteinases: structure, function, and biochemistry. *Circ Res,* 92**,** 827-39.

VU, T. H., SHIPLEY, J. M., BERGERS, G., BERGER, J. E., HELMS, J. A., HANAHAN, D., SHAPIRO, S. D., SENIOR, R. M. & WERB, Z. 1998. MMP-9/gelatinase B is a key regulator of growth plate angiogenesis and apoptosis of hypertrophic chondrocytes. *Cell,* 93**,** 411-22.

WAGENSEIL, J. E. & MECHAM, R. P. 2007. New insights into elastic fiber assembly. *Birth Defects Res C Embryo Today,* 81**,** 229-40.

WAGENSEIL, J. E. & MECHAM, R. P. 2009. Vascular extracellular matrix and arterial mechanics. *Physiol Rev,* 89**,** 957-89.

WAGENSEIL, J. E. & MECHAM, R. P. 2012. Elastin in large artery stiffness and hypertension. *J Cardiovasc Transl Res,* 5**,** 264-73.

WAHLGREN, C. M., LARSSON, E., MAGNUSSON, P. K., HULTGREN, R. & SWEDENBORG, J. 2010. Genetic and environmental contributions to abdominal aortic aneurysm development in a twin population. *J Vasc Surg,* 51**,** 3-7; discussion 7.

WANG, W., SCHULZE, C. J., SUAREZ-PINZON, W. L., DYCK, J. R., SAWICKI, G. & SCHULZ, R. 2002. Intracellular action of matrix metalloproteinase-2 accounts for acute myocardial ischemia and reperfusion injury. *Circulation,* 106**,** 1543-9.

WANG, Y., AIT-OUFELLA, H., HERBIN, O., BONNIN, P., RAMKHELAWON, B., TALEB, S., HUANG, J., OFFENSTADT, G., COMBADIERE, C., RENIA, L., JOHNSON, J. L., THARAUX, P. L., TEDGUI, A. & MALLAT, Z. 2010. TGF-beta activity protects against inflammatory aortic aneurysm progression and complications in angiotensin II-infused mice. *J Clin Invest,* 120**,** 422-32.

WANG, Y., KRISHNA, S. & GOLLEDGE, J. 2013a. The calcium chloride-induced rodent model of abdominal aortic aneurysm. *Atherosclerosis,* 226**,** 29-39.

WANG, Y., KRISHNA, S., WALKER, P. J., NORMAN, P. & GOLLEDGE, J. 2013b. Transforming growth factor-beta and abdominal aortic aneurysms. *Cardiovasc Pathol,* 22**,** 126-32.

WANG, Z. & GRIFFIN, M. 2012. TG2, a novel extracellular protein with multiple functions. *Amino Acids,* 42**,** 939-49.

WATANABE, K., FUJIOKA, D., SAITO, Y., NAKAMURA, T., OBATA, J. E., KAWABATA, K., WATANABE, Y., MISHINA, H., TAMARU, S., HANASAKI, K. & KUGIYAMA, K. 2012. Group X secretory PLA2 in neutrophils plays a pathogenic role in abdominal aortic aneurysms in mice. *Am.J.Physiol Heart Circ.Physiol,* 302**,** H95-104.

WEINBAUM, J. S., BROEKELMANN, T. J., PIERCE, R. A., WERNECK, C. C., SEGADE, F., CRAFT, C. S., KNUTSEN, R. H. & MECHAM, R. P. 2008. Deficiency in microfibril-associated glycoprotein-1 leads to complex phenotypes in multiple organ systems. *J Biol Chem,* 283**,** 25533-43.

WERNECK, C. C., VICENTE, C. P., WEINBERG, J. S., SHIFREN, A., PIERCE, R. A., BROEKELMANN, T. J., TOLLEFSEN, D. M. & MECHAM, R. P. 2008. Mice lacking the extracellular matrix protein MAGP1 display delayed thrombotic occlusion following vessel injury. *Blood,* 111**,** 4137-4144.

WILLIAMS, H., PEASE, R. J., NEWELL, L. M., CORDELL, P. A., GRAHAM, R. M., KEARNEY, M. T., JACKSON, C. L. & GRANT, P. J. 2010. Effect of transglutaminase 2 (TG2) deficiency on atherosclerotic plaque stability in the apolipoprotein E deficient mouse. *Atherosclerosis,* 210**,** 94-99.

WILLIAMS, S. E., BROWN, T. I., ROGHANIAN, A. & SALLENAVE, J. M. 2006. SLPI and elafin: one glove, many fingers. *Clin Sci (Lond),* 110**,** 21-35.

WOLINSKY, H. & GLAGOV, S. 1967. A lamellar unit of aortic medial structure and function in mammals. *Circ Res,* 20**,** 99-111.

WONG, G. T. 2002. Speed congenics: applications for transgenic and knock-out mouse strains. *Neuropeptides,* 36**,** 230-6.

WOZNIAK, G., NOLL, T., AKINTURK, H., THUL, J. & MULLER, M. 2001. Factor XIII prevents development of myocardial edema in children undergoing surgery for congenital heart disease. *Ann N Y Acad Sci,* 936**,** 617-20.

XIONG, W., KNISPEL, R., MACTAGGART, J. & BAXTER, B. T. 2006. Effects of tissue inhibitor of metalloproteinase 2 deficiency on aneurysm formation. *J Vasc Surg,* 44**,** 1061-6.

XIONG, W., MACTAGGART, J., KNISPEL, R., WORTH, J., PERSIDSKY, Y. & BAXTER, B. T. 2009. Blocking TNF-alpha attenuates aneurysm formation in a murine model. *J Immunol,* 183**,** 2741-6.

XIONG, W., ZHAO, Y., PRALL, A., GREINER, T. C. & BAXTER, B. T. 2004. Key roles of CD4+ T cells and IFN-gamma in the development of abdominal aortic aneurysms in a murine model. *J Immunol,* 172**,** 2607-12.

YABLUCHANSKIY, A., MA, Y., IYER, R. P., HALL, M. E. & LINDSEY, M. L. 2013. Matrix metalloproteinase-9: Many shades of function in cardiovascular disease. *Physiology (Bethesda),* 28**,** 391-403.

YAKUBOV, B., CHEN, L., BELKIN, A. M., ZHANG, S., CHELLADURAI, B., ZHANG, Z. Y. & MATEI, D. 2014. Small molecule inhibitors target the tissue transglutaminase and fibronectin interaction. *PLoS One,* 9**,** e89285.

YAN, C. & BOYD, D. D. 2007. Regulation of matrix metalloproteinase gene expression. *J Cell Physiol,* 211**,** 19-26.

YOSHIMURA, K., AOKI, H., IKEDA, Y., FUJII, K., AKIYAMA, N., FURUTANI, A., HOSHII, Y., TANAKA, N., RICCI, R., ISHIHARA, T., ESATO, K., HAMANO, K. & MATSUZAKI, M. 2005. Regression of abdominal aortic aneurysm by inhibition of c-Jun N-terminal kinase. *Nat.Med.,* 11**,** 1330-1338.

ZACCHIGNA, L., VECCHIONE, C., NOTTE, A., CORDENONSI, M., DUPONT, S., MARETTO, S., CIFELLI, G., FERRARI, A., MAFFEI, A., FABBRO, C., BRAGHETTA, P., MARINO, G., SELVETELLA, G., ARETINI, A., COLONNESE, C., BETTARINI, U., RUSSO, G., SOLIGO, S., ADORNO, M., BONALDO, P., VOLPIN, D., PICCOLO, S., LEMBO, G. & BRESSAN, G. M. 2006. Emilin1 links TGF-beta maturation to blood pressure homeostasis. *Cell,* 124**,** 929-42.

ZADELAAR, S., KLEEMANN, R., VERSCHUREN, L., DE VRIES-VAN DER WEIJ, J., VAN DER HOORN, J., PRINCEN, H. M. & KOOISTRA, T. 2007. Mouse models for atherosclerosis and pharmaceutical modifiers. *Arterioscler Thromb Vasc Biol,* 27**,** 1706-21.

ZAIDI, S. H., HUI, C. C., CHEAH, A. Y., YOU, X. M., HUSAIN, M. & RABINOVITCH, M. 1999. Targeted overexpression of elafin protects mice against cardiac dysfunction and mortality following viral myocarditis. *J Clin Invest,* 103**,** 1211-9.

ZAMBONI, P. & GEMMATI, D. 2007. Clinical implications of gene polymorphisms in venous leg ulcer: a model in tissue injury and reparative process. *Thromb Haemost,* 98**,** 131-7.

ZHANG, L. & WANG, Y. 2015. B lymphocytes in abdominal aortic aneurysms. *Atherosclerosis,* 242**,** 311-7.

ZSOLDOS, Z., REID, D., SIMON, A., SADJAD, S. B. & JOHNSON, A. P. 2006. eHiTS: A new fast, exhaustive flexible ligand docking system. *J.Mol.Graph.Model.*